HANDBOOK OF SENSORS AND ACTUATORS

Volume 7

Series editor S. Middelhoek

K. Iwansson, G. Sinapius and W. Hoornaert (editors)

Measuring Current, Voltage and Power

ELSEVIER

Measuring Current,

Voltage and Power

HANDBOOK OF SENSORS AND ACTUATORS

Series Editor: S. Middelhoek, Delft University of Technology, The Netherlands

Volume 1	Thick Film Sensors (edited by M. Prudenziati)
Volume 2	Solid State Magnetic Sensors (by C.S. Roumenin)
Volume 3	Intelligent Sensors (edited by H. Yamasaki)
Volume 4	Semiconductor Sensors in Physico-Chemical Studies (edited by L. Yu. Kupriyanov)
Volume 5	Mercury Cadmium Telluride Imagers (by A. Onshage)
Volume 6	Micro Mechanical Systems (edited by T. Fukuda and W. Menz)
Volume 7	Measuring Current, Voltage and Power (by K. Iwansson, G. Sinapius and W. Hoornaert)

HANDBOOK OF SENSORS AND ACTUATORS 7

Measuring Current, Voltage and Power

Kaj Iwansson
European Patent Office
Rijswijk, The Netherlands

Günther Sinapius
Europäisches Patentamt
München, Germany

Winfried Hoornaert
European Patent Office
Rijswijk, The Netherlands

1999
ELSEVIER
Amsterdam - Lausanne - New York - Oxford - Shannon - Singapore - Tokyo

ELSEVIER SCIENCE B.V.
Sara Burgerhartstraat 25
P.O. Box 211, 1000 AE Amsterdam, The Netherlands

First edition 1999

Library of Congress Cataloging in Publication Data
A catalog record from the Library of Congress has been applied for.

ISBN: 0 444 72001 4

♾ The paper used in this publication meets the requirements of ANSI/NISO Z39.48-1992 (Permanence of Paper).

Printed & bound by Antony Rowe Ltd, Eastbourne
Transferred to digital printing, 2005

The need for a
Handbook of Sensors and Actuators series

The arrival of integrated circuits, like microprocessors and memories with extremely good performance/price ratios has had a profound influence on many areas of technical endeavour. In the measurement and control field, modern electronic circuits have been introduced on a large scale leading to very sophisticated systems and novel solutions. However, in these measurements and control systems, sensors and actuators are frequently applied that were conceived many decades ago. Consequently, it has become necessary to improve these devices in such a way that their performance/price ratios would be in more agreement with that of modern electronic circuits.

The demand for these new devices initiated worldwide research and development programs in the field of sensors and actuators. Many generic sensor technologies have been examined, from which the thin- and thick-film, glass fibre, metal oxides, polymers, quartz and silicon technologies are the most important.

A growing number of publications on this topic started to appear in a wide variety of scientific journals until, in 1981, Elsevier Science started the publication of the scientific journal *Sensors and Actuators*. It has since become one of the leading journals in this field, publishing papers on sensors and actuators made in various technologies.

When the development of a scientific field expands, the need for handbooks arises, wherein the information that appeared earlier in journals and conference proceedings is systematically and selectively presented. The sensors and actuators field is now in this position. For this reason, Elsevier Science took the initiative to develop a series called

Handbook of Sensors and Actuators

which contains the most meaningful background material that is important for the sensors and actuators field. Titles on thick film sensors, magnetic sensors, intelligent sensors, semiconductor sensors, mercury cadmium telluride imagers and micro mechanical systems have been published. Coverage of subjects such as pressure sensors, radiation sensors, microsystems technology, piezoelectric sensors, robot sensors and accelerometers will soon follow.

The series comprises one- and multi-author handbooks. Great care is given to the selection of the authors and editors. They are all well-known scientists in the field of sensors and actuators and have impressive international reputations.

Elsevier Science and I, as editor of the series, are delighted that these handbooks have already received such a positive response from the sensors and actuators community. We hope that the series will be of great use to many scientists and engineers working in this exciting field.

Simon Middelhoek
Handbook of Sensors and Actuators
Series Editor

This Page Intentionally Left Blank

SUMMARY

This authoritative new book focuses on recent developments in the instrumentation for sensing voltages and currents. It covers new trends and challenges in the field, such as measurements of biocurrents, the increased speed of the components for data taking, testing of computers and integrated circuits where the measurement of rapid voltage and current variations on a very small geometrical scale is necessary. The first chapter concentrates on recent methods to sense voltages and currents, while the rest of the book investigates the applied side, covering for instance electrical power and energy measurements. The main purpose of this volume is to illustrate commonly employed techniques rather than track the scientific evolution and merits and therefore mainly covers patent literature aimed at industrial applications. It is an exciting addition, justifying the series' claim to cover state-of-the-art developments in both the applied and theoretical fields of sensors and actuators.

This Page Intentionally Left Blank

Preface

The measurement of voltages and currents is a common task in the field of electricity and electronics. From a technical point of view it is useful to identify schematically different steps of such a measurement. In a first step a voltage or a current is sensed, intermediate steps such as amplification, transmission and further treatment may follow to yield the result in the final step. Today in most cases microprocessors perform the final steps of such measurements. Analog-to digital converters digitise a voltage that is proportional to the value to be measured and a processor performs further computations and handles the storage and the display of the results. The prerequisite for such measurements are sensors or transducers that respond in a known way to the voltage or current to be measured. The emphasis of this book is put on recent developments of the instrumentation for sensing voltages and currents.

Aside from the general trend towards smaller, cheaper and more reliable instrumentation, new demands have arisen. New applications, like measurements of biocurrents, ask for higher sensitivities. Computers and integrated circuits pose new challenges. To exploit the increased speed of the components for data taking, suitable sensors are required. The accuracy that can be achieved depends more than ever on the first step, the acquisition of the raw data. The influence of the measurement process on the results becomes more crucial. Testing of integrated circuits themselves is a completely new application. For such tests one has to measure rapid voltage and current variations on very small geometrical scales. Here, as well as in the traditional high voltage applications, contactless measurements play an important role.

The organisation of this book is as follows: In the first chapter different methods to sense voltages and currents are described. For the sake of completeness most commonly used methods are mentioned, we concentrate, however, on those developed recently. The following chapters address the subject from the side of different applications in which voltages and currents are sensed.

This publication mainly covers patent literature[1]. The reason for the emphasis on patent literature is, aside from our professional bias as patent examiners at the EPO, that patents, as opposed to scientific publications, are aimed at industrial application, i.e. at instruments that can be built. Since the main purpose of this publication is to illustrate commonly employed techniques rather than to track the scientific evolution and merits in particular fields, in general those publications that illustrate a particular measurement principle best have been cited. The citation of a particular reference does therefore not imply that this is the first or most pertinent publication in the respective field.

We want to dedicate this book to the late **Dieter Kuschbert**, a very friendly, generous and competent person in whose directorate in the DG1 of the EPO in The Hague the project of this text evolved, and to our families who patiently let us spend many evenings and weekends on the project.

Finally, we would like to thank our employer, the **European Patent Office** for giving us support and time, and **Myriam Torbitzky**, who did the desktop publishing part with great dedication.

The Hague and Munich
August 1998

[1]Except for the US numbers, which refer to published patents, most of the other patent publication numbers refer to patent applications, which may differ from the granted patents.

This Page Intentionally Left Blank

EUROPEAN PATENT OFFICE

This is Volume 15 of the EPO Applied Technology Series. The following books have appeared previously in this series:

Volume	1	CARDON & FRANSEN	Dynamic Semiconductor RAM Structures
Volume	2	LAMMINEUR & CORNILLIE	Industrial Robots
Volume	3	BRACKE et al	Inorganic Fibres & Composite Materials
Volume	4	HOORNAERT	Reverse Osmosis
Volume	5	GEISLER et al	Optical Fibres
Volume	6	JACOBS et al	Nickel & Cobalt Extraction Using Organic Compounds
Volume	7	CRISTOL	Solid State Video Cameras
Volume	8	CORNILLIE & DAVIES	Microprocessors
Volume	9	MICHIELS & DE HERDT	Molecular Sieve Catalysts
Volume	10	DERAEDT	Methods of Abating Residual Formaldehyde in Industrial Resins
Volume	11	DHEERE	Universal Computer Interfaces
Volume	12	HERMANN	Protein Folding
Volume	13	ONSHAGE	Mercury Cadmium Telluride Imagers
Volume	14	SIDERIS	Methods for Monitoring & Diagnosing the Efficiency of Catalytic Converters

This Page Intentionally Left Blank

Table of Contents

CHAPTER 1 - SENSORS AND TRANSDUCERS

This Page Intentionally Left Blank

CHAPTER 1

SENSORS AND TRANSDUCERS

1.0 INTRODUCTION

To measure voltages or currents one usually exploits observable effects related to these variables (e.g. the deflection of the needle of a galvanometer). Galvanometers date from the discovery of the interaction between an electric current and a magnetic needle by Oersted in 1819. Galvanometers made accurate analogue current measurements possible. Due to the lack of comparable devices for voltage measurements, for a long time voltage measurements have been done as current measurements. For digital measurements the contrary is true. The analog-to-digital voltage converter (ADC) is the most commonly used analog-to-digital interface. Thus, most digital current measurements are done as voltage measurements.

A number of devices are employed to transform the voltage or current to be measured into a form suitable for further processing. In the first place there are voltage/current dividers and measuring amplifiers. A second group of devices transform an input variable into another variable. These we call sensors. This chapter deals with commonly used sensors and effects related to the voltage or current to be measured. The distinction between measuring circuits and sensors is not always easy. Bridge arrangements, like the Wheatstone-bridge, will not be covered.

The choice of the sensor depends on the variable to be sensed and the response required. The response of the sensor may be for example a voltage or a current within a predetermined range of values relative to/at a chosen potential or a change of polarisation of polarised light. Depending on the physical effect involved, the response can e.g. be linear (Pockels) or quadratic (Kerr). Arrangements with compensation decrease the sensitivity to distortions in the response and increase both, the measuring range and the resolution. A variable that can be measured more easily, e.g. a reference, is applied to the sensor to compensate for the effect due to the variable to be sensed and the sensor is used as a comparator to detect when the compensating variable equals the variable to be measured.

The different kinds of sensors can be grouped into two categories: contacting and contactless. The output from contactless sensors is galvanically isolated from the source of the signal. Usually contactless sensors affect the variable to be measured less. Due to the less direct nature of the measurement, however, precision may also be less. Fiberoptic sensors, made from crystals and optical fibres only, offer the advantage that they are less sensitive to electric and magnetic stray fields than sensors containing electronic circuitry.

For most sensors estimates for their sensitivities have been given. Due to the numerical uncertainty of the experimental data, a lack of detail concerning some experimental parameters and the bias of "typical results" the respective values represent order of magnitude estimates. In those cases where some numerical values necessary for these estimates have not been indicated in the respective publications, whenever possible these values have been taken from a physics textbook [1].

In this book SI units are used unless explicitly otherwise stated.

1.1 VOLTAGE SENSORS

1.1.1 Overview

The range of voltages to be measured ranges from several kV in gas-insulated power installations to mV on electrostatically charged surfaces. Voltage sources in power lines have considerable current sourcing capabilities over long periods of time; electrostatic charged surfaces deliver short current pulses only. For the testing of integrated circuits one has to measure MHz voltage signals with µm spatial resolution.

Measuring the voltage at a point P_1 one determines the electric potential difference U with respect to a reference point P_2, e.g. ground. The potential difference between two points P_1 and P_2 corresponds to the line integral of the electric field E along any path s that connects these points:

$$U = -\int_{P_1}^{P_2} \vec{E}\, d\vec{s} \tag{1}$$

When P_1 and P_2 are connected by an electrical conductor (having a resistance R) and a current source is provided, a current flows; its magnitude is determined by Ohm's law.

The most common way to measure a voltage U_S between two points is to connect them through a (high) resistance R and a galvanometer (with a combined resistance R_M) and to measure the current through there. When a current flows, however, the output resistance of the voltage source, R_S, and its current sourcing capability have to be taken into account. The voltage drop, U_M, across R and the galvanometer is related to the voltage U_S by:

$$U_M = \frac{R_M}{R_M + R_S} U_S \tag{2}$$

The measurement error, i.e. the difference between U_M and U_S decreases with increasing R_M which implies that in such a measurement very low currents have to be measured with high accuracy. Limitations due to the current sourcing capability of the voltage source can be overcome with a feedback arrangement. In such a circuit a compensating current is provided to cancel the current from the source. The voltage is then obtained from the measured compensating current and the values of the resistors involved.

If the points P_1 and P_2 are not connected by an ohmic resistance but by a capacitor which is disconnected after an appropriate period of time, the DC voltage between these points can be derived from the charge stored in the capacitor (cf. Equ. 5). With a circuit, in which the capacitor is disconnected from the points P_1 and P_2 before the voltage measurement, voltages at an arbitrary potential with respect to the measurement circuit can be measured [2]. The charge stored in the capacitor can be determined by any suitable method, e.g. by connecting it to a constant current source and measuring the time of discharge [3].

Voltage can be measured directly with electronic valves or transistors which for a unipolar voltage act as amplifiers with a very high input resistance, cf. Section 1.1.2. More recently Josephson junctions have been used for DC voltage measurements, cf. Section 1.1.3.

The methods described thus far use contacting sensors. A sensor, e.g. a galvanometer, is conductively connected to both, the point whose potential is to be measured and the reference point. A contactless probe that transforms the voltage at P_1 into another electrical variable does not have an ohmic contact with that point. To measure a current related quantity, e.g. a displacement current with a capacitive probe (Section 1.1.4), the probe must still be connected to the reference point. The same holds for the anode in field emission or secondary electron probes (Section 1.1.5). In the latter case not the current but the field dependent energy of the electrons is measured to determine a voltage.

A complementary method to measure the voltage between two points consists in sensing the associated electrical field instead of a current. For this purpose all electric field sensors can be used. Sections 1.1.6 to 1.1.8 cover probes for electric field related phenomena other than current. Section 1.1.6 covers electrometers. Sensors made from materials whose optical or mechanical properties depend on the electric field are treated in Sections 1.1.7 and 1.1.8. These sensors are contactless, they do not require conductive connections to either of the two points whose potential difference is to be sensed.

1.1.2 Transistors

Nowadays transistors (bipolar or FETs) have taken over from electronic valves in most voltage measurements. The voltage to be sensed is connected to the base and the emitter (gate and source). If the voltage has the correct polarity and magnitude, a collector (drain) current flows. With a single transistor unipolar voltages from DC up to high frequencies can be sensed. The finite base resistance of bipolar transistors (megohms) is the main disadvantage compared to electronic valves. These transistors act as high resistance current amplifiers. FETs do not have this drawback because their gate resistance is orders of magnitude higher.

Transistors used as voltage sensors provide a collector (drain) current whose magnitude is a function of the voltage applied. With a symmetric arrangement of the transistors such circuits are suited for bipolar voltage signals. If the transistor in the circuit is configured as an emitter(source) follower, the voltage drop over the emitter (source) resistor equals the input base (gate) voltage. The output resistance of the circuit is much lower then its input resistance because the transistor acts as an impedance transformer.

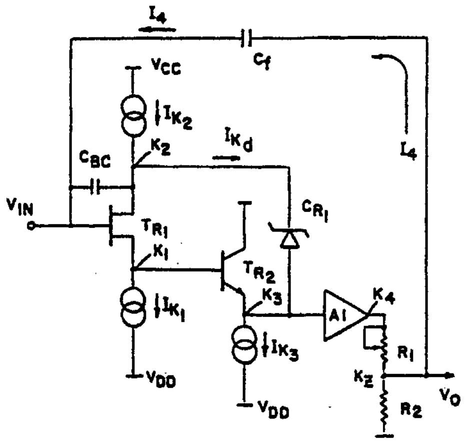

Figure 1 [4]

Circuit for High Impedance Broad Band Probe

C_{BE} is small because the gain K_1 at the emitter is almost 1 for an emitter follower. In order to minimise C_{BC}, the gain K_2 is tied to a value close to K_1 by the Zehner diode CR_1 which (for AC) couples the collector to the emitter. The transistor TR_2 provides a current I_{K3} to make the current I_{K1} equal to the current I_{K2}. C_{BS} is reduced by the mechanical design of the circuit. Due to the current I_4 the capacitance C_f acts as a "negative impedance", i.e. it can be used to compensate the remaining capacitances.

When high frequency signals are to be measured, the internal capacitances of the transistors may cause problems. The input capacitance C_{ip}, of the circuit shown in Figure 1 [4] depends on the base-to-substrate capacitance, C_{BS}, the base-to-emitter capacitance, C_{BE}, and the base-to-collector capacitance, C_{BC}, and is further influenced by the Miller effect, which describes the increase of the base-to-collector capacitance and which gives rise to a multiplicative factor (1 - K), where K is the gain of the transistor:

$$C_{ip} = C_{BS} + C_{BE} + C_{BC}(1 - K) \quad (3)$$

Each capacitance C_{BX} in Equ. 3 represents an effective capacitance, the value of which, due to the Miller effect, is given by the product of the mechanical capacitance and the term $(1 - K_X)$, where K_X is the gain measured at the respective terminal X of the transistor TR_1.

If one only wants to know whether a voltage exceeds a reference value, one may use a differential amplifier (comparator). The main components of these devices are bipolar transistors. They provide a binary output, i.e. their output voltage is at one of two levels depending on which of the two input voltages is higher. The operation of ADCs consists of multiple voltage comparisons, either in parallel or sequential (successive and single/dual slope type).

1.1.3 Josephson Junctions

When two superconductors are coupled through a small tunnelling barrier, special (Josephson) effects occur. In this section we are only concerned with the AC Josephson effect, further applications of the Josephson junctions are discussed in Section 1.2.12.

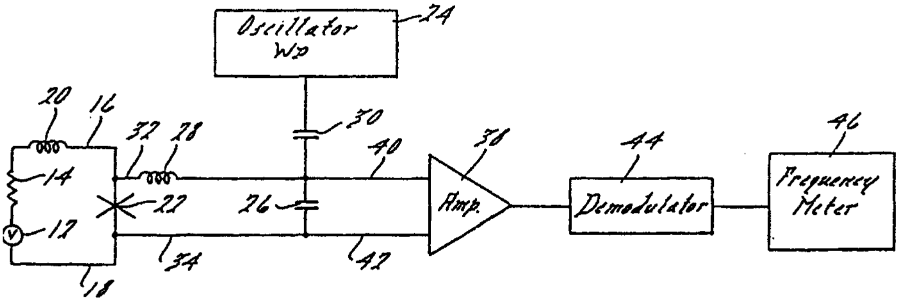

Figure 2 [5]

Superconducting Circuit Means

Superconducting leads (16, 18) couple a voltage source (12) with an internal resistance (14) to the Josephson junction (22). The Josephson junction is chosen such that its critical current $i_e = \Phi_0/L$ is about 10^{-5} A, where L is the magnitude of the inductance (20) of the superconducting leads. Capacitor (26) and inductance (28) form a resonance circuit whose resonance frequency is matched to the frequency f_{osc} of the RF oscillator (24). Junction (22) mixes the frequencies f and f_{osc} to provide two sidebands $f_{osc} \pm f$ and acts as parametric amplifier. After demodulation f is applied to a frequency meter. With this circuit a measurement of $4 \cdot 10^{-16}$ V with a S/N of 10 has been achieved with a source resistance of 10^{-10} Ohms at 4.2 °K.

When a current greater than the critical current is driven through a Josephson junction, a DC voltage U appears across that junction. This voltage in turn gives rise to a supercurrent that oscillates with a frequency f:

$$f = \frac{U}{\Phi_o} \tag{4}$$

Φ_o is the magnetic flux quantum associated with a Cooper pair, its value is $2 \cdot 10^{-15}$ Wb (1 Weber = 1 Vs). With the above equation the voltage to be measured can be derived from the observed frequency. A suitable circuit is shown in Fig. 2 [5].

1.1.4 Capacitive Sensors

1.1.4.1 DC Voltage

Capacitive sensors are used to measure DC and AC electric fields and voltages. Their field of application ranges from circuit boards to power lines. A capacitive sensor consists of a conductive surface that, together with the sample surface, forms a capacitor. The relation between voltage, U, capacitance, C, and the charge, Q, stored in a capacitor is:

$$Q = U\,C \tag{5}$$

In the simple case of an idealised parallel plate capacitor (having plates with a surface area a, a plate distance d and a capacitance $C = (\varepsilon_0\, a)/d$) the corresponding equation for the electrical field $|E| = U/d$ reads:

$$Q = \varepsilon_o\,|\vec{E}|\,a \tag{6}$$

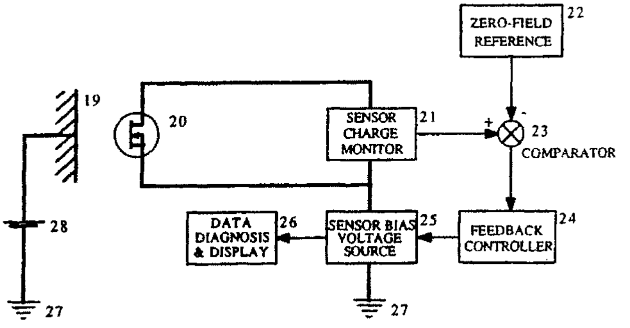

Figure 3 [6]

Potential Analyser

Charge incurred in the sensor (20) by the surface potential of the sample surface (19) alters the impedance of a semiconductor channel within the sensor. The deviation in the charge dependent impedance of the sensor from a calibrated zero-field reference (22) is used by a feedback controller (24) to alter the base potential of the sensor to eliminate the deviation signal. In this state, the surface potential of the sensor matches that of the sample thus forming a zero-field condition, as a result no charge is induced in the sensor. The surface potential difference between the sample and the sensor is then equal to the sensor base voltage, which is directly measured by a voltmeter. Due to the absence of induced charge in the zero-field condition the measurement is independent of the sample/sensor separation (typically < 0.5 mm).

According to Equ. 5 the charge stored on the sensor electrode gives a measure of the voltage. One approach consists in a measurement of this charge. The first instruments used for this purpose were leaf electrometers. Other devices that measure the coulomb force between electrodes are treated in Section 1.1.6. Any other charge measuring method will do as well.

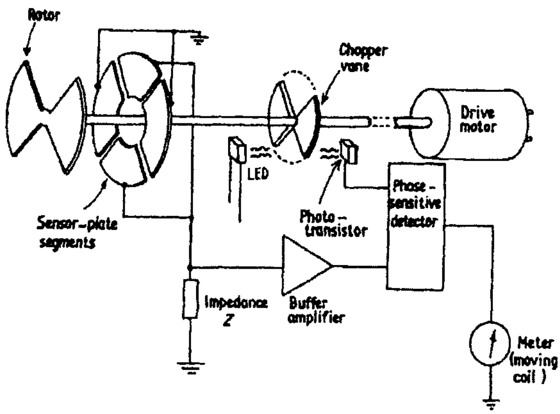

Figure 4 [7]

Schematic Diagram of Field-Mill System with Polarity-Sensing Circuit

A signal representing the rotor position is provided to the phase-sensitive detector. With the phase sensitive detector not only the magnitude but also the polarity of the electric field can be determined.

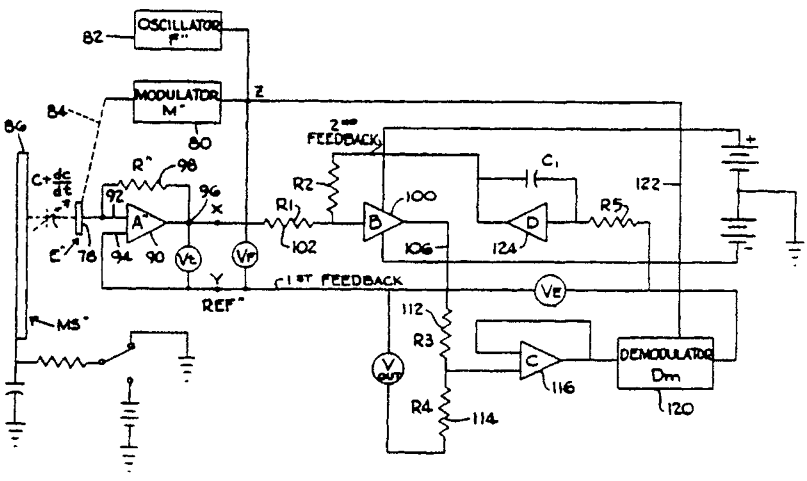

Figure 5 [8]

High Speed DC Non-Contacting Electrostatic Voltage Follower

A vibrating capacitance detector is coupled to a surface containing both wideband electrostatic AC and DC potentials. The detector is connected to the inverting input of detector amplifier (90) the output of which is connected to a high bandwidth amplifier (100). A first feedback path is provided from the high bandwidth amplifier to the non-inverting input of the detector amplifier which provides both, a signal which is equal to and follows the wideband electrostatic AC potentials on the measured surface and a signal at the vibrating capacitance modulation frequency, representative of the DC potential of the measured surface. A second feedback path includes a demodulator (120) and integrator (124, C_1) to monitor the first feedback path and to provide a DC correction signal to the high bandwidth amplifier to null the signal on the first feedback path which is representative of the vibrating capacitance modulation of the DC potential. As a result, the monitored signals on the first feedback path will be driven to follow, and exactly match all wideband AC and DC electrostatic data on the measured surface.

The field-effect probe of Fig. 3 [6] consists of an unshielded semiconductor similar to a MOSFET. Its conductivity depends on the amount of charge induced. It is operated in a bridge arrangement with a negative feedback to balance the charge.

The second approach avoids the difficulty of charge measurements and uses the time derivative of Equ. 5 or 6 to obtain a resulting current. The field mill in Fig. 4 [7] consists of a rotor that periodically shields the sensor-plate segments (stator) such that an alternating electric field is observed. Alternatively a capacitive probe can be vibrated in a direction normal to the sample surface to cause a variation of the capacitance (and of the electric field). According to Equ. 5 the resulting current is proportional to the DC voltage. Additional AC voltages require special signal treatment, see e.g. Fig. 5 [8].

1.1.4.2 AC Voltage

In the case of alternating voltages or fields the time derivatives of Equ. 5 or 6 have to be used. For sinusoidal signals with a frequency f capacitive sensors act as an impedances with a magnitude of $1/(2\pi f\ C)$. Following Maxwell's equations the term dE/dt in the time derivative of Equ. 6 is referred to as "displacement current". In the sensor shown in Fig. 6 [9] the insulation of the conductor acts as dielectric of the capacitor. Fig. 7 [10] shows a sensor with a shielded probe for circuit testing. A measurement with such a probe will only moderately affect the operation of the circuit under test. Since the accuracy of the measurement crucially depends on the knowledge of the distance between the probe and the test point, such a probe is better suitable for the measurement of the timing characteristics of signals than for absolute voltage measurements.

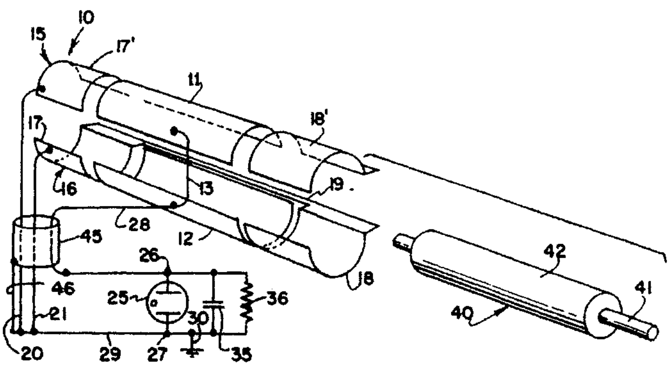

Figure 6 [9]

Capacitive Pickup Device for Pulsating High Voltage Measurements

The device derives a measurable voltage which is a linear function of the magnitude of pulsating high voltage of the order of 15 to 40 kilovolts in an insulated conductor. The pickup device includes a pair of electrically conducting plates (15, 16), the plates being centrally relieved to accommodate the pickup plate members (11, 12) and adapted to be connected to ground to reduce the influence of fringe fields.

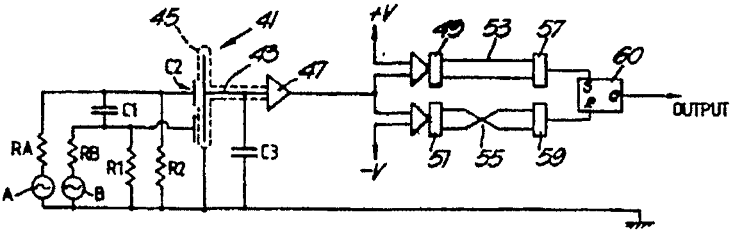

Figure 7 [10]

Electric Circuit Testing Equipment

The shielded probe unit (41) is capacitively coupled to a selected point in the circuit. The signals picked up by the probe unit are conditioned to produce an output signal corresponding only to signals picked up by the unit from the selected point. The conditioning of the signals allows the pick-up of unwanted signals to be tolerated.

1.1.5 Electron Current Analysers

1.1.5.1 Applications

This section deals with sensors used for **integrated** or **printed circuits**. In circuit **testing** the variable of interest usually is not just a voltage but also the timing characteristic of voltage signals at different locations of the circuit. Thus, a high spatial and temporal resolution is required. These requirements are best met by devices that analyse the electron current emitted from the area of interest.

High spatial resolution can be achieved with tunnel microscope like devices, i.e. with a very fine probe-tip at some distance above the surface of the circuit. The probe current depends on the potential difference between sample and probe-tip. For signal tracing in circuits, rapid scans over the whole circuit area have to be performed. Only particle or laser beam devices meet the speed requirements. The potentials are derived from the energy of the emitted secondary electrons. A comparison of electron beam testers (EBT) and electro-optical testers (cf. Section 1.1.7) shows a superior spatial resolution for EBTs (less than 0.1 μm) whereas for the temporal resolution electro-optical devices do better (about 1 ps) [11].

1.1.5.2 Tunnelling and Field Emission

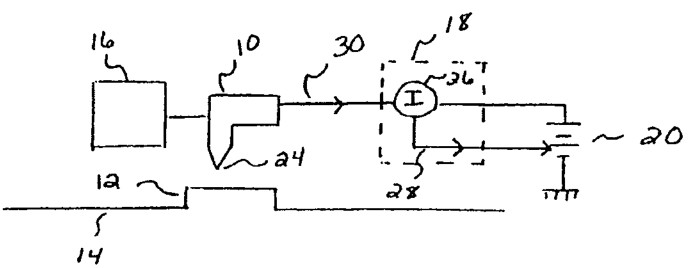

Figure 8 [12]

Use of STM-like System to Measure Node Voltage on Integrated Circuits
A sensing needle (10), which is connected to a supply voltage (20), is positioned directly above a node (12) on an integrated circuit (14). Tunnelling or field emission current is produced in the sensing needle due to the difference in potential between the sensing needle and the node. The system is operated so that the supply voltage is regulated to obtain a fixed current level. Thus, a change in the voltage level to be measured causes an identical change of the supply voltage.

When a probe tip (supplied with a voltage U_2) is held in very close proximity to a conductor (at U_1) a tunnelling current flows, its magnitude depends on the potential difference. For this to occur the size of the probe tip as well as the distance, d, between the tip and the surface have to be as small as fractions of micrometers. For a fixed distance d (i.e. a fixed tunnelling resistance R) the tunnelling current I depends only on the potential difference:

$$I = \frac{(U_2 - U_1)}{R} \tag{7}$$

The system shown in Fig. 8 [12] is suitable for tunnel and field emission currents. The expected sensitivity is better than a millivolt. For the detection of a tunnel current the probe-surface distance is about one nanometer. With such a small distance the system may be operated at atmospheric pressure. When the distance d is increased, field emission becomes the dominant process. Then, however, vacuum is necessary. Equ. 7 still holds - with a different value for R. For a sampling operation the electron emission can be triggered by a pulsed laser or particle beam.

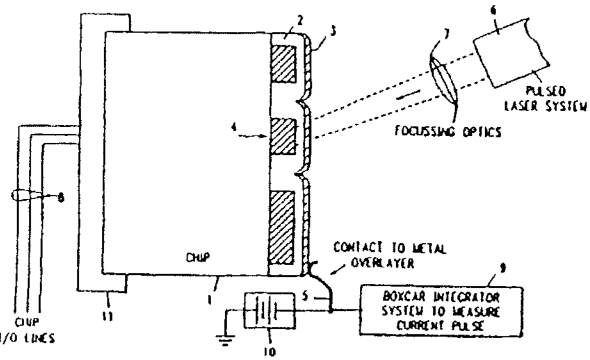

Figure 9 [13]

Noncontact Testing of Integrated Circuits

The metal test pads (4) of an integrated circuit chip-to-test (11) are covered with a photon-transmissive passivation layer (2) susceptible to photon assisted tunnelling which in turn is covered with a thin conductive photon transparent overlayer (3). For the measurement the test pads are accessed through the passivation layer and conductive overlayer by a pulsed laser to provide voltage-modulated photon-assisted electron tunnelling to the conductive overlayer. The conductive overlayer acts as a photoelectron collector for the detector. A chip-to-test which is properly designed for photon assisted tunnelling testing has test sites accessible to laser photons even though passivated.

Laser assisted tunnelling also allows the measurements of voltages in circuits passivated with nonconductive layers up to about 1 μm thick (cf. Fig. 9 [13]). One measures the tunnel current to a transparent conductive overlayer. The passivation layer lowers the threshold energies for electron emission as compared to air. Photon energies of less than 3 eV are sufficient to cause tunnelling when a suitable insulation layer is present.

1.1.5.3 Secondary Electrons

When an object (at potential U_1) is hit by a sufficiently energetic laser or particle beam secondary electrons (with charge e_0) are emitted. Their kinetic energy, T, at an analyser (at potential U_2) is given by:

$$T = T_0 + e_0(U_2 - U_1) \tag{8}$$

The emission energy T_0 depends on the work function of the material from which the electrons are emitted and the traversed thickness before emission. An energy analysis of the secondary electrons yields the potential of the emitting object. Variation of the emission energy and field gradients above the circuit tend to limit the sensitivity. This is no serious handicap if only signal levels of either zero or five volts are measured. Secondary electron energy analysers require vacuum chambers.

In a scanning operation the position of the primary beam and the electron signal must be correlated. Depending on the frequency of the signal either real time sampling (up to about 100 MHZ) or stroboscopic sampling is suitable. Commonly the scanning operation is triggered in a predetermined time relation to the voltage signal of interest.

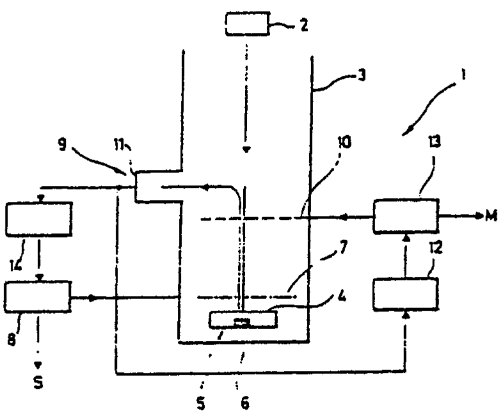

Figure 10 [15]

Contactless Measurement of the Voltage in an Object with an Insulating Surface

A primary electron beam is directed onto the insulating surface (4) of the object (5). The energy of the electrons in the secondary-electron flow generated at the surface of the object is measured and the potential of the conducting zone under the surface is derived. In order to increase the measurement precision, an alternating electrical absorption field is applied above the object and the measurement of the energy of the secondary electrons is carried out in synchronism with the alternating field.

Electron beam testing is the best-established technique. The technology for the required electron beams is known from Scanning Electron Microscopes (SEM). The range of the electron allows voltage measurements on passivated components covered by thin insulation layers. However, when the beam hits insulating materials, the problem of electrostatic charging arises, and when conductors are hit, signals may be induced in the circuit to be tested. These effects can be minimised by keeping the primary and the secondary electron current equal. For most materials this occurs at electron energies between 0.2 and 3 keV [14]. At these energies the penetration depth is less than 5 μm and the electrons do not reach sensitive parts of the circuit underneath. The amount of possibly hazardous Bremsstrahlung decreases with decreasing electron energy. Typical beam currents are in the nA range. EBT devices provide a voltage resolution of several millivolts (cf. Fig. 10 [15]).

Particles other than electrons will produce secondary electrons as well. The use of heavier ions offers some advantages. Due to their much shorter penetration depth more energetic beams have to be used which reduces the sensitivity of the primary beam to electric or magnetic stray fields considerably. Ion beams, however, may cause sputtering on the surface of the circuit. This can be used to remove passivation layers to gain access to conducting leads or to repair faults on the circuit. On the other hand thin conductors may be damaged. Appropriate precautions to prevent a damage of the circuitry are necessary [16]. Ion beams (e.g. α-particles) are less commonly used than electron beams.

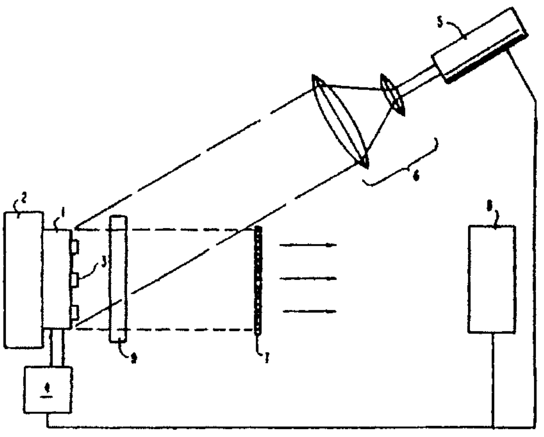

Figure 11 [17]

Full Chip Integrated Circuit Tester

Contactless probing of an integrated circuit is carried out by flooding the surface of the integrated circuit (1) with pulsed ultraviolet laser light, causing photoelectron emission as a function of the potentials at micropoints (3) on the integrated circuit, converting this two-dimensional electron pattern into a corresponding relatively long duration pattern of luminescence by a luminescent target (7), and reviewing the result by video/computer scanning (8). Measurements can be performed either in vacuum or in air, with or without insulating passivation layers present on the chip to monitor instantaneous voltages (logic states and AC switching waveforms) for a full two-dimensional array of micropoints simultaneously.

To generate secondary electrons with a laser beam, photon energies above 4 eV (corresponding to a laser wavelength of less than 300 nm) are necessary. With a sufficiently intense laser it is possible to map the potential distribution over a larger circuit area at once. Such a system is shown in Fig. 11 [17]. With a photo yield of about 10^{-4} electrons per absorbed photon each laser pulse generates about $6 \cdot 10^4$ electrons/μm^2 over a circuit area of 100 mm^2. Appropriate electron optics is required to obtain a distortion-free intensity profile of the secondary electron distribution from which position sensitive electron detectors can recover the two dimensional voltage distribution. Sensitivities of about 1 mV and 5 ps are reported [17].

1.1.6 Electrometers

Charges of an equal sign repel each other, those of an opposite sign attract each other. The Coulomb force F between two charges q_1 and q_2 at a distance r along the direction of a unit vector e is given by:

$$\vec{F} = -\frac{1}{4\pi\varepsilon_0}\frac{q_1 q_2}{r^2}\vec{e} = q_1 \vec{E}_2 = \frac{q_1 U}{r}\vec{e} \qquad (9)$$

E_2 is the electric fields originating at q_2 and U the corresponding voltage, ε_0 is the dielectric constant.

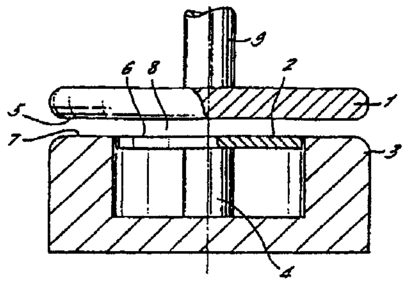

Figure 12 [18]

High Voltage Voltmeter

The high voltage voltmeter, which operates by measuring the electrostatic attraction between two electrodes when a voltage is applied, comprises a high voltage electrode (1), an earth electrode (2) and a guard electrode (3).The attractive force experienced by the earth electrode is measured by a measuring means (4) incorporating e.g. a strain gauge, which gives an electrical signal indicative of the applied voltage. The electrodes are mounted either in vacuum or in a dielectric gas, e.g. sulphur hexafluoride.

When a direct voltage U is applied to a capacitor-like structure, the charge distribution gives rise to a force F between the electrodes. For a parallel plate capacitor ($C=(\varepsilon_0\, a)/d$) it can be easily calculated using Equation 9:

$$\vec{F} = q\vec{E} = \frac{C\,U}{2}\vec{E} = \frac{\varepsilon_0\, a}{2}\frac{U^2}{d^2}\vec{e} \qquad (10)$$

where a is the area of one plate and d the distance between the plates. In the Kelvin type electrometers the force is measured with a balance. In the device shown in Fig. 12 [18] a strain gauge is used to measure the force. A voltage of 100 kV gives rise to a force of 3.5 Newtons (d = 10 mm, electrode diameter = 100 mm). Fig. 13 [19] shows a device similar to the gold-leaf electroscope where the force is not measured directly but where the deflection is converted into an optical signal.

More recently microelectromechanical (MEM) components have been employed in electrometers. The device shown in Fig. 14 [20] comprises a 28 microns thick and 2000 microns long cantilever which forms part of a MEM resonator. For a potential difference between 0 and 40 V a (nonlinear) variation of the resonance frequency from 14.5 to 11.5 kHz is observed with this device.

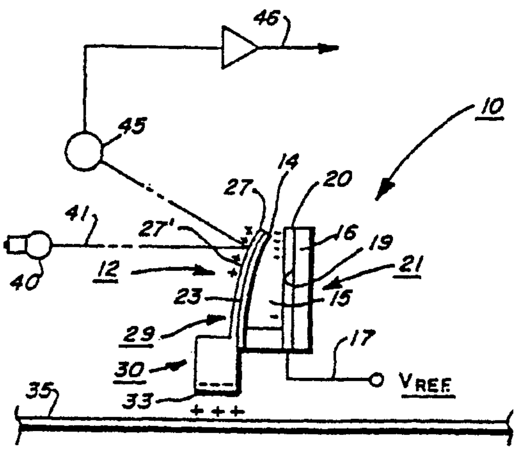

Figure 13 [19]

Electrostatic Voltmeter

An electrostatic voltmeter (10) comprises a microdeflector probe (12) for measuring the charge on a surface (35). The probe comprises a flexible finger (14) cantilevered on a base (16) which is electrically biased to a predetermined potential V_{ref}. A sensing electrode (27) on the finger has a portion (33) which is positioned adjacent to the surface, whereby a charge representative of the charge on the surface is induced on the sensing electrode. The potential difference between the finger and the base causes the finger to deflect. This deflection is converted to a signal representing the charge on the surface by directing a beam (41) of light on the finger and detecting the reflected beam.

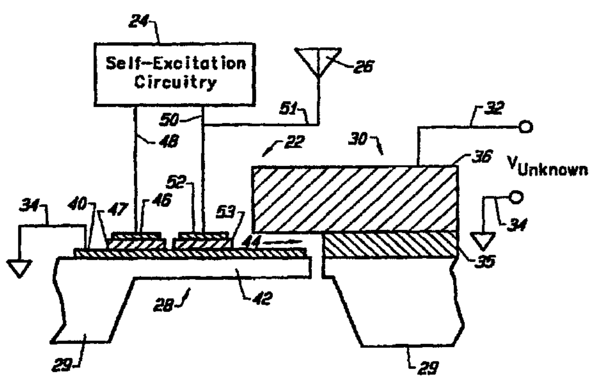

Figure 14 [20]

Microelectromechanical-Based Power Meter

The MEM resonator comprises a cantilever (28) and an associated plate (30). A variable frequency signal from a self-excitation circuitry (24) is applied to an electrode (52) which together with a piezoelectric film (53) and a ground plate (40) forms a drive transducer. A corresponding feedback transducer (46, 47, 50) controls the self-excited oscillation of the cantilever. An electric field across the gap (44) between the cantilever and the associated plate deflects the cantilever and thereby changes its resonance frequency. Output device (26) provides an output representative of the frequency shift. For measurements of line-to-line voltages between powerlines, the cantilever ground plate (40) is connected to a powerline and a conducting plate (36) of the associated plate to an electrode plate located close to the powerline.

Atomic force microscopes or scanning force microscopes (SFM) are used for high accuracy and high spatial resolution DC voltage measurements on integrated circuits. Since SFMs are less sensible to surface conditions than scanning tunnel microscopes (STM), no special preparation of the surface is required. The force on the conducting SFM tip close to a conducting surface is (in analogy to Equ. 10) proportional to the square of the potential difference. A potential difference $U = U_{DC} + U_{\omega} \sin \omega t$ causes a vibration of the tip with an amplitude A:

$$A \sim U_{DC}^2 + 2\,U_{DC}\,U_{\omega} \sin \omega t + \frac{U_{\omega}^2}{2}(1 - \cos 2\omega t) \qquad (11)$$

For the measurement the tip is biased with an AC voltage having a frequency ω such that the tip will vibrate at the frequency 2ω. If there is a vibration at the frequency ω, it is due to a DC voltage The amplitude of this vibration is proportional to the product of the DC and AC voltages and can be varied by applying a DC bias voltage to the tip. The bias voltage at which the vibration at the frequency ω stops, corresponds to the DC voltage to be determined. An instrument of this type is shown in Fig. 15 [21].

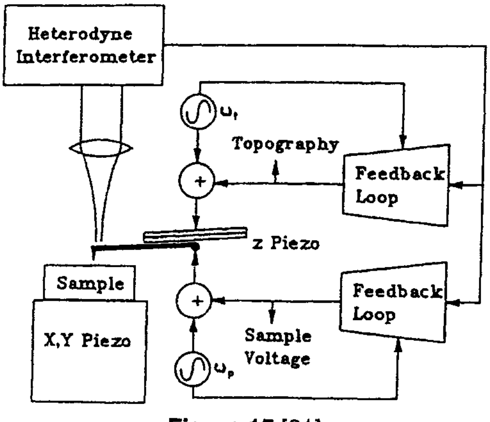

Figure 15 [21]

Potentiometric SFM

Tip vibration is sensed by a heterodyne interferometer and the signal passed to a lock-in amplifier. The lock-in output is a measure of the amplitude of vibration of the tip at ω_p and hence of the DC potential between tip and specimen. The lock-in output is fed back to the tip to obtain zero amplitude of oscillation at ω_p, at which point the DC tip voltage is equal to the voltage on the specimen directly below the tip.

1.1.7 Electro-Optical Sensors

1.1.7.1 Electro-Optical Phenomena

This section covers sensors whose optical properties change in response to electric fields. The sensors currently used are based on one of the following effects:
- the linear electro-optic effect - Pockels cells
- the quadratic electro-optic effect - Kerr cells
- change of optical transmissivity due to excitonic electroabsorption - multiple quantum well devices (MQW)
- change of optical transmissivity due to variations of the alignment of liquid crystals (LC), the Franz-Keldysh effect or electrochromism.

Electric fields give rise to linear birefringence in some materials. This phenomenon is called the electro-optic effect. Linear birefringence of a material causes different components of polarised light to travel at different speeds. Field measurements with Kerr and Pockels cells consist of the detection of the resulting phase shift between the different components and the corresponding change of polarisation. Measurements of the changes in optical absorption or transmissivity are easier to perform. The field of application of related sensors is, however, rather restricted.

The Kerr effect is observed in liquids of polar molecules; the Pockels effect in some non-centro-symmetric crystals. In Kerr cells a phase shift is induced between the components with a polarisation parallel and perpendicular to the electric field, thus, the electric field has to be perpendicular to the direction of propagation of the light. In Pockels cells the electric field can be parallel or perpendicular to the direction of propagation of the light. Due to the tensor character of the Pockels effect, the phase shifts depend on the direction of the light and the orientation of the polarisation vector with respect to the crystal axes. Their linear response to the electric field makes Pockels cells more suitable for lower fields as compared to Kerr cells. The relatively large phase shifts can be observed with simple analysers, so that usually sophisticated interferometers are not required.

1.1.7.2 Pockels Cells

In general the tensor of the Pockels effects has 18 non-zero coefficients. In some highly symmetric crystals only three are non-zero, in uniaxial crystals they are different whereas in cubic crystals they are identical. $Bi_{12}SiO_{20}$ (BSO), $Bi_{12}GeO_{20}$ (BGO) and $Bi_4Ge_3O_{12}$ are not birefringent in the absence of a field, $NH_4H_2PO_4$ (ADP), KH_2PO_4 (KDP), $LiNbO_3$, $LiTaO_3$ and quartz exhibit natural birefringence. The relation between the electrical field strength E and the phase shift δ is given by:

$$\delta = \frac{2\pi}{\lambda} \ell \, n_0^3 \, r \, E \tag{12}$$

where λ is the wavelength of the incident light (e.g. 1 µm), n_0 the index of refraction of the Pockels crystal (1.5 for KDP), r its electro-optic coefficient ($r \sim 25 \cdot 10^{-12}$ m/V for KDP [1]) and ℓ the length of the cell (e.g. 10 mm). With these parameters an electric field of $3 \cdot 10^5$ V/m causes a phase shift of $\pi/2$. The measuring system consists of: a laser light source, a polariser (to polarise the light at an angle of -45° with respect to the crystallographic axis of the crystal), the crystal and an analyser at an angle θ with respect to the axis.
A $\lambda/4$ plate somewhere between the polariser and analyser provides an additional phase shift of $\pi/2$.

The intensity I of the light leaving the analyser is given by [24]:

$$I = \frac{I_0}{2}\,(1 + \sin 2\theta \cdot \sin \delta) \qquad (13)$$

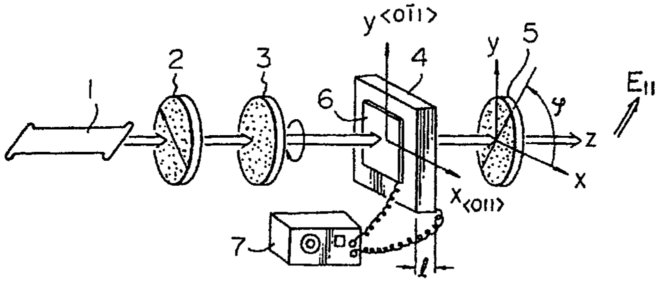

Figure 16 [22]

Pockels Cell Voltage and Electric Field Measuring Device

The device includes a polariser (2), a quarter-wave plate (3), an electro-optic crystal (4) consisting of a material having an optical rotatory power, and an analyser (5). The angle of orientation φ of the analyser, relative to the optical axis of the crystal, is set to the product of θ and ℓ, where θ represents the optical rotatory power of the crystal near the centre of the temperature range at the installation environment and ℓ represents the thickness of the crystal. The specified relation between φ and θ·ℓ maximises the temperature stability of the device by ensuring that the sensitivity of the device is substantially independent of temperature.

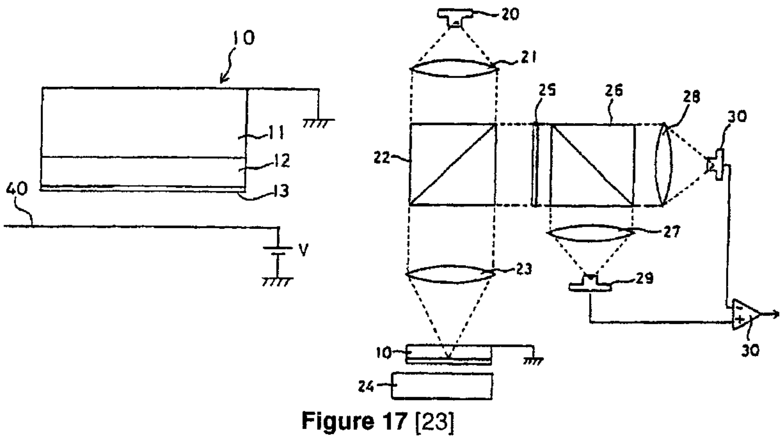

Figure 17 [23]

Potential Sensor Using an Electro-Optical Crystal

The monolithic sensor (10) consists of a high-resistance (>10^5 ohms cm) compound semiconductor (12) which is grown on a low-resistance (<10^{-1} ohms cm) compound semiconductor (11) and covered by a reflecting dielectric film (13). The lattice constants and the thermal expansion coefficient of the semiconductors (11, 12) are similar. Their large band gaps allow the use of light of a short wavelength such that a high sensitivity can be achieved. Linearly polarized light from the laser diode (20) is directed onto the sensor, whose anisotropy depends on the potential applied to the object of measurement (24). The reflected light is deflected by the half-mirror (22) through half-wave plate (25) to the beam splitter (28) from where it is directed into light receiving elements (29, 30).

With an angle θ of +45° or -45° (the orientation of the analyser being perpendicular or parallel to the polariser) one obtains the maximum intensity variation. The sensor is mounted between two electrodes and is suited to measure one component of the electric field, cf. Figure 16 [22]. Figure 17 [23] shows a probe for integrated circuits with a Pockels cell: the probe structure (left) and the apparatus (right).

An ellipsoidal crystal Pockels sensor which is traversed by three light beams with appropriate directions of propagation and polarisations is suitable to detect all three field components [24]. For such a detector the crystallographic symmetry of the sensing element can be either uniaxial 622, 422 or $\bar{4}2m$, or cubic $\bar{4}3m$ or 23. The three perpendicular axes of the ellipsoid are directed along the three orthogonal crystallographic axes of the highest crystal symmetry. In each measurement channel a light beam from a monochromatic light source is polarised along a respective crystallographic direction, reflected at the opposite end of the crystal, analysed and detected. The spherical shape of the sensor minimises the distortion of the electric field. If multimode polarisation conserving fibres are used, polariser and analyser can be at a remote position. The reflection of the beam at one end of the sensor doubles the effective length of the sensor and leads to the cancellation of some of the distortions.

Pockels cells are commonly employed for a wide range of applications, from probes for integrated circuits to high voltage measurements. They can be used for frequencies up to above one GHz. Because of their thermal sensitivity, temperature compensation may be necessary.

1.1.7.3 Kerr Cells

Kerr cells have long been employed for measurements of high voltages and high voltage pulses. Polar liquids like benzene, water, acetone, chlorobenzene and nitrobenzene are commonly used in these cells. The phase difference d between light polarised parallel and perpendicular to the electric field E is:

$$\delta = 2 \pi \ell b E^2 \tag{14}$$

where b is the (temperature dependent) Kerr constant (e.g. $b \approx 10^{-12}$ m V^{-2} for nitrobenzene [1]), ℓ the length of the cell (e.g. 50 mm). An electric field of $3 \cdot 10^6$ V/m causes a phase shift of about π. An experimental set-up is shown in Fig. 18 [25]. A laser beam is polarised at -45°with respect to the electric field, passes the Kerr cell and an analyser at 90° with respect to the polariser. The intensity at the output of the crossed polariser/analyser as a function of the phase shift and the maximum intensity I_o is:

$$I = I_0 \sin^2 \frac{\delta}{2} \tag{15}$$

Typical applications of Kerr cells cover electrical fields in the range 10^5 to 10^7 V/m, the frequency response is linear up to about 100 MHZ [26]. Many materials used for Kerr cells also exhibit the Cotton-Mouton effect (cf. Section 1.2.9).

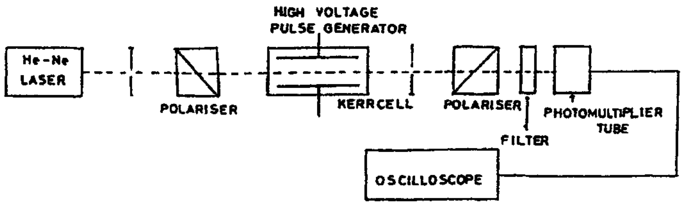

Figure 18 [25]

Arrangement with a Kerr Cell

1.1.7.4 Multiple Quantum Wells

A more recent electro-optic sensor is based on the change of the optical transmittivity of a "semi-insulating" multiple quantum well (MQW) structure for photons, cf. Fig. 19 [27]. It comprises a semiconductor material with $\rho > 10^6$ ohm cm. For photons with an energy corresponding to the energy of excitonic absorption, this material has a fixed transmittivity (T_1) in a given bias field. An additional field leads to a broadening of the absorption peak and therefore results in a change in transmittivity (from T_1 to T_2).

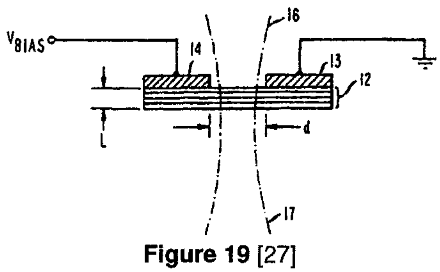

Figure 19 [27]

Electrooptic Apparatus for the Measurement of Ultrashort Electrical Signals

Coplanar striplines (13, 14) are fabricated on the MQW structure (12). When an electrical signal is applied to the striplines, a perturbed field ($E_{bias} + E_{signal}$) is generated and leads to a broadening of the excitonic absorption peak. The modulation of the transmitted photon beam images the applied electrical field E_{signal}.

1.1.7.5 Other Absorption Effects

Several effects lead to field dependent changes of the optical transmissivity of certain materials. Most of these effects occur only in a narrow field range where they show a strong field dependence. Therefore they are often employed for binary sensors (comparators) to detect whether a voltage exceeds a certain threshold. Liquid crystals are the most common devices of this type.

Nematic liquid crystals show several electro-optic effects. In the nematic phase the molecules are still arranged in (already broken) layers. The field dependent deformation of aligned phases (DAP effect) is employed for most analogue field measurements. It causes a decrease in transmissivity proportional to the applied field. For a 10 μm thick cell this occurs between 1.5 and 5 volts [1]. The response time is in the order of several microseconds. Figure 20 [28] shows an application of a liquid crystal cell for voltage measurements.

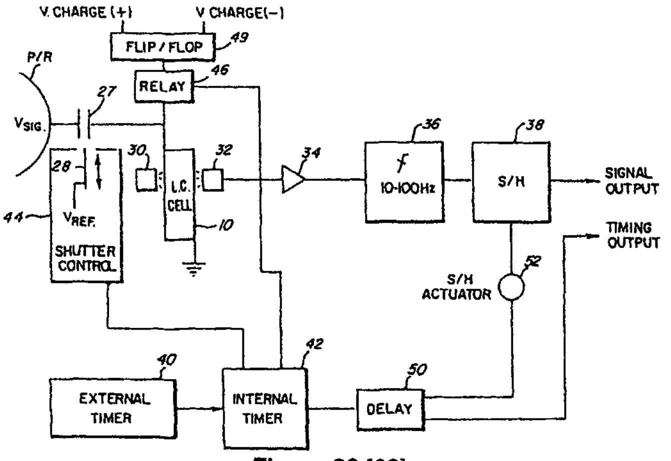

Figure 20 [28]

Liquid Crystal Voltmeter

The device comprises a liquid crystal cell (10) electrically connected to a charged surface and having a light transmissivity varying with applied voltage. Light from a light source (30) is directed through the liquid crystal cell to a light detector (32) which detects changes in the intensity of light. A saturation level biasing voltage is periodically applied to the liquid crystal cell to set the cell to a reference level to clear the cell of transient polarization effects.

The Franz-Keldysh effect causes in certain semiconductors a field dependent shift of the optical absorption band edge to lower energies. Fields of about 1 kV/mm lead to a measurable decrease of the transmissivity for light with an energy less than the band gap of the semiconductor. For CdS and ZnS absorption occurs at wavelengths of 500 and 300 nm respectively. Figure 21 [29] shows a device based on this effect.

Electrochromic materials change colour when a DC potential is applied. This change in light absorption is due to a change of oxidation state of the material (thus electrochromic materials strictly speaking are not contactless sensors because they require an electric connection). Solids like WO_3 or aqueous mixtures of potassium tungstate are electrochromic. A list of other suitable materials is given in [30]. For voltage measurements μm thin films or cells of these materials are mounted between two electrodes. They change colour at voltages close to one volt and it takes about a second (the time scale of redox reactions) for the colour to change. The life time of such a sensor is limited to several hundred colour changes.

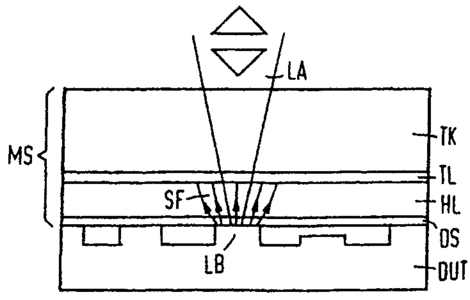

Figure 21 [29]

Method for Optically Measuring Electrical Potentials

A laser probe beam (LA) is directed onto a point (LB) at which the potential is to be measured. The measuring sensor (MS) has carrier crystal (TK) which is transparent for the laser beam (LA) and which carries a transparent conductive layer (TL) and a mirrored dielectric semiconductor (HL), the light absorption characteristic of which is varied in dependence on the stray electrical field from the electrical potential at the point (LB).

1.1.8 Piezoelectric and Electrostrictive Materials

1.1.8.1 Measuring the Deformation

Piezoelectric crystals become polarized when they are deformed, and a charge and an associated electric field build up. This behaviour is called the piezoelectric effect. The reverse piezoelectric effect causes a piezoelectric crystal to deform when exposed to an electric field. Depending on whether the electric field and the deformation are parallel or mutually perpendicular, one speaks of a longitudinal and a transverse effect. The relative deformation, $\Delta L/L$, is a linear function of the applied electric field, E, and the piezoelectric coefficient, d, for the respective crystal orientation:

$$\frac{\Delta L}{L} = d\,E \tag{16}$$

For piezoelectric ceramics (PZT) d is about $0.5 \cdot 10^{-9}$ m/V [31].

A more recent approach to field measurements employs electrostriction instead of the inverse piezoelectric effect. An applied electric field, E, induces a strain in electrostrictive ceramics which causes a deformation, $\Delta L/L$. The deformation is proportional to the square of the field strength and to an effective electrostrictive coefficient, M:

$$\frac{\Delta L}{L} = M\,E^2 \tag{17}$$

For Ba : PZT the value of M is about 10^{-16} $(m/V)^2$ [32].

A simple sensor with these materials consists of a first piezoelectric or electrostrictive material to which the voltage to be measured is applied and which transmits the resulting mechanical waves to a second piezoelectric crystal which reconverts them into a voltage, cf. Figure 22 [33]. In this reference it is suggested to use as first material an electrostrictive material in order to prevent ageing and the risk of depolarisation of the material in high electric fields and also to reduce the size of the sensor.

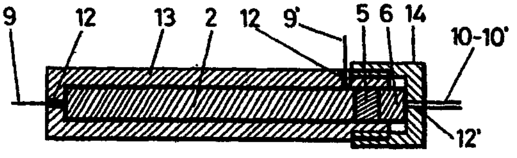

Figure 22 [33]

Voltage Transformer Based on Mechanical Waves

The primary voltage is applied through two electrodes (9, 9') to a first piezoelectric or electrostricive material (2) acting as transmitter. The transmitter is coupled via a dielectric body (5) to the second piezoelectric material (6) acting as receiver and providing the output voltage on two electrodes (10, 10'). The housing consists of a tube (13) with a cover (14) to adjust the pressure on the sensor elements.

Various other techniques can be employed for electric field measurements with piezoelectric or electrostrictive materials. The most common way is to bond an optical fibre to the material. The change of the length of the fibre causes a phase shift in the transmitted light that can be measured with an interferometer. The phase shift depends on ΔL, the wavelength of the light, λ, the refraction index of the fibre, n, and a factor, f, that accounts for the coupling between the sensor and the fibre:

$$\delta = \frac{2\pi}{\lambda} n f \Delta L \qquad (18)$$

Since for the measurement of magnetostriction similar methods are employed, reference is also made to Section 1.2.10.

1.1.8.2 Piezoelectric Crystals with Optical Fibres

This type of sensor consists of a piezoelectric crystal with an optical fibre bonded to it. To measure e.g. a voltage in a gas-insulated power appliance, the sensor is positioned somewhere between the conductor and the housing and the orientation of the crystal is chosen such that it senses the electric field associated with the voltage between conductor and housing. The phase shift induced by an electric field of 100 V/m can be derived from Equs. 16 and 18 to about 0.004 radians for a 1 cm sensor and a 1 µm laser.

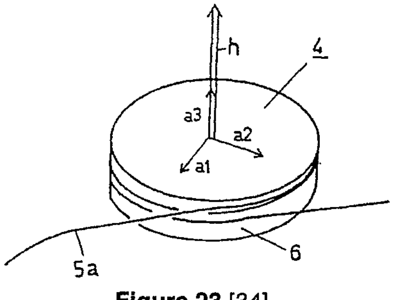

Figure 23 [34]

Optical-fibre Sensor

The sensor for measuring a particular directional component of an electrical field comprises a piezoelectric body (4) and a glass fibre (5a) which is rigidly connected to the piezoelectric body in a given length section. A crystal class and a crystallographic orientation of the piezoelectric body is selected such that only the directional component of the electrical field which is parallel to a given body axis (h) of the piezoelectric body causes a change in a length of the glass fibre by means of an inverse piezoelectric effect. The change in length is measured interferometrically.

Simple polariser/analyser arrangements will not suffice to determine phase shifts of this magnitude accurately. Usually interferometers of the Mach-Zehnder, Fabry-Perot or two-mode [31] type are used. In the Mach-Zehnder arrangement coherent light from a laser is sent through two single-mode fibres where the first one is bonded to the piezoelectric crystal and the second one serves as reference. In a two-mode interferometer one needs only one dual-mode fibre. The two modes undergo different phase shifts. An additional modulator (e.g. a piezoelectric crystal) serves to adjust the working point, i.e. to set the phase shift in the absence of a field (to e.g. $\pi/2$).

With the homodyne detection technique one compensates the phase shift due to the electric field and the result is obtained from the magnitude of the compensating variable. In Mach-Zehnder interferometers the compensation can be done either on the reference or the measurement path, in the two-mode interferometer it is done in the measurement path. Because of the temperature dependence of the length variation, measuring and compensating elements should be at a similar temperature.

The choice of the crystal depends on the application, e.g. whether one wants to employ the parallel or the transverse effect. Fig. 23 [34] shows a disk-shaped sensor. To increase the observed phase shift one simply has to wind the fibre a couple of extra times around the sensor. Though this is true for all sensors, it is more obvious for disk-shaped ones. Tables about crystal classes suitable for different sensor geometries are given in [34]. For the disk-shapes, polyvenylidenfluorid (PVDF), piezoelectric ceramics Lithiumniobat and quartz are appropriate.

A special class of crystals, like, e.g. GaAs, allows the simultaneous measurement of all three components of the electric field [35]. For some of these crystals the sensitivities differ according to the orientation.

1.1.8.3 Piezoelectric Electroacoustic Sensors

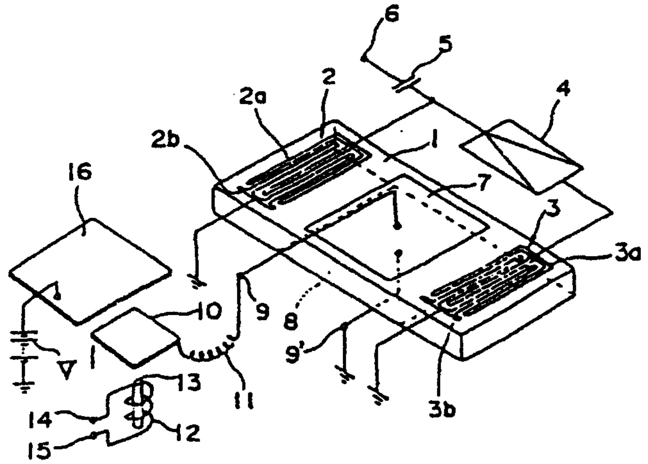

Figure 24 [36]

Electrostatic Voltage Sensor

The sensor includes a surface acoustic wave oscillator with a surface acoustic wave propagating medium (1) and transmitting and receiving transducers (2,3) coupled to the medium. A voltage collection member (10) vibrated with a constant frequency faces the charging plate (16) to be measured. The oscillating signal is applied to the electrode (7) and thereby causes a variation of the surface acoustic wave delay. Voltage is measured through the resulting variation of the oscillation frequency which is obtained at the terminal (6).

Piezoelectric electroacoustic sensors transform an electric field into a change of the resonance frequency of an oscillator. Such an oscillator comprises a transmitter and a receiver mounted spaced apart on a piezoelectric plate and connected by a feedback line. Any length variation, $\Delta L/L$, of the piezoelectric material (e.g. $MgNbTiZrPbO_3$ or $LiNbO_3$), which acts as delay means for surface acoustic waves, leads to a frequency variation, $\Delta f/f$. A device based on surface acoustic waves (SAW) is shown in Fig. 24 [36].

To avoid problems that arise when a piezoelectric element is exposed to a DC field for a longer time (creep phenomenon), the DC voltage is modulated before being applied to the sensor. The circuitry to evaluate the frequency changes from the frequency modulated resonance signal may incorporate means to compensate for temperature drift. Over a voltage range from -1 kV to +1 kV a linear response of about 1V/kV has been observed [36].

A more recent approach is based on Lamb waves that propagate within the sensor plate. For this purpose transmitter and receiver electrodes have counter-plate earth electrodes on the reverse side of the sensor plate. Fig. 25 [37] shows an example of the response of this type of sensor at different resonance frequencies.

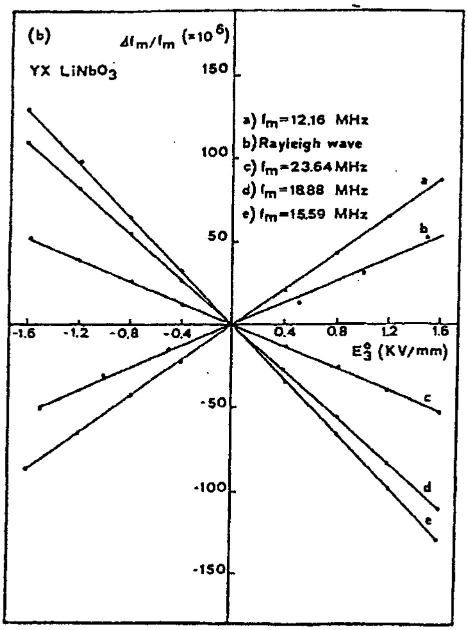

Figure 25 [37]

Fractional frequency changes as a function of the applied electric field for a selected number of Lamb modes and for the Rayleigh (surface) wave propagating in YX $LiNbO_3$ plates.

1.1.8.4 Electrostrictive Sensors

The quadratic field dependence of the electrostrictive effect allows the amplification and frequency shifting of the signal to be measured when a DC and one or more AC fields [32], [38] are superimposed. When the electrical field $E = E_{DC} + E_\omega \cos \omega t + E_\Omega \cos \Omega t$ is squared, a DC term and frequency mixed terms with frequencies Ω, ω, $\omega \pm \Omega$, 2Ω and 2ω arise and cause length variations at these frequencies, e.g.

$$\left(\frac{\Delta L}{L}\right)_\omega = 2\, M\, E_{DC}\, E_\omega \cos \omega\, t \tag{19}$$

Measurements of low frequency, Ω, fields with piezoelectric materials suffer from a noise spectrum with a $1/f$ characteristic. In order avoid this noise one applies a high frequency electric field, E_ω, and measures the phase shift at $\omega \pm \Omega$. Figure 26 [32] shows the strain on the crystal at the frequencies $\omega \pm \Omega$ as a function of the carrier amplitude E_ω. The other application is the measurement of weak fields. According to Equation 19 the phase shift can be amplified by a strong DC or AC bias field.

With an optical fiber attached to a 150 mm crystal, a 1 μm laser and fields of 10^4 V/m and 100 V/m a phase shift of about $3 \cdot 10^{-4}$ radians can be expected. The analysis of the phase shift is done with interferometers as for piezoelectric crystals.

In an investigation [38] of two materials that exhibit the electrostrictive effect, barium-doped lead zirconate titanate (Ba :PZT) and a lead magnesium niobate/lead titanate(PMN)-based ferroelectric relaxor, a (frequency dependent) resolution of 1nV/√Hz for 15 cm of fiber has been observed with PMN.

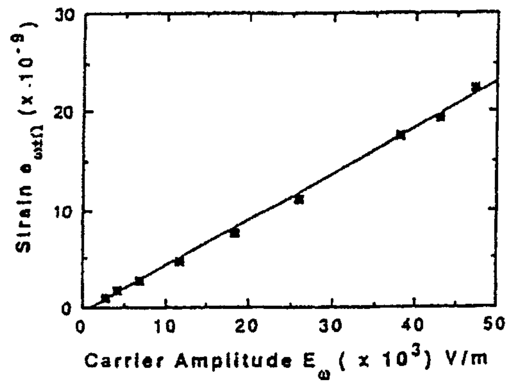

Figure 26 [32]

Dependency of the strain $e_{\omega\pm\Omega}$ on the dither amplitude E_ω for $E_\Omega = 1000$ V/m

1.2 CURRENT SENSORS

1.2.1 Principles

The most fundamental way to measure an electrical current is based on its very definition, i.e. the movement of charge carriers. One "simply" counts the number of charge carriers per unit time. This method is used for currents of charged particle beams (an application not covered by this book), e.g. with a Faraday cup. In most applications, however, one is concerned with much higher currents in conductors, e.g. wires, where one wants to measure currents without interrupting them.

In the same way as voltage measurements can be performed as current measurements, current measurements can be performed as voltage measurements. Ohm's law gives the relation between the current flowing through a resistor (of known resistance) and the resulting voltage drop. This method is mainly used for high currents (Sect. 1.2.3) and in computerised measuring systems with ADCs.

The oldest method to measure direct current exploits the Lorentz force, i.e. the force acting on charged particles in a magnetic field (Section 1.2.6). Electric currents give rise to magnetic fields on their own such that most magnetic field sensors can be used as current sensors. The sensors described in Sections 1.2.7 to Section 1.2.13 respond to the magnetic field, i.e. to different field related phenomena. Hall elements (Section 1.2.7) and semiconductor magnetoresistances (Section 1.2.8) sense the Lorentz force. With magnetooptical and magnetostrictive sensors changes of optical properties or of the dimension of the sensors are observed (Sections 1.2.9 and 1.2.10). Magnetic resonance probes (Section 1.2.11) respond to the field dependent energy splitting of electron or nuclear energy levels. SQUIDS (Section 1.2.12) sense the magnetic flux. Section 1.2.13 covers various other magnetic field sensors like ferromagnetic sensors that are magnetised by magnetic fields and where this magnetisation leads to different observable effects. Alternating magnetic fields due to alternating currents cause variations of the magnetic flux. Inductive sensors, e.g. coils with or without magnetic cores, are described in Section 1.2.14.

The use of SI units leads to a minor inconvenience when dealing with magnetic fields. Magnetic fields are represented by the field vector H, its dimension is A/m. Some equations, however, are expressed in terms of the magnetic flux density B, given in Tesla, $1\ \mathrm{T} = 1\ \mathrm{V\ s\ m^{-2}}$ (the conversion to Gaussian CGS units is as follows: $1\ \mathrm{A/m} = 4\pi\cdot 10^{-3}$ Oe and $1\ \mathrm{T} = 10^4$ G). Whereas in the Gaussian CGS system B and H are identical in vacuum, in the SI system they are related through the vacuum magnetic permeability μ_o ($\mu_o = 4\pi\cdot 10^{-7}$ Vs/Am):

$$\vec{B} = \mu_o \vec{H} \tag{20}$$

Because of the identity of B and H in vacuum in the Gaussian CGS system, also B is frequently referred to as magnetic field. For magnetic field responsive current sensors the external magnetic field due to the current to be measured is the primary input. Therefore all magnetic flux densities cited in this text refer, unless explicitly otherwise stated, to the vacuum magnetic flux density, which is related to the magnetic field through equation 20.

The relation between an electric current I and the resulting magnetic field is given by Maxwell's equations. The line integral of the magnetic field H along a path s that encloses a conductor carrying a current I is:

$$\oint \vec{H}\, d\vec{s} = I \tag{21}$$

The strength of the magnetic field at a distance r from a conductor is:

$$H = \frac{I}{2\pi r} \tag{22}$$

Cf. page 150

Inside a coil with n windings per length ℓ that carry a current I, the magnetic field is given by:

$$H = \frac{n}{\ell} I \tag{23}$$

When a magnetic material is placed in a magnetic field H, it becomes magnetised with a magnetisation M:

$$M = (\mu - 1)\, H = \chi\, H \tag{24}$$

where $\mu = (M + H)/H$ is the magnetic permeability and $\chi = \mu - 1$ the magnetic susceptibility. Ferromagnetic materials have high susceptibilities χ (e.g. Fe $\approx 10^4$). χ is much smaller for paramagnetic ($\chi > 0$) and ($\chi < 0$) diamagnetic substances. Susceptibility and the permeability of ferromagnetic materials depend on both the field strength and previous magnetisation (hysteresis). The relation between M and H is linear only at lower magnetic fields, at higher field strengths M saturates. Because of this most current sensors that use ferromagnetic cores are operated as zero field detectors, i.e. as current comparators. A feedback circuit provides a compensating current to cancel the magnetic field.

When a ferromagnetic substance is exposed to a magnetic field H, the resulting magnetic flux density B_m inside the material exceeds B_o, the value in the vacuum. This is due to the magnetisation of the substance. The enhancement corresponds to the permeability μ:

$$\vec{B}_m = \mu_o (\vec{H} + \vec{M}) = \mu_o\, \mu\, \vec{H} = \mu\, \vec{B}_o \tag{25}$$

Another important quantity in this context is the magnetic flux, Φ. The variation of the magnetic flux is mainly used in the context of induction (Section 1.2.14). The flux is defined as the integral of the magnetic flux density B over a surface S, e.g. the area enclosed by the winding of a coil:

$$\Phi = \int_S \vec{B}\, d\vec{a} \tag{26}$$

The unit for the flux is Weber (Wb), 1 Wb = 1 Vs.

In various applications a sensor is placed in a gap of an annular magnetic core that surrounds a current carrying conductor to enhance the magnetic field at the sensor. Because of the flux conservation the magnetic field in the gap, H_g, of an annular core (magnetic permeability μ, radius r, gap width d) is:

$$H_g = \frac{\mu\, I}{d\,(\mu - 1) + 2\pi\, r} \tag{27}$$

Cf. page 150

There are two asymptotic cases, in both cases H_g is greater than the field in the absence of the magnetic core (cf. Equation 22):

- $d << r/\mu$, the second term in the denominator of Equation 27 dominates and the field in the gap is amplified by a factor μ;
- $d\,\mu >> r$ (for highly permeable iron cores μ is > 1000), the first term in the denominator dominates and the magnetic field is amplified by a factor $2\pi \cdot r/d$.

One advantage of magnetic cores arises from the fact that external magnetic fields cancel in the integral around the closed loop (cf. Equation 21). When weak currents are to be measured, either form of amplification or shielding is mandatory to eliminate the influence of the earth's magnetic field (about 20 A/m). At strong magnetic fields, however, saturation of the core occurs.

1.2.2 Charge Integration

To perform a simple current measurement by charge integration, one can monitor the slope of the voltage across a capacitor while it is charged or discharged by the current to be measured. In the circuit shown in Figure 27 [39] the collected charge is used to control a transistor.

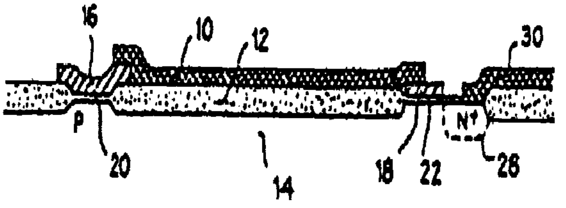

Figure 27 [39]

Measuring Device for very Low Currents

Electric charges, the flux of which constitues the current to be measured, are collected on the conducting electrode (10) which is connected to the insulateed gate (16) of a FET and a conducting layer (18). The charges on the electrode are compensated by the injection of charge carriers from the semiconducting zone (14) through a thin insulating layer (22). This is done by accelerating the charge carriers in the semiconducting zone (14) such that they can pass the insulating layer (22). The frequency and the duration of the accelerating periods depends on the current through the FET.

1.2.3 Shunts

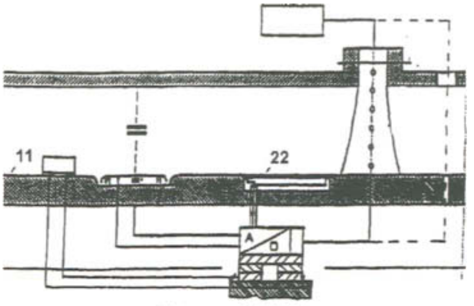

Figure 28 [40]

Current Transformer

For the measurement of transient, rapidly varying short-circuit currents, etc., in particular in gas-insulated, metal-encapsulated switch-gear a current transformer is mounted in at least one power line (11). The current transformer has a length of thin-walled tubing (22) which conducts transient short-circuit currents occurring in the power line (11) and whose external diameter is equal to the external diameter of the power line (11). The voltage drop along a line at the surface of the length of tubing (22) is used as a measure of the transient short-circuit current.

It is a well-known technique to determine the (high) current that flows through a conductor from a measurement of the voltage drop across a resistor (current shunt). However, at high frequencies the thickness of the shunt is crucial: its resistance corresponds to the ohmic resistance only if its thickness is equal to or less than the penetration depth (skin effect). In the example shown in Fig. 28 [40], the current on a power line is determined from the voltage drop across a thin tubing.

1.2.4 Calorimetric Methods

These methods are in fact based on power measurements. We have included them in the section dealing with current sensors because they require a current to flow. When an electric current, I, passes through a conductor with resistance R some power, P, is dissipated:

$$P = R\,I^2 = \frac{U^2}{R} \tag{28}$$

The resulting temperature rise of the conductor can be measured with any suitable temperature sensor and be used to determine either U or I. The response time of corresponding sensors crucially depends on the size and the thermal properties of the conductor and the coupling of the conductor to the sensor. An application in which the sensor immediatly responds to temperature changes of the conductor is the measurement of infrared radiation from power transmission lines, cf. Figure 29 [41].

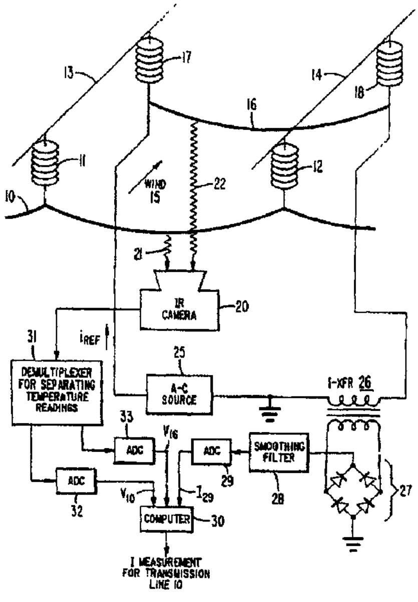

Figure 29 [41]

Measurement of the Current Flow in an Electric Power Transmission Line
The construction of a high-tension line with counterwound helical conductors around a supporting core minimizes the surrounding magnetic field and thus reduces the skin resistance of the line as compared to its bulk resistance . Infrared radiation from the I^2R losses in the line is thus linearized and the current in the line can be directly measured by sensing the infrared radiation from the line using using infrared detectors. Radiation from a hot line (10) and a reference line (16) is compared. A current of about 1000 (100) A leads to a heating of 45 (0.45) °C of a 220 V line at 35 °C exposed to a cooling cross wind in the example given. The cited resolution of the infrared cameras is 0.05 - 0.5 °C.

In another approach a sensing material which exhibits an observable temperature dependent effect is either placed next to the current carrying conductor or used as conductor. If the observable effect occurs at a given threshold temperature, a tapered conductor (i.e. a conductor with a smoothly varying resistance along the current path) can be used to provide an analog indication over a predetermined current range. If the observable effect is irreversible, the sensor acts as maximum sensor.

In one sensor of this type the sharp melting line of Tempilaq paint on the surface of a tapered resistor provides an analog indication of the maximum power [42]. Thermooptical sensors on the other hand exhibit reversible colour changes. A number of cholesteric liquid crystals for thermooptical sensors are listed in [43]. Figure 30 [44] shows a thermooptical sensor with a tapered resistor. Recently this type of sensors has been incorporated into battery labels to measure a (small) discharge current [45] through a known resistance and to derive the battery voltage in order to assess the charge condition.

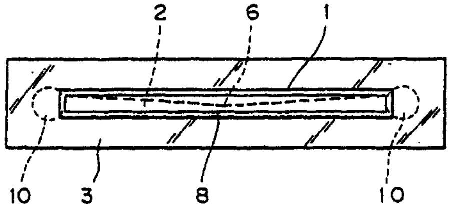

Figure 30 [44]

Voltage Measuring Sheet

The shape of the tapered resistor (2) with a narrow central portion (6) is indicated by the dashed line. A layer (1) of a decolouring agent that loses its colour at about 40 °C is in thermal contact with the conductor and is related to a scale pattern.

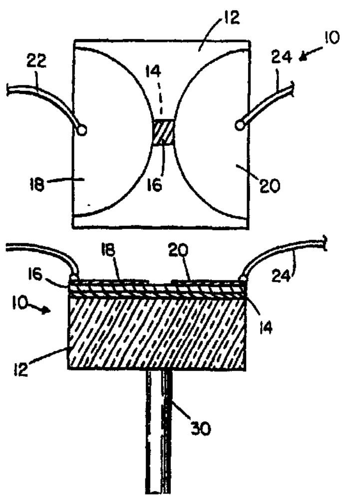

Figure 31 [46]

Thermooptical Current Sensor

The current to be measured is applied (18, 20, 22, 24) to a resistive or semiconducting element (16) to increase the temperature of this element and of the optical resonator (14). The change of the optical property of the resonator is detected through the modulation of the wavelength spectrum of light directed into and reflected from the resonator through the optical fiber (30) abutting the transparent substrate (12).

Optical resonators with temperature dependent optical properties can be used to sense a range of currents. In the device shown in Fig. 31 [46] a current is measured through the modulation of the wavelength spectrum of light by a temperature dependent optical resonance property of the sensing element. This particular sensor has been optimised for a short response time.

1.2.5 Sensing the Energy of the Magnetic Field

A conductive ring that surrounds a current carrying conductor contains a magnetic flux. The energy stored in a ring with volume V (i.e. cross section a times circumference) is:

$$W = \frac{1}{2} B\, H\, V = \mu\, \mu_o \frac{a^2\, I^2}{V} \tag{29}$$

When such a ring is interrupted by an air gap, the stored energy (given by a similar expression as above) leads to an attractive force between the pole pieces of the gap. Different methods can be employed to measure this force, which depends on the current I, e.g. a measurement of the strain on the ring, with a strain gauge or measurement of the movement of the pole piece with optical means [47]. With a variant of the first method current pulses between 1000 and 250 000 A have been measured in a resistive spot welding machine [48].

1.2.6 Measuring the Lorentz Force on the Conductor

Charge carriers that move at an angle, α, with respect to magnetic field lines are deflected. The deflecting force acts in a direction perpendicular to the plane formed by the directions of the particle's velocity and the magnetic field. The force F on a charge q that moves with a velocity v in a magnetic field with a flux density B is given by the vector product:

$$\vec{F} = q\,(\vec{v} \times \vec{B}) \tag{30}$$

There is some confusion in the terminology: German texts refer to F as the Lorentz force, in other texts the electric field dependent (q E) term often is included in the expression for the Lorentz force. Rewriting Equation 30 in terms of the current I passing through a conductor of a given length ℓ, one obtains the force that acts on that conductor due to the magnetic flux density B:

$$\vec{F} = I\,(\,\vec{\ell} \times \vec{B}\,) \tag{31}$$

Since electric currents give rise to magnetic fields, a force acts between two parallel current carrying conductorss:

- an attractive force, if the currents flow in the same direction, and
- a repulsive force, if they flow in opposite directions.

The strength of the force F (in N) on each conductor can be derived from Equations 22 and 31:

$$F = \mu_o \frac{I_1 I_2 \ell}{2 \pi r} = 2 \times 10^{-7} I_1 I_2 \frac{\ell}{r} \tag{32}$$

where I_1 and I_2 (in A) are the respective currents and r (in m) is the distance between the conductors. Different arrangements are used to exploit the Lorentz force on the current carrying conductor for current measurements.

They differ by the source of the magnetic field and how the Lorentz force is measured. Measurements according to Equation 31 rely on a known external magnetic field. When the force between two conductors is measured according to Equation 32 one may either work with one known current (I_1 or I_2) or feed the same current through both conductors ($I_1 = I_2$). In the later case the force is a quadratic function of the current.

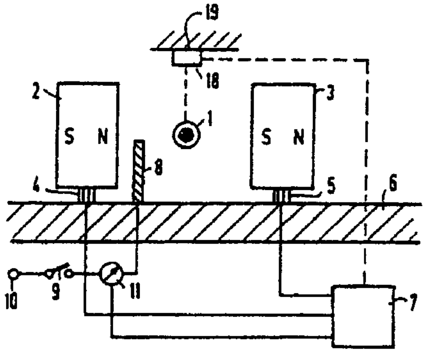

Figure 32 [49]

Measuring Electric Current in Conductor

A high current conductor (1) passes between two magnets (2, 3). The Lorentz force on the magnets is sensed with transducers (4, 5). In an alternative embodiment, the force on the conductor (1) is measured (18). Conductor (8) is used for calibration.

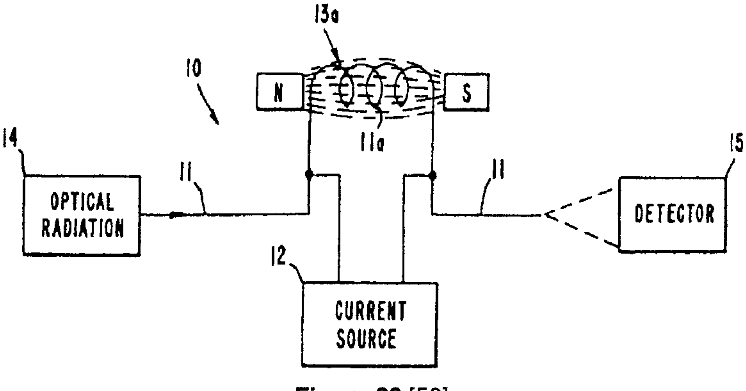

Figure 33 [50]

Fiber Optic Transducer for Measuring Current or Magnetic Field

A multi-mode optical fiber, which serves as the sensor, is composited with a metal capable of conducting electricity. Optical radiation is introduced into the fiber from a source which may be either coherent or incoherent. An electrical current is applied to a portion of the electrically conducting fiber and a magnetic field is applied to the current-carrying fiber. A known value of one permits a determination of the presence or absence of the other through electromotive forces on the metallic conductor in the magnetic field, which induce differential phase shifts (coherent optical radiation input) or losses (incoherent optical radiation input) between the fiber modes. These phase shifts or losses are detected by a suitable detector. For a magnetic flux density of 10^{-1} T good linearity is obtained in the 5 to 2,000 mA current range.

In all these setups the Lorentz force on at least one of the interacting components, i.e. one conductor or the source of the magnetic field, is measured. Various methods to measure the force may be used, e.g. spring loaded meters, piezoelectric sensors, resilient members or stress induced phase shifts in optical fibres.

Moving coil instruments are the best known devices of this type (for moving iron instruments cf. Section 1.2.13.3). They consist of a rotatable coil mounted in the gap of a magnet. Direct current that flows through the coil gives rise to an angular force on the coil. With appropriate springs to bias the coil, a linear relation between current and angular deflection can be obtained.

The related figures illustrate
Fig. 32 [49]: an arrangment with either moving magnets or a moving conductor;
Fig. 33 [50]: a moving conductor with fixed magnets and a fibre sensor;
Fig. 34 [51]: two moving conductors with a piezoelectric transducer.

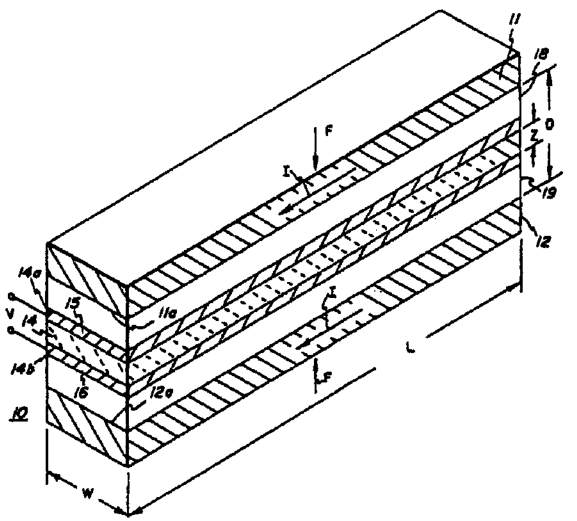

Figure 34 [51]

Current Sensor

A current sensor, integratable with power switching and control circuitry on a common substrate and insulatable from current-carrying conductors, utilizes a piezoelectric element (14) located between a pair of current-carrying conductors (11, 12). The conductors carry a current flowing in the same direction, causing an attractive force there between to act upon the piezoelectric element (14) and generate a voltage proportional to the square of the conductor currents. With a pair of sensors, each in a different portion of a half-bridge circuit, and associated electronics a sensor output proportional to the instantaneous value of the sensed current is obtained.

1.2.7 Hall Elements

The Hall effect describes the action of an external magnetic field with a given flux density, B_z, on a current, I_x, in a conductive plate. The Lorentz force, F_y, acting on the charge carriers moving with a velocity v_x deflects them in the y direction. The magnitude of the resulting electric field, E_y, is such that the electrostatic force on the charge carriers q compensates the Lorentz force:

$$q\,E_y + (-\,q\,v_x\,B_z) = 0 \tag{33}$$

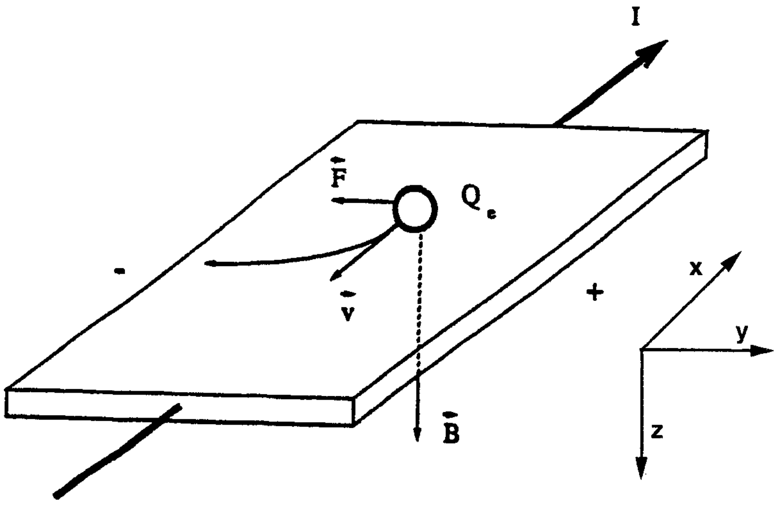

Figure 35 [303]

Hall Effect

The coordinate system has been added in this figure to illustrate the equation above:
Current I_x results from electrons ($q = -|e_o|$) moving with a velocity $v_x = -|v_x|$. A magnetic field $B_z = |B_z|$ gives rise to the Lorentz force $F_y(B_z) = -(-|e_o|)(-|v_x|)|B_z| = -|e_o v_x B_z|$. The resulting electric field $E_y = -|E_y|$ in turn gives rise to a force $F_y(E_y) = (-|e_o|)(-|E_y|) = |e_o E_y|$.

The electric field gives rise to a voltage U_H (Hall voltage) along the y direction. Its magnitude depends on the thickness on the conductor, d, and the Hall coefficient, R_H, of the material:

$$U_H = R_H \frac{I_x B_z}{d} \tag{34}$$

When the charge carriers are electrons, the Hall coefficient is negative, about $-5 \cdot 10^{-11}$ m^3/C for copper and up to -10^{-4} m^3/C for InAs-semiconductors [1].

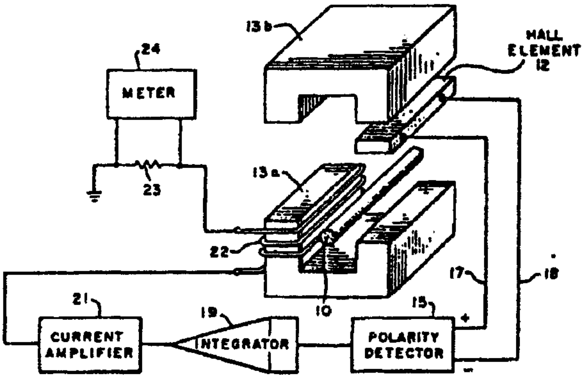

Figure 36 [54]

Sensing System for Measuring a Current
A current flowing through a conductor, is measured by initially passing an energizing magnetic flux through a Hall element (12) to produce a Hall voltage proportional to the sensed current. To eliminate temperature, gain and non-linear effects normally associated with a Hall element, the amplitude of the Hall voltage is effectively ignored and only is polarity is detected (15) and employed to control the operation of an integrator (19) to develop a cancelling current to establish an equal, but opposite cancelling flux in the Hall element. With a zero net flux, the integrator will hold the cancelling current at the level required to cancel the initial energizing flux. Since the cancelling current needed to null the energizing flux will be proportional to that flux, the current may be used to produce (23) a control voltage to represent the measured currrent.

Typical values for the thickness, d, the length, x, and width, y, of Hall elements are: $1 < d < 100$ μm, $0.5 < x,y < 10$ mm. The current, I_x, is chosen such that the resolution is highest but excessive heating of the Hall element is avoided. Usually values below 1 A are used. Solid state, GaAs ion implanted devices achieve a resolution of 1 V/T with $I_x = 5$ mA [52].

When direct currents are to be measured, the offset voltage of the Hall device has to be corrected for. A circuit suitable for this purpose is described in [53]. Two applications of Hall elements are shown in Figs. 36 [54] and 37 [55].

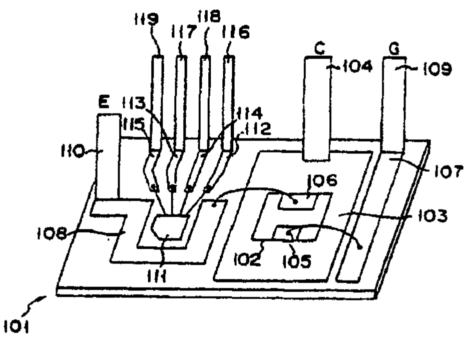

Figure 37 [55]

Composite Semiconductor Device with Overcurrent Detection
An insulating substrate (101) includes a conductive layer (103) on which a power semiconductor element (102) is mounted through its main electrode. The other main electrode of the semiconductor element is connected to one end of a U-shaped conductive layer (108) such that a load current through the semiconductor element also flows through the conductive layer (108) and produces a magnetic field which is detected by a current detector (111) such as a Hall element.

1.2.8 Magnetoresistance Elements

Magnetoresistance is responsible for the change of resistance in metals and semiconductors when they are exposed to magnetic fields. Different materials and arrangements of materials exhibit different magnetoresistance effects. Magnetoresitance is measured by passing a sense current through the magnetoresistive material. Thus far the following effects have been studied, the following brief discussion is based on the references indicated:

- magnetoresitance in semiconductors like InSb, NiSb [56];
- anisotropic magnetoresistance (AMR) in ferromagnetic materials like Permalloy [57];
- giant magnetoristance (GMR) in systems in which the magnetic moments in different layers or clusters change between an antiparallel and a parallel orientation [58];
- giant magnetoresistance (GMR) in epitaxal films [59] (somtetimes also referred to as "colossal magnetoresistance").

For comparitive purposes these effects are best characterised by the ratio $\Delta R/R$ with the corresponding magnetic field range. Two definitions for the ratio $\Delta R/R$ are used concurrently:

$$\begin{aligned} \Delta R/R_H &= (R_{H=0} - R_H)/R_H \\ \Delta R/R_{H=0} &= (R_{H=0} - R_H)/R_{H=0} \end{aligned} \tag{35}$$

where $R_{H=0}$ and R_H are the resistance values in the absence of an external magnetic field or current to be measured and when the maximum field for the respective effect is applied respectively. If $\Delta R/R$ is small, both values are close to each other. Since the measurement of currents usually consists of the determination of the magnitude of the currrent (as compared to no current), we shall refer to $\Delta R/R_{H=0}$ in the following and convert the published values accordingly.

Semiconductor sensors are sensitive to external magnetic fields perpendicular to the direction of the sense current. The field dependence of a semiconductor magnetoristance can be described by:

$$R(B) = R_o + a\,B^2 \tag{36}$$

To obtain a linear relationship between the resistance and the magnetic field one can bias the sensor with an external bias field $H_o >> H_x$, where H_x is the external field to be measured. If the H_x^2 term is negligible, the following linear relationship holds between the resistance R and the flux density B_x:

$$R(B) = (R_o + a\,B_o^2) + 2\,a\,B_o\,B_x \tag{37}$$

In the corresponding reference [56] a linear $\Delta R/R_{H=0}$ response of $\approx \mp 1.1$ % for $\Delta B = \pm 2$ mT corresponding to $\Delta I = \pm 1$ A is reported. Figure 5 of this reference, however, suggests that the unlinearised $\Delta R/R_{H=0}$ value is considerably higher, i.e. because of the above sign convention for $\Delta R/R_{H=0}$ has a more negative value.

The variation of the specific resistivity, ρ, of an anisotropic magnetoristance like a premagnetised Permalloy strip follows a $\cos^2\theta$ dependence, where θ is the angle between the direction of the sense current and the direction of magnetisation of the strip:

$$\Delta\rho = \rho - \rho_\perp = \Delta\rho_{max} \cos \Theta^2 = (\rho_\| - \rho_\perp) \cos \Theta^2 \tag{38}$$

where $\rho_\perp$ and $\rho_\|$ are the specific resistivities for orthogonal and parallel orientation of the directions of the sense current and the magnetisation of the strip, respectively. The strip typically consists of a 20 - 100 nm thin evaporated or sputtered layer of Permalloy which initially is magnetised along the strip parallel to the direction of the sense current. When an external magnetic field is applied in a plane orthogonal to the strip, the direction of magnetisation in the sensor plane is rotated whereby the angle θ increases and the resistance decreases. The variation of the resistance vs. the magnetic field follows a bell shaped curve. Typical value for the saturation field strengths at which the magnetisation aligns with the applied field are between $\approx 10^2$ and 10^5 Am^{-1}. In the cited example [57] a curve with a nonlinear response of $\Delta R/R_{H=0} \approx 2$ % for $\Delta B = \pm 2$ mT ($1.6 \cdot 10^3$ Am^{-1}) is shown. A linearisation of the response over a limited field range can be achieved by arranging highly conductive equipotential strips (barber poles) at 45° with respect to the direction of original magnetisation on the sensor strip.

With zero field measurements, in which a feedback circuit responsive to the voltage drop across the sensor controls a compensation field (current), no linearisation of response of the sensor is required. Suitable bridge arrangements help to reduce the effects of the (considerable) temperature dependence of the magnetoresistance in semiconductors and the AMR in permalloy of about 0.06% $°K^{-1}$ and 0.25% $°K^{-1}$ respectively. One example each of a sensor based on semiconductor magnetoresistance and AMR is shown in Figures 37 [60] and 38 [61].

GMR on the other hand leads to considerably higher $\Delta R/R$ values. So far GMR sensors primarily have been used as magnetic field sensors. They are particuarly useful for applications where a high signal-to-noise ratio is required like in reading heads for magnetic data carriers. Probably because of their still limited $\Delta R/(R \cdot \Delta H)$ resolution, which at room temperatures is not much better than that for AMR sensors, these sensors have not yet been employed on a larger scale for current measurements. Nevertheless some of their properties are summarized below.

The first type of giant magnetoresistances comprises layers or clusters of ferromagnetic materials separated by non-magnetic materials. In the absence of a magnetic field the magnetic moments of neighbouring domains are antiparallel. In this configuration the resistance is highest. Upon application of a magnetic field the relative orientation of the magnetic moments of the different changes until, at a specific saturation field strength, H_S, all are parallel. Resistance is lowest in this configuration. According to a simple model this change in resistance is due to the spin dependence of the electron scattering in the magnetized domains. Spin-dependent scattering on the interfaces between the different materials is also thought to contribute to GMR.

Two commonly used structures for this first type of giant magnetoresistances are the following:

- multilayer structures of up to about 50 ferromagnetic and non-magnetic layers in alternation (like Fe/Cr or Co/Cu). By an appropriate choice of the thickness of the non-magntic layers antiferromagnetic coupling between neighbouring magnetic layers, i.e. their antiparallel orientation in the absence of a field, can be achieved. Typical values for the thickness of the layers which commonly are produced by sputtering are in the order 10^{-9} m. With Co/Cu multilayers a nonlinear response of $\Delta R/R_{H=0} \approx 41$ % has been observed for $\Delta B \approx \pm 1$ T at room temperature [58].
- grannular allloys containing nanometer sized clusters of ferromagnetic material.

The second type of giant magnetoresistances consists of expitaxial, single crystaline La-Ba-Mn or La-Ca-Mn oxide films. They are produced by laser deposition and are about 100 to 200 nm thick. The $\Delta R/R$ ratios of both types of giant magnetoresistances are highly temperature dependent. Because of thermal fluctuations the ratios are generally much higher at temperatures as low as 4.2 °K than at room temperatures. The properties and in particular the temperature dependence of the $\Delta R/R$ value of the second type of giant magnetoresistances can be significantly influenced by annealing, i.e. the particluar annealing conditions. With annealed La-Ca-Mn-O films a nearly isotropic, nonlinear $\Delta R/R_{H=0}$ response of ≈ 93 % has been observed for $\Delta B \approx \pm 6$ T at 260 °K [59].

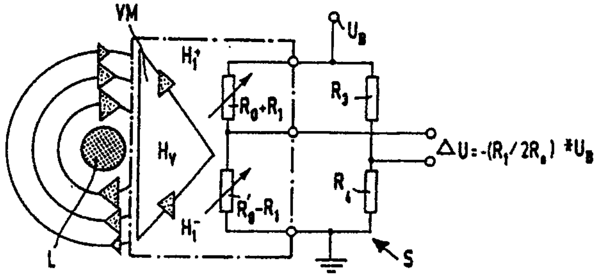

Figure 38 [60]

Test Arrangement for Electronic Circuits

The device to measure currents in bus-like conductors forms part of a small probe head. It comprises a serial arrangement of two biased magnetoresistances that sense one component of the magnetic field, H_I, only. When a bias field H_V parallel to H_I is applied, the magnetoresistances sense the sum and the difference of H_V and H_I respectively.

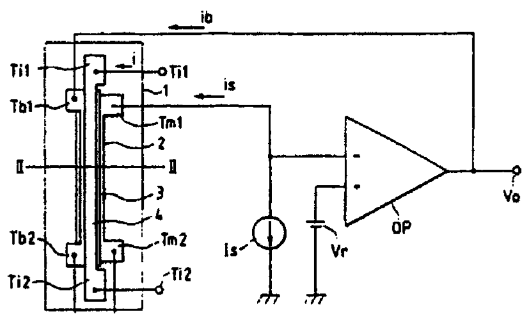

Figure 39 [61]

Current Sensor System

The sensing portion is composed of a ferromagnetic magnetoresistance element (2), a bias conductor (3) and a current conductor (4) all arranged on an insulating substrate (1). When a current flows through the conductor (4) the resistance of the magnetoresistance element changes accordingly. An amplifier (OP) provides a feedback current to cancel the change of resistance and an output signal (V_o).

1.2.9 Magnetooptical Sensors

1.2.9.1 The Magnetooptical Effect

There are three effects that change the optical properties of materials in magnetic fields:

- the Faraday effect, i.e. the rotation of the polarisation of linearly polarised light
- the Cotton-Mouton effect, i.e. field induced birefringence
- the magnetooptic Kerr effect, i.e. the magnetisation dependent rotation of the polarisation of polarised light on reflection from magnetised materials

Nowadays mainly the Faraday effect is employed for current sensing. For the sake of completeness we will briefly describe the Cotton-Mouton effect as well. The magnetooptic Kerr effect, which is exploited rather for the determination of the magnetisation of ferrites than for the measurement of currents, will not be covered here.

Liquids with anisotropic molecules exhibit the Cotton-Mouton effect, i.e. birefringence in a transverse magnetic field. The phase difference induced between the light components, parallel and perpendicular to the magnetic field, is proportional to the square of the applied magnetic field. For a light wave that traverses a Cotton-Mouton cell of a given length length, ℓ, exposed to a magnetic field, H, the phase shift, δ, between the respective components amounts to:

$$\delta = 2 \pi \ell C H^2 \tag{39}$$

C is the (temperature dependent) Cotton-Mouton constant ($C \approx 4 \cdot 10^{-14}$ m/A^2 for nitrobenzene [1]). A magnetic field of $\approx 4 \cdot 10^7$ A/m along a 10 mm cell causes a phase shift of about π. To measure the phase shift polariser/analyser arrangements like for Kerr cells (cf. Section 1.1.7.3) can be used. Most liquids that exhibit the Cotton-Mouton effect also exhibit the Kerr effect.

1.2.9.2 Faraday Sensors

Optically active materials (e.g. sugar solutions) rotate the polarisation of linearly polarised light. Under the influence of a magnetic field inactive isotropic materials rotate the polarisation of a light beam parallel to the field vector. The fact that only the field component parallel to the direction of propagation is rotated is expressed by the scalar vector product:

$$\alpha = V \int \vec{H} \, d\vec{\ell} \tag{40}$$

where α is the angle of rotation (in degrees), H the magnetic field vector, $d\ell$ represents the path of the light in the sensor, V is the Verdet constant of the sensor material.

Two types of Faraday sensors are employed: optical (silicate) fibres and bulk material. In both cases light from a (laser) source is polarised before being sent through the sensor. To determine the magnetic field (current), one measures the rotation angle at the output of the sensor. Suitable materials for sensors preserve the polarisation of the light beam and do not rotate the plane of polarisation in the absence of a magnetic field. High signals can be obtained with fibres wound several times around the current carrying conductor. In order to preserve the polarisation, single mode fibres are used.

Some bulk materials, however, have a much higher Verdet constant than fibres. Typical values for fibre sensors are $V = 2.5 \cdot 10^{-4}$ deg/A [62] and $\ell = 1$ m. Thus a magnetic field of $\approx 2 \cdot 10^5$ A/m is required to observe a phase shift of about $\pi/4$.

If the sensor forms one loop around a conductor that carries a current I, Equation 21 can be used to express the integral in Equation 40 in terms of I:

$$\alpha = V I \tag{41}$$

For a sensor placed inside a coil with N_C turns Equation 23 yields:

$$\alpha = V N_C I \tag{42}$$

Light that is reflected back at the end of the sensor and passes the sensor in the opposite direction undergoes a second Faraday rotation. This feature is referred to as "nonreciprocal" and can be derived from Equation 40. Most distortions are reciprocal and thus cancel when reflection is used.

We will shortly mention the various sources of error and the different methods employed to measure the Faraday rotation, a comprehensive treatment with the relevant references can be found in [62]. Impurities, bends and stress induce linear birefringence, torsion leads to circular birefringence. Vibration is another source of error. By twisting a bent fibre one can compensate the effects of linear birefringence through circular birefringence. The value of the Verdet constant varies with temperature and frequency, e.g. for optical fibres $(dV/dT) \approx V \cdot 10^{-4}$ °K^{-1}. Paramagnetic and ferromagnetic bulk materials with a much higher Verdet constant than silica fibres exhibit a more pronounced temperature dependence. Diamagnetic glasses, however, offer higher Verdet constants at a reasonable temperature stability [62].

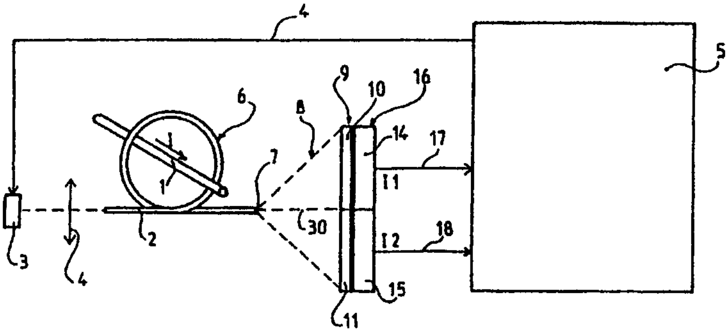

Figure 40 [63]

Device for Measuring Current with an Optical Fibre

The device measures, using the Faraday effect in a monomode optical fibre (2), the intensity (I) of the current in a conductor (1). It comprises a polariser-splitter (9) constituted, for example, by two coplanar half-discs (10,11) of polarising sheet, the preferred polarisation orientations of which make the desired angle 90° or 45°. Photodiodes (14, 15) constituted by a two-quadrant photodetector (16) in the form of a disc of the same diameter as that (9) formed by the polariser-splitter, are arranged downstream of the polariser-splitter. The phodiodes are connected to an electronic unit (5).

The simplest way to measure the Faraday rotation consists in an arrangement with crossed or aligned polariser and analyser at the input and the output of the sensor. The intensities observed have a $\sin^2\alpha$ or $\cos^2\alpha$ dependence. The difference signal from two analysers at ± 45° relative to the polariser follows a sin (2α) dependence. To achieve higher resolutions various interferometer designs can be used, e.g. Sagnac, Fabry Perot. With two light beams of different frequencies heterodyning techniques can be employed. This transforms the angle of the Faraday rotation into a phase modulation of a high frequency signal. Two applications of the Faraday effect are given in Figs. 40 [63] and 41 [64]. With the device shown in Figure 41 currents between 10 and 150 mA have been detected with a linear response in the frequency range from 25 to 125 Hz.

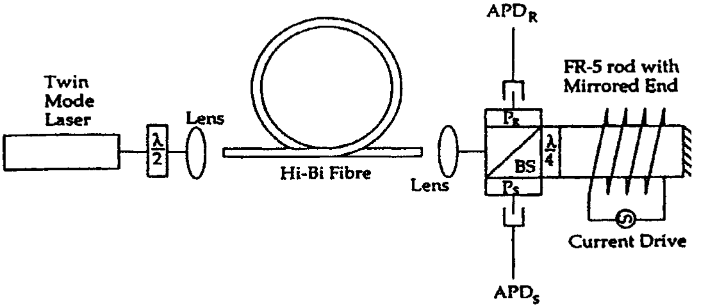

Figure 41 [64]

Current Sensing Using Faraday Rotation and a Common Path Optical Fiber Heterodyne Interferometer

Orthogonally polarised outputs of a two-frequency laser source are rotated with a λ/2 plate to the eigenaxis of a birefringent monomode fibre and transferred to the bulk sensor which is made of glass with a Verdet constant of ≈ $5 \cdot 10^{-3}$ deg/A. Part of the beam is directed into a reference detector (APD_R). The other part passes a λ/4 plate. The two emerging (orthogonal) circularly polarised modes pass the sensor, are reflected back, and pass the sensor again. They are detected after a back-transformation into linearly polarised states (through the λ/4 plate) at the signal detector (APD_S). The angle of the Faraday rotation is recovered electronically.

1.2.10 Magnetostrictive Sensors

1.2.10.1 Magnetostriction

Ferromagnetic materials are elastically deformed when exposed to magnetic fields:

$$\frac{\Delta L}{L} = g\,H \qquad (43)$$

For Ni g is in the order of 10^{-9} m/A [65]. For Fe, Co, Ni the deformation reaches values of $\Delta L/L \approx 10^{-5}$ at saturation. With magnetostrictive current sensors the current is derived from this deformation (length variation). All methods for length measurements with an appropriate resolution can be used. As with piezoelectric sensors (cf. Section 1.1.8) different approaches are employed to measure this deformation:

- through the change of resistance of resistive leads attached to the magnetostrictive material;
- through phase shifts (due to the length variation of the fibre or to strain induced birefringence in the fibre) in a light beam transmitted through an optical fibre bonded to the crystal;
- through the delay of a surface acoustic waves.

An example for the first approach in which, to increase the signal, the conductor has a meander like shape is shown in Fig. 42 [66].

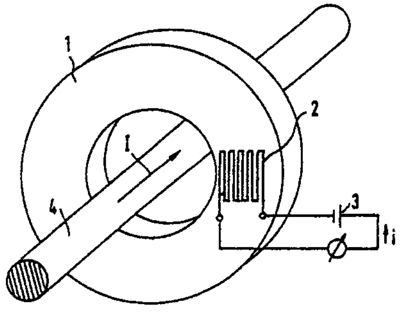

Figure 42 [66]

An annular body (1) which consists of magnetostrictive material surrounds the conductor (4). Conductor tracks (2) made of length dependent resistance are applied on the annular body (1). The resistance of the conductor tracks is a measure of the current (I) through conductor (4).

1.2.10.2 Magnetostrictive Materials with Optical Fibres

Measurements of length variations with optical fibres have been treated in detail in Section 1.1.8.2. Piezoelectric and magnetostrictive sensors with optical fibres look alike. However to avoid distortions due to the Faraday effect (cf. Section 1.2.9.2), the direction of propagation of the light must be perpendicular to the magnetic field vector.

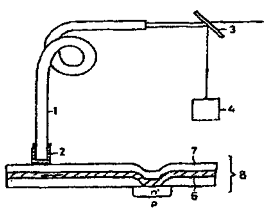

Figure 43 [67]

Measuring Device for Current on Wiring of Intergrated Circuit

When the tip of an optical fiber (1) covering a magnetostrictive material (2) is positioned on the wiring (6) of an integrated circuit (8), the material (2) is strained by a magnetic field generated by a current on the wiring, and thereby a stress is given to the fiber. A laser beam (5) in the fiber is modulated when it is reflected on the end surface and its propagation mode is changed. The beam is reflected by a half mirror (3) and falls on a photodetector (4) which delivers an output corresponding to the change in the propagation mode, and a current can be read from this output.

Certain materials like e.g. silica fibres exhibit the photo-elastic effect, i.e. stress induced birefringence. When such a fibre is wound around a magnetostrictive element, the length variation causes stress such that the magnetic field can be derived from the induced birefringence. With a nickel cylinder on which a monomode silica fibre of length ℓ was wound and through which a polarized light beam (λ = 0.633 μm) was propagated, the change of the state of polarisation Ψ has been measured. With a suitable detector for two polarisation states and an appropriate magnetic bias field ($\approx 5.6 \cdot 10^3$ A/m) a linear response $\Delta\Psi/(\ell \cdot H) \approx 2.2 \cdot 10^{-4}$ rad A^{-1} has been observed for H between 0.2 and 80 A/m [65]. In this field range a 200-mm long sensor would for example have of response of about $4 \cdot 10^{-5}$ rad A^{-1}. In a more qualitative measurement only the change of the propagation mode is observed (Fig. 43 [67]).

1.2.10.3 Magnetostrictive Materials and Surface Acoustic Waves

A surface acoustic wave sensor for current measurements is a resonance circuit, whose resonance frequency depends on the length of a magnetostrictive delay line. It consists of a transmitter and receiver with a feedback loop and a magnetostrictive delay line. Typically the delay line is made of Yttrium-Iron-Garnet (YIG) and Gallium-Gadolinium-Garnet (GGG), its length and thickness are several mm and μm respectively. Since the dependence of the resonance frequency on the magnetic field is linear only for a limited range of magnetic field strengths, a compensation coil is required to limit the field to be sensed to this range. In the arrangement shown in Fig. 44 [68] the sensor is mounted in the gap of a magnetic core with two coils, one for the current to be measured and the other one for a compensating current.

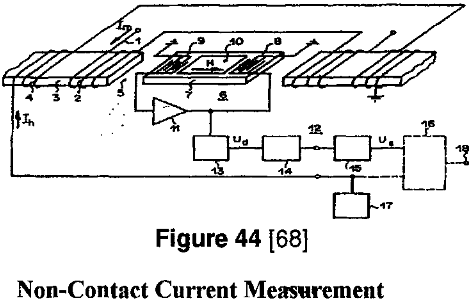

Figure 44 [68]

Non-Contact Current Measurement

1.2.11 Magnetic Resonance

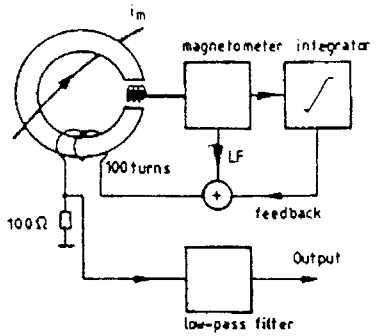

Figure 45 [70]

ESR Current Sensor

The ESR probe is made of $AcTCNQ_2$, a material that is rather cheap and easy to handle. With this sensor a current resolution of about 10 mA $Hz^{-1/2}$ has been achieved.

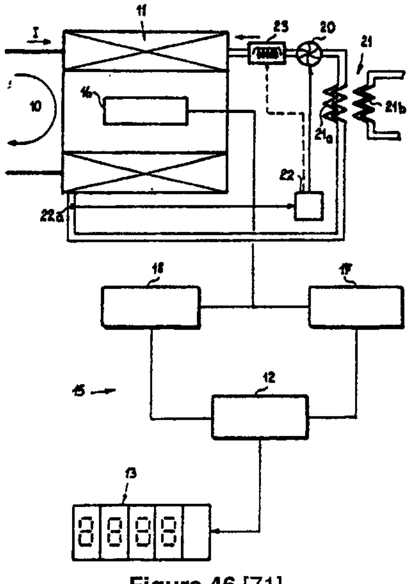

Figure 46 [71]

Device for Measuirng a Direct Current Intensity

A coiled magnet (11) is mounted in series in the circuit (10) wherein the current to be measured circulates, the temperature of the magnet is stabilized and the magnetic field is measured at the centre of the magnet by means of a NMR probe (16).

Magnetic resonance is a well-known technique in material sciences and for chemical analysis (electron spin resonance, ESR, and nuclear magnetic resonance, NMR). When an electron/nucleus is exposed to a magnetic field, its magnetic energy levels split according to the orientation of its magnetic moment (parallel or antiparallel to the magnetic field). An external RF field perpendicular to the magnetic field stimulates transitions between the energy levels. The energy difference ΔE is given by:

$$\Delta E = g \, \mu \, B = h \, f_o \tag{44}$$

For electrons/protons the value for the g factor is about 2/5.58 and μ corresponds to the Bohr magneton, $\mu_B = 9.27 \cdot 10^{-24}$ J/T or the nuclear magneton, $\mu_N = 5.05 \cdot 10^{-27}$ J/T [1], h is the Planck constant, f_o is the Larmor frequency, i.e. the frequency of the precession of the spin. Its value for electrons and protons, f_e and f_p, can be derived from the expression for the energy difference:

$$f_e = 2.8 \; 10^{10} \; Hz/T; \quad f_p = 4.3 \; 10^{7} \; Hz/T \tag{45}$$

In spin resonance magnetometers (current metres) a test probe is exposed to the magnetic field and the field is determined from the Larmor frequency. When the frequency of an inductively coupled RF circuit is swept, absorption is observed at the Larmor frequency. The frequency is in the GHz/100 MHz range for ESR/NMR. In general NMR magnetometers are used for flux densities down to several mT [69]. Modern ESR systems give a resolution down to the nT range. NMR is observed in nuclei with a nonzero nuclear spin (e.g. hydrogen s=1/2) only. To achieve accurate results, both temperature stability and field homogeneity over the whole probe have to be ensured. One example each for an ESR and a NMR current sensor is shown in Figures 45 [70] and 46 [71].

1.2.12 SQUIDS

Superconducting **QU**antum **I**nterference **D**evices (SQUIDS) have been used for the measurement of magnetic fluxes and related quantities since the mid-1960s. SQUIDS consist of a superconducting ring interrupted by one or two Josephson junctions respectively (RF and DC SQUIDS). They act as magnetic flux sensors with a resolution of about 10^{-19} Wb. We will briefly summarize some of their basic properties on the basis of two review articles [72], [73] where further details can be found. We start with RF SQUIDS because they are simpler to understand. Commercially RF SQUIDS were available long before DC SQUIDS. Today, however, because of their higher accuracy (see below) DC SQUIDS are more common. The discovery of high temperature superconductors helped to promote SQUIDS.

When a moving charge is exposed to a magnetic field, its wave function acquires a phase shift. For the wave function to be single valued, the phase shift accumulated over a closed loop must be a multiple of 2π. The pase shift θ acquired by a Cooper pair (two electrons) circulating in a superconducting ring is related to the magnetic flux Φ_i through the hole surrounded by the ring:

$$\theta = 2\pi \frac{2\,e}{h} \Phi_i = 2\pi\, n \tag{46}$$

(h is the Planck constant and e the charge of the electron).As a consequence the magnetic flux through the hole is quantized as well - in units of Φ_o
($\Phi_o = 2\cdot 10^{-15}$ Wb):

$$\Phi_i = n \frac{h}{2e} = n\, \Phi_o \tag{47}$$

The application of an external flux Φ_e causes a supercurrent, i_s, to maintain the flux quantisation. The magnitude of the current is determined by the flux, $i_s \cdot L$ (L is the selfinductance of the ring), required:

$$n\, \Phi_o = \Phi_e + i_s\, L \tag{48}$$

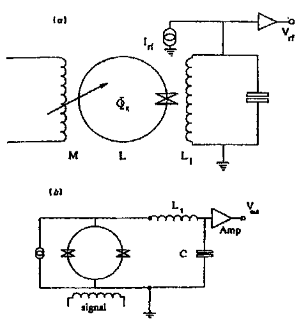

Figure 47 [73]

SQUIDS, the Josephson Effects and Measurement
(a) Schematic diagram of RF SQUID with L-C circuit readout
(b) Schematic diagram of DC SQUID readout system

In a superconducting ring with one Josephson junction (RF SQUID) the situation changes due to the Josephson effect: the junction acts as tunnelling barrier and introduces an additional phase shift $\delta\theta$ in the wave function according to

$$i_s = i_c \sin \delta\theta \tag{49}$$

where i_C is the critical current of the junction. When a modulating RF flux $\Phi_e(t)$

$$\Phi_e(t) = \Phi_{RF} \sin \omega t + \Phi_x \tag{50}$$

is applied (with $\Phi_{RF} < i_c \cdot L$; f is typically about 20 MHz), new features appear. Both, the supercurrent i_s and the enclosed flux Φ_i become multi-valued functions of the external flux Φ_e. For $\beta = (2\pi\ i_c L/\Phi_o) > 1$ the internal flux Φ_i passes through a hysteresis loop.

While this loop is performed, a flux quantum Φ_o is absorbed and consecutively emitted. The necessary energy ($\Phi_o{}^2/2L$) is absorbed from the RF field. This absorption can be detected through a change in the RF voltage U_{RF} at a RF circuit inductively coupled to the SQUID. For $n\ \Phi_o < \Phi_x < (n+1/2)\ \Phi_o$, U_{RF} depends linearly on Φ_x. The dependence is given by:

$$\Delta V_{RF} \sim \omega_{RF} \sqrt{\frac{Q\ L_{RF}}{L}}\ \Delta \Phi_x \tag{51}$$

where Q and L_{RF} are the quality factor and the inductance of the RF circuit.The DC SQUID consists of a superconducting ring with two Josephson junctions that are resistively shunted through resistors (R). The device is biased with a direct current that exceeds the critical current of the junctions. The direct voltage (U) that appears at the junctions leads to an oscillation (frequency f) of the phase shift, θ, introduced at the junction (AC Josephson effect):

$$\frac{d\theta}{dt} = \frac{2\pi V}{\Phi_o} \tag{52}$$

When an external flux is applied, the circulating current and therefore the direct voltage becomes a periodic function of this flux. The modulation depth is $R \cdot \Phi_o/I$ for a flux variation of $\Phi_o/2$.

As SQUIDS act as very accurate flux to voltage converters in a very limited flux range ($\Phi_o/2$) only, they must be operated with some kind of compensation and have to be shielded against external fluxes, cf. Fig. 48 [74].

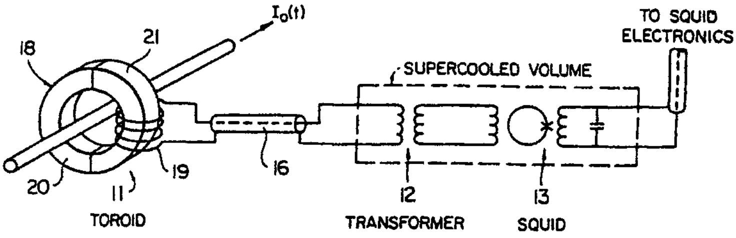

Figure 48 [74]

Method and Apparatus for Measuring Magnetic Fields and Electrical Currents in Biological and Other Systems

The measurement probe is at room temperature from where the signal is transferred into the supercooled housing of the SQUID which also contains the inductive coupling elements. Superconducting impedance matching transformers increase the resolution.

Sensitivities of several 10^{-11} T for magnetic fields (10^{-13} A for currents and 10^{-20} V for DC voltages) have been achieved. The flux resolution is about $10^{-6}\ \Phi_0\ Hz^{-1/2}$ for DC SQUIDS as compared to about $10^{-4}\ \Phi_0\ Hz^{-1/2}$ for RF SQUIDS. The resolution is worse for RF SQUIDS because the absorbed energy has to be bigger than the thermal fluctuations in the order of kT. This leads to an upper limit of about 10 nH for L at T = 10 °K.

The good voltage resolution of SQUIDS results from the fact that the voltage measurement is performed as a current measurement with a small measuring resistance. A circuit with a flux-locked loop and current compensation with a dynamic range from 10^{-13} to 10^{-9} V is described in [75].

1.2.13 Other Magnetic Field Sensors

1.2.13.1 Transistors

Magnetic field responsive transistors operate similarly to Hall elements. They are constructed in a planar configuration and have two collectors that share the emitter current equally. When a magnetic field is applied perpendicular to the emitter/collector plane, the current is deflected by the Lorentz force. As a result the current distribution between the two collectors becomes asymmetric. A field resolution of ≈ 0.1 A/m has been achieved with this kind of device [76].

Figure 49 [77] shows a device where the measurement range can be extended by attenuation or intensification of the magnetic field.

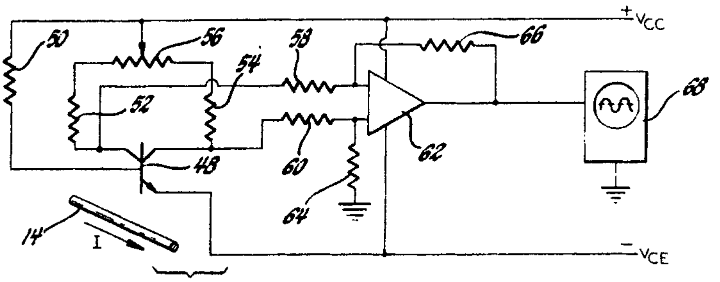

Figure 49 [77]

System for Calibrated High Level Current Measurement

Transistor (48) provides a differential output voltage proportionate to the magnetic field created by the current in the conductor (14). Calibration of the current sensor is effected by the intensifying or shunting the magnetic field to permit measurement of low and high current levels respectively. The field incident on the transistor is intensified by use of a magnetic material to direct the magnetic flux on the transistor to sense low current levels. High current levels are sensed by interposing magnetic material between the transistor and the conductor to provide a shunt path for shunting the magnetic field in a calibrated fashion such that the field at the transistor is maintained within the operational limits of the device.

1.2.13.2 Reeds

Reed switches (two blades of resilient ferromagnetic material, facing each other, sealed in a glass tube) are actuated by magnetic fields. One type opens when there is no field and closes when the field strength exceeds a specified value (e.g. $H = 10^2$ A/m). When such a reed switch is equipped with a compensating coil, it operates as a measuring instrument for (DC) currents. The reed switches whenever the superimposed fields from the current to be measured and the compensating coil exceed a predetermined value (Fig. 50 [78]).

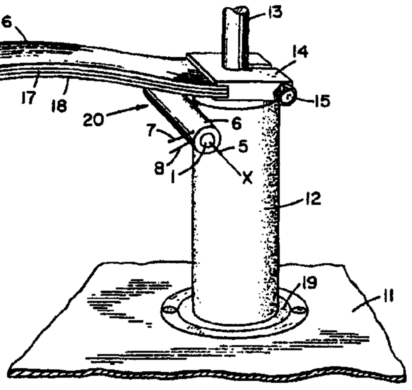

Figure 50 [78]

Current Measuring Apparatus Employing Magnetic Switch

Reed relay (20) consists of a sealed glas tube (1) which contains two reeds and is surrounded by an actuacting coil. To measure the current through the conductors (16, 17, 18), the magnitude of the current through the actuating coil is increased at a constant rate and the instant at which the reed switch changes its state is recorded. The magnitude of the current through the actuating coil when the switch changes its state is a measure of the current through the conductors.

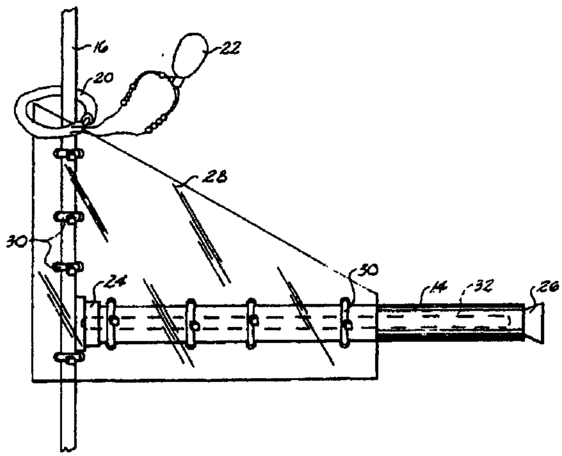

Figure 51 [79]

Lighting Current Detector

The apparatus for measuring the intensity of current produced in an elongated electrical conductive member (16) by a lightning strike includes an elongated strip of magnetic material that is carried within an elongated tubular housing (14). Initially a predetermined electrical signal is recorded along the length of the strip of magnetic material. One end of the magnetic material is positioned closely adjacent the conductive member so that the magnetic field produced by current flowing through the conductive member disturbs a portion of the recorded signal directly proportional to the intensity of the lightning strike.

1.2.13.3 Different Magnetisation Sensors

When ferromagnetic materials are exposed to magnetic fields, their magnetisation changes (cf. Equation 24). Various properties related to the magnetisation change as well. The sensors described here either exploit just the change in magnetisation or respond to related parameters.

Moving iron amperemeters are the oldest type of magnetisation responsive devices. They consist two soft iron plates placed in the field of a fixed coil, one of which is movable and connected to an indicator. The magnetic field from a direct or an alternating current passing through the coil magnetises both plates in the same way. Their mutual repulsion is transformed into a deflection of the indicator. Correction irons, e.g. ferromagnets, mounted close to the moving iron are used to adjust the indication characteristic of such an instrument.

When a premagnetised sensor is exposed to a magnetic field, part of the premagnetisation gets lost. Placed next to a conductor they thus can serve as peak current detectors. The current is derived from the loss of the premagnetisation. Such a device may be a magnetic data carrier where the loss of data is measured (Fig. 51 [79]).

Some magnetic properties of anisotropic magnetic materials change linearly with the applied magnetic field. Magnetic fields move the direction of the saturation magnetisation (e.g. in ferromagnetic magnetoresistances -Section 1.2.8). In the device shown in Figure 52 [80] an AC coil is placed over the probe to sense the change of its (magnetisation dependant) self-inductance L.

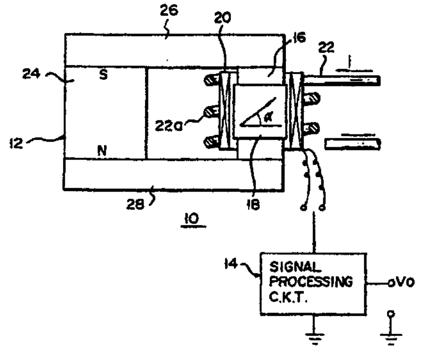

Figure 52 [80]

Current Sensor Having an Element Made of Amorphous Magnetic Metal

The current sensor comprises an element (18) located near a conductor (22) and made of amorphous magnetic metal whose magnetic property varies in accordance with the intensity of a magnetic field generated from a current flowing through the conductor. It further comprises magnetic field-applying means (24) applying a DC-bias magnetic field to the element, a coil (20) exhibiting electrical property corresponding to the magnetic property of the element (18), and output means (14) for outputting a signal corresponding to the electrical property of the coil. The coil has a specific positional relationship with the element, such that at least part of the magnetic flux generated by said coil passes through the element.

In materials with unbalanced magnetic moments (ferrites) oscillations and waves of the magnetic moments can be excited (magnetostatic spin waves). Microwave radiation in the GHz range coupled in a slab of yttrium iron garnet (YIG) produces such an oscillation. Because of this interaction, the microwave signal is delayed on its passage through the probe. The delay time depends on geometrical factors of the probe, the frequency, and the magnetic field. The sensor shown in Figure 53 [81] provides an intensity signal, V_m, which reflects the field dependent phase shift, $\delta\phi$:

$$V_m = 1 + \cos(2\,\delta\phi - \theta) \tag{53}$$

where θ is a phaseshift introduced by an additional delay line which is chosen to achieve maximum sensitivity, e.g. $\theta = -\pi/2$ or $-\pi$. The reported sensitivity is 0.1 mA over a dynamic range of six orders of magnitude using suitable alternators.

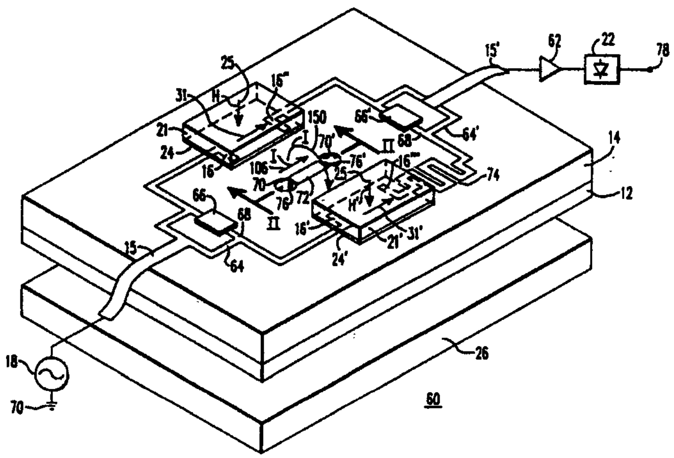

Figure 53 [81]

Wide Band Large Dynamic Current Sensor

Two YIG delay lines in parallel (24,24') are exposed to the same bias field (H, H'). A current (I) that passes through a conductor (72) produces a field (150) that adds with an opposite sign to the bias field in the probes. The intensity of the sum of the transmitted signals can be expressed in terms of the different phase shifts acquired, i.e. $+\delta\phi$ and $\theta - \delta\phi$ where θ is a delay caused by the delay line (74) on the right-hand side.

1.2.14 Inductive Measurements

1.2.14.1 Simple Coils

Alternating currents give rise to an alternating magnetic flux, Φ, in the vicinity of the conductor. An alternating flux that passes through an opening of a conductive loop induces a voltage U_{ind}. This fact is expressed by Faraday's law of induction (equivalent to the integral form of Maxwell's second equation):

$$U_{ind} = \oint \vec{E}\, d\vec{s} = -\frac{d}{dt}\left(\int_s \vec{B}\, d\vec{a}\right) = -\frac{d}{dt}\,\Phi \qquad (54)$$

A simple inductive sensor consists of a coil with one or more windings. Its both ends are connected through a measuring resistor. The voltage drop over the resistor is proportional to the alternating current. For a circular coil (radius r) with a single winding Equation 22 can be used to determine the induced voltage:

$$|U_{ind}| = \mu_o \frac{a}{2\pi\, r}\, \frac{d\, I}{dt} = 10^{-7}\, 2\pi\, r\, \frac{d\, I}{dt} \qquad (55)$$

where a is the area of the winding, $a = \pi\, r^2$. Figure 54 [82] shows the principle of an inductive sensor. Arrangements to measure also direct currents inductively are discussed in Section 1.2.14.3.

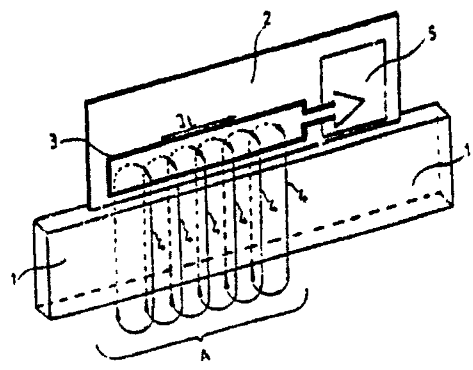

Figure 54 [82]

Device for the Potential-Isolated Measurement of Alternating Currents

Primary conductor (1) and inductive loop (3) are inductively coupled by field lines (4).

To avoid capacitively coupled distortions, the whole coil can be mounted in a nonferromagnetic housing. The influence of magnetic stray fields can be reduced by using a pair of antiparallel coils in series (astatic coils), cf. Figure 55 [83].

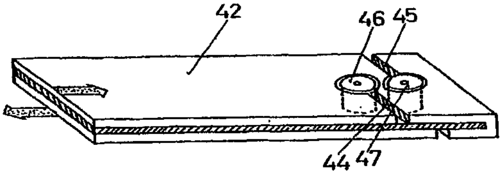

Figure 55 [83]

Current Transformer for a Static Electricity Counter

The current transformer on the secondary side is provided with a secondary winding consisting of two astatically designed coils (46, 47) laying next to one another and connected in series. As a result external parasitic magnetic fields have practically no effect on the transmission of the measured value. A large output signal is achieved by a large magnetic coupling of the primary conductor (42) and the secondary coil without the use of ferromagnetic materials.

1.2.14.2 Rogowski Coils

Coils wound on a nonmagnetic core that surround a conductor are referred to as Rogowski coils. Such a coil consists of many inductive loops perpendicular to the magnetic field H. Integration of Equation 55 around the circumference s of the core yields:

$$|U_{ind}| = \mu_o\, n\, a\, \frac{dI}{dt} = 1.26 \cdot 10^{-6}\, n\, a\, \frac{dI}{dt} \tag{56}$$

a being the cross section of the individual windings and n the number of windings per unit length. In the derivation of the above expression it has been assumed that the magnetic field is constant over the cross section of the windings. For a straightforward analysis of the results the radial dimension of such a coil should be rather small. The advantage of Rogowski coils over a simple winding is twofold:

- extraneous fields cancel in the integral around the closed loop (provided they are uniform over this range)
- the signal is higher than for a single coil only.

The voltage U_{ind} gives rise to a current I_c that is related to the current to be measured:

$$|U_{ind}| = I_c\, R + L\, \frac{dI_c}{dt} = \mu_o\, n\, a\, \frac{dI}{dt} \tag{57}$$

whereL is the inductance of the coil and R the combined resistance of the coil and measuring circuit.

Two simple solutions arise when one of the terms of Equation 57 is negligible:

- when $I_c\, R >> L\, dI_c/dt$ one has to integrate the voltage over a measuring resistor to obtain I; with a = 10^{-4} m^2 and n = 500 m^{-1} a 10 MA/s current pulse yields a signal of about 0.6 V;
- when $I_c\, R << L\, dI/dt$ (short circuited coil,) the device acts as current transformer with $I_c = I/N$, where N is the number of windings.

A shielded Rogowski coil is shown in Figure 56 [84]. In order to facilitate the measurements, Rogowski coils can also be made in shape of a belt that can easily be mounted around a conductor.

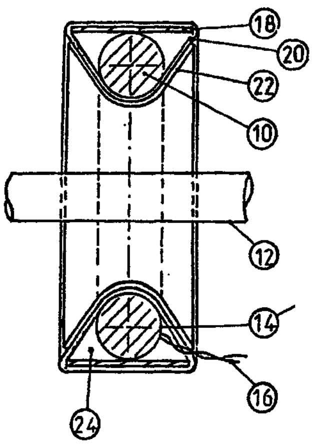

Figure 56 [84]

Current Transformer with Non-Magnetic Core

The Rogowski coil (14) is provided with a mangetic shielding (18) against extraneous fields, an inner electrostatic shield (22) to prevent capacitive coupling between the coil and the conductor (12) and an insulating layer (20).

1.2.14.3 Coils with Magnetic Cores

Alternating current transformers consist of a magnetic core with a primary and a secondary coil with N_1 and N_2 windings. Ideally input and output current I_1 and I_2 are related through:

$$I_2 = \frac{N_1}{N_2} I_1 \tag{58}$$

With a sufficiently large resistor R in the secondary circuit, I_1 can be derived from the voltage drop $U = I_2 R$. Low and high frequency components can be isolated with appropriate circuitry, cf. Figs. 57 [85] and 58 [86]. The response of a transducer can further be modified by introducing nonlinear portions into the flux path, cf. Fig. 59 [87].

Soft magnetic materials with high permeability, low coercive force and linear B-H characteristic are chosen as core materials for alternating current transducers. For high frequency applications the frequency dependence of the permeability has to be taken into account. In some metallic amorphous alloys it is constant up to about 100 kHz [88].

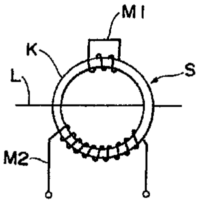

Figure 57 [85]

Apparatus for Assessing Insulation Conditions

The short-circuited tertiary winding (M1) has a low resistance for low frequency components. It therefore cancels the low frequency flux and thus acts as a high-pass for the secondary coil (M2).

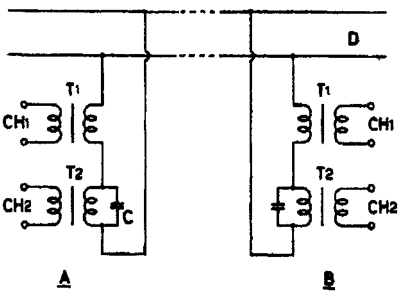

Figure 58 [86]

Branching and Inserting Circuit for Data Transmission Line

The capacitance (C) connected in parallel to the primary winding of the second transformer (T2) coil acts as a low-pass for the secondary winding (CH2).

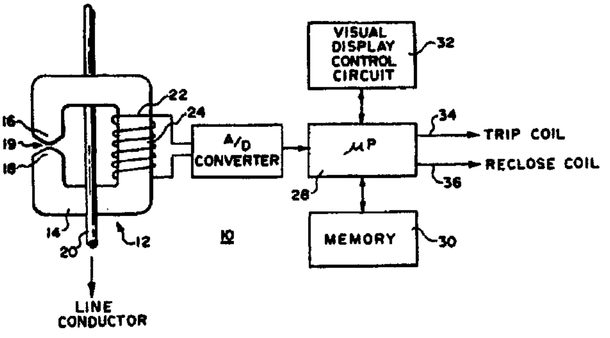

Figure 59 [87]

Non-Linear Alternating Current Transducer

Yoke (14) has an air gap (19) to exhibit a nonlinear magnetic response to current changes in the line conductor (20) and to provide a logarithmic output across the secondary winding (22). Because of the logarithmic response the relative accuracy of the transformer output is uniform over a wide range of primary currents.

As soon as a secondary current flows in a current transformer, power is transferred to the secondary side, and the primary current is affected. When the primary current is purely AC, zero flux transformers offer a suitable alternative. In the circuit shown in Fig. 60 [89] there is no feed back into the primary circuit and Equation 58 holds exactly.

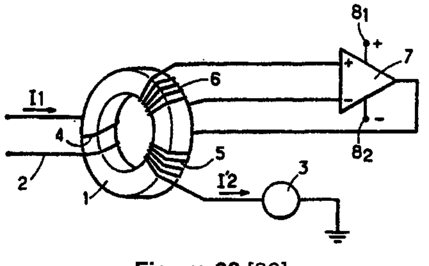

Figure 60 [89]

Device for Generating a Secondary Alternating Current whose Strenght is Proportional to that of a Primary Current

The voltage induced in the sense coil (6) controls an amplifier (7) that drives a current through the compensation coil (5). When the amplifier has a negligible offset and an infinite amplification the flux induced has the same magnitude and opposite sign as the flux from the primary coil (4).

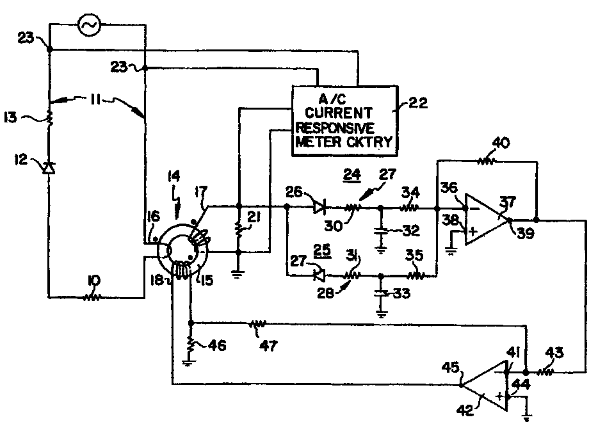

Figure 61 [90]

Current Measuring and DC Magnetic Flux Compensating Apparatus

DC magnetic flux bias imposed on a magnetic core (15) of a current transformer (14) is compensated in response to an indication of the amplitude and duration of opposite polarity secondary winding current components. In a second embodiment, the magnetic bias is compensated by responding to the integral of the secondary current. The integral of the secondary current is a measure of the magnetic core flux variations. The durations of the positive and negative flux variations are compared.

To measure direct currents one exploits the fact that they give rise to DC bias flux in the magnetic core. This flux offset alters the operation characteristics of the transformer such that amplitude and duration of the positive and negative half waves differ. In the circuit shown in Fig. 61 [90] a compensating DC flux is derived from this asymmetry.

In the arrangement shown in Figure 62 [91] the DC flux is detected through the difference of the amplitudes of the positive and negative half waves required to drive a core alternatingly into opposite saturations. Saturation is detected through the vanishing self-inductance of the AC coil, which acts as "flux gate". Induction of the AC signal onto the primary conductor is prevented by driving two identical AC coils in opposite directions. For this kind of converters core materials with a steep linear magnetisation curve that flattens off rapidly at saturation are required. The field to be measured must be well below the hard saturation field and the AC field should be considerably higher.

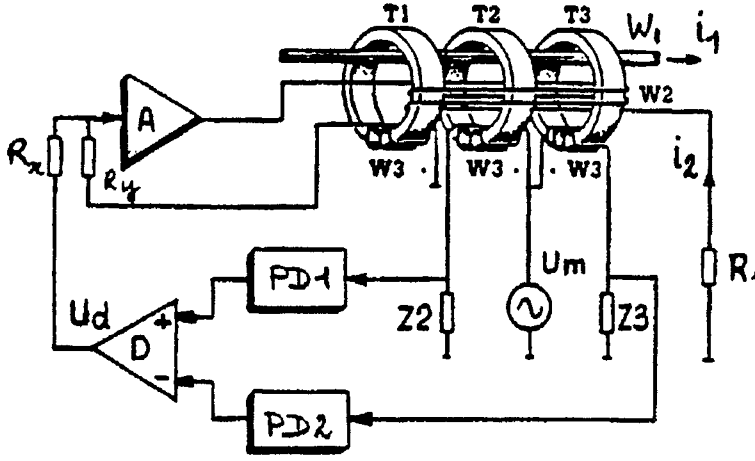

Figure 62 [91]

Circuit for the Detection of an Asymmetry in the Magnetization Current of a Magnetic Modulator

Two tertiary coils (W3) are wound in opposite directions on two cores (T2, T3) and fed by an AC reference voltage (Um) to drive the cores periodically into saturation in both directions. Upon saturation the voltages across the impedances (Z2, Z3) sharply rise. Any DC magnetic flux Φ_{DC} in the two cores due to a direct current in the primary coil (W1) gives rise to an asymmetry in the voltages over the two impedances which appear at the outputs of two peak detectors (PD1, PD2). An amplifier (A) provides a direct current to the secondary coil (W2) which compensates the magnetic flux Φ_{DC}. Any alternating current (accompanied by a magnetic flux Φ_{AC}) in the primary coil induces a signal in the tertiary coil on an additional core (T1) which gives rise to an alternating current through the secondary coil which compensates the magnetic flux Φ_{AC}. The secondary current (i_2) is an image of a primary direct or alternatiung current (i_1).

1.2.14.4 Planar-Type Detector

When an alternating primary current passes through a first ferromagnetic plate which faces a similar second plate, eddy currents are induced in the second plate. If the frequency of the current is sufficiently high (MHz) and the geometry of the plates is chosen accordingly , the skin effect is observed, i.e. the current densities of both, the primary and the induced eddy current, peak on the surfaces of the respective plates. Figure 63 [92] shows a device with 5 µm thick plates in which this effect is exploited to measure currents in the 10 to 100 MHz range. The sensitivity of the sensor crucially depends on the matching of the output impedance of the power source and the impedance of the transmission line between the power source and the detector. Its frequency range can be increased by decreasing the capacitance between the plates.

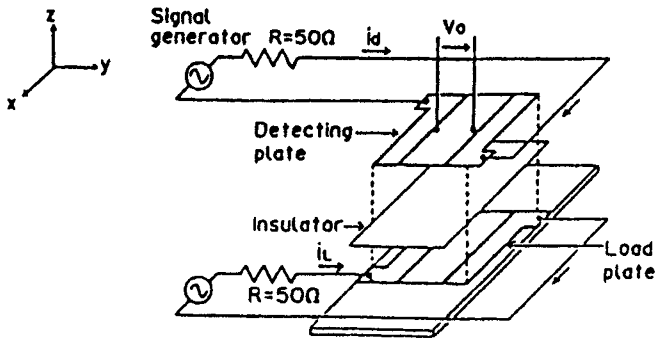

Figure 63 [92]

Planar-Type Current Detector

Two ultra-thin permallow plates with sputtered electrodes are mounted facing each other. The load current (i_L) is sent through the load plate and a detecting current (i_d) in the opposite direction through the detecting plate. Due to the skin effect the applied currents and the induced eddy currents flow in opposite directions on the outer surfaces of the plates such that the current density on the outer surface of the plates is minimised when both currents are equal. To measure the amplitude and phase of the load current of a known frequency one adjusts the amplitude and the phase of the measuring current such as to minimise the voltage drop (Vo) across the outer side of the upper plate.

This Page Intentionally Left Blank

CHAPTER 2

MEASURING HIGH VOLTAGES AND CURRENTS

2.1 MEASURING HIGH VOLTAGES

2.1.1 Introduction

High voltage technology has many applications: electrical energy is transported at 765kV or more, higher voltages are used in electrostatic generators, in pulsed power machines and in EMP simulators.

Improved insulation techniques make it possible to use higher voltages in power generators. This means that lighter and cheaper stator bars can be used for a given power level.

There is thus a need for measuring high voltages for control, monitoring and test purposes.

The term "high voltage" is unclear. In a "small signal" apparatus and in various consumer products, the sector voltage, e.g. 220 V, is considered as high. The national electricity code (USA) defines "low voltage" as less than 24 V [297].

A common distinction relative to electric power generation and transport is:

LV (Low Voltage)	0-1 kV
MV (Medium Voltage)	1-100 kV
HV (High Voltage)	100-230 kV

In this chapter we refer to "High Voltage" in this later sense, and also include the higher MV and anything above HV, i.e. EHV and UHV.

Measuring high voltages brings particular difficulties:

- The high voltage and power levels and the associated hazards for people and equipment put a high demand on isolation.
  Insulations and procedures used for lower voltages are inadequate. Consider for instance that the break through voltage for air (50Hz AC) is about 5.9 kV/cm [305].
  Material impurities or surface deposits which are without consequence at low voltages create unwanted discharges at high voltages.

- The high levels call for principles of measure that can cope with the enormous range of input values.
- It is difficult to keep a good sensitivity while measuring large values.
- The high voltages (and associated currents) may induce disturbances in the measuring equipment.
- The high field strength can deteriorate the materials used in the measuring devices.

We have two approaches to HV measurements: Scale down the voltage and use LV measuring methods or use dedicated HV measuring methods.

The down scaling can be done with voltage transformers or with voltage dividers - resistive, reactive or combined reactive and resistive. In view of the voltages involved, these devices can be very costly and bulky.

Capacitive voltage dividers do of course only work with AC - typically 20Hz - 100 MHZ.
Resistive dividers can operate from DC to 100 kHz.
RC voltage dividers can operate from DC to +/- 2 MHZ.

For comparison we note that a small-signal current or voltage transformer for MV or HV has an upper frequency limit of about 20 kHz.

Direct measurements are more and more done by optical methods, mostly using the Pockels or the Kerr effects, see ch. 1.1.7. These methods can be used for direct, absolute, measurements, and nature supplies insulation: Pockels cells are made of dielectric crystals (glass), and Kerr cells are based on dielectric liquids. They use light as signal carrier. Contrary to conventional transformers, Pockels and Kerr cells can measure high frequency voltage changes. Additionally, they do not disturb the electric field.

2.1.2 Electro-optical Transducers

Kerr cells

Kerr-cell voltage measuring transducers (ch.1.1.7.3) were the first to be developed. Figure 64 [334] shows a design from 1929. Up to that date Kerr cells had been used for low frequency HV measurements. The new design was suitable for use in the MHz range, and featured compensation for light source intensity variations:

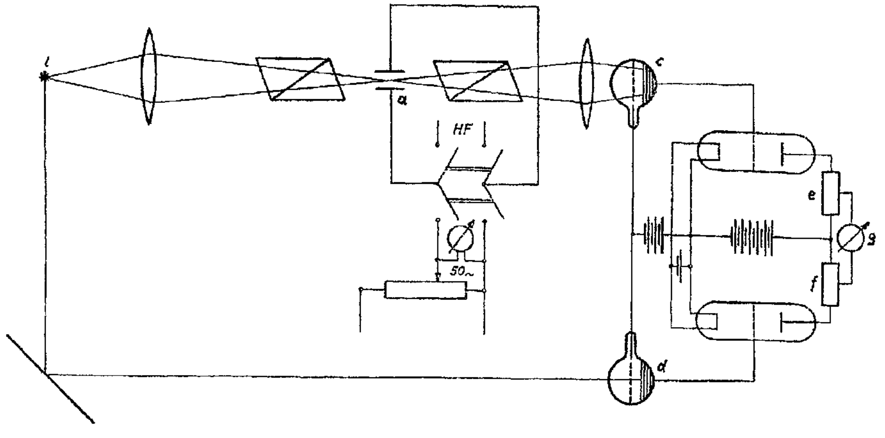

Figure 64 [334]

Kerr cell voltage measuring arrangement with compensation for light intensity variations.

The signals corresponding to a reference beam and a measuring beam are combined over resistances (e) and (f), which are being adjusted to give a zero current through the galvanometer (g).

(a) is a Kerr cell with nitro benzol, (c) and (d) photocells and (I) a light source. Polarizing and analysing Nicol prisms are placed before and after the Kerr cell.

The instrument does a relative measurement:

A 50 Hz reference source is to be adjusted to give the same output as the unknown HF signal.

Further down in this chapter we will illustrate how, many years later, reference beams are being used for analog purposes in Pockels and Faraday devices

Some **disadvantages** with using Kerr cells for HV measurements are:

- Excessive heating of the liquid, due to the high electric field
- Immersed electrodes lead to formation of space charges near the electrodes
- Capacitance of the two parallel electrodes and their leads
- Expensive insulation of the electrode cables is needed

[304] proposes a technique reducing these problems.

Pockels cells

Recent years have seen an intensive development of Pockels cell devices (cf. ch. 1.1.7.2) for HV applications (and for small signal ultra fast events as well).

In a Pockels cell the voltage to be measured can be applied lengthwise to two ends of the cell via transparent electrodes (Fig. 16 and Fig. 68), alternatively via one transparent and one reflecting electrode (Fig. 17)

It can also be applied laterally across the cell as in Figure 71 [313]. Crystals having Pockels effect have different directional characteristics depending on crystal structure and cut.

The main problems under investigation are on one hand how to deduct an unambiguous measurement value from the periodic output signal of a polarimetric set up, and on the other hand how to eliminate various types of disturbances; Pockels cells are sensitive to temperature and pressure changes. Optical and electronic components before and after the cell are subject to disturbances and ageing.

First, let us look at the problem with the **periodic output**. Consider the relation output/input as a continuos sinusoidal function.

We realize that the **sensitivity** around the extreme values is very low.

When the signal to be measured does not vary much, it is thus interesting to arrange the operating point of the transfer function at 50% of the maximum. This gives us optimal sensitivity and linearity. See Figure 65 [307].

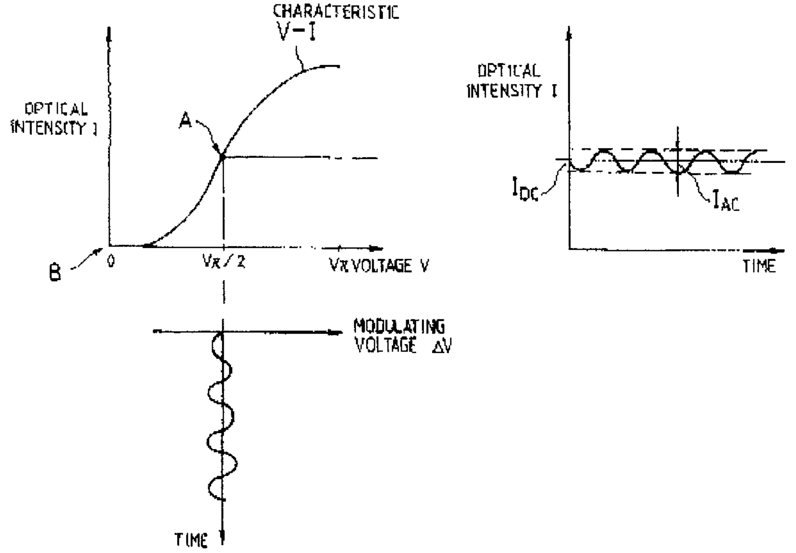

Figure 65 [307]
Transfer Characteristics of Pockels cell

A way to arrange the operating point is to phase shift the light beam. See Figure 66 [307].

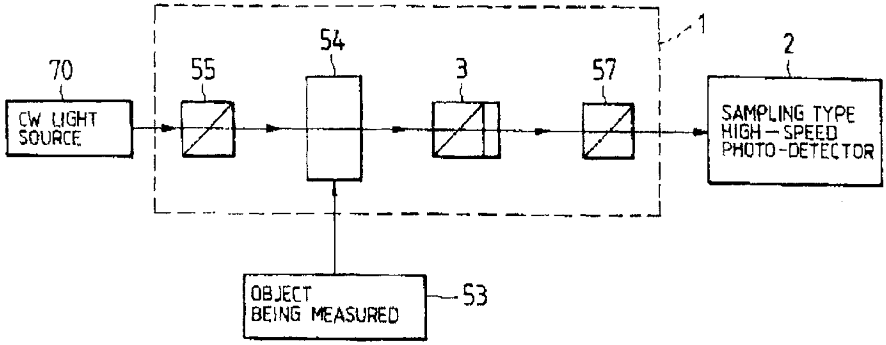

Figure 66 [307]

Pockel Cell Voltage Sensor with Phase Compensator

The voltage detector comprises a CW (continuous wave) light source 70, and optical modulator 1 for modulating the output CW light beam of the CW light source 70 with the output voltage of an object 53 to provide an optical intensity signal corresponding to the voltage, and a sampling type high-speed photo detector 2 for detecting the optical intensity signal. The CW light source 70 comprises, for instance, a He-Ne laser or a semiconductor laser. The optical modulator 1 comprises a polarizer 55 for extracting a specified polarization component from the CW light beam, a Pockels cell 54 for changing the polarization of the output light beam from the polarizer 55 with the output voltage of the object 53 to provide emergent light beams having various polarization components corresponding to the voltage waveform of the object 53, a phase compensator 3 for adjusting the phases of the emergent light beams from the Pockels cell 54, and an analyser 57 for extracting an emergent light beam having a specified polarization component from the emergent light beams from the phase compensator 3 to thereby provide an optical intensity signal corresponding to the voltage waveform of the object 53. The phase compensator 3 comprises, for instance, a Soleil-Babinet compensator for changing the phase of the output light beam of the Pockels cell to shift the operating point of the optical modulator 1 [307].

The second problem related to the periodic transfer function is that one cannot directly determine an absolute value or the direction of a voltage change if the voltage goes beyond the half wave voltage, which in KDP (potassium dihydrogen Phosphate) is about 11300 V [308]. Other types have a half wave voltage V_π of 2 kV [310].

A first solution to this problem consist in counting cycles. This solution is sensitive to signal loss, and is therefore not very practical.

A second solution is to use two phase shifted light beams and associated electronics. See Figures 67 A and B [308]. A feed back arrangement maintains the peak to peak intensity of the two beams constant.

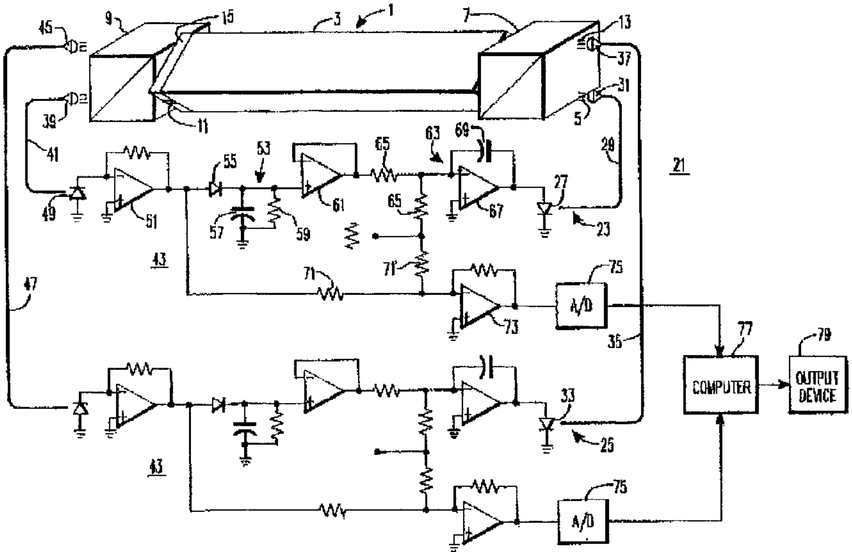

Figure 67 A [308]

Pockels Cell Device with Two Phaseshifted signal

The figure illustrates schematically a complete voltage measuring system. This system 21 includes the sensor 1 comprising the crystal 3, the first and second polarizers 7 and 9 respectively, and the one-eighth wave plates 11 and 15. The system 21 also includes first and second light sources 23 and 25 which generate the two collimated light beams 5 and 13 respectively. The light source 23 includes a light emitting diode (LED) 27. Light produced by the LED 27 is transmitted by optic fiber cable 29 and passed through collimating lens 31 to produce the first collimated light beam 5. Similarly the LED 33 in second light source 25 produces light which is transmitted by the optic fiber cable 35 and passed through collimating lens 37 to produce the second collimated light beam 13. Light from the first beam 5 exiting the second polarizer 9 is gathered by lens 39 and conducted through fiber optic cable 41 to a first electronic circuit 43. Similarly, the second beam exiting the second polarizer 9 is focused by lens 45 on fiber optic cable 47 which directs the light to a second electronic circuit 43.

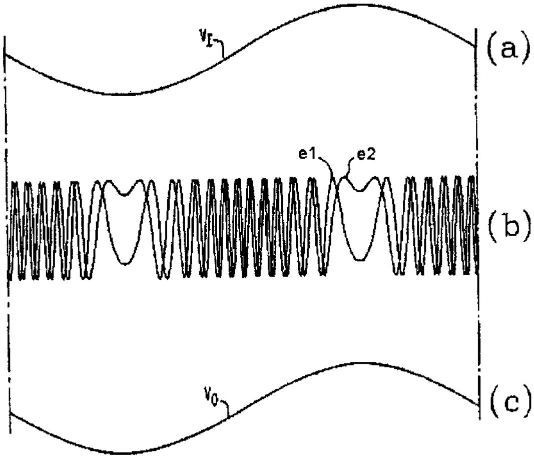

Figure 67 B [308]
Waveform Diagram

The figure illustrates on a comparative time basis the voltage waveform VI to be measured, the quadrature electrical signals e1 and e2 generated in response to the voltage waveform a by the system of Figure 67A, and the output waveform V0 generated by the system of Figure 67 A which is representative of the voltage waveform a.

This arrangement does imply extra components and costs, and does create new problems due to temperature effects and varying optical constants along the two optical paths. It could be caused by inhomogeneous tension in the crystal or varying characteristics of the respective phase shifters.

A variant of the idea of employing two phase shifted beams, engaging less and smaller components is shown in Figure 68 [309].

This apparatus uses a single light source and a single beam which is reflected at the far end of the Pockels crystal. Exiting the crystal, the beam is split in two parts which are then phase shifted in relation to each other. A microprocessor takes the intensity of the two signals to calculate the unknown voltage.

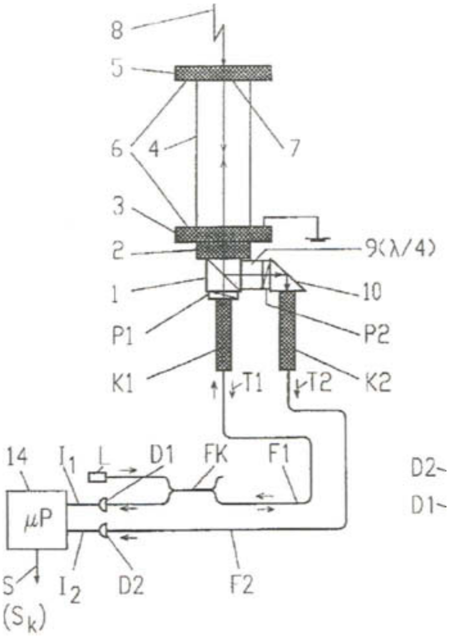

Figure 68 [309]

Pockels Cell Device with Beamsplitter

The HV measuring system uses an electro optical sensor, with an electro optical crystal (4), exhibiting a phase shift in the light in dependence on the applied HV (8).

- The crystal is supplied with a linearly polarised input beam, with a given polarisation angle relative to the electro optical axis of the crystal, with detection of 2 back reflected partial beams (T1, T2) provided by a polarisation analyser (1) with a given relative phase shift provided by a quatre wavelength plate, via respective photo detectors (D1, D2). Pref. the polarisation angle of the input light beam is between 30 and 60 degrees.
- ADVANTAGE - Uses single optical channel for reduced overall size.

A third solution consist in employing two Pockels cells of different sensitivity. One for large and one for small signal variations. We will illustrate the same principle applied to a Faraday current sensor at the end of this chapter (Fig. 116).

Interferences and unwanted variations in sensitivity have numerous sources, such as:

- Intensity variations of light sources due to e.g. temperature changes or ageing
- Drift in the characteristics of photoelectric converters (usually photodiodes)
- Varying optical properties of components such as sensor crystals and phase shifting plates. The causes can again be ageing, temperature changes or mechanical influence.

Intensity variations of the light sources can be compensated for by the use of a **reference beam** in a manner similar to the one illustrated with the Kerr cell in Figure 64 above.
Here the adjustment was manual. Today one does this with some kind of automatic calculation or feed back.

A development of the reference beam method consist in using a laser light source with two frequency components (utilizing the Zeeman effect). See Figure 69 [311]. Here the reference beam is used to eliminate the effect of intensity variations of the light source (7). The "superheterodyne demodulation method" of this device additionally eliminates the influence of drift in the characteristics of the photodiodes (10) and (13), and has the added advantage of extending the measuring range to +/- 3π rad.

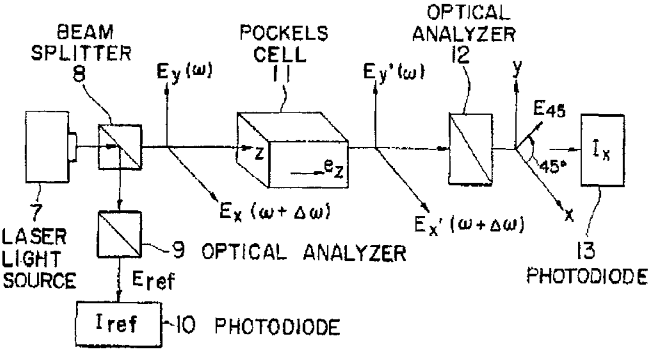

Figure 69 [311]
Twin Frequency Pockels Cell Device

The explanation of the functioning is somewhat lengthy, and we refer to the original document for more details.

A way of compensating for external influences is to insert an additional Pockels cell, activated by a known alternating voltage, in the optical path. An arithmetic unit can then calculate an interference free voltage value.

An elegant way of determining a temperature independent AC voltage, is to normalize the two orthogonal output signals (corresponding to S- and P-polarized light) with the DC component of the output of the corresponding opto electrical transducers. See Figure 70 [312].

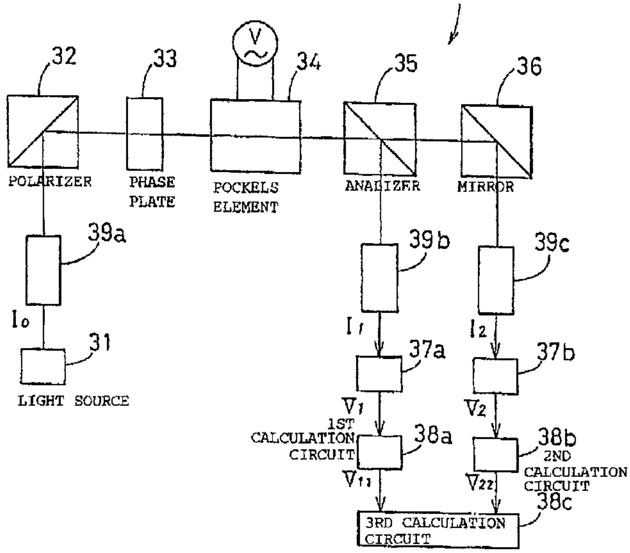

Figure 70 [312]

Pockels Cell Device with Normalised Output

The first calculation circuit 38a calculates an equation V11 = (V1 - DC1)/DC1 based on the first electric signal V1 to produce an output signal V11 therefrom, while the second calculation circuit 38b calculates an equation V22 = (V2 - DC2)/DC2 to produce an output signal V22 therefrom. In the equations, DC1 is a direct current component of the first electric signal V1, and DC2 is a direct current component of the second electric signal V2. The third calculation circuit 38c calculates an equation V3 = 1/[(alpha /V11) - (beta /V22)] based on the output signalsV11, V22 to produce an output signal V3 therefrom. Assuming that the intensity of the incident light beam from the light source 31 is I0 and that each value of alpha , beta is "1", the respective intensities I1, I2 of the output light beams received by the first and second light-receiving elements 38a, 38b are represented by the following equations (3), (4), and the output signals V11, V22 are represented by the following equations (5), (6).

"(3)" I1 = (I0/2) (1 - GAMMA z - k. DELTA T)
"(4)" I2 = (I0/2) = (1 + GAMMA z + k. DELTA T)
"(5)" V11 (V1 - DC1)/DC1 = (- GAMMA z)/(1 - k. DELTA T)
"(6)" V22 (V2 - DC2)/DC2 = (GAMMA z)/(1 + k. DELTA T)

Thus, the output signal V3 of the third calculation circuit 38c is represented by the following equations (7) and (8).
"(7)" V3 = 1/[(alpha /V11) - (beta /V22)]
k : Temperature change ratio of the phase difference applied by the phase plate

DELTA T : Temperature difference from 25 DEG C

alpha and beta are constants. V3 is proportional to the applied voltage "V".

A development of this principle is to concurrently intensity normalize and temperature compensate the signal. See Figure 71 [313].

This apparatus is based on the realization that the temperature dependence of the AC and DC signals parts of the two light signals are different. Knowing this one can deduct a measure which is proportional to the temperature from the corresponding electrical signals. The temperature value is then used for correcting the intensity normalized signal.

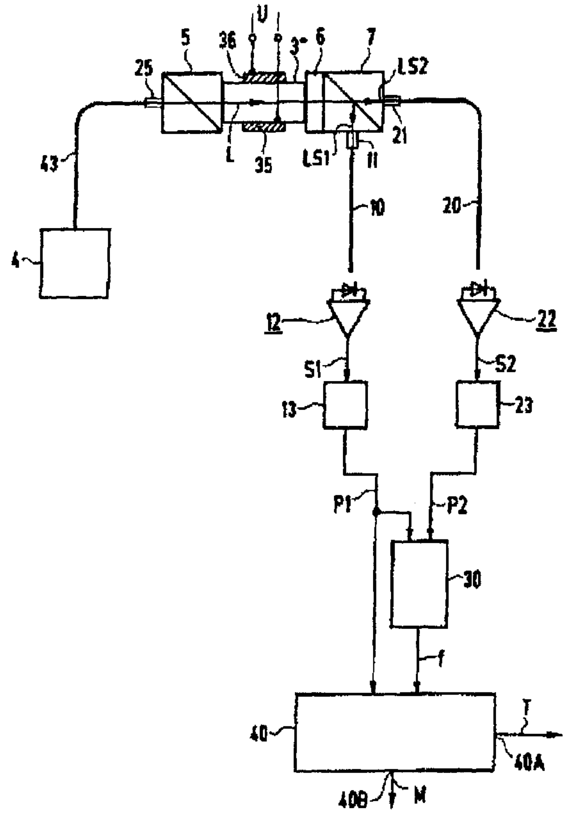

Figure 71 [313]

Pockels Cell with Temperature and Intensity Compensation

The AC voltage to be measured is applied to a Pockels element (3) and alters the polarisation of light (L) travelling through the Pockels element. The transmitted light is split into two differently-polarised light signals (LS1,LS2), which are converted into electrical intensity signals (S1,S2). A function value (f) for temp. is obtained from at least one intensity signal. This function value and at least one of the two intensity signals is used to provide a temp. compensated measurement signal (M). The two intensity signals are pref. intensity normalised before the function value is obtained.

[314] compensates for temperature induced errors by first measuring the dielectric constant of the electro optic material of the Pockels cell. The constant is found to be nearly proportional to the reciprocal of the absolute temperature. Thus the product of (temperature dependent) halfwave voltage and dielectic constant is nearly independent of temperature. See Figures 72 A and B [314].

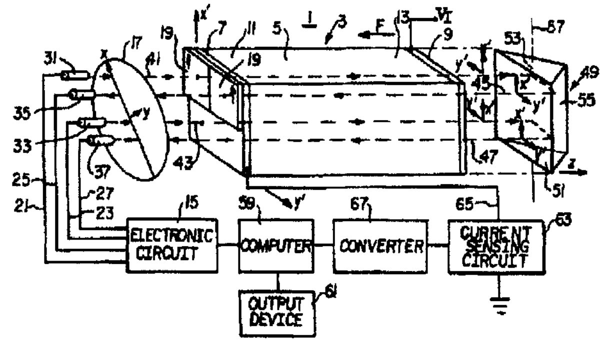

Figure 72 A [314]

Temperature Compensated Pockels Cell

As the dielectric constant and the halfwave voltage of electro-optic crystals having a fourfold axis of rotary inversion are oppositely dependent on the absolute temperature, but their product is nearly independent of temperature, temperature compensation in an ac voltage measuring system utilizing such an electro-optic crystal is provided by measuring the time averaged current through the crystal. Good electric isolation is achieved by a current sensing circuit which produces a pulsed light signal having a pulse rate proportional to the time averaged current through the crystal. The pulsed light signal is converted to an electrical signal for input to a digital computer which calculates therefrom, and from a reference current and voltage measured at a reference temperature, and a time averaged voltage measurement, a temperature correction factor which is applied to the crystal halfwave voltage used by the computer in calculating the instantaneous value of the voltage to be measured. A look up table containing empirically derived values related to the calculated correction factor can be used to generate a correction factor adjusted for leakage through the crystal, fringing of the field produced by the voltage to be measured, and residual temperature dependence of the electro-optic crystal. In a practical embodiment of the invention, shield rings surround both ends of the electro-optic crystal to reduce fringing of the electric field.

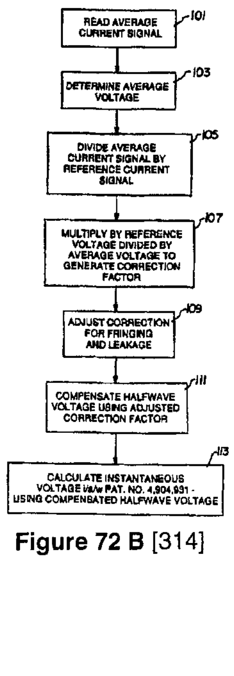

Figure 72 B [314]

2.1.3 Non-Electro-Optical methods

In [341] trends in high-voltage test and measuring technology are described. Micro electronics are playing an important role in the whole process of measuring, starting with the so called intelligent sensors. Digital techniques and microcomputers made intelligent measuring apparatus feasible.

A consequence of this is that the level of signal voltages must be adapted.

An output of a classical voltage transducer (voltage transformer) typically used to be 100 V, and it sourced a load of a few W.

This has to be adjusted to the working range of say +/- 10 V of microprocessor supported systems. The small power need of these systems imply that the input resistance has to be high (in the MΩ range).

Another trend is that the measuring transducers become more "general purpose" and can be used in circuit breakers, control systems etcetera with a minimum or no adaptions.

It is possible to use more classical instrumentation like an oscilloscope [93]. Care has to be taken to insulate the sensitive instrument entry and to the common mode rejection.
The use of electro-optics is important. Advantages are a higher transfer rate and noise immunity (Fig. 73) [93].

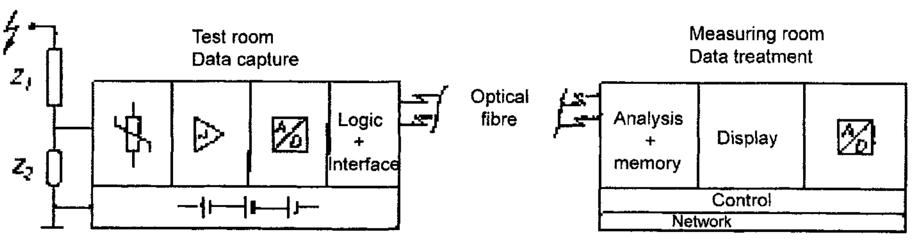

Figure 73 [93]
HV Measuring System
The use of an optical link isolates the HV side from the data treatment side.

Figure 74 [95] shows a high voltage measuring system with a very high input impedance. A control signal is fed back to adjust a reference source to match the source under test. This avoids loading the source under test during the final measurement.

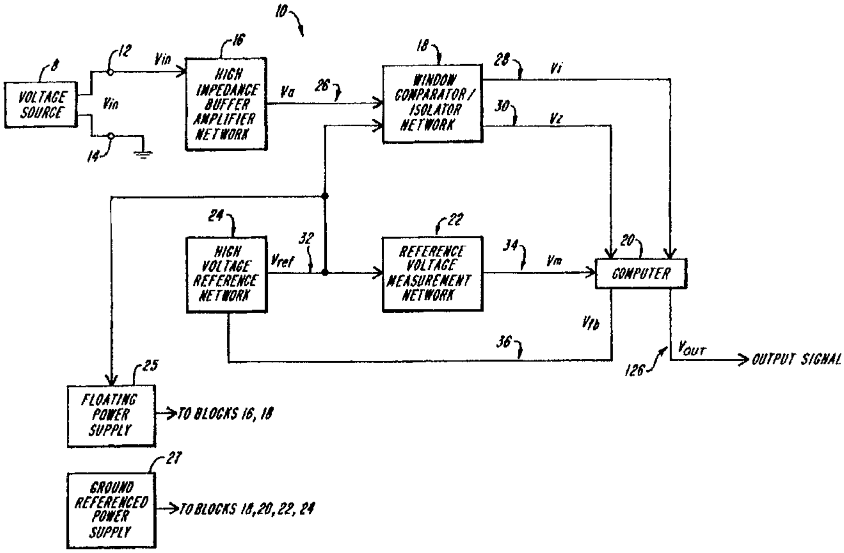

Figure 74 [95]
High Impedance System for Measuring Voltage

Other solutions for measuring at high-voltage potential are shown in [96] and [97]. Figure 28 uses a measuring converter inside the contour of the conductor. A transmission circuit converts the measurement signal into light signals in light-guides.

Figure 75 [97] has a display that can be seen from the outside world.

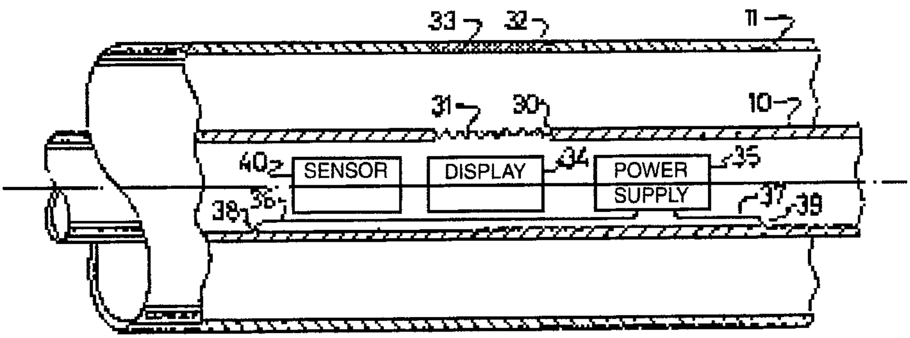

Figure 75 [97]
Applied Voltage Indicator for CurrentConverter

Measuring ac-Voltages

A new ac high voltage sensor uses a piezoelectric transducer and a strain gauge. This sensor detects the mechanical strain of the transducer on which a foil strain gauge is cemented. Tests ascertained that the strain was directly proportional to the voltage measured, with errors less than 2 % for voltages up to 26000 Vpp (Fig. 76) [98].

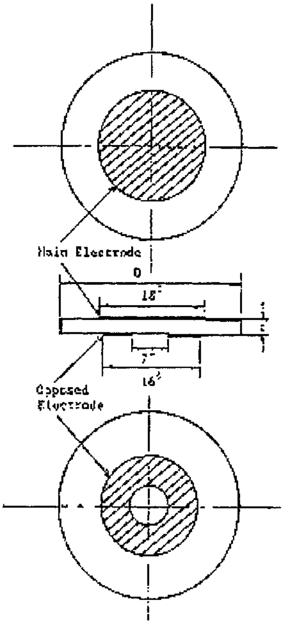

Figure 76 [98] ©1988 IEEE
Shape and Dimension of a Piezoelectric Transducer

A sensor for voltages and currents uses a Rogowski coil in a non-magnetic metallic screening mounted inside the screening tube of a conductor. The metallic screening forms together with the tube and the conductor a capacitive voltage divider (Fig. 77) [99].

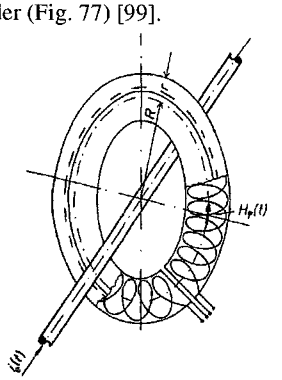

Figure 77 [99]

One way to tackle like problems of high-voltage measurements is the use of voltage dividers, which enable us to handle a small fraction only in a more classical way. We know a number of voltage dividers such as resistance dividers, capacitance dividers and inductive dividers.

Transformer voltage dividers [100, 101] have become very popular. They are much more accurate than capacitance or resistance dividers. A divide decade is an autotransformer (Fig. 78) [100] with ten taps and a switch assembly. A number of decades can be connected one after the other. In order to minimise the magnetic flux leakage a toroidal magnetic circuit should be used. To reduce active loss in the winding, the wire cross section must be as large as possible. Attention must be given to the contact resistance of the switches.

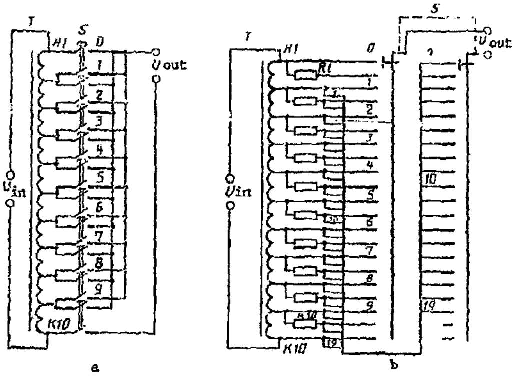

Figure 78 [100]
Modular Transformer Voltage Dividers in Measuring Equipment

An inductive voltage divider using a microprocessor is shown in Figure 79 [101]. Use is made of a combination of an inductive divider and a 12 bit multiplying D/A converter. A sensible choice of the transformation ratio of the inductive divider makes that 1 MSB of the DAC equals $Ui/2^{13}$ and 1 MSB equals $Ui/2^{24}$. Ui is the input. A computer determines the divide ratio. An IEC bus is used for communication.

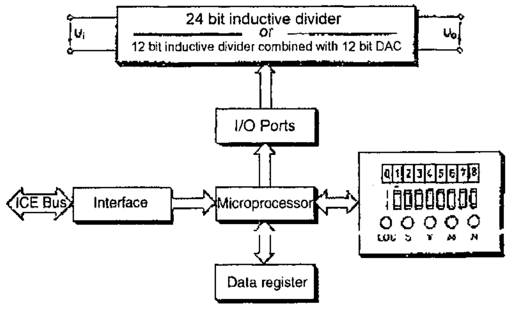

Figure 79 [101]

Satellite communications can be used in remote sensing on energised high voltage conductors [102]. Sensor modules for electrical, mechanical or environmental parameters in the vicinity of the high voltage conductor digitise and communicate the measured quantities via a communications subsystem mounted on and powered by an energised high voltage conductor without requiring a circuit interruption.

The subsystem modules are toroidal in shape and can be mounted on an energised high voltage conductor using a hot-stick (Fig. 80) [102].

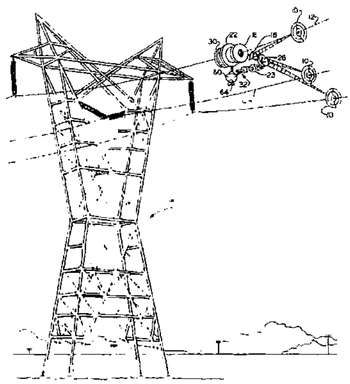

Figure 80 [102]
Line-mounted, Movable, Power Line Monitoring System or Environmental Parameters Beyond Line-of-Site Distance

An example of a sensor module for measuring both voltage and current is described in [103]. Figure 81 [103] shows a dielectric insulator incorporating a sensing capacitor for forming a capacitive divider with capacitor (5). Capacitor (13) incorporated in the same dielectric at the same temperature as (4) acts to correct the temperature induced faults using the differential amplifier (6). Coils (18) and (21) measure the current in the conductor (3).

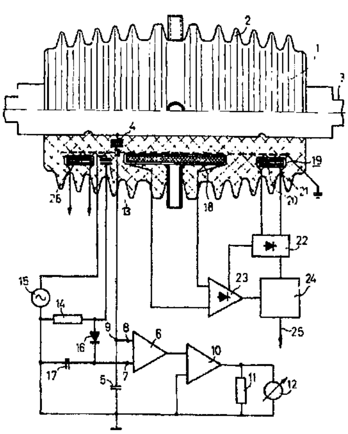

Figure 81 [103]
Current and Voltage Measurering Device with Moulded Resin Bushing

Another example is shown in Figure 82 [104]. An open air coil is located in an encasement in the cast resin body for maintaining the primary conductor in the top of the cast resin body. A keeper assembly maintains the primary conductor in the groove and provides an electrical connection from the primary conductor to the voltage measuring apparatus.

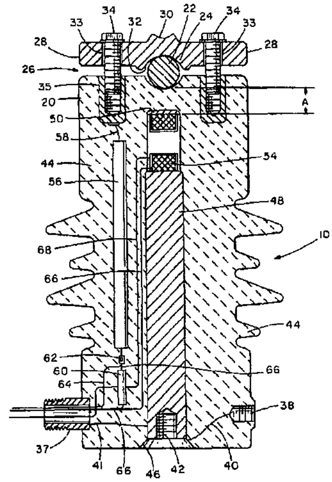

Figure 82 [104]

Line Secured Current and Voltage Sensing Apparatus

A resistive divider compensated for parasitic capacitances is shown in Figure 83 [105]. A right angled triangular sheet of electrical conductive material is formed in a semi-cylinder and interposed between a resistor (R3) and the screening (4). So the part of the parasitic alternating current between the screen (4) and the sensor is compensated by an alternating current between the additional electrode (5), connected to the high voltage, and the resistor (R3).

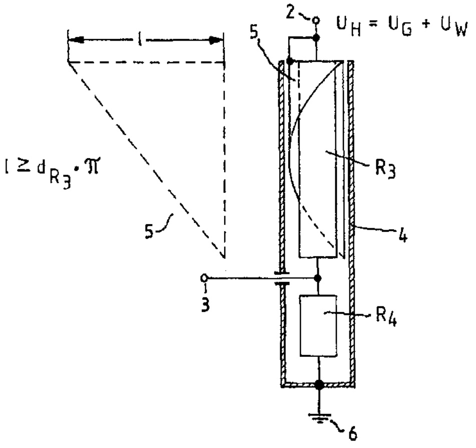

Figure 83 [105]

Compensation for Parasitic Capacitances in a Screened Resistance Device

Figure 84 [106] shows a line mounted apparatus for measuring line potential. The module is doughnut shaped and opens like a pair of jaws. The potential difference between ground and the power conductor (3) is integrated to a voltage proportional to the current flowing in the equivalent capacitance formed by the outer surface of the module and ground.

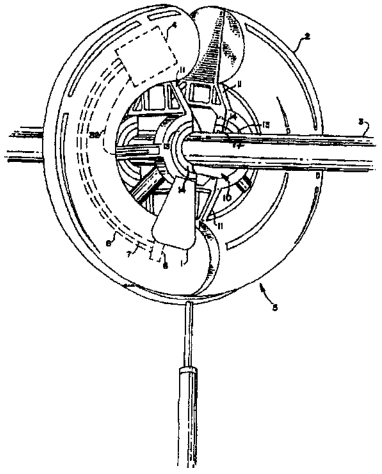

Figure 84 [106]
Line Mounted Apparatus for Measuring Line Potential

Figure 85 [107] gives an example of a mobile system for monitoring electrical and other parameters along a power corridor [107]. The system has two propulsion modules with e.g. linear induction motors deriving their power from the power conductor. The module 20 carries e.g. corona detection and a transmitter.

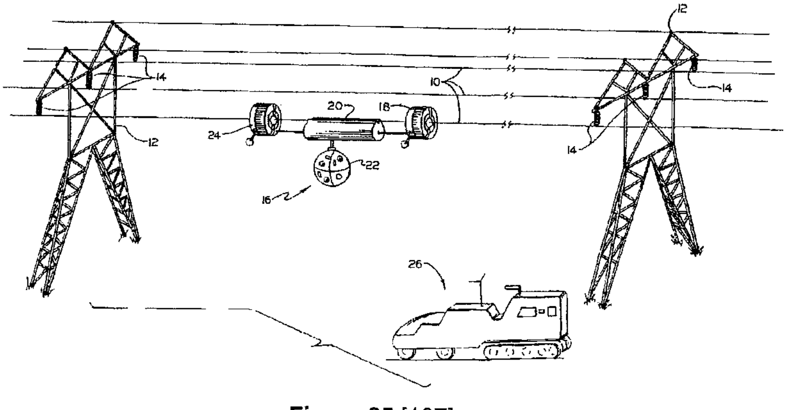

Figure 85 [107]
Line Mounted Apparatus for Measuring Line Potential

Figure 86 [108] shows a technique for detecting the voltage of AC high voltage lines. A radar wave is transmitted to the lines and is reflected when the AC voltage drops to threshold level. Reflection continues until the AC voltage cycles to the threshold level on its second half of the cycle. A time interval is calculated for radar reflection and non-reflection, and a ratio thereof is calculated and displayed.

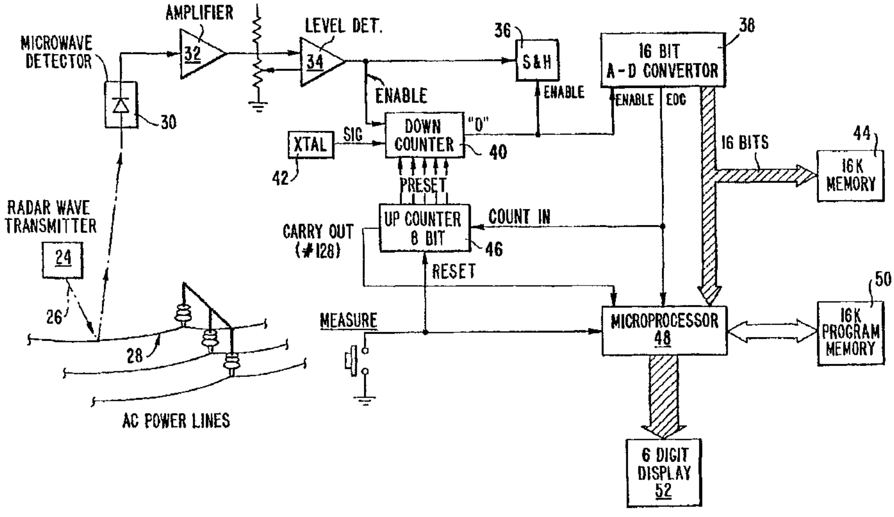

Figure 86 [108]

Remote Measurement of High Voltage AC with Radar

a Generation of impulse voltage
b Measurement of impulse voltage
1 Impulse-voltage generator
2 Front capacitor
3 Test object
4 Damping resistor
5 High-voltage lead
6 Voltage divider
7 Measuring table
8 Oscilloscope or digital recorder
9 Screened chamber
10 Grounding system

2.1.4 Measuring Impulses and Transients

The parameters involved in HV impulse measurements are the level and waveform, and ambient conditions like temperature, humidity and clearances from grounded or energised structures [109]. Problems arise with systems of large dimensions. When the HV component is made of several sections, then it is possible to test the linearity of each section and to verify the absence of nonlinear phenomena (corona) of the complete device at the highest voltage levels.

If the system can be considered as linear, one approach is to deduce its behaviour by its step response, that can be considered as a fingerprint of the system. It is even possible to calculate, for a given excitation, the response of the system [110]. With that aim, the measuring system is represented by a chain of distributed and concentrated elements, each one simulated by a quadrupole. By step-by-step computation one can proceed from the input to the output for each input signal. It is also possible, by a deconvolution procedure, to proceed in the other direction, from an output signal to the time input signal (Fig. 87) [110].

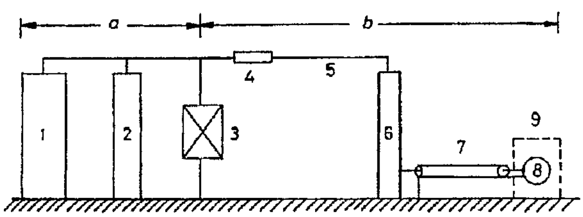

Figure 87 [110]

Accurate Method of Representation of High-Voltage Measuring Systems and its Application in High-impulse-voltage Measurements

a Generation of impulse voltage b Measurement of impulse voltage
1 Impulse-voltage generator 6 Voltage divider 2 Front capacitor
7 Measuring cable 3 Test object 8 Oscilloscope or digital recorder
4 Damping resistor 9 Screened chamber 5 High-voltage lead
10 Grounding system

A further example is shown in Figure 88 [111]. It is a broadband measuring system for transients from 1 Hz to 1 MHz. Use is made of a capacitive voltage divider C1/C2, what makes the circuit suitable for high voltage reasurements. The circuit generates output signals Uo which are replicas of the input signals.

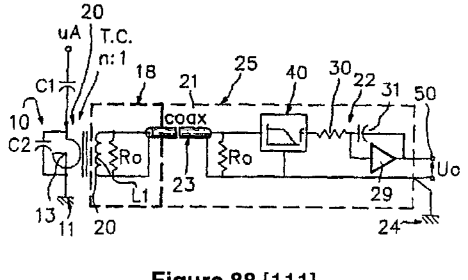

Figure 88 [111]

High Voltage Measuring Circuit Coupled to the Capacitive Grounding Tap Bushing of an HV Device

Very fast transients have been studied in a 765 kV substation, purpose of which is to determine the practical overvoltages that may occur in gas insulated substations during sudden voltage collapses in SF_6. The main cause of which are disconnector operations: when a disconnector switches an open ended busbar, a sequence of reignitions occurs, each reignition being at a different voltage level. In this way travelling waves are generated (Fig. 89) [112]. (The measurement system covers a signal bandwidth up to 500 MHz).

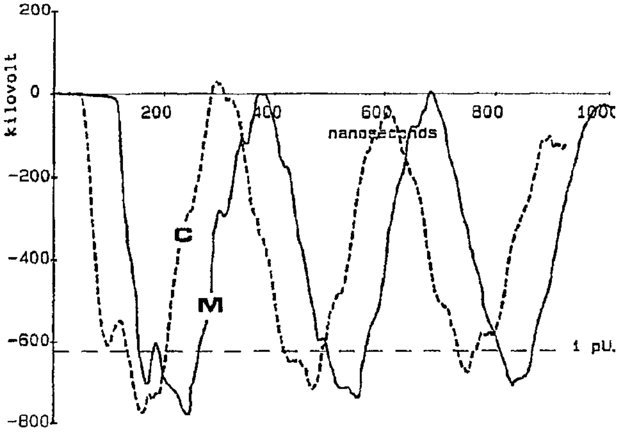

Figure 89 [112]
High Voltage VFT Measurements and Calculations in a 765 kV Pilot Installation
M : measured C : calculated

A voltmeter for remotely sensing high voltage impulses uses a condenser that is discharged through a spark gap. The frequency at which this occurs is a function of the voltage measured, and is displayed in volt. Radioactive material within the chamber insures a constant breakdown voltage (Fig. 90) [113].

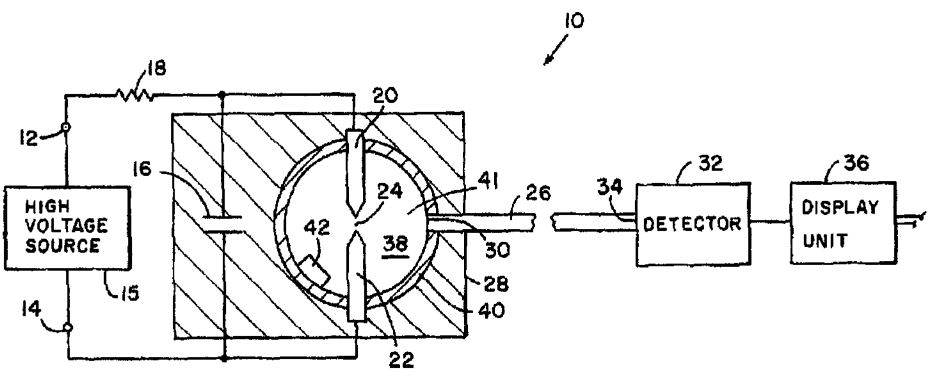

Figure 90 [113]
Voltmeter for Remotely Sensing High Voltages

2.1.5 Measuring dc Voltages

A recently developed method for measuring high dc voltages uses an electron speed-filtering system. Figure 91 [114] shows the experimental setup: non-energetic electrons are emitted by an electron gun and accelerated by a high-voltage U. The electrons enter the rectangular cavity resonator and are deflected by a microwave field of an $H_{1,0,p}$ mode due to Coulomb and Lorentz forces. At five discrete accelerating voltages between 40 and 100 KV the deflected electrons leave the cavity through a second aperture in the end face. They are detected with a Faraday cup (3). Experiments were carried out with a superconducting niobium cavity at LHe temperature.

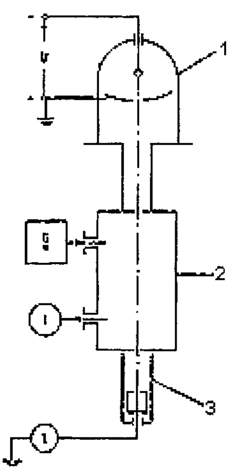

Figure 91 [114] ©1991 IEEE
Basic Arrangement of the Experimental Set-up
1) electron gun 2) speed-filter 3) detector

Figure 92 [115] shows a Kilovoltmeter based on electro-osmosis engendered by a strong electric field.

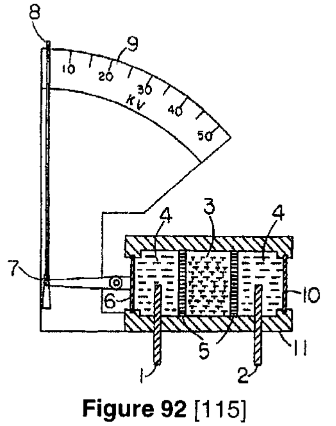

Figure 92 [115]
Electroosmotic Kilovoltmeter

Another simple equipment detects the existence of an unsafe voltage on mobile appliances. In Figure 93 [116] a metal plate (14) is mounted below the chassis (10) of the mobile cabin, and the voltage V3 between the plate (15) and the mobile cabin (10) is detected by a differential amplifier (16), that feeds a threshold detector (18) which senses when V3 reaches a level corresponding to a dangerous potential V2 between the cabin and ground.

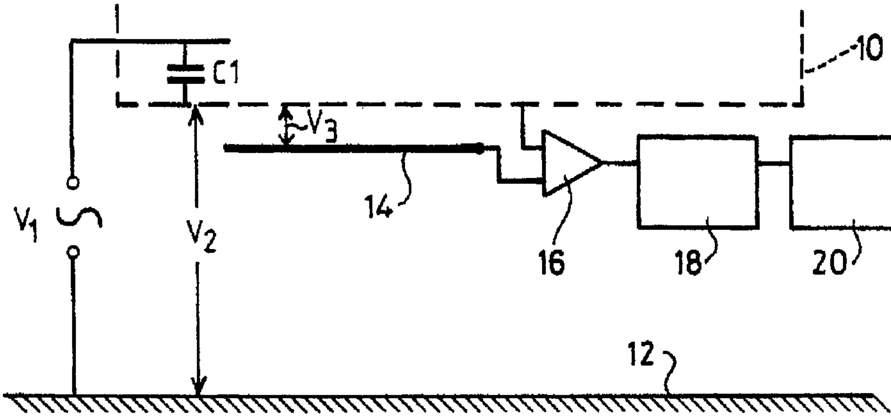

Figure 93 [116]
Detection of Unsafe Voltages on Mobile Equipment

Measuring dc voltage in a static convertor can be achieved according to Figure 94 [117]. Normally this dc voltage is measured by means of a sensitive voltage divider (4). Such a voltage divider is quite expensive so alternatives are welcome. The measurement can be supplemented using a capacitive voltage divider (6). The time derivative at variable dc voltage in cases of faults can be taken out from terminal (13). The dc voltage can be calculated using a wattmeter (7) on the ac line (10). The dc current is measured by a transductor (9) and a division circuit (8) yields the dc voltage under disregarding of all power loss [that can be calculated and taken into account].

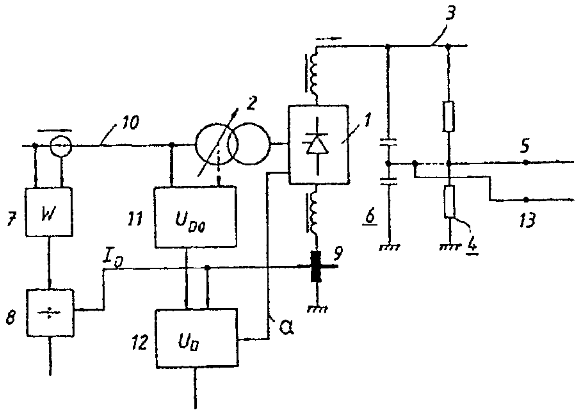

Figure 94 [117]
Measuring DC Voltage in a Static Convertor

Figure 95 [117] shows another method simulating dc voltage by means of a capacitive voltage divider in both ac and dc lines ((7) and (8)). Valve 1 is connected between these two lines. Tappings from (7) and (8) are connected to a voltage measuring device (9) to which there are also connected the control pulses for the valves (1) and (4) in phase R of the bridge. When valve (1) is conducting its voltage is zero while it has full voltage when (4) is conducting. The voltage between (7) and (8) is measured in (9) by switching on this element by the central pulses from valves (1) and (4). This yields two measuring values: the first corresponding to zero voltage and the difference between the two values corresponding to full voltage or mean value for the whole convertor.

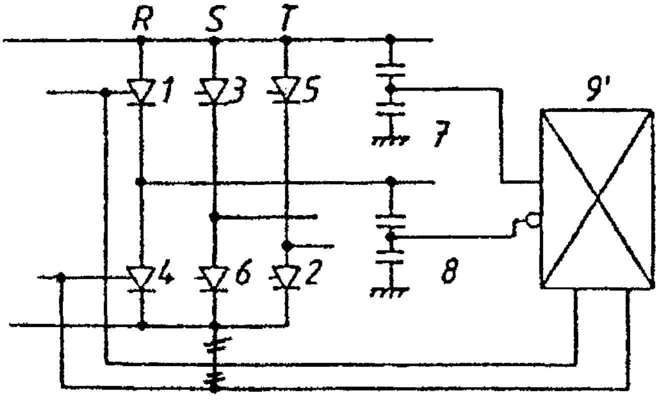

Figure 95 [117]
Measuring DC Voltage in a Static Converter (Diagram B)

Another subject is the detecting of a high voltage electric field. Figure 96 [118] shows a capacitive electric field sensor utilising a pair of electrodes shielding a device within the sensor which generates a signal responsive to the intensity of the electric field. This signal is transmitted by means of a fibre optic so as to isolate the sensor electrically. Other examples are [119] and [120].

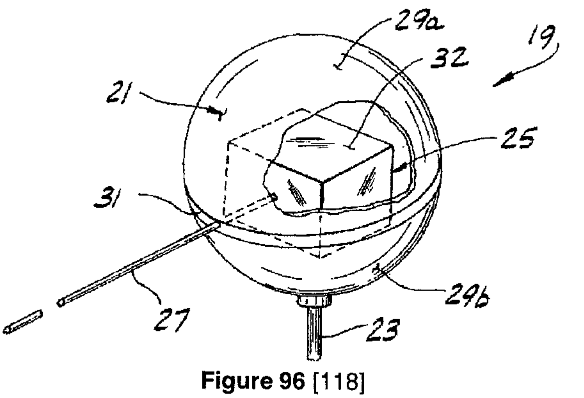

Figure 96 [118]
Apparatus for and Method of Measuring a High Voltage Electric Field

A differential static voltmeter senses the static voltage which occurs as a vertically oriented gradient in the earth's atmosphere [121]. The signal produced is a measure of the disposition of the probes relative to a line usually parallel to the earth's surface. This voltmeter is useful as a pitch and roll reference in airborne vehicles.

Surface potentials can be measured using an electrooptic element (22) with an electrode (24) facing the surface (20). An oscillator (35) and amplifier (25) are connected to a reference electrode (25) of the electrooptic element (22). The light transmitted by the crystal (23) of the element is measured by a photo element (30). A detector (31) determines the time at which the electrical field becomes zero and delivers a trigger signal to sample and hold circuit (32) that loads the momentary value of the oscillator (35). This value is output via circuit (33) (Fig. 97) [122].

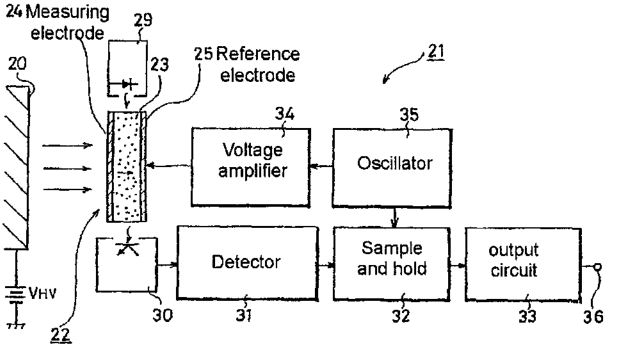

Figure 97 [122]
Surface Potential Measuring Sensor

Another optical electrostatic field apparatus uses a laser (1) and a sensor (3) surrounded by a polymer sheet (4) generating, under the influence of the field, the second harmonic of the light wave. Fibre optics (20) and (23) transport the incident and reflected waves of the laser (1) to the sensor (3) and further to the optical measuring system (7) - (10). This apparatus can be used for measuring the field between high voltage coaxial cables (Fig. 98) [123].

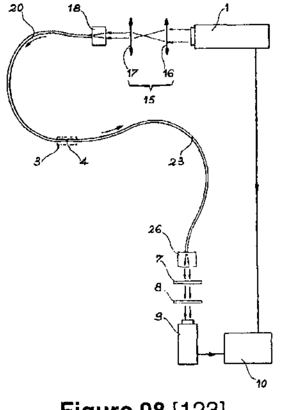

Figure 98 [123]

An absolute voltmeter measuring up to 30 KV within +/-0,3 % uses the electrostatic force on a movable disk [124]. The force on the disk (see Figure 99) is counteracted by a suspended weight of known value. Electrical strain gauges detect the difference between the two forces, and the spacings between the electrodes is adjusted by the micrometer head until the deflection is zero.

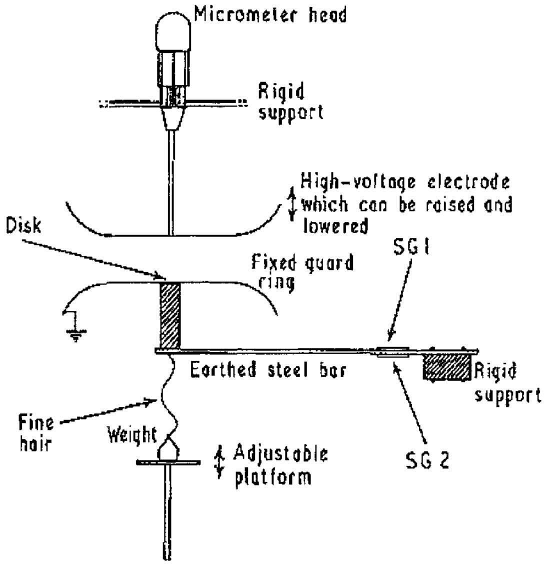

Figure 99 [124]
Principle of the Absolute Voltmeter

A high speed voltage follower employs a vibrating capacitance detector coupled to an electrode (86) carrying both wideband electrostatic ACC data and dc potentials, see Figure 5 [8]. A first feedback path is provided from the output of a high bandwidth amplifier 100 to the non-inverting input (94) of a detector (90) which provides both a signal which is equal to and follows the wideband electrostatic ac potential on the electrode (86), and a signal, at the vibrating capacitance modulation frequency, representative of the dc potential on (86).

A second feedback path includes a demodulator and integrator (124) to monitor the first feedback path to provide a dc connection to the amplifier (100) to null the signal on the first feedback path representative of the vibrating capacitance modulation of the dc potential. An electrostatic probe employs a vibrating transparent detector and is disposed in a path of radiation which is directed onto a measured electrostatic surface.

Figure 100 shows a pair of conductive spherical shells that are carried by a balloon into an electrical field which induces equal and opposing charges on the shells [126]. Rotation of the shells causes the charges to alternate. This signal is fed to an amplifier and then to a transmitter.

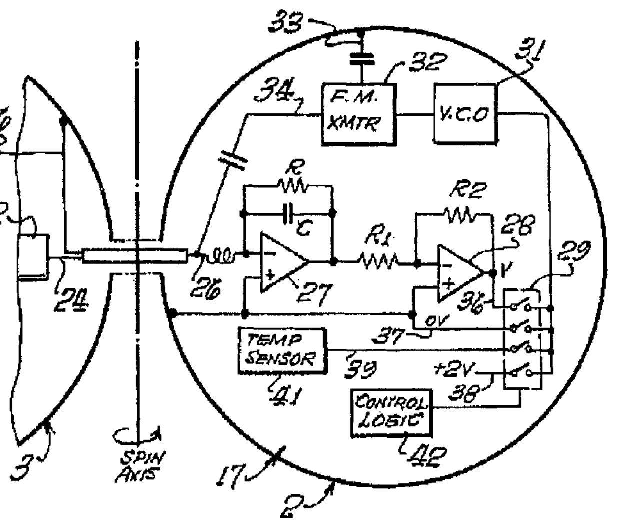

Figure 100 [126]
Electrical Field Sensing and Transmitting Apparatus

A panoramic electrostatic field sensor has a central electrode [127]. A for detecting a field about an 60° arc (see Figure 101). A housing (B) with windows (22) and (28) permits the electrode (A) to "see" the electrostatic field. A cap (C) with a slot (32) rotates between (A) and (B) and an amplifier (D) can activate an indicator.

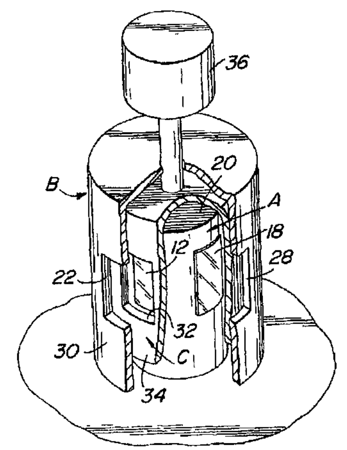

Figure 101 [127]
Panoramic Electrostatic Field Sensor

In Figure 102 [128] a turning fork is used to alternately couple and de-couple a sensitive electrode (6).

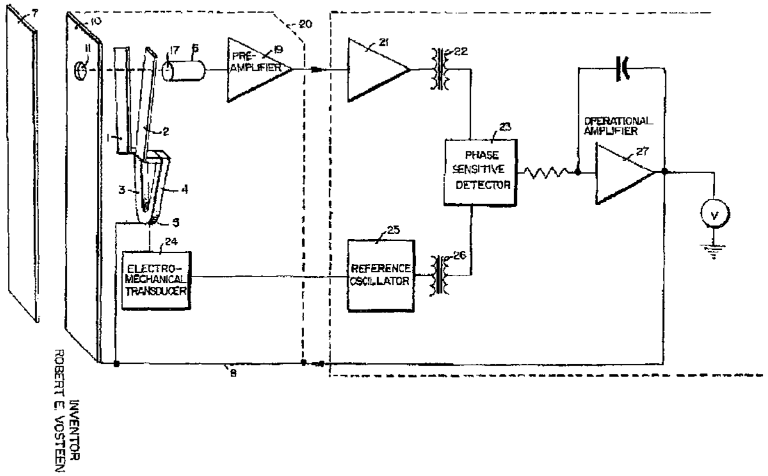

Figure 102 [128]

Electrostatic Field Modulator having a Tuning Fork

A rapid responding generating voltmeter [129] shown in Figure 103 and comprises two sets of stator segments. Each set has a time-varying capacitance but the sum is constant. Two circuits respectively sense the voltage (e_1), and (e_2) across the said capacitors and a summing circuit yields an output proportional to the high dc voltage measured.

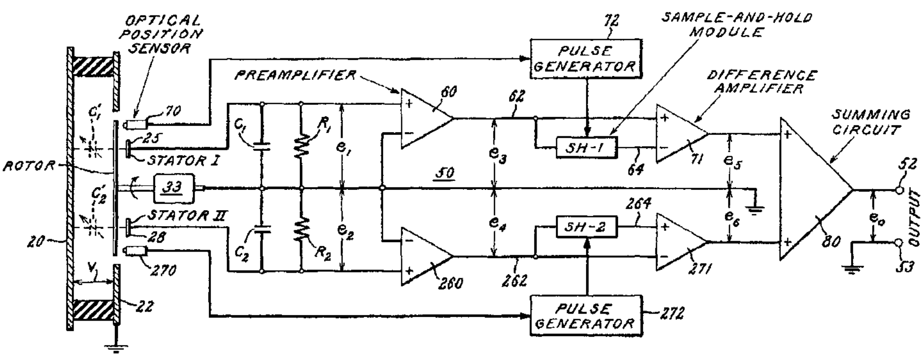

Figure 103 [129]

Arrangement for Measuring a Current

Further examples are described in [130] to [139].

2.2 MEASURING HIGH CURRENTS

2.2.1 Introduction

The classical way to measure high currents is by use of shunts, current dividers or current transformers. It is also possible to measure the magnetic field generated by the current to be measured, or to measure the force between conductors. Use also can be made of optical modulators influenced by the magnetic field created by the current.

2.2.2 Non-Electro-Optical methods

An example of a current divider is proposed in Figure 104 [140], where (1) shows a main conductor and (2) a measuring conductor, the current in which is proportional to the output Ua of the amplifier and independent of temperature.

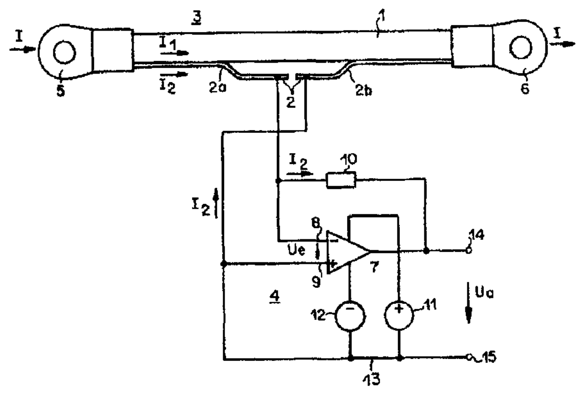

Figure 104 [140]

Another example shows the use of the force between conductors in order to measure the current. In Figures 105 [141] and 106 [142] the rails (2) and (3) carry each half of the DC current and the force is transmitted to a carbon resistance (9) acting as a force measuring cell.

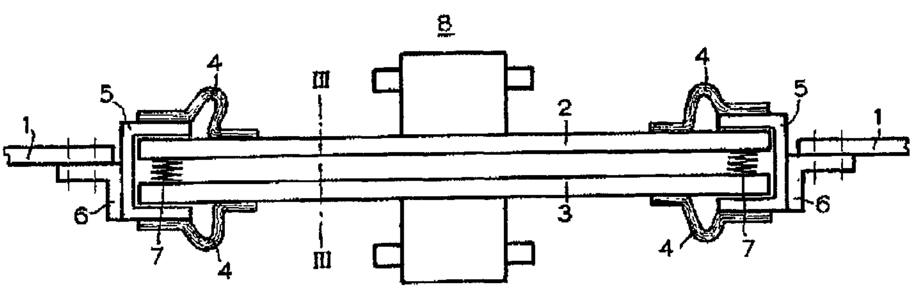

Figure 105 [141]
Current Sensing transducer for Power Line Current Measurements

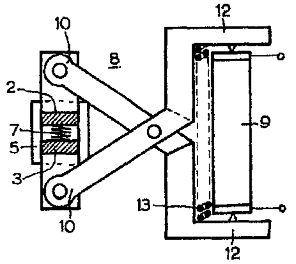

Figure 106 [142]
Current Sensing transducer for Power Line Current Measurements

[143] uses a current divider together with a compensated transformer (Fig. 107).

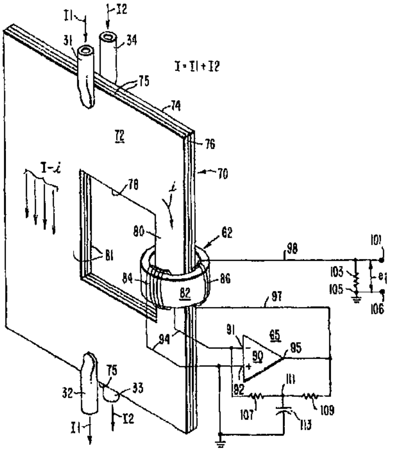

Figure 107 [143]
Simplified Block Diagram of the System for AC EHV Transmission Line

A resolution of better than 1 in a current of 200A was obtained by [144] using a SQUID sensor at 4° K. The ultimate resolution of this sort of system is discussed and found to be possibly one part in 10^8 with no constraints on the maximum current.

YIG-tuned devices (cf. ch. 1.2.13.3) are used in DC and AC transmission lines [145] see Figure 108. A YIG-tuned microwave oscillator is situated in the magnetic field created by the current to be measured. The oscillator frequency follows the line current variations linearly (see [146]). So, a FM signal is created that is transmitted and captured by a FM receiver.

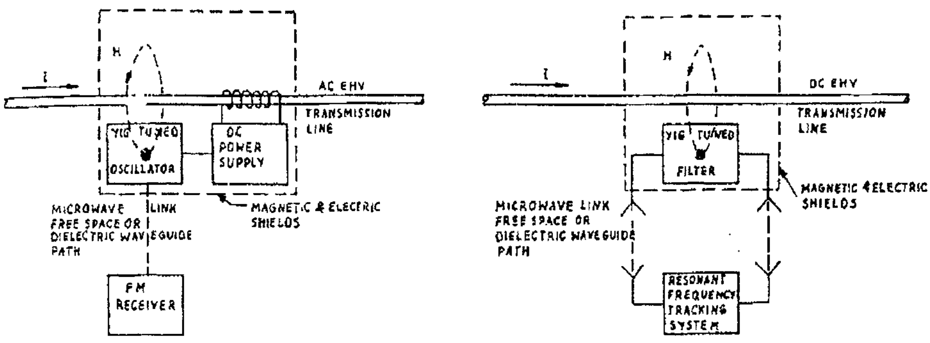

Figure 108 [145]

[71] describes a MNR (magnetic nuclear resonance) shunt for measuring high current. The temperature of a magnet (11) by the current to be measured is stabilised and the magnetic field at the centre of the magnet is measured by means of a MNR probe (Fig. 46).

A method to balance noise is described in [147]. In Figure 109 noise would normally be generated in the measuring circuit by changes in the magnetic field surrounding the conductor as a result of changes in current flow in the conductor. This would cause errors in the current measurement. A multi-turn coil is included in the measurement circuit in such a way that the voltage induced into the coil by changes of the magnetic field compensates the noise voltage induced into either part of the measuring circuit. The exact magnitude of the voltage induced in the coil is controlled by a variable resister so that it can be equated to the noise voltage.

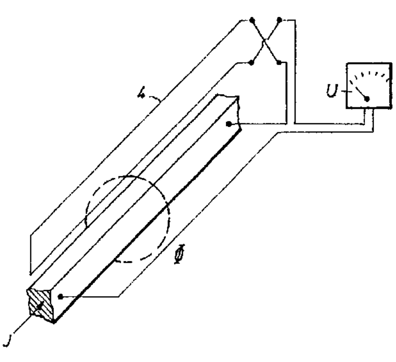

Figure 109 [147]

Apparatus for the Noise-Compensated Measurement of High D.C. Current

A similar technique is used in [148] in a welding machine (Fig. 110).

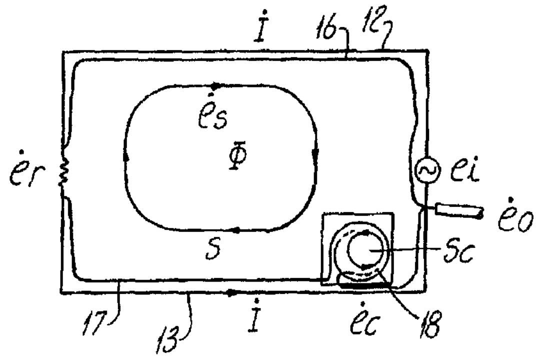

Figure 110 [148]
Measuring Current in Welding Machines

In [149] Hall generators are used to measure the magnetic flux created by the measured current (Fig. 111).

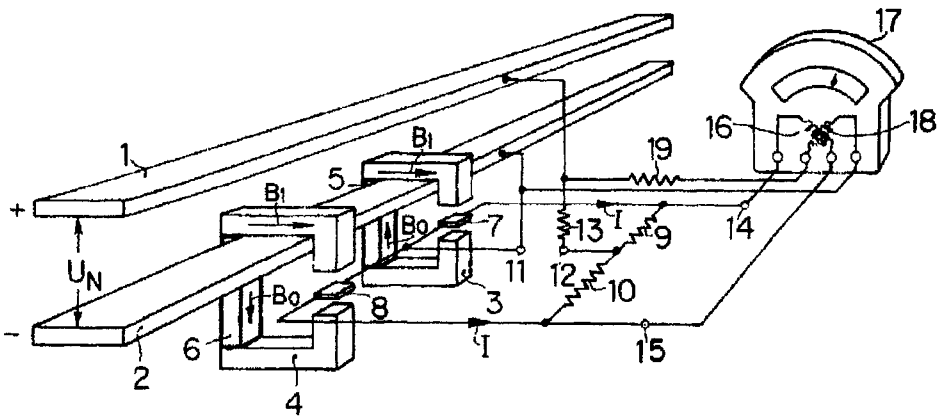

Figure 111 [149]

A compensation technique for measuring a DC current using a measuring transformer is described in [150]. A single-coil (Fig. 112) wound on a Ferrite core surrounding a current path is driven from a voltage controlled contact current source. The coil drive current is modulated with a fixed frequency squarewave. The average voltage across the coil is sensed and integrated providing an output signal proportional to the current being measured and also provides a negative feedback to the voltage controlled current source via the modulated drive current in a direction which compensates for the effects of the current flowing in the conductive path. Figure 113 gives further details.

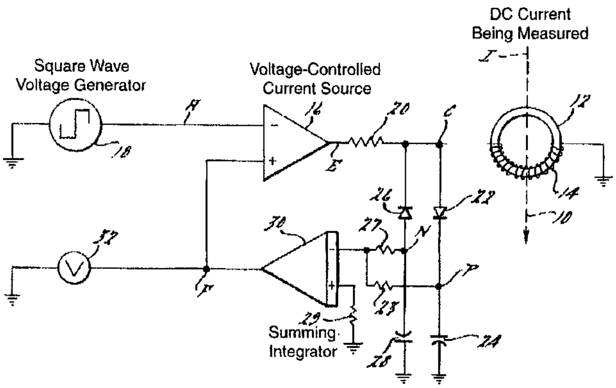

Figure 112 [150]
Single-Coil Current Measuring Circuit (Figure 1)

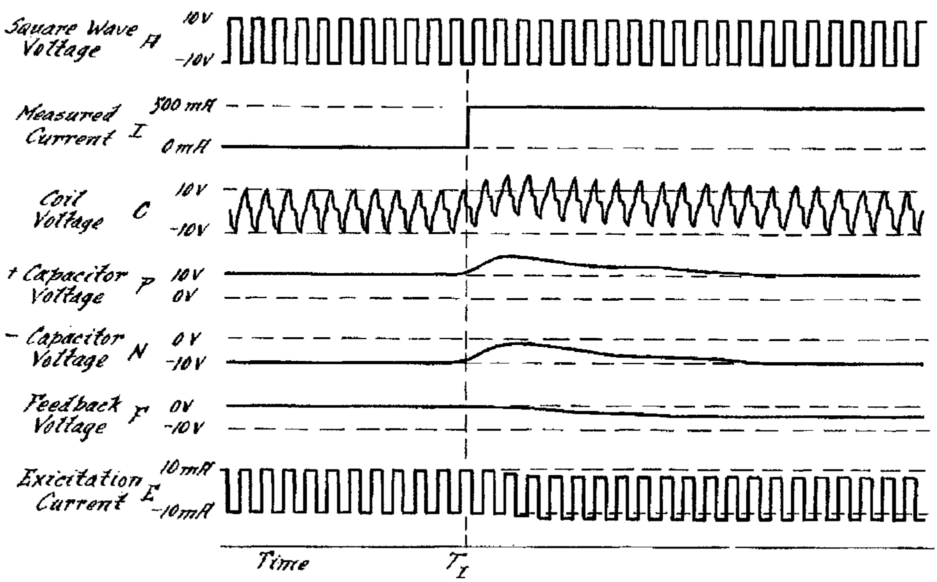

Figure 113 [150b]
Single-Coil Current Measuring Circuit (Figure 2)

A detector for indicating the occurrence of a surge current (Fig. 114) is described in [151]. Two clamps (18) and (19) make electrical connection with the conductor at two locations along its length. A rectifier (30) - (33) develops an actuator signal to drive an electromechanical counter (23).

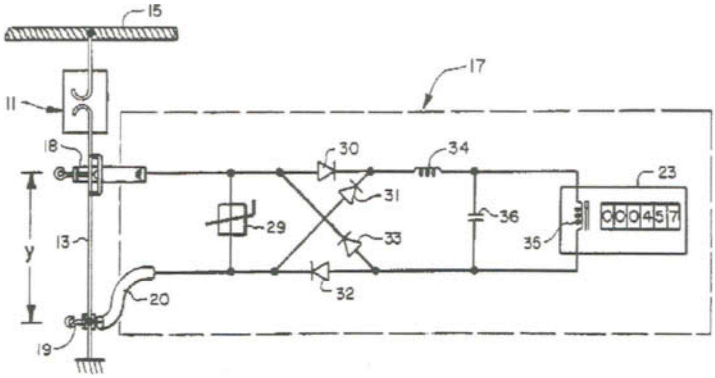

Figure 114 [151]

Linear Signal Isolator and Calibration Circuit for Electronic Current Transformer

[152] shows an optical data transmission system for use with current sensors on AC high voltage :ransmission lines (Fig. 115). The system uses a high-emitting diode transmitter, sending its signals via a filter optic light pipe to a photodiode receiver at ground potential, and to a silicon photodiode in a feedback configuration.

A DC reference signal is superimposed on the AC current data signal to provide system gain calibration. The DC signal is utilised, in a feedback loop, to control the gain of an AC signal amplifier in the 'eceiver and to thus stabilise system calibration.

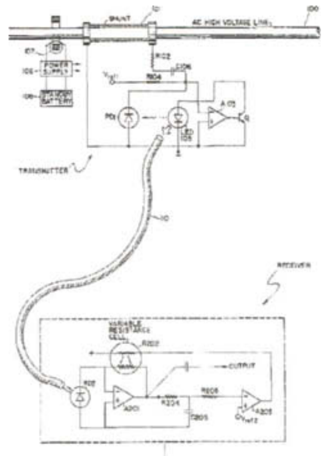

Figure 115 [152]

2.2.3 Faraday cells

Faraday cells (cf. Ch. 1.2.9.2) are a kind of magneto optic sensors. Just as Pockels cells they have the advantage of being non-conductive, they are relatively small and light, they do not exhibit hysteresis and they have a large dynamic range and frequency response. They sense the magnetic field surrounding a conductor, that is proportional to the unknown current (cf. Ch. 4.2.5.2, HALL ELEMENTS AND FARADAY SENSORS). Faraday sensors can be made of opto fibres or of solid crystals.

The **problems** associated with Faraday sensors are very similar to the ones of Pockels cell voltage measuring sensors:

Intensity variations due to e.g. temperature and mechanical influences on the actual Faraday cell or to associated optical components such as light sources (e.g. laser diodes), opto fibres, phase shifting plates and photo detectors (e.g. photodiodes).

Just as with Pockels cells, the output of the polarimetric measuring device is a periodic sinusoidal signal, with its low sensitivity around the extreme values, and its being non-monotonous.

The **solutions** giving better stability are similar to the ones being applied to Pockel devices: Using reference beams, normalising with DC components, measuring temperature and using a known relation of the temperature influence.

The extension of the **measuring range** beyond the half voltage is also being done in an analog manner compared to Pockels devices: Counting zero crossings, using two phase shifted signals, or employing two sensors with different sensitivity.

An arrangement combining temperature and/or vibration compensation, having a high sensitivity over an extended range of currents is illustrated in Figure 116 [315]

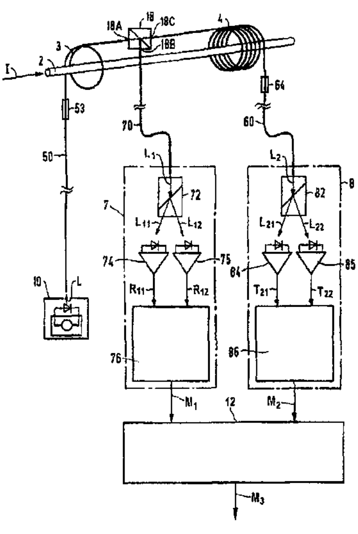

Figure 116 [315]

Faraday Device Combining Sensor Coils of Different Sensitivity

It employs two transmission mode Faraday sensors "3" and "4" made by annealed optical fibres with low linear birefringence and for practical purposes ignorable circular birefringence. The sensors have different sensitivities which can be varied by altering the number of turns.

The signals are intensity normalised in a conventional manner.

This device, which employs digital processing means and a look-up table, has a monotonous transfer function as seen in Figure 117 [315].

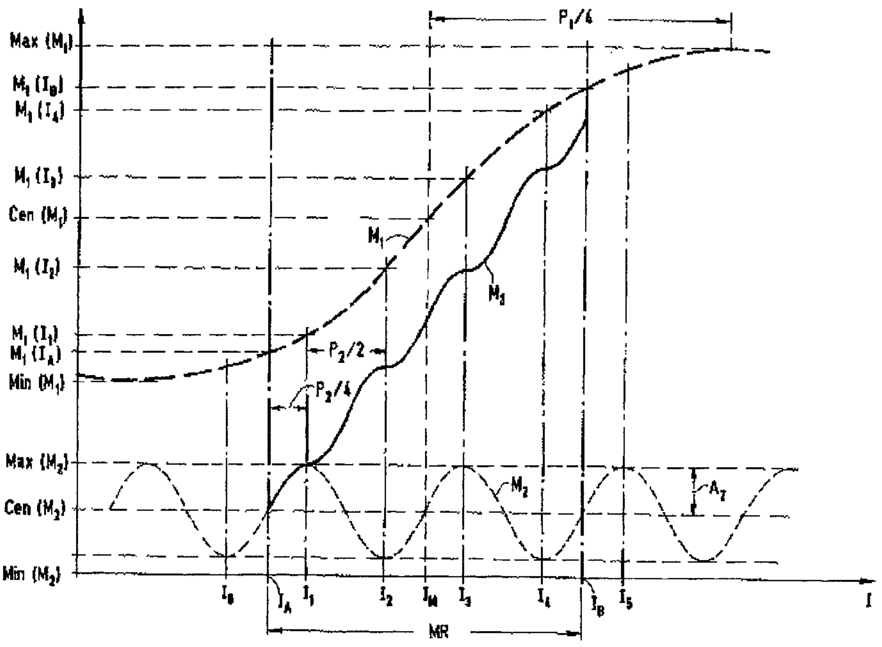

Figure 117 [315]

Waveform Diagram for the Device of fig. 116

M_1 is the signal obtained from the sensing coil "3". M_2 is the signal obtained from sensing coil "4". M_3 is the output signal.

Parallel to developing the optical and electronic signal processing means, a number of improvements of the actual sensors have been done:

In glass sensors the optimal, linear polarization state of the light beam can be disturbed at the reflection of the beam within the glass block, which can lead to a loss of sensitivity of the sensor and possibly to a non-uniform distribution of the sensitivities along the light beam paths before, between and after the reflection. If this occurs, the sensor becomes susceptible to current effects from external conductors, as well as from the conductor carrying the current to be measured, so that an accurate measurement cannot be obtained.

Figure 118 [316] illustrates a device capable of maintaining the linear polarisation state of the light beam after reflection irrespective of the input azimuth or of polarisation of the beam. The sensing glass block is shaped so that the light beam is incident on each of said further faces substantially along the normal to said face, thereby minimising reflection at the further faces and reducing polarization errors.

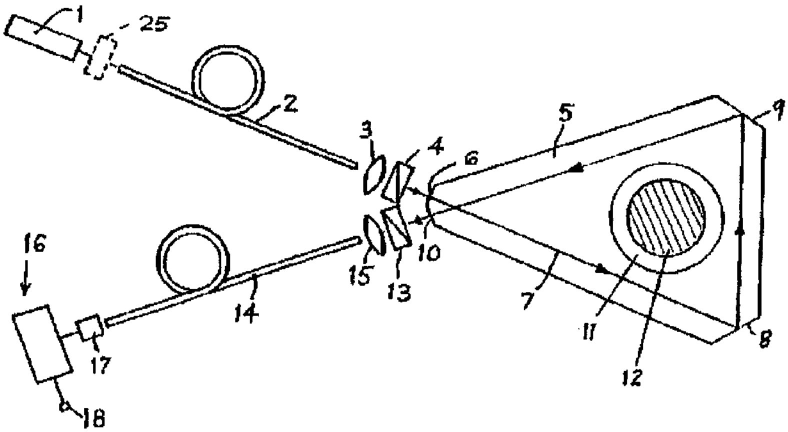

Figure 118 [316]
Polarisation Maintaining Faraday Sensor Geometry

This device can be made in two parts for easy mounting on an existing conductor.

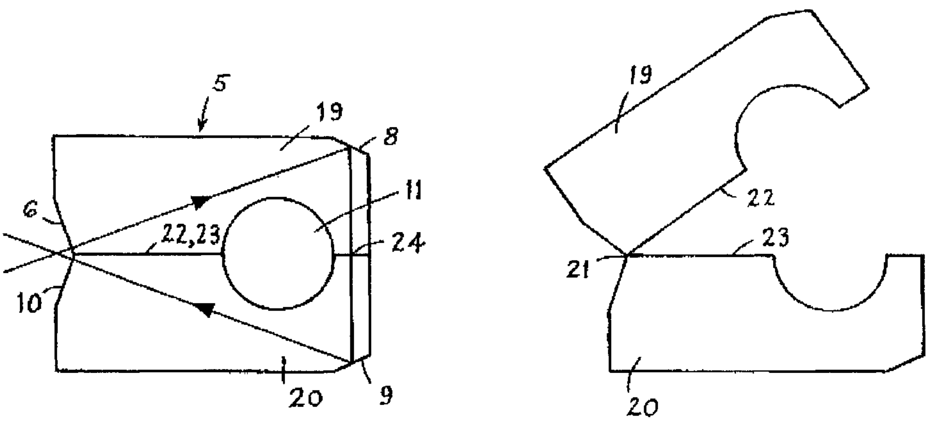

Figure 119 [316]
Demountable Faraday Sensor

[317] displays another design of a demountable Faraday sensor. See Figure 120 [317].

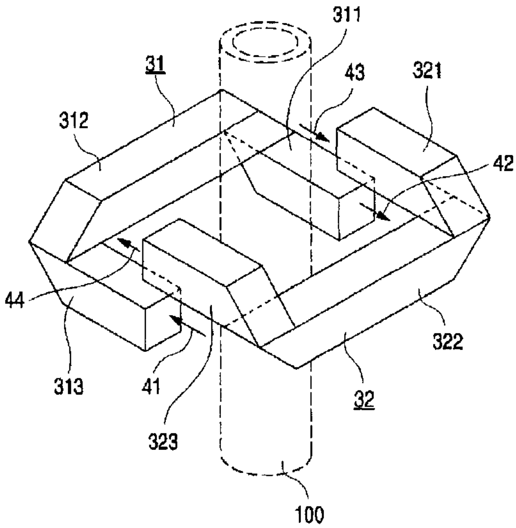

Figure 120 [317]
Demountable Farady Sensor

Elimination of an influence due to e.g. Pockels effect (sensitivity to the electric field) in a Faraday sensor can be done by arranging the light path as in Figure 121 [318].

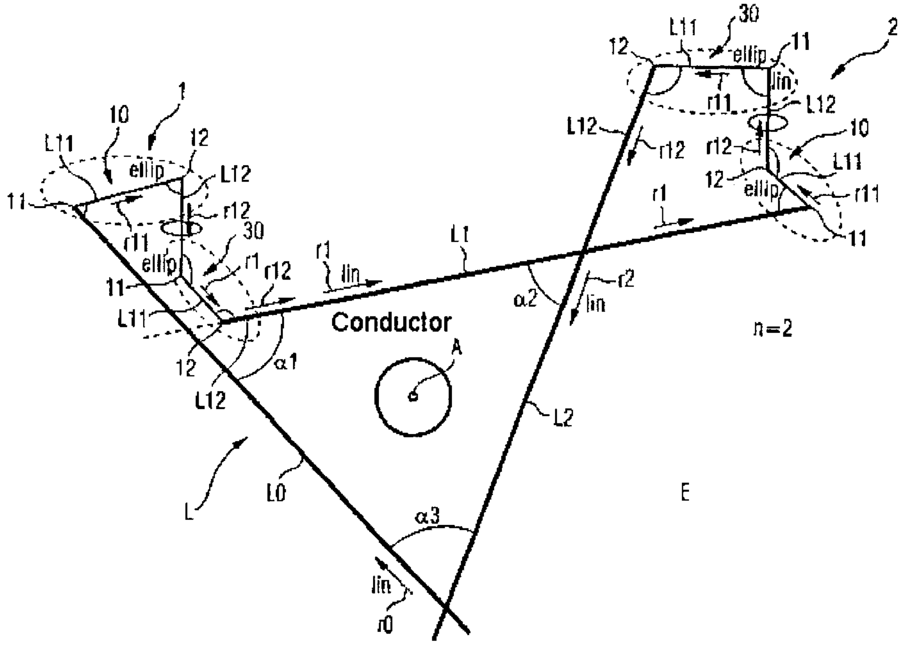

Figure 121 [318]

Faraday Sensor Light Path with Elimination of Pockels Effect Influence

The arrangement has a number of beam switching units (1,2..) corresponding to the number of corners the generated beam is to have. The first unit (1) is arranged in an input light beam of the predetermined polarisation and generates a first deflected output beam of the predetermined polarisation. The output beam propagates in a propagation direction which, together with the propagation direction of the input beam, forms a predetermined first angle associated with the first beam switching unit (1). The same happens for each successive beam switching unit.

Each unit is made up of at least two consecutive polarisation maintaining beam reversal units, at least one at the input and one at the output. A first beam fed from one of these unit in a correct propagation direction generates a first reflected beam propagating in a perpendicular direction. The first reflected beam generates a second reflected beam perpendicular to the first reflected beam and also to the first beam. A predetermined polarisation of the first beam is maintained in the second reflected beam. In each beam switching unit, the input or output beam and the input and output side beam deflection units are arranged relative to each other such that the propagation directions match.

CHAPTER 3

SHIELDING AGAINST INTERFERENCES

3.1 INTRODUCTION

Interference is a problem in many kinds of electrical apparatus. Most of the known solutions can be applied to equipments for measuring currents or voltages, but a few special considerations should be made. We must take precautions to keep the signal free of external influences which would corrupt the measuring result without noticeably changing the actual sensing of the variable to be measured. Very selective shielding procedures must thus be used.

The interference problem is different for measuring very small and very large values.

For small values of useful signals, we want to avoid all kinds of noise, even very weak ones.

This type of interference is examplified by Figures 126 and 127 below.

When measuring at high voltage or current levels weak interference is unimportant, because of the strong useful signals. Unfortunately, the electromagnetic fields are very strong, so capacitive or inductive coupling of unwanted signals to the measuring equipment easily occur. Shielding in this context is demonstrated in Ch. 3.2. We can also get so called self effects [301].

3.2 SHIELDING CURRENT TRANSDUCERS

An example with a current measuring transformer is shown in Figure 122 [300]. The disturbing capacitive coupling between the primary conductor and the transducer is eliminated by inserting a shield around the primary. This shield can be made of an electrically conducting material such as copper. The magnetic field, which we want to measure, is not affected.

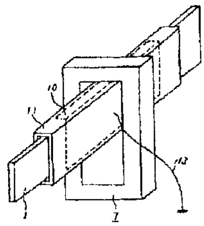

Figure 122 [300]

Electrostatically Shielded Current Transformer

The shield can serve as a capacitive voltage transducer. This is illustrated in Figure 123 [332]

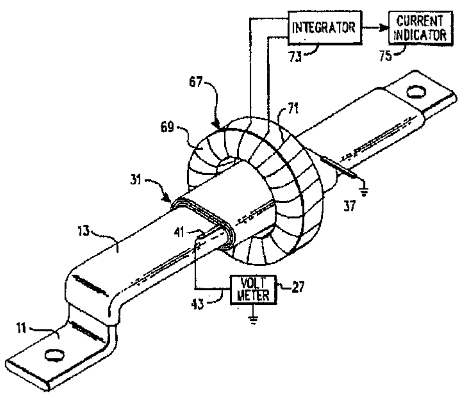

Figure 123 [332]

Integral capacitive divider busbar voltage measuring apparatus. - aligns mutual inductor sensor with integral capacitor divider so outer layer serves as voltage shield

The insulation layers 13 and 35 are made of identical electrically insulating material, however, the thickness of the second insulation layer 35 is substantially less than that of the layer 13. Furthermore, preferably the second conductive layer 37 is coextensive with the first conductive layer 15 so that the effective plate areas of the two capacitors are the same. Thus, the relative capacitance of the two capacitors 17 and 33 is related inversely to the relative thickness of the dielectrics and hence the capacitance of capacitor 17 is substantially less than that of capacitor 33 so that the voltage across the capacitor 33 as measured by the voltage meter 27 is a small fraction of the voltage between the bus bar 11 and ground. In the exemplary device, the thickness of insulation layer 13 is about 20 times greater than that of insulation layer 35.

The common plate of the two capacitors is connected to the voltmeter 27 through terminal 41 and lead 43, while the outer conductive layer 37 is grounded The current sensor comprises a mutual inductor 67 through which the bus bar passes. In the exemplary embodiment of the invention, the mutual inductor 67 has a toroidal low permeability core 69 on which the secondary winding 71 is wound. The bus bar 11 passing through the toroidal core 69 forms a one turn primary winding. As is known, such mutual inductors generate a voltage across the secondary winding which is proportional to the derivative of the current in the primary winding, in this case, the current in the bus bar 11. This secondary voltage is applied to an integrator 73 to produce a signal proportional to the current in the bus bar. This output of the integrator 73 is applied to a current indicating device 75. [332]

Instead of placing the electric shield around the primary conductor, we can put it around the secondary winding. Figure 56, (ch. 1.2.14.2) shows a "coreless" current transformer electrically shielded in this way. This transformer is additionally provided with a magnetic shield, 18, on the outside. The inside and the sides of the measuring coil are left exposed to the useful magnetic field emanating from the primary conductor.

A solution suitable for high current (>1000A) 3 phase systems is seen in Figure 124 [182]. This device includes a shield (50) of magnetizable material covering the part of the magnetic circuit (12) which is exposed to the neighbouring disturbing conductor. The shield does not cover the secondary winding (16), as this would have introduced an unwanted magnetic shunt.

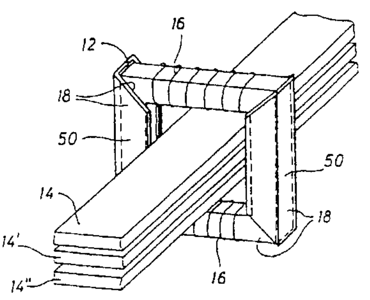

Figure 124 [182]
Magnetically Shielded Current Transformer

3.3 INTERFERENCE AND SHIELDING

Before developing on interference and shielding, we note that when it is not feasible to shield, or when the shielding is incomplete, one can measure the interference field separately, and then deduct it from the measured signal. In some cases the effort of measuring the interference is smaller than the one involved with shielding. We do not elaborate further on this subject.

With the **electro- or magneto-optic** sensors now being used for measuring voltages or currents, one must not only consider electric/magnetic interference, but also non-electric interference, such as pressure or temperature induced signals.

Interference from external magnetic fields (e.g. from adjacent conductors) on a Faraday current sensor can be minimized by making the sensing loop closed (closing the line integral in Ampère's law. Cf. equ. 72, page 150 and equ. 21, page 24) and protecting in- and output ports.
[340] describes how magnetic interference on a Faraday current sensor can be eliminated this way.

The optical sensors have certain advantages:

A Faraday current sensor is insensitive to the electric field and a Pockels voltage sensor is insensitive to the magnetic field. At least if we use ideal materials (cf. Ch. 2.2, Figure 121).

Electric conductors-acting as antennas- and parts will of course need to be protected as usual.

The **sensitivity** of electrical measuring systems to electromagnetic interference (EMI) increases due to the increasing complexity of circuits, higher sensitivity, higher speed and higher packing density [154].The most important measures to be taken against EMI are shielding, grounding, location of components, filtering and overvoltage protection.

It is important to consider the EMI problem during an early stage in design and to spend expensive engineering time to look at the minute details i.e. where components should be located; how the circuit wiring should be routed; what type of cabling and connectors should be used; and where cabling shields should be grounded [155]. An understanding of the behaviour of electric and magnetic fields is needed to solve the interference problem correctly.

Use can be made of lumped circuit elements to model how these fields behave and to gain insight into their qualitative behaviour and predict the dependence of the resulting interference on system parameters.
In this context, **noise** is defined as any signal other than the useful signal, and is composed of extrinsic and intrinsic noise. Intrinsic noise is for example Johnson noise in a resistor.

Extrinsic noise needs three conditions:

1. **A noise source**
2. **A coupling mechanism**
3. **A susceptible receiver**

If reduction of the noise source is not possible, usually its coupling can be reduced. Again these mechanisms can be classified in four groups:

1. **Conductive**
2. **Capacitive [Electric field]**
3. **Inductive [Magnetic field]**
4. **Radiative [Far field]**

An example of **conductive coupling** is signal and power return currents flowing through the same conductor (Fig.125) [155]. The solution is to isolate the signal, low level and high-level power supply circuits.

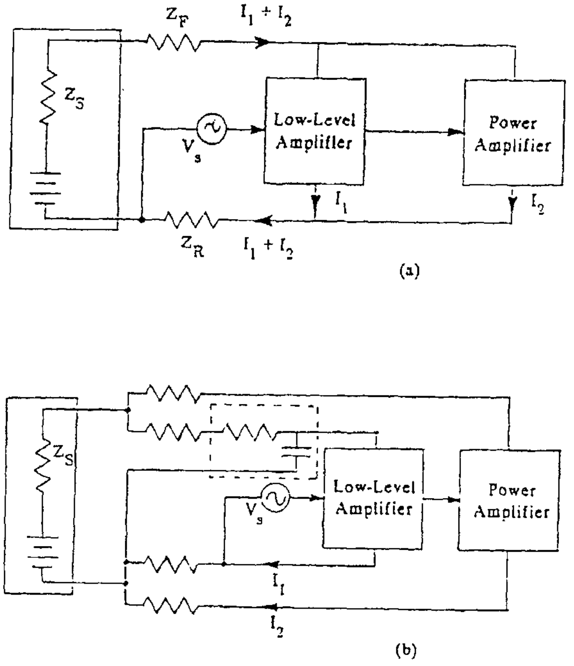

Figure 125 [155] ©1987 IEEE
Grounding and Shielding Electronic Instrumentation

Capacitive interference from coupling with an earth current is shown in Figure 126 [156], where a sensor (MU) and an input amplifier is shown. The housing of the sensor (MU) has to be connected to earth (E1), the housing of the input amplifier may not be earthed, but has a certain capacitance to earth (here (E2)). In industrial environments currents always circulate in earth so there is a potential difference between (E1) and (E2), that is represented here by (U_o), creating an AC current via (C1) - (C4) and a faulty AC voltage over the input resistor (R_e). This voltage is fully amplified and must be kept low, even in case damping arrangements are used (Fig. 126). This is done by arranging for that C1 = C2 and C3 = C4, and keeping them small, twisting the conductors, and having a big distance from earth.

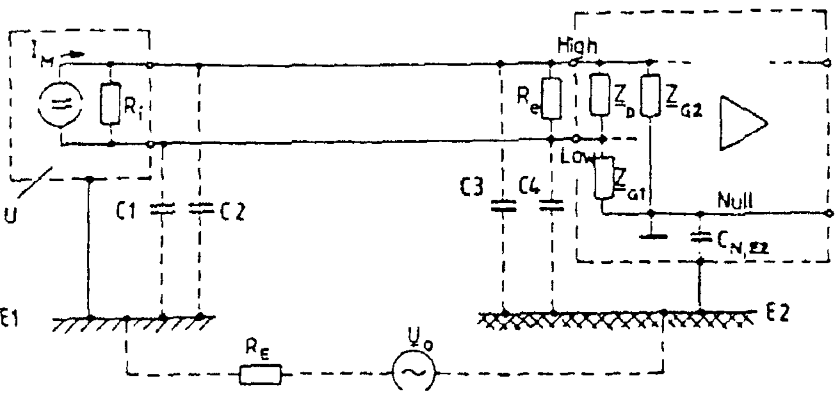

Figure 126 [156]
Capacitive Coupling

Inductive interference is shown in Figure 127 [156].

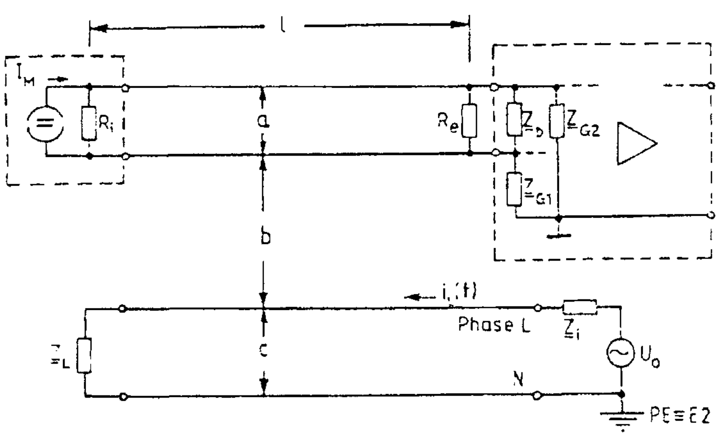

Figure 127 [156]
Inductive Coupling

A source is feeding the load (Z_l), creating a fault voltage

$$U = M\frac{di}{dt} \text{ wherein } M = \frac{\mu_o - 1}{2_n} \ln \frac{1-\frac{a}{b}}{1-\frac{a}{b}-c} \tag{59}$$

To limit the interference, the distance b has to be maximised and a and c have to be minimised. A further limitation of both capacitive and inductive interference is obtained by twisting the signal leads some 30 times per meter.

Radiative interference is dealt with in [157]. Here a noise source emits electromagnetic waves, captured by a receiver-circuit. The induced voltage is

$$V_o = |E_o| \cdot h_{eff} \tag{60}$$

wherein h_{eff} respresents the effective antenna length (Fig. 128) [157].

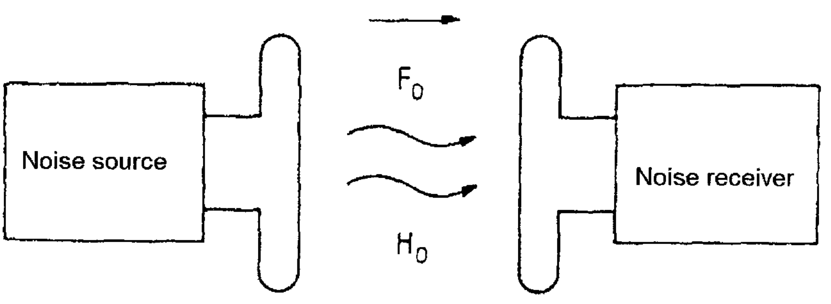

Figure 128 [157]
Radiative Interference

Electromagnetic interference (EMI) can be suppressed by an enclosure [158]. The amount of EMI suppression is termed shielding effectiveness (SE). The SE is determined by the material and construction, seams and apertures and also by the EMI sources and receptors [159].

Figure 129 [160] shows an electrostatically shielded indicator (7) having its pointer shielded by an unipotential element enveloping the pointer. The pointer moves between two parallel, spaced strips of electrically conductive glass connected together.

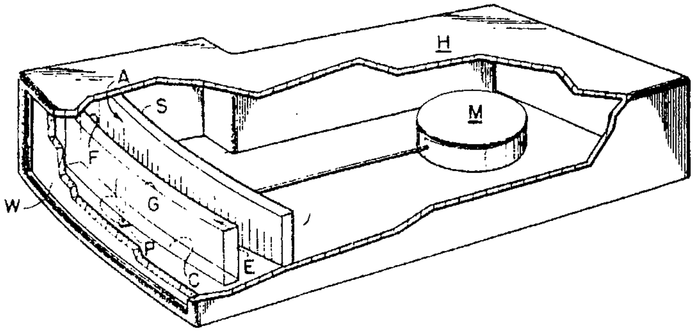

Figure 129 [160]
Electrostatically Shielded Indicator

Another example is shown in Figure 130 [161], where an antistatic test mask (with a number of openings through it for access of test probes) is used.

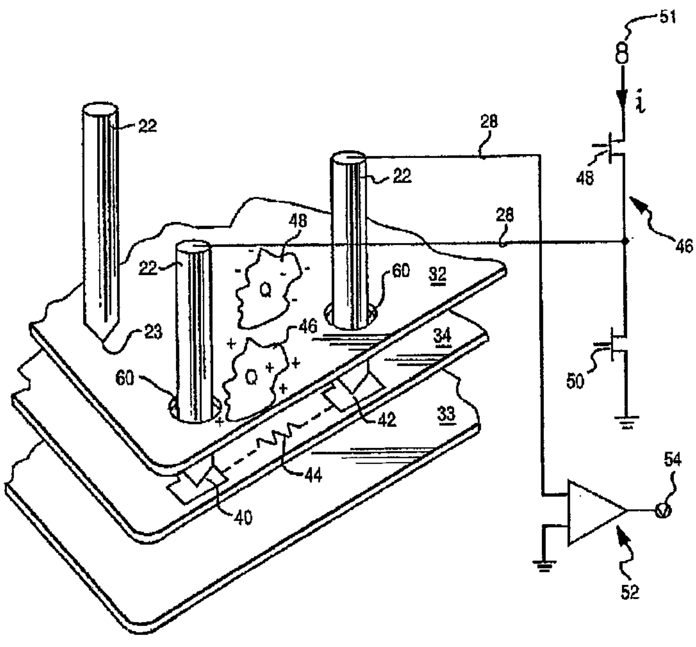

Figure 130 [161]
Antistatic Mask for Use with Electronic Test Apparatus

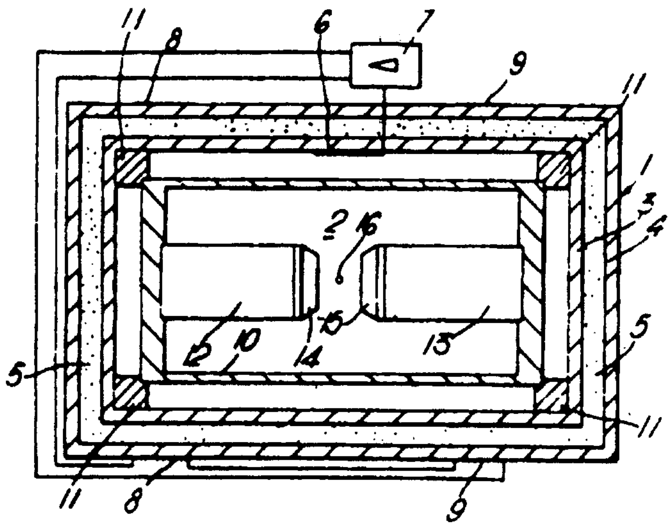

Figure 131 [165]
Magnetic Shield Arrangement for a High Flux Homogeneous Field-Producing Magnet

Magnetic shielding is illustrated by reference [162] to [173]. Reference [163] refers to the use of diamagnetic materials for shielding. Reference [165] shows in Figure 131 an enclosure used in a nuclear magnetic resonance spectrometer requiring constant magnetic field conditions. A coil is mounted around the enclosure for maintaining a constant magnetic field within the enclosure when a field correcting current flows in the coil. A transducer is positioned inside the enclosure for providing a signal responsive to the departure from the constant field condition, and an amplifier is coupled to the transducer and coil for delivering the field correcting current to the coil in response to the signal from the transducer.

Reference [172] describes a high -Tc oxyde superconductive magnetic shield, working at 77K. The attenuation of the magnetic field is good enough for neuromagnetic measurements with a SQUID magnetometer.

PCs are easily transformed into powerful measuring instruments through hardware upgrades. An external chassis for I/0 modules provides the greatest accuracy because sensitive acquisition hardware is isolated from noise within the PC enclosure [174].

In [175] a laminate is used for protecting the electric components (Fig. 132) [175]. The laminate has the form of a plurality of layers which give protection against electromagnetic radiation and also permit thermal management control of the printed circuit board. Reference [176] uses time filtering of spurious pulses by means of timing circuits. Spurious pulses are suppressed in a duration range of from nanoseconds to milliseconds.

Figure 133 [177] shows a well-designed chassis that shields instruments from external noise and reduces internally generated noise.

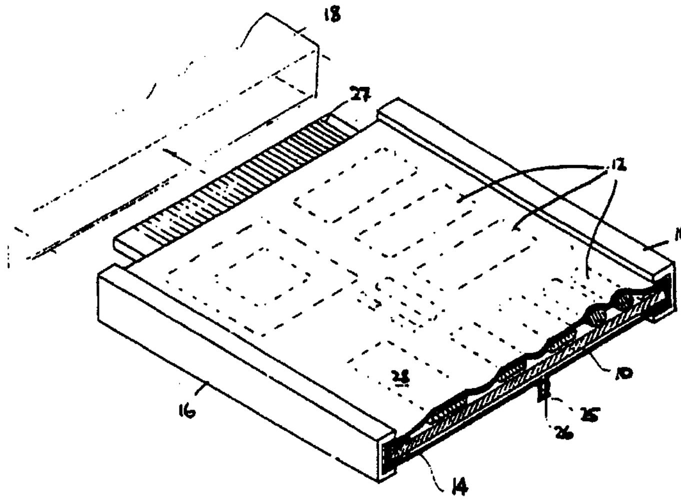

Figure 132 [175]
Circuit Protection Apparatus

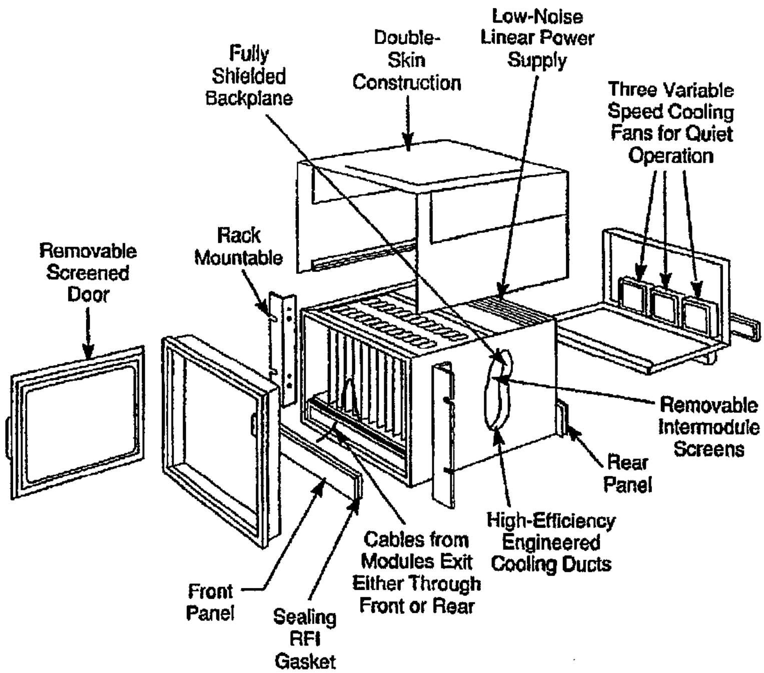

Figure 133 [177]
VXUbus Meets the Needs of RF ATE

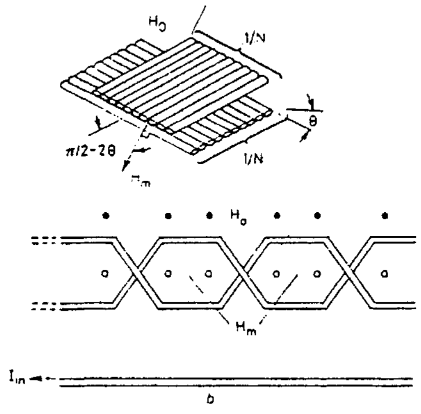

Figure 134 [178]
Principles of Coupling

Shielded coaxial cables are described in reference [180]. Imperfect shields coupling mechanisms are illustrated in Figure 134 [178]. Transfer admittance coupling may be represented by a through capacitance between the centre conductor and the exterior return path. On the other hand transfer impedance may be represented by a mutual inductance which couples exterior fields to the interior and vice versa. Shielding of HVDC transmission lines by parallel shield wires is described in [181].

Figures 135 and 136 [181] show the shield wires in a test site.

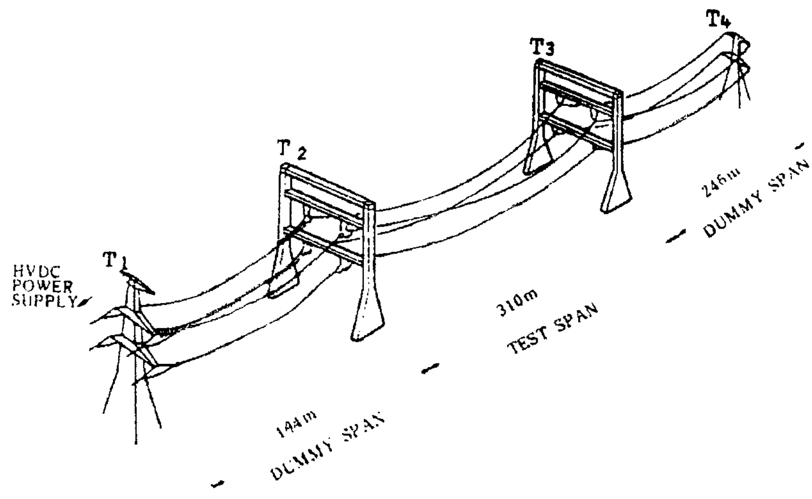

Figure 135 [181] ©1989 IEEE
Shiobara HVDC Test Line (Bipolar Double Circuit Line)

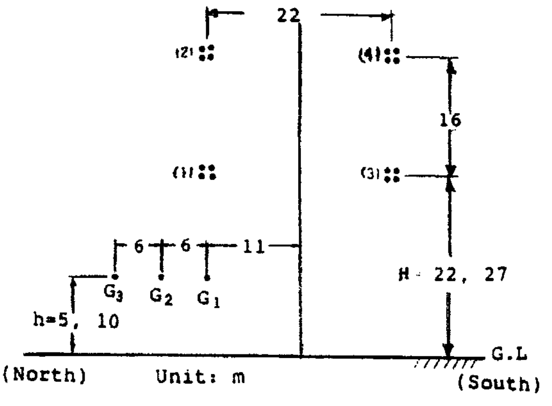

Figure 136 [181] ©1989 IEEE
Arrangement of Shield Wires under HVDC Test Line

G1, G2, G3 : Shield Wires
(1), (2) (3), (4) : 4 x 3.84 cm
(Conductors of test line)
(1), (4) : -650kV, (2), (3) : +650kV

A current transformer is shielded by ferro- or ferrimagnetic material (Fig. 124) [182] above.

Figure 137 shows a thermal and electromagnetic shield for a power meter [183]. The shield comprises a metal-organic laminate of black and white polyester layers bonded to both sides of an aluminum foil.

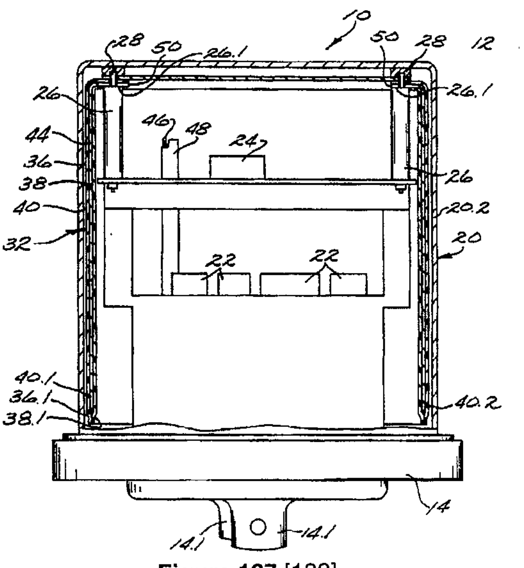

Figure 137 [183]
Thermal and Electromagnetic Shield for Power Meter

References [184] to [191] describe screening plastics for EMI shielding. Plastics are transparent to electromagnetic interference and thus require special treatment to protect against this growing and hazardous form of "air" pollution.

Another technique reducing electromagnetic interference [192] is shown in Figure 138. EMI absorbing material, e.g. in the form of split ferrite cores is fixed in holes stradling the protected conductor path. A clip is used to secure the EMI-absorbing material. No soldering or special tools are required.

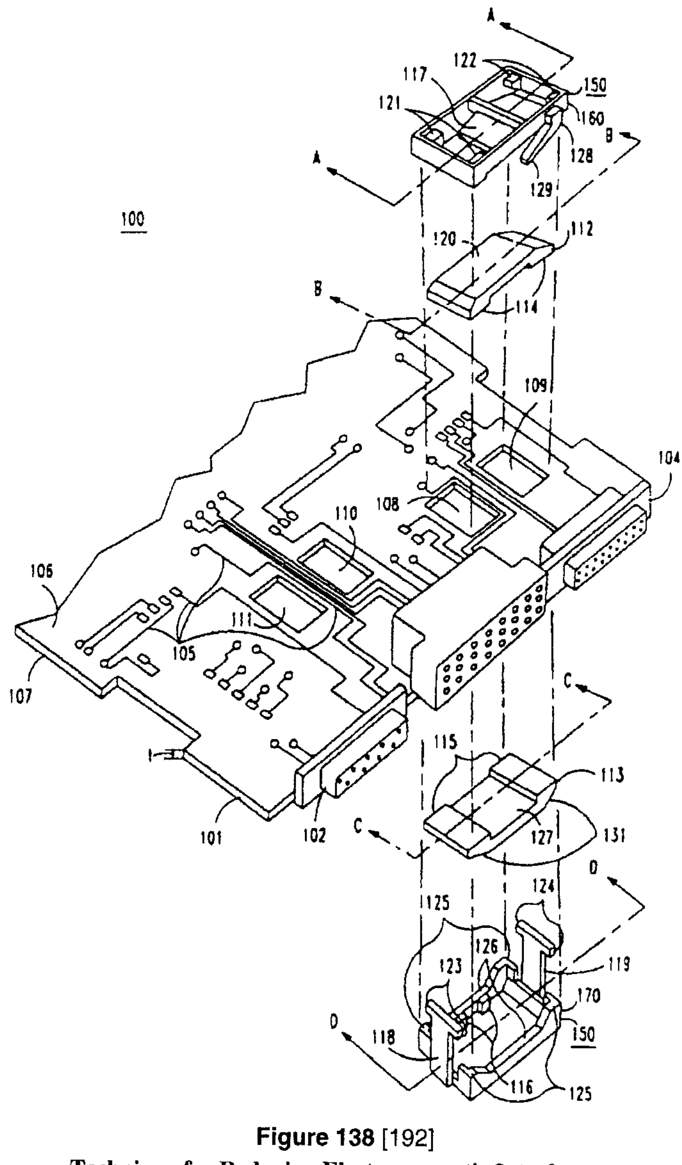

Figure 138 [192]
Technique for Reducing Electromagnetic Interference

References [184] to [191] describe screening plastics for EMI shielding. Plastics are transparent to electromagnetic interference and thus require special treatment to protect against this growing and hazardous form of "air" pollution.

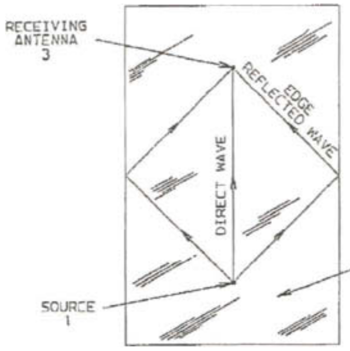

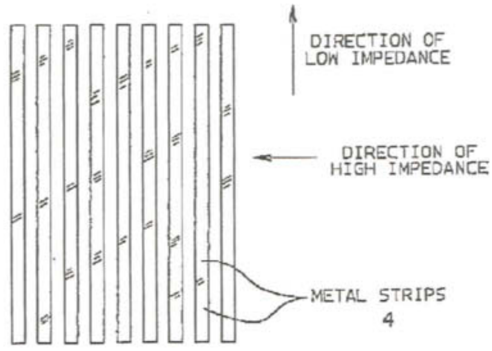

Figure 139 [193]
Conventional Ground Plane

Figure 140 [193]
Grated Ground Plane

Courtesy of International Business Machines Corporation

Another technique reducing electromagnetic interference [192] is shown in Figure 138. EMI absorbing material, e.g. in the form of split ferrite cores is fixed in holes stradling the protected conductor path. A clip is used to secure the EMI-absorbing material. No soldering or special tools are required.

A **ground plane** [193] constructed of parallel metal strips reduces reflections of electromagnetic waves

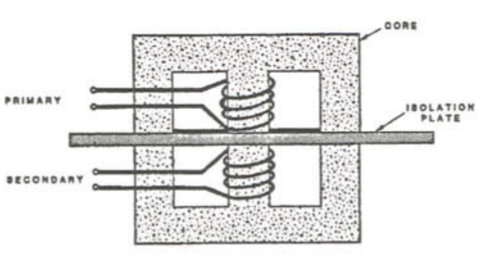

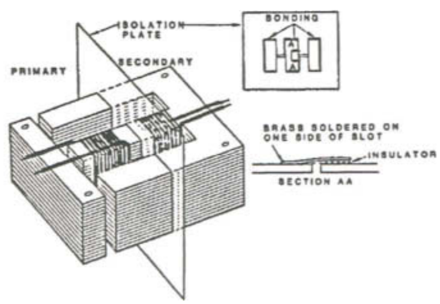

Figure 141 [194] ©1985 IEEE
EMP Isolation Transformer

Figure 142 [194] ©1985 IEEE
EMP Isolation Transformer Concept

*) Reprinted by permission from the IBM Technical Disclosure Bulletin, copyright 1989 by the International Business Machines Corporation.

Reference [195] describes the **measurement of shielding effectiveness** in superconductive composites. The recent advent of high temperature superconductors has opened the door to a wide range of research. The Meissner effect, which states that superconductors are perfectly diamagnetic, suggest shielding applications. A flanged coaxial test fixture (Fig. 143) was selected to measure the shielding effectiveness of $YB_{a2}Cu_3O_{7-x}$.

This design allows for circulation of liquid nitrogen inside the fixture, so as to maintain the sample below its critical temperature.

The sample splits a 50 Ω coaxial line in two, and the insertion loss is being measured to assess the shielding efficiency of the sample.

The result of the test indicate that there are remaining problems to be solved when testing super conducting shields.

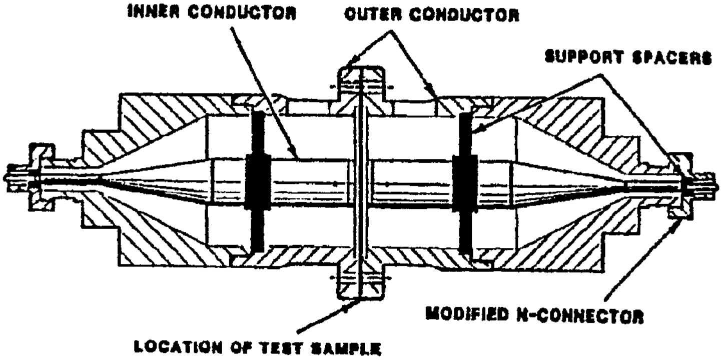

Figure 143 [195] ©1989 IEEE
Flanged Coaxial Test Fixture

For **low-current** applications the technique of **guarding** will minimize the current leakage:
A conductor surrounding, or arranged adjacent to, a low current line or conductor is maintained at the same potential as the line or circuit.
Shielding, guarding and the use of kelvin connections for low-voltage measurements are for example discussed in [302]

This Page Intentionally Left Blank

CHAPTER 4

MEASURING POWER

4.1 INTRODUCTION

By "power" we mean the product of current and voltage, measured in Watts. The word is often used when referring to energy (power x time, Ws) in conjunction with electricity consumption and utility meters. It is also used to express the proportion of signal power that falls within a certain frequency band, "spectral power" (e.g. in %), of a complex signal.

A Watt hour energy meter is a power meter with an integrating component added. Therefore energy meters are also treated in this chapter, when measuring power is the essential characteristic.

Most common power meters are ac instruments, or work both for ac and dc. Some dedicated dc instruments are treated below.

Power can be sensed directly, e.g. with Hall or thermal devices, or indirectly via combined current and voltage measurement.

4.1.1 Definitions

This chapter treats mainly currents at utility power frequencies (50-60HZ). Let us recall some definitions (sinusoidal voltage and current in a 2 phase current).

Instantaneous Power	$p(t) = u(t)\, i(t)$		**(61)**
Apparent Power	$S = U\, I$	[W]	**(62)**
Active Power	$P = U\, I \cos\alpha$	[W]	**(63)**
Reactive Power	$Q = U\, I \sin\alpha$	[VAr]	**(64)**
Power Factor	$\varphi = \cos\alpha = P/S$		**(65)**
Average Power	$p_{av} = 1/T \int_0^T u i\, dt$	[W]	**(66)**

where

U = effective voltage [V]

I = effective current [A]

α = phase angle between voltage and current

u = instantaneous voltage [V]

i = instantaneous current [A]

φ = power factor

Power Vector $S = P + j\,Q + kD$ (j,k are imaginary unity vectors) **(67)**

$|S|$ = Apparent Power [VA]
P = Active Power [W]
Q = Reactive Power [VAr]
D = Distortion Power [VA] (contribution from distorted wave forms).
If voltage and current have the same waveform D = 0. Then $P^2 + Q^2 = S^2$

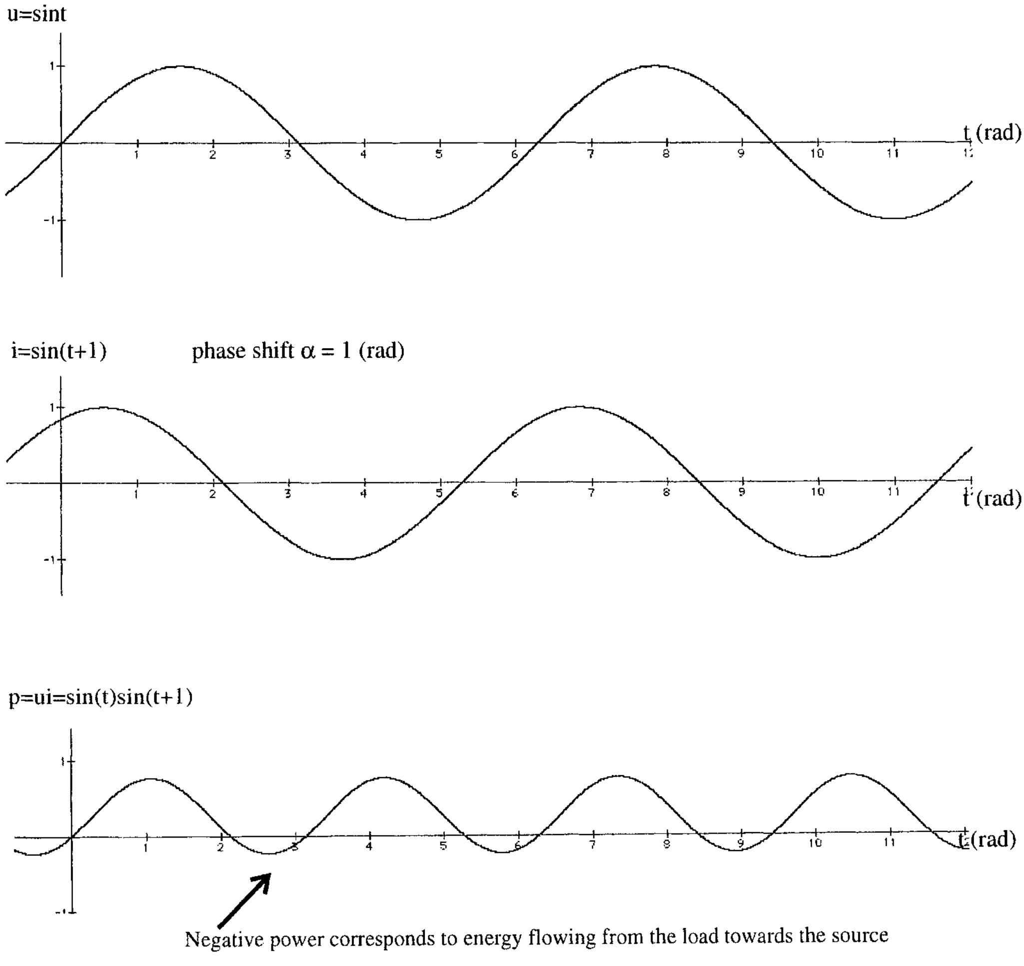

Figure 144
Voltage, current and power wave forms

The definition of time-dependent electric power consumed by a load is: p(t) = i(t) u(t). One can measure p(t) directly, or measure i(t) and u(t) and multiply them.

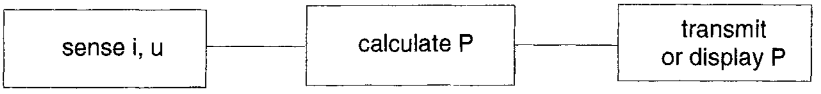

Figure 145

Measuring i and u and multiplying in real time is theoretically straightforward, but turns out to be difficult to do.

Digital technology performs this by sampling, more or less simultaneously, the current (i) and the voltage (u), and then multiplying the samples pair wise (Fig. 146) [196]. The illustrated device additionally averages the power-value.

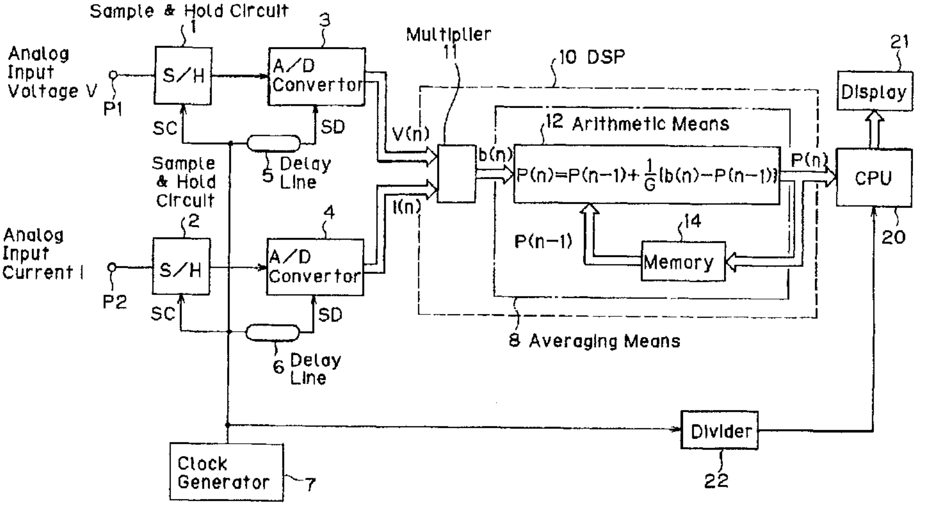

Figure 146 [196]

Sampling Type Power Measuring Device

A sampling type power measuring device measures an analog input signal by performing sampling on the analog input signal converting each value picked up by sampling into digital form and processing the digital values. Exponential averaging calculation is performed directly on the digital values; therefore no provision nor time is needed for regulating a sampling period this shortening the time of measurement.

4.2 MEASURING PRINCIPLES

4.2.1 Overview

The standard methods for measuring power are:

- Measuring a non electric effect of power absorption.
- Measuring an electric effect of power absorption.
- Using the exponential or square-law characteristics of semiconductors, and applying Ohm's law.
- Measuring current or voltage, knowing the impedance.
- Measuring current and voltage separately, and multiplying the values.

A digital DC-power meter works like its AC-cousin but with DC-sensors: Measure i and u and multiply.

In order to achieve a high accuracy in measuring on AC signals, high speed sampling and large range analog to digital converters (ADC's) are required. Such a meter, although simple in principle, becomes expensive. Even at lower precision, an electronic meter is costly due to components such power supply, protection elements, sensors and shielding.

This is one of the reasons for inventing other, cheaper designs. Others being linked to aspects like maintenance and compatibility with existing systems, components and standards

Compensation for non-linearity of the transducers is implemented in precise instruments.

Using the data on t, p, i and u, combination instruments, like those just cited in [196], elaborate information such as average power (Pave $=1/T\int I(t)\, u(t)\, dt = I\, V \cos\alpha$ [VA]), reactive power (IU sin α [VAR]),maximum power and consumed energy.

An elementary analog device can function as in Figure 147 [198].

High frequencies are usually measured via diode detectors or by thermal methods.

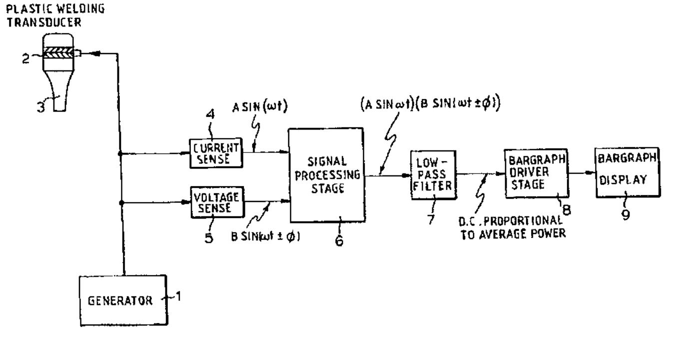

Figure 147 [198]

Indicating Power Developed by Ultrasonic Transducer

Analog device for measuring and displaying power supplied by a generator to a plastic welding transducer. Note the similarity with the digital power meter of fig. 146.

4.2.2 Direct Sensing Of Power

4.2.2.1 Measuring a Non-Electric Effect of Power Absorption

Non-Thermal Methods

Most fluids have variable states of their constituent atoms or molecules such that when energy is applied, visible spectra may result. These could be, for example, emission, absorption or fluorescent spectra and may be discrete or continuous. By using certain characteristics of the spectra an indication of power levels may be given. A spectrum may be produced by electrons changing state and emitting or absorbing photon, or also, in the case of molecules, by interactions of rotational and vibrational states with incident energy [207].

Figure 148 [207] exploits the phenomena of power dependent light emission in an absorbing gas, and detects the light with a photo detector.

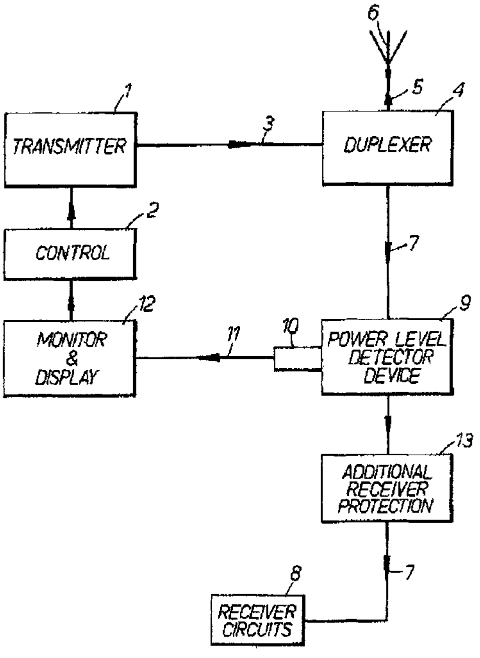

Figure 148 [207]

Apparatus for Monitoring Power

A power level detector device (9) acts to protect receiver circuits 8 from too high a level of incident power. When power at the device (9) is above a certain threshold level the gas contained by the device (9) generates an emission spectrum of electro- magnetic energy. This energy is detected by a photodetector (10) which produces an electrical signal to control the power of a transmitter (1) and hence the power transmitted to the receiver circuits (8).

Thermal Methods

Electric power absorbed by a solid or a fluid induces physical changes. Usually the temperature raise following resistive heat production in the load (Joule's law) is measured $\delta Q = RI^2dt$. **(68)**

Calorimetric measurements of electric power can be very precise, especially at high power levels. They are therefore being used for standards [201] and for calibration. Their simplicity and transparency make them popular in high voltage, radio and microwave applications. Radio engineers use them for measuring output power of radio transmitters.

Figure 149 [199] shows a calorimetric device for measuring power of an incident RF wave. The device determines the temperature difference between in- and outgoing cooling water. Dissipated power = P (Kw) = const x f x ΔT, where f = massflow (kg/s)and ΔT = temperature change. **(68 bis)**

In this apparatus the electric radio frequent power is absorbed by the water, but the same principle could of course be used with current producing heat in a resistive load, cooled by liquid.

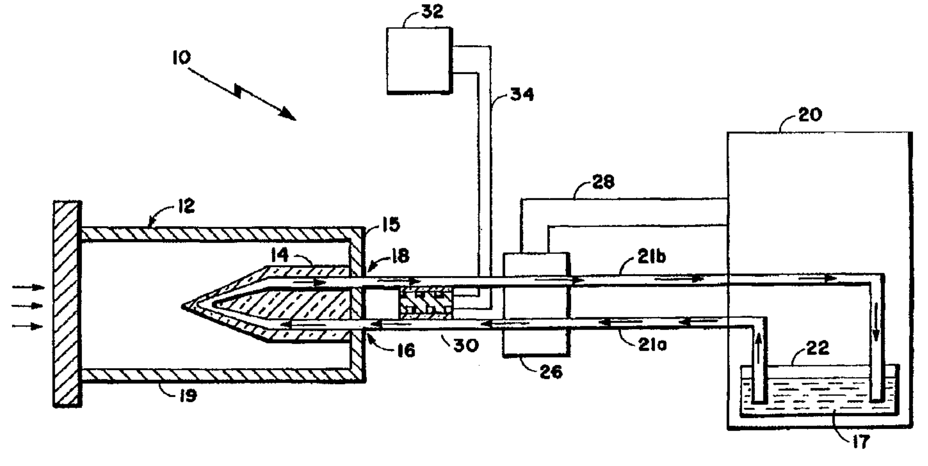

Figure 149 [199]

Power Measurement Calorimeter

One type of measurement device widely used for measuring high RF power signals is the waterload. In using a waterload, the high level RF power is absorbed in a matched-impedance section of a transmission line that is wholly or partially filled with a flowing stream of liquid, usually water. It is generally desired that the liquid itself dissipate all of the incident power, so that the temperature difference between the liquid entering the load and the liquid leaving the load can be measured by calibrated thermocouples, thermistors, or thermometers. One of several techniques can then be used for relating the desired absolute RF power to the corresponding rise in temperature.In one type of waterload, a water filled chamber is disposed at an end portion of a housing and input and output ports are provided to the chamber such that, a pressurized water supply is provided to the chamber. In this way cool water is provided to the load through the input port and the heated water is removed from the chamber from the output port.

Instead of measuring ΔT directly, one can measure heat dependent expansion (Fig.150) [200].

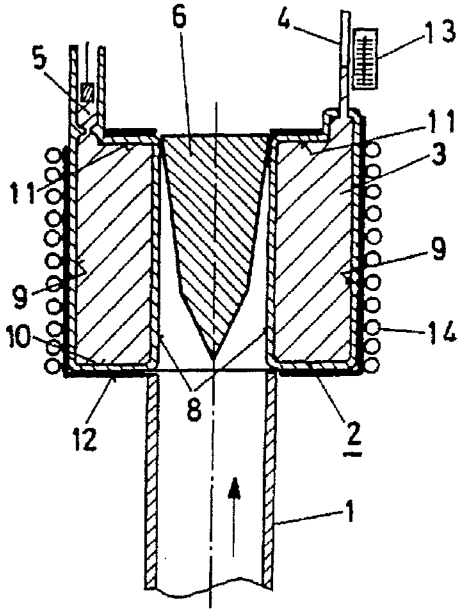

Figure 150 [200]

Microwave Pulse Energy Measurement by Absorbent Liquid Heating

A vessel (2) placed coaxially across the waveguide end (1) contains a quantity of absorbent liq. (3) in the space between concentric cylindrical walls (8, 9). A capillary tube (4) with a graduated scale (13) and a compensating tube (5) extend upward from the cover (11) of the vessel (2). A conical reflecting wedge (6) blocking the inner cylinder scatters the incident microwave energy uniformly around the inner wall (8), through which microwaves penetrate into the absorber (3). The outer wall (9), base (10) and cover (11) are coated with reflecting material (12) to prevent radiative loss. The absorbed energy is evaluated from the rise of liq. in the capillary (4).

There are other ways of using the thermal transformation: In [203] current and voltage proportional currents can be used to heat resistors that in their turn influence a bimetallic spring which rotates a pointer. It is used as a maximum demand meter in combination with a normal Wh-meter [203].

Optical thermometers, as recently developed, are being used - see Figure 151 [205].

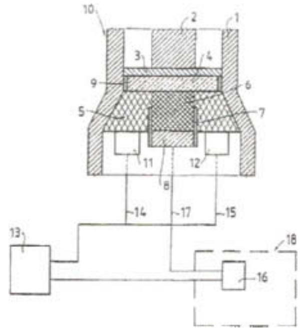

Figure 151 [205]
Sensor and Device for the Measurement of Radiant Energy,in Particular the Energy Associated with Radio-Frequency, Microwave and Light Radiation Signals

The sensor provides a termination for the guide along which the signal is propagated which termination is capable of completely absorbing the incident energy and converting it into heat. The termination is in thermal contact with a monocrystal or with a layer of crystals for example of ruby (oxide of aluminium) which is capable of being illuminated by one or more sources of light with a predetermined and sinusoidally modulated wavelength in order to emit fluorescent radiation at a second wavelength the phase displacement of which with regard to the modulating phase is a function of the temperature of the termination and thus a function of the incident energy. For radio-frequency and microwave measurements the termination terminates the coaxial cable or the wave-guide with the characteristic impedance and comprises a layer of metal deposited on the monocrystal or on the layer of ruby crystals. In the case of measurements of optical power the termination is constituted by a black body which the input optical fiber abuts the black body being in a thermal exchange relationship with the monocrystal or with the layer of ruby crystals.

A similar principle is used in the now well known **battery tester**, where the power dissipated in a thin film resistor is sensed by a layer (e.g. a liquid crystal) that changes colour with temperature (thermochromic transformation) [206] (Fig. 152).

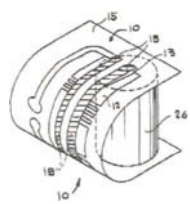

Figure 152 [206]
Battery Tester and Method for Making the Tester

A device (14) for testing a battery particularly a small portable battery (25 or 26) comprising a flexible transparent substrate (15) on which is deposited a narrow band of a black absorbant material (18). A conductive material (10) which tapers outwardly in opposite directions from a central point (11) to a pair of outer terminals (13 or 17) is then deposited atop the substrate (15) on the same side of the substrate (15) as absorber layer (18). A layer of a cholesteric liquid crystal material (15') is then deposited on the substrate (15) on the opposite side from the black absorber layer (18). The conductive material (10) is an epoxy cement-based conductor preferably silver printed or painted directly on to the substrate (15). An indicator scale (19-22) is located along sections of the tapered conductive material (10). To test a dry cell battery (25 or 26) the terminal ends (13 or 17) of the conductive material (10) are placed in contact with the battery terminals causing a current to flow which heats the conductive material (10) the heat being most intense at the central point (11) and radiating outwardly. The heat is transferred through the thin substrate (15) to the liquid cystal layer (15) which results in a color change in the liquid crystal. The traverse of the color change along the length of the indicator scale (19-22) outwardly from the central point (11) is proportional to the current or voltage output condition read on the indicator scale (19-22) which is calibrated accordingly.

4.2.2.2 Using Thermo-electric Conversion or Resistivity Change

We have several useful transformations from heat to an electrical variable.

- Thermoelement give a voltage as an output signal.
- Resistors, e.g. thermistors, that change resistance with temperature. When used for measuring the power of radio frequent or microwave radiation they are called Bolometers.
- The characteristic curves of semiconductors change with temperature.

Whereas calorimetric methods are absolute in character, the transformations just mentioned imply relative measurements, and thus rely on calibrations. The principle is this:

1) The current to be measured heats up a resistor in a manner proportional to power. The resistor looses some unknown amount of heat to the surrounding. For each input power level, the thermal equilibrium temperature is different.

2) The temperature, or temperature change, of the resistor is sensed by a temperature sensitive element with an electrical output which is proportional to the power to be measured.

In the case of the thermoelement, it is possible to lead the signal to be measured directly through it, and use it as a measurement resistor (Fig. 153) [202] below.

4.2.2.2.1 Thermocouples

The heat difference between the hot and cold junctions, whether induced by Joule's effect in the element or by heat transfer, creates a measurable voltage by the Seebeck and Thomson effects [335].

Thermocouples can also be used as multipliers (i x u) in power measuring instruments: See ch. 4.2.5, "Thermal Converters".

Thermocouple sensors have been used for many years, especially for measuring at RF and microwave frequencies. They can however be used at lower frequencies or DC as well. An instrument based on AC/DC conversion using thermocouples, designed for power frequencies, i.e. 45-65 Hz is described in [201]. This instrument was developed as a standard.

Thermocouple sensors are faster than calorimetric devices.

The meter of [202] (Fig. 153) shows how radio frequent power creates a low level (e.g. 160 nV for 1 mW of applied RF power) DC-signal when applied to a thermocouple pair (106). The low level output of the thermocouple is chopped at 220 Hz to facilitate processing.

The low chopping frequency reduces the interfering effect of "spiking" caused by the chopper.

The meter perform synchronous detection and a microprocessor in a feed back loop is used to zero and calibrate it automatically.

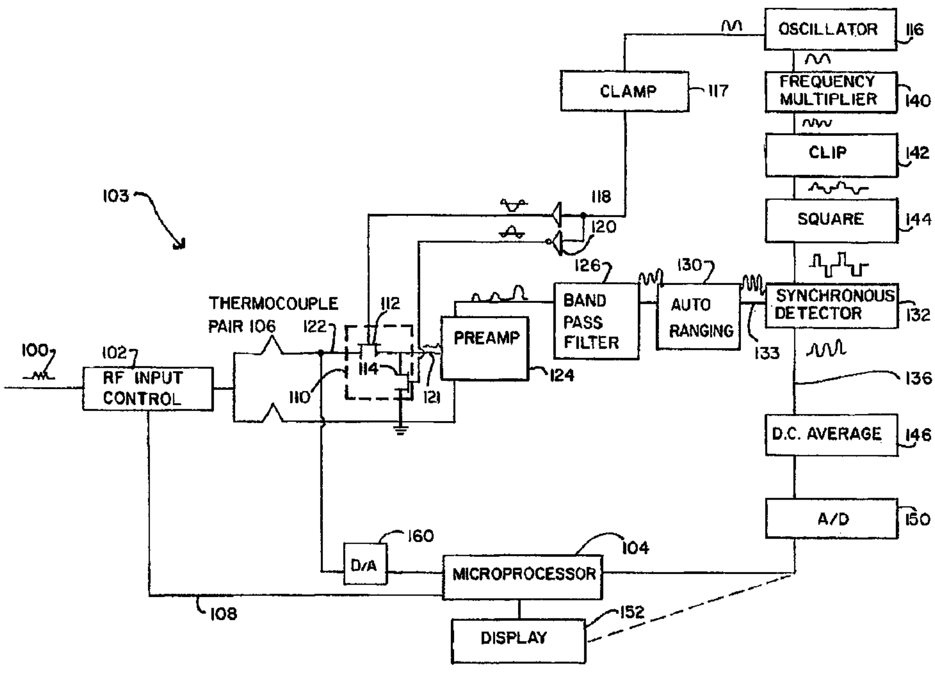

Figure 153 [202]
Thermocouple Power Meter

An RF input 100 is shown entering an RF input control element 102 of a thermocouple power meter 103. Also entering the RF input control element 102 is an input line from a microprocessor 104. The RF input control element 102 selectively permits any one of several RF inputs to be applied to a thermocouple pair 106—including the RF input 100 and a zero input or a reference input such as one milliwatt selected by the microprocessor 104 via line 108.

The thermocouple pair 106 converts the RF input, if any, exitting the control element 102 into heat and thereafter into a d.c. signal in conventional fashion. The amplitude of the d.c. signal generated by the thermocouple pair 106 is low and difficult to measure with accuracy. Accordingly, the d.c. signal from the thermocouple pair 106 is passed through a chopper stage 110 that includes a series chopper 112 and a shunt chopper 114. The series chopper 112 and the shunt chopper 114 are driven to operate complementarily, one being ON (or conductive) when the other is OFF (or non-conductive). For simplification, capacitors and resistors and the like that would be included in a detailed circuit diagram are omitted, such elements being within the knowledge of one of ordinary skill in the art to include.

The low end sensitivity of thermocouples is not very good.

Figure 154 [319] illustrates how a thermoelectric measurement converter can be integrated in a single chip. The circuit measures the product of two instantaneous values.

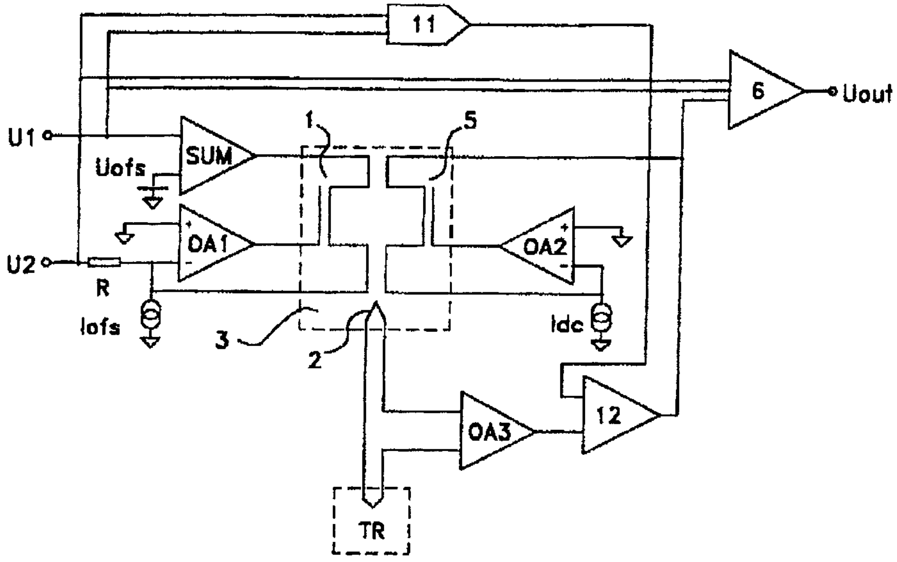

Figure 154 [319]
Integrated Thermoelectric Measurement Converter

FET transistors (1) and (5) act as controlled resistors and are seated on a heat insulating layer (3). FET (1) is coupled to the input signals. FET (5) performs an automatic compensation for the thermal influence of power change on FET (1). Temperature sensor (2) measures the temperature difference between the layer (3) and the reference body (TR). A feed-back system drives the voltage, and thus the power on transistor (5) so as to establish temperature balance between the layer (3) and the reference body (TR).

The integrated device, which shape is illustrated in Figure 155 is manufactured by epitaxial growth. Here the substrate (20) is mounted on multiple Peltier-elements (29) which cool the device so as to lower the noise level.

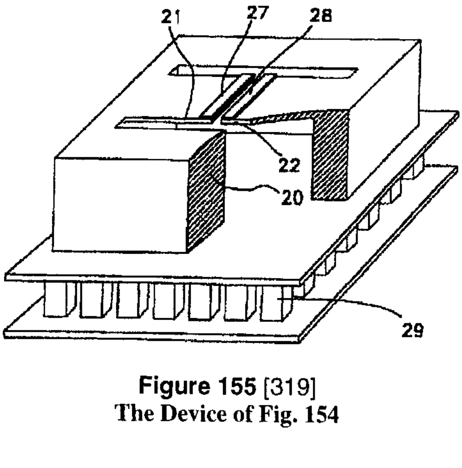

Figure 155 [319]
The Device of Fig. 154

4.2.2.2.2 Semiconductors as Temperature Sensors in Power Measuring devices

The **characteristic curves** of semiconducting elements change with temperature. A transistor which is heated will give a higher collector-emitter current for a fixed base-emitter voltage.

Figure 156 [336] shows a circuit arrangement exploiting this principle. (The dashed lines indicate thermally isolated monolithic semiconductor islands 96 and 98):

The input is at T1-T2, and resistor 42 heats up transistor 52, which collector-emitter current thus varies in a way proportional to power.

This operational mode is relatively insensitive to noise and operates linearly at very small signal levels.

At higher amplitude levels the diode 60 conducts, and the resistor 44 is effective in heating island 98, and establishing thermal equilibrium.

The output signal 92 over T7-T8 is in this case proportional to the square of the input power.

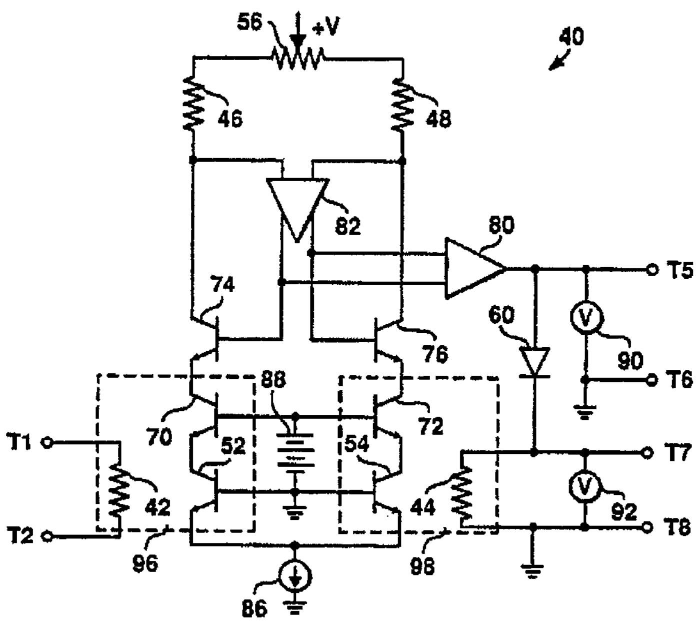

Figure 156 [336]
Power Measuring Device Comprising Transistor Heat Sensors
The circuit has a linear feed back part with an output T5-T6. For small signal amplitudes the feed back through amplifier 82 brings the islands 96 and 98 into thermal equilibrium (power dissipated in transistor 72 heats island 98). It has to be noted that in this mode of operation the diode 60 is not conducting, because the forward bias over it is to small.

Combing the two outputs, T5-T6 and T7-T8 in an additional stage is illustrated in Figure 157 [336].

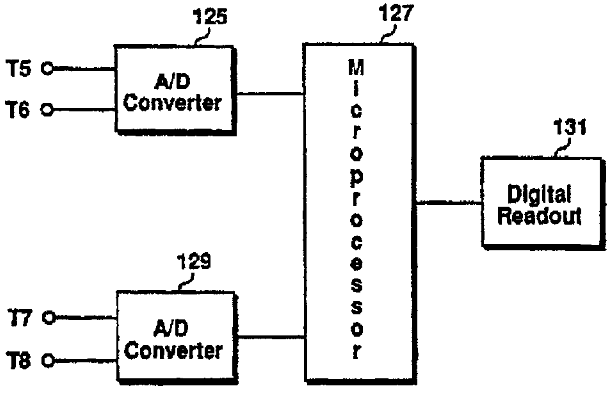

Figure 157 [336]
Automatic means for combining the indications of the meters 90 and 92 in "fig. 156"

This instrument has a good linearity, sensitivity and accuracy over a wide dynamic range of measured signals.

4.2.2.2.3 Resistive Sensors

Bolometer elements (resistance change with microwave power absorption) such as **Baretter** (positive temperature coefficient) elements and **thermistors** (negative temperature coefficient) are being used in microwave applications. Resistive sensing of microwave power is faster than using thermocouples. Baretters are faster than thermistors [331]. Traditionally they are inserted in Wheatstone bridges. Figure 158 [208] shows an example of the use of a Baretter element.

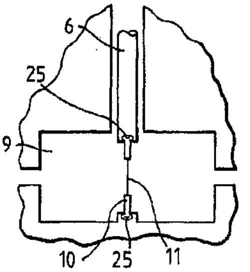

Figure 158 [208]
Baretter Elements

A known method of measuring microwave power is to suspend a very thin wire in a waveguide section with a moulded D.C. lead out. When illuminated by microwave the resistance of the wire changes considerably. It is normal to operate barretters at constant resistance by means of a D.C. self balancing bridge. The change in D.C. bias power when microwave power is absorbed by the element is known as the D.C. substitute power and the ratio of this to the incident power is the effective efficiency. This is less than unity because of dissipation in the structure which does not result in a change in the element resistance, microwave leakage and differing power co-efficients of resistance for D.C. and microwave heating.

A method of measuring **microwave** power is to suspend a very thin wire in a waveguide section with a grounded DC lead out. When illuminated by microwaves the resistance of the wire changes considerably. It is normal to operate barretters at constant resistance by means of a DC self -balancing bridge. The change in DC bias power when microwave power is absorbed by the element is known as the DC. substitute power and the ratio of this to the incident power is the effective efficiency. This is less than unity because of dissipation in the structure which does not result in a change in the element resistance, microwave leakage and differing power coefficients of resistance for DC and microwave heating.

A self-balancing system with bolometer element without a Wheatstone bridge is shown in Figure 159 [209]

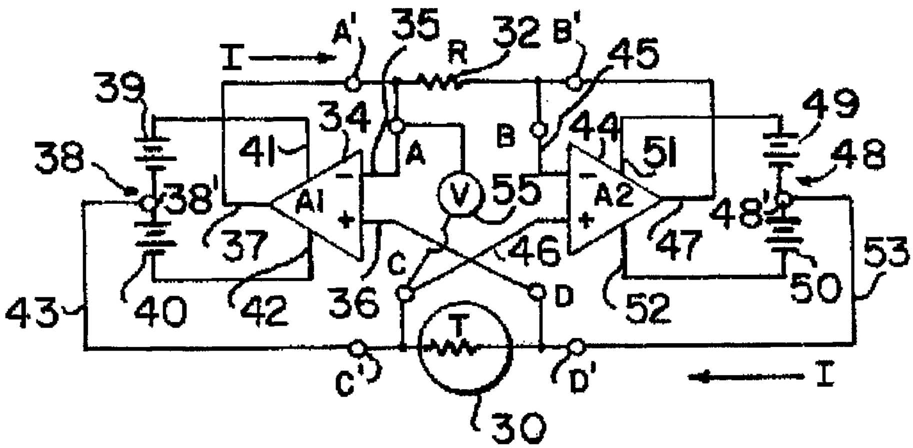

Figure 159 [209]
Self-Balancing D.C.-Substitution Measuring System

A self-balancing D.C.-substitution R.F. power measuring system includes first and second high gain differential operational amplifiers, a bolometer element, and a reference resistor element. The amplifiers and the two elements are connected in a current loop with one of the elements connected between the output terminals from the differential amplifiers and the other of the elements connected between center points of isolated dual power supplies associated with each of the amplifiers. The inputs to one amplifier are connected from an adjacent end of one of the elements and the far end of the other element, while the inputs to the second amplifier are connected to the far end of the one element and the adjacent end of the other element. Current flows out of one amplifier and into the other. The current is driven to a value which maintains the potential between the input terminals of the first amplifier essentially equal to zero and the potential between the input terminals of the second amplifier essentially equal to zero. Thus, the current drives the value of the bolometer element to a resistance which is equal to the resistance of the reference element. An output connection to a voltmeter may be taken between corresponding ends of the elements. The bolometer element may be a thermistor or a barretter. The system may also be used in a hot-wire anemometer. In another version of the system, the current loop is established with one of the elements connected between the output of one amplifier and the center point of the power supply of the other amplifier and the other of the elements connected between the output of the other amplifier and the center point of the power supply of the one amplifier; the input connections to the amplifiers are taken from the same points, but with the input leads to the second amplifier interchanged.

Digital technology eliminates the need for bridges. See Figure 160 [210].

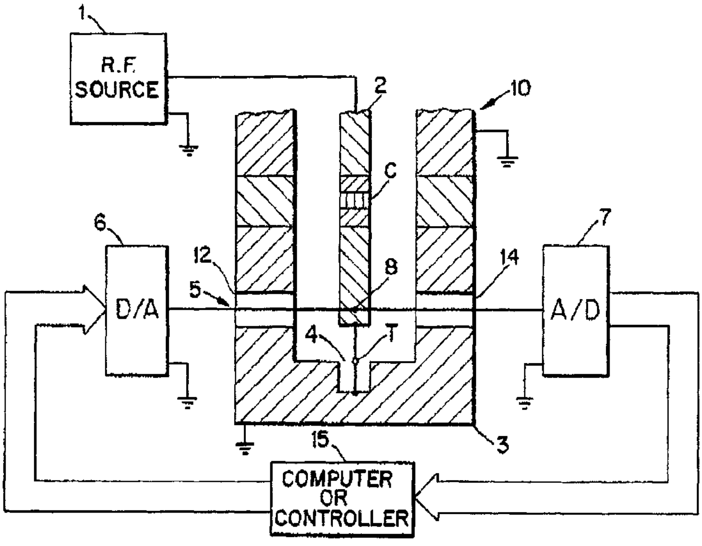

Figure 160 [210]
High Frequency Power Sensing Device

The device uses a single thermistor, directly converts a digital signal to the current through the thermistor, and converts the voltage across the thermistor to a digital signal. The change of the digitized dc signals from no RF power to power to be measured provides the measure of RF power by the substituted dc method. The above approach eliminates the need for bridges and voltmeters between the power sensor and computer circuits. This approach permits the computer to set the dc resistance of the thermistor to the proper value to provide optimum matching at the desired frequency and to calculate the dc power dissipated in the thermistor. The present invention using only a single thermistor, eliminates the need for bypass capacitors and the nonlinearity error produced by thermistor pairs. The dc blocking capacitor in this invention, not being an integral part of the power sensor, is interchangeable permitting a wide range of operating frequencies with a single basic power sensor.

4.2.3 Using the Square Law Characteristics of Semiconductors

"Square law" instruments are dedicated to the measuring of radio and microwave frequencies at low power levels. They exploit the square law relation between voltage and current in e.g. a diode's transfer curve (i=u*u for small u). They also use the fact that the square of current or voltage over a known impedance according to Ohms law, gives the power

$$P=UI=U^2/Z \quad (69)$$

The signal to be measured, or a fraction thereof, is passed through a diode, or a diode junction, working in the square law region. The output is proportional to the signal power applied to the diode. It is a half cycle rectified signal, smoothed by the inherent capacitance of the diode.

Figure 161 [326] illustrates the principle circuit arrangement.

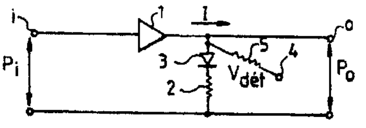

Figure 161 [326]
Diode Signal Power Detector

V_{det} is the power proportional voltage, and the resistor (5) adapts the output impedance.

Diode detectors have **a shorter reaction time**, microseconds instead of seconds, and better sensitivity than thermal or resistive detectors [211] [331]. The problem of temperature dependence can be solved (Fig. 162) [212].

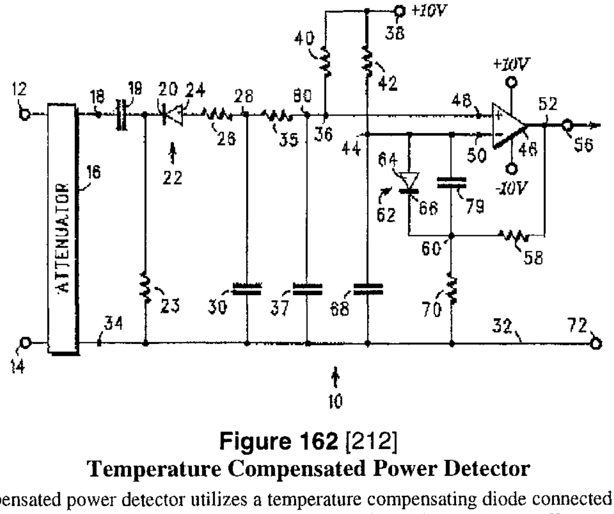

Figure 162 [212]
Temperature Compensated Power Detector

A temperature compensated power detector utilizes a temperature compensating diode connected to an inverting input of an amplifier to enable the amplifier to substantially cancel out undesirable temperature effects caused by a power level detector diode coupled to the non-inverting input of the amplifier. As a result the amplifier output voltage tends to remain constant over temperature in response to a fixed power level being applied to the detector. A lookup table is utilized to determine the power level corresponding to a power detector output voltage of a particular magnitude.

To increase the **dynamic range** when measuring radio-frequency power one can combine thermocouples with diode sensors (Fig. 163) [204].

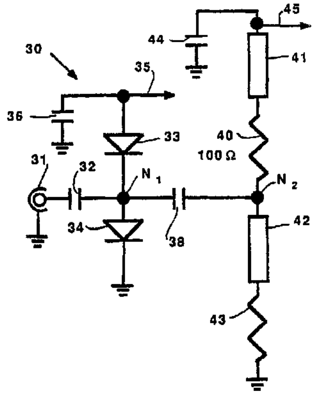

Figure 163 [204]
Wide Dynamic Range Radio-Frequency Power Sensor

A wide dynamic range radio-frequency power sensor (30) having a low-power sensor portion and a high-power sensor portion is described. Both sensing portions are connected to an input signal at the same time without the use of a signal splitter. In the preferred embodiment a single radio-frequency load serves both sensor portions. Each sensor portion has its own output terminal (35-45). The low-power sensor portion comprises a pair of diodes (33-34).The high-power sensor portion (which includes the radio-frequency load) may comprise a pair of diodes preceded by an attenuator (84) or a pair of thermocouples (41-43).

Diodes are the most common devices, but the diode junction in for example a **FET** can be used as well (Fig.164) [213]. In this circuit the current Io is proportional to the power of the signal at "30".

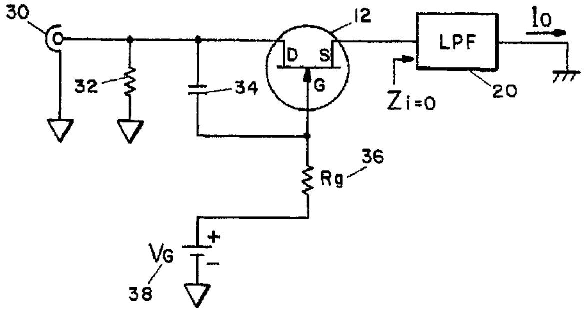

Figure 164 [213]
Broadband RF Power Detector

Measuring of waves in free space is not treated here, but the above methods can be used in conjunction with an antenna for radiation power measurements.

4.2.4 Measuring Current or Voltage,

knowing the impedance

$$P=UI \Leftrightarrow P=U^2/R = RI^2 \quad (70)$$

The "Square law" detectors described above utilize this principle, but it is not limited to high frequency applications. Figure 165 [215] shows a suitably designed measuring scale that translates the linear measurement of voltage to the indication of power. Naturally, the impedance must be known if one wants to display the power in absolute values.

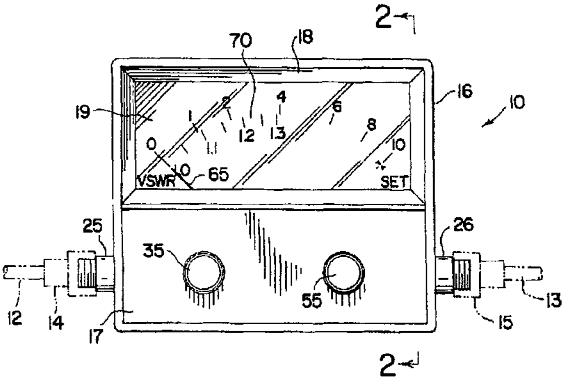

Figure 165 [215]
VSWR Meter Circuit Using Variable RF Attenuator

Measuring the current instead of the voltage with a current transformer and using the transformation formula P =RI*I (R = 50Ω) is being done at radio wave frequencies.

4.2.5 Sensing Current and Voltage separately and multiplying

4.2.5.1 Introduction

Sensing currents and voltages as such is treated in Chapter 1. Sensors of particular importance are: Hall sensors, magneto resistive sensors, inductive and capacitive sensors, shunts, magneto- or electrooptic sensors and current transformers with or without a magnetic core.

Figure 166 [261] shows a simple design using an inductive current sensor and a capacitive voltage sensor.

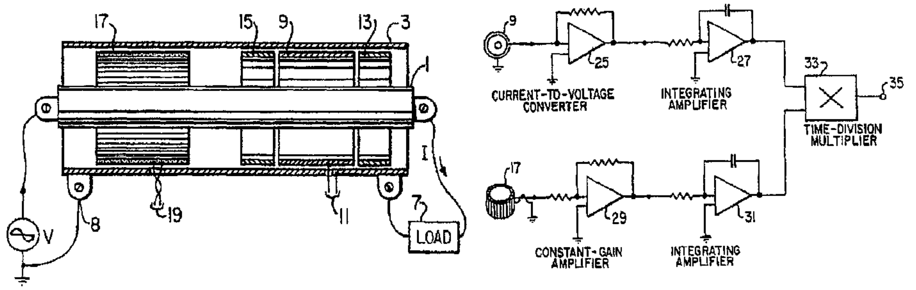

Figure 166 [261]
Voltage and Current Sensing Power Detector

In Figure 167 [333] a **thermoelectric sensor** measures the effective current, I, which is then multiplied by the effective voltage V and the power factor φ to establish the active power P.

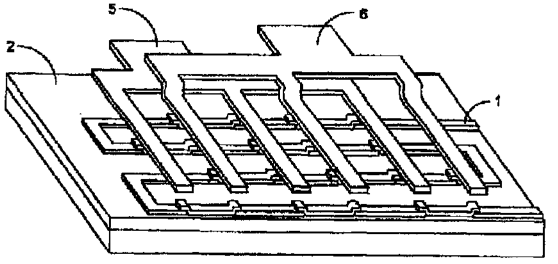

Figure 167 [333]
Thermoelectric Power Sensor

Thermoelectric sensor for measuring true effective current consumed by appliance e.g. water heater or domestic or industrial premises - has resistors for actual and comparison currents in contact with alternate thermocouple junctions in series circuit.

The sensor measures the current by comparing the heat generated by the current in resistor (5) with that from a known comparison current in resistor (6). The resistors are in contact with alternate thermocouple junction in series in a circuit (1). The current difference between the two resistors generates a proportionate EMF i.e. error signal in the circuit due to unequal heating of the thermocouple junctions.

This EMF is amplified and processed by an electronics system which automatically adjusts the comparison current in resistor (6) to cancel the EMF. From the known value of the comparison current, the electricity consumption can be automatically calculated and the valve transmitted via an interface to a remote recording point.

ADVANTAGE - Readily miniaturised and produced at low cost by conventional microsystems metal deposition and engraving processes, while increasing reliability.

Hall sensors and **magneto resistive** sensors are suitable for solid state integration (Fig.146). A possible circuit design is shown in fig. 168 [216]. This design is based on a magneto resistive current sensor, a voltage divider (RC and RD), and a pulse width modulator producing a power proportional output pulse train.

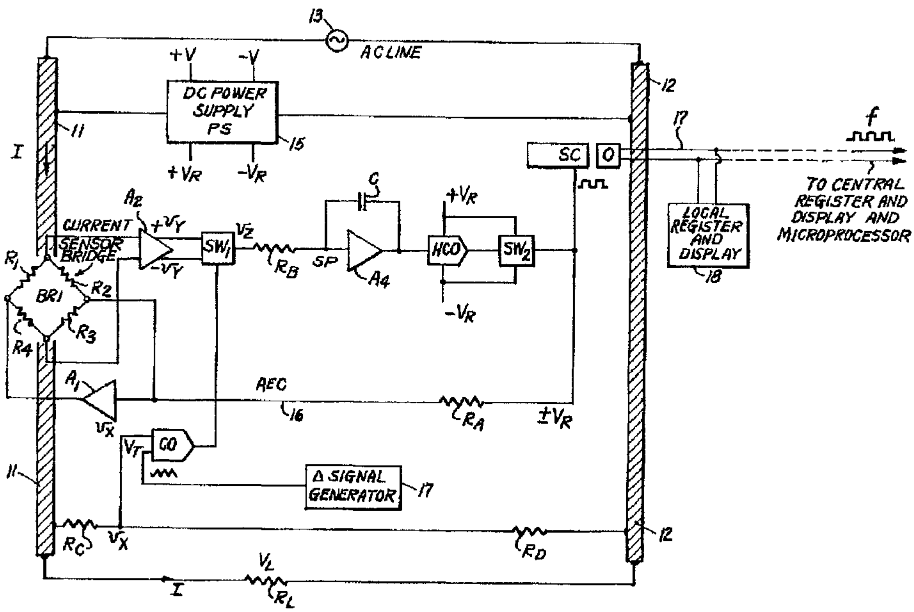

Figure 168 [216]

Low-Cost Self-Contained Transformerless Solid State Electronic Watthour Meter Having Thin Film Ferromagnetic Current Sensor

The low cost, light weight, small size ferromagnetic current sensing device employed in the watthour meter preferably comprises a thin film magnetoresistive magnetic field sensor formed by semiconductor integrated circuit fabrication techniques on a common substrate with other components of the solid state meter circuit. The thin film magnetoresistive magnetic field sensing device preferably is fabricated in the form of a balanced Wheatstone bridge with each arm of the bridge comprising a magnetoresistive magnetic field sensor wherein each field sensor is magnetically coupled to the power supply conductor to be measured. In this arrangement, the two diagonally opposite terminals of the bridge are connected across the input and output terminals of a constant current output amplifier supplied with an input supply current and the two remaining diagonally opposite terminals of the bridge are connected across a set of current indicating input terminals to the multiplier circuit means of the watthour meter. In a preferred embodiment of the invention the watthour meter circuit includes automatic error correction circuit means for feeding back an automatic error correcting polarity reversing signal from the output thereof to the input of the multiplier circuit means for reversing the polarity of one of the input signals to the input of the multiplier circuit means whereby long term errors due to drift, thermal changes and the like are averaged out of the product signals being derived by the multiplier circuit means during each quantizing period operation of the meter.

With Hall elements, sensing the current and multiplying by the voltage can be done simultaneously (Fig. 169) [217].

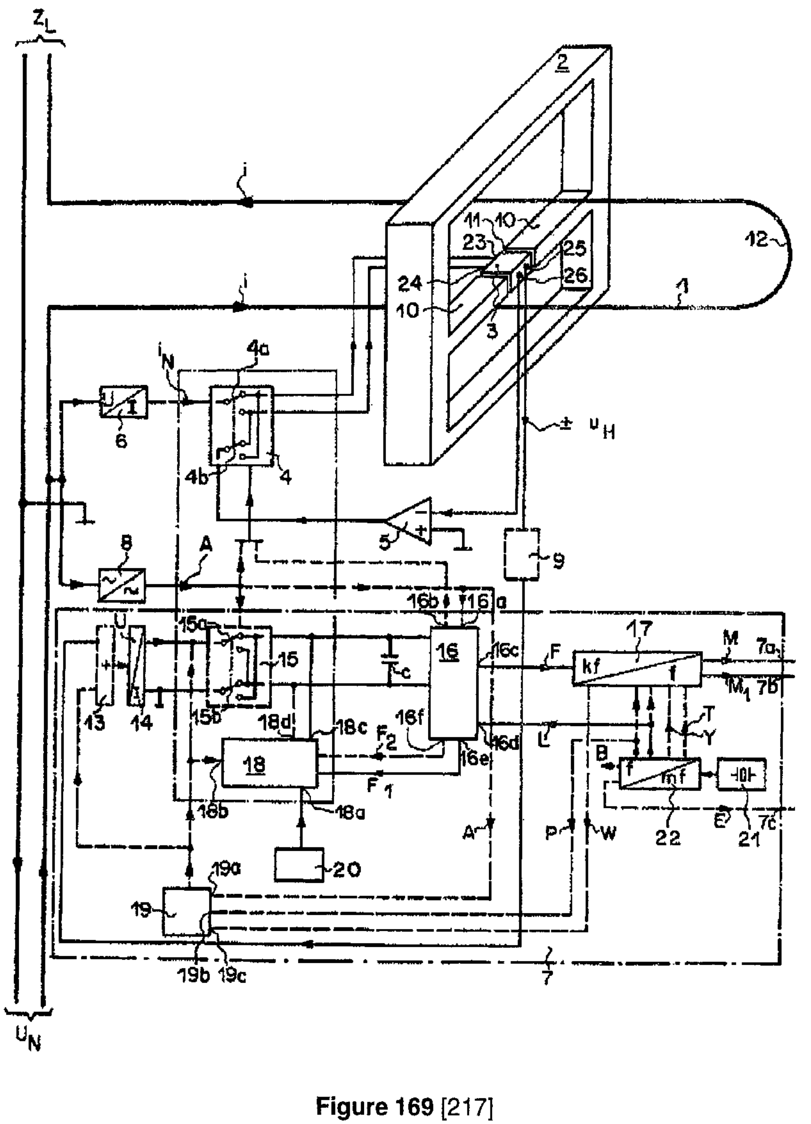

Figure 169 [217]
Electricity consumption meter

A conductor (1) carrying current (i) and a voltage-current converter (6) are provided, the latter converting the supply voltage (Un) into a current (in). The proportional current passes through a Hall effect element (3). The element lies at the centre of a ferromagnetic core in the air gap, lying in the central bar of a figure of eight. The conductor passes through both openings of the core around the Hall element. The output voltage produced by the element is proportional to the product of the current and voltage (in times Un), and is applied to a voltage frequency converter (7) producing a pulse signal of frequency representing the power consumption.

4.2.5.2 Analog Multiplication

The commonly used devices are:

- Ferraris wheels, Electrodynamometers annd Electrostatic Wattmeters
- Hall elements and Faraday sensors
- Thermo elements
- Solid state multipliers, such as 4 quad, log antilog devices
- Single electronic components e.g. transistors
- Discrete electronic circuits

Ferraris Wheels

The classical electricity meter is based on this device. It is still the most common one in household Watthour meters, because of its comparably low price and reliability. Ferraris type energy meters are also treated in Chapter 5. The torque on the aluminium wheel is proportional to the average AC-power transmitted by the line. A current coil creates Eddy currents in the wheel. These interact with the field set up by the voltage-coil to turn the Ferraris disc (Fig. 170) [218]. The theoretical treatment of the phenomena is complex [297].

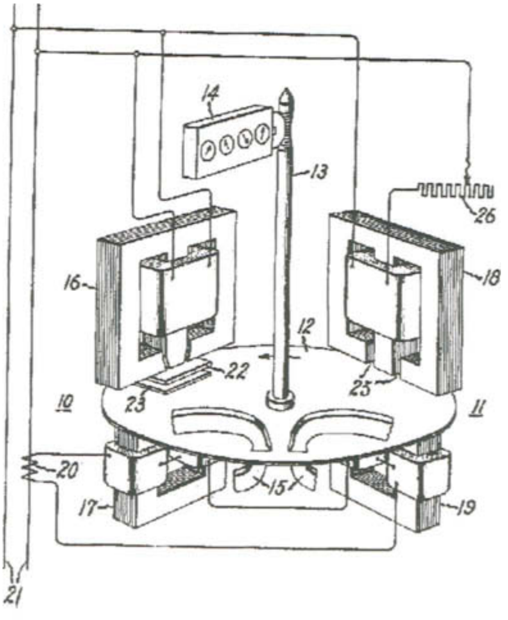

Figure 170 [218]
Volt-Ampere-Hour Meter

The meter torque is the sum of the troques of the two dirving elements and remains substantailly proportional to volt-amperes over a considerable power factor range. The meter shaft is indicated at **13**, the register at **14** and the damping magnets, partially broken away at **15**.

To be noted is that the Ferraris wheel meter does not measure any DC-component. It can be used for DC after an DC-AC conversion by e.g. **transductors**, as in Figure 171 [219].

(A transductor is a DC-AC converter employing a magnetic core. The DC current to be measured constitutes the primary winding. An auxiliary winding on the secondary side is fed by an AC source, periodically reversing the saturation of the core).

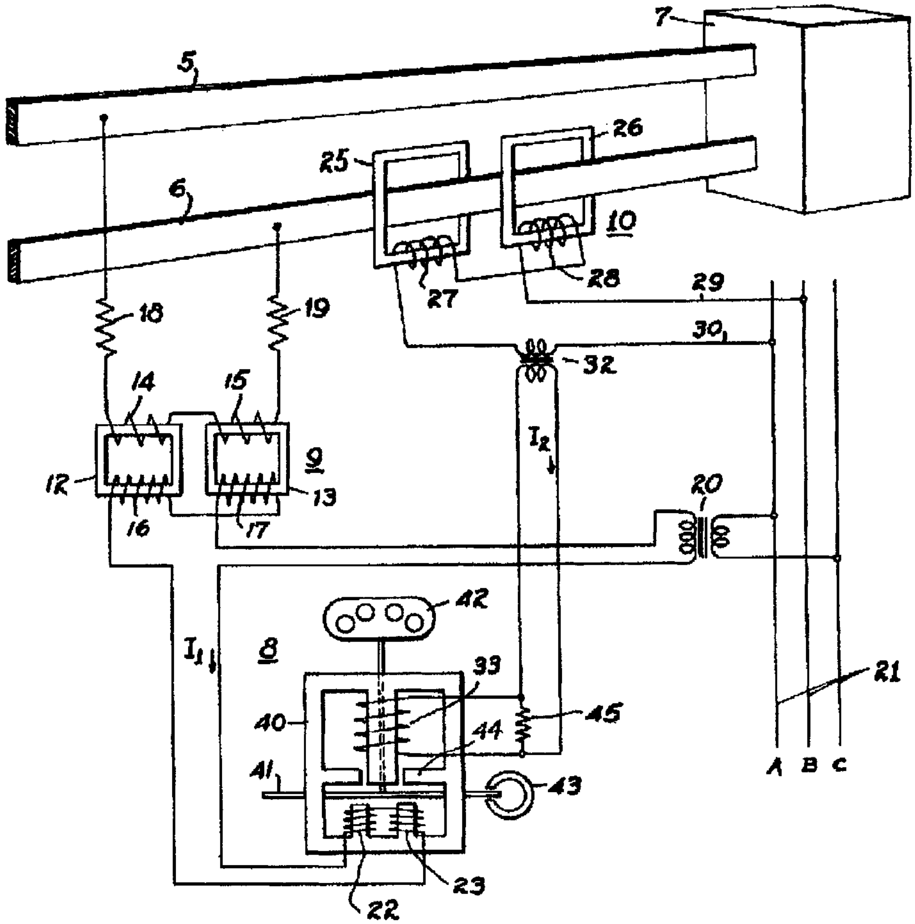

Figure 171 [219]
A Power-Measuring Device

5 and **6** represent the positive and negative line conductors of a D.C. power feeder or distribution bus which, in the case of electrolytic cell or pot line operation for aluminum production, is adapted to carry high current, medium voltage D.C. power supplied from a suitable source indicated at **7**. A typical circuit often is designed to carry as much as 100,000 amperes at 600 volts, and needs to be metered with sustained accuracy. To attain this objective, the system of this invention utilizes an induction meter **8**, a voltage transductor **9** and a current transductor **10**. The two transductors convert the voltage and current quantities of the D.C. power circuit to proportional alternating current quantities. These are then applied to the meter in proper relation to each other in such manner as to effect accurate integration of their product in terms of D.C. kilowatt hours.

Due to the wide spread use of Ferraris type meters, it has become interesting to electronically simulate their functioning. Figure 172 [220] shows a circuit for this.

The circuit is based on the notion that the Ferraris wheel respond only to the fundamental component at mains frequency plus interacting similar harmonics of the mains voltage and load current. Further, it assumes that for the common case of sinusoidal voltage, the power formula can be simplified to:

$$P = \frac{1}{T} v_1 \dot{i}_1 \cos^2 t dt \qquad \textbf{(71)}$$

where v_1 and i_1 are the fundamental frequencies.

When voltage and current are out of phase, this yields the well known expression for power in a linear load (Ch. 4.1.1), P=UIcos α. **(63)**

The circuit employs an active analog filter to extract the fundamental, 50Hz, current, voltage and phase shift values which are converted to power and energy values by a microprocessor.

This circuit arrangement is claimed to be in total agreement with a Ferraris wheel meter when the supply voltage is an undistorted sinusoidal. An inaccuracy of +/- 1% is expected when the mains voltage has a 5% third harmonic distortion.

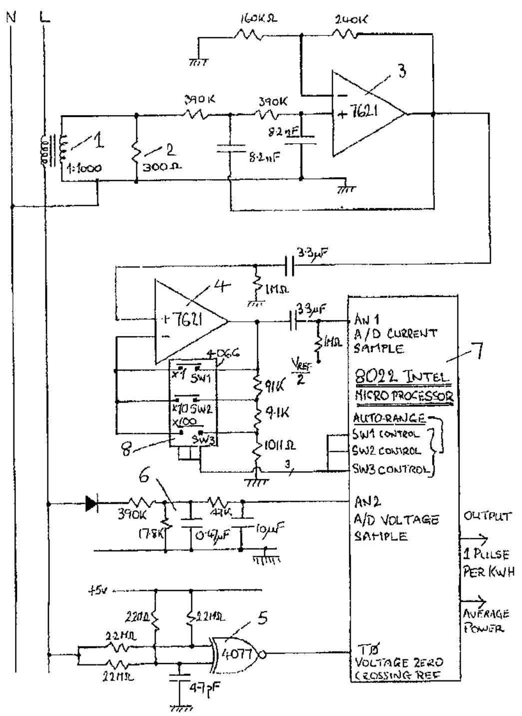

Figure 172 [220]

Electronic Apparatus for Metering and Measuring Electrical Energy Consumption in a Manner which Simulates the same Measurment as Effected by a Rotating Disc Electromechanical Meter.

A problem with the Ferraris wheel is its non linearity. **Electronic error compensation** using a microcomputer yield good results, but is complicated (extra components). It is shown in Figure 173 [222].

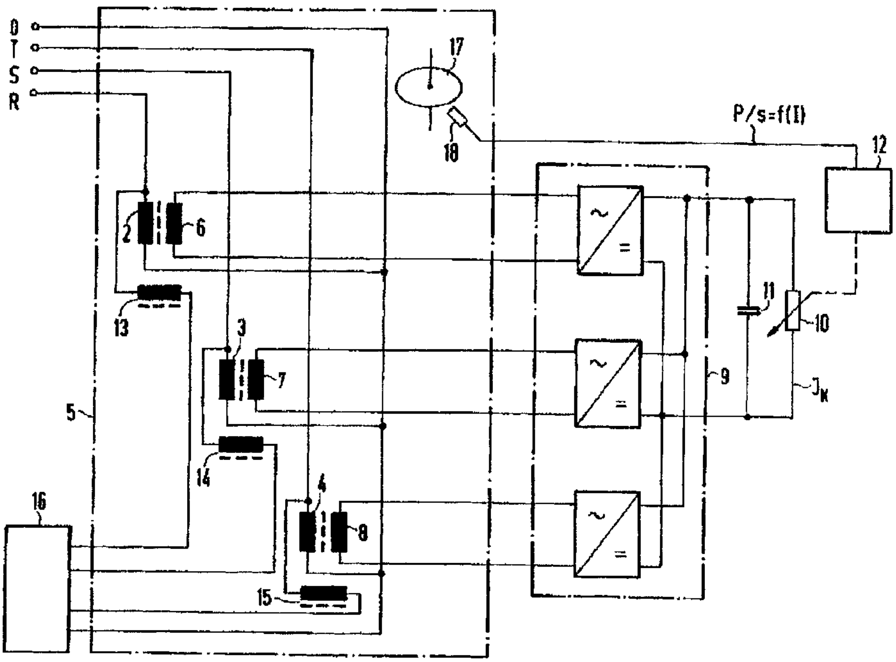

Figure 173 [222]
A Power-Measuring Device

The voltage windings (2-4) of a three-phase wattmeter (5) are provided with auxiliary windings (6-8) wires to a rectifier (9) which supplies compensatory DC to an adjustable resistive load (10) in parallel with a smoothing capacitor (11). The compensation current (IK) is adjusted by a controller (12) in accordance with the current drawn by a load (16) from the three current windings (13-15). This quantity is measured by a tachometer (18) counting the revolutions of a disc (17), wired to the controller (12), which may be a microcomputer Error compensation circuit in induction wattmeter.

The classical error compensation is performed by an adjustable permanent magnet "15" in Figure 170. Another problem with the Ferraris wheel is its lack of precision. Mechanical parts wear. It does not cope well with certain electrical charge conditions and it is basically only measuring the fundamental frequency component (50/60 Hz).

Electro dynamometer

If one replaces the permanent magnet in a moving coil instrument (d'Arsonval) with coil(s), i.e. an electromagnet, one gets an electro dynamometer. In Figure 174 [233] (1) and (2) represent current and voltage coils).

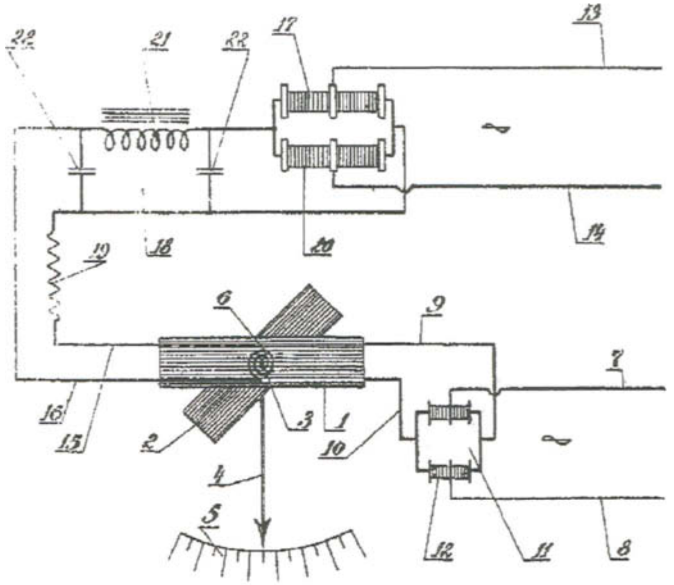

Figure 174 [233]
Electrodynamometer

See also standard textbooks such as [230] or [258], for further details. It is a most commonly used wattmeter. It cannot respond to high frequency signals and is inaccurate at low power factors due to instrument or transformer phase shift. The just cited [233] eliminates the phase problem by rectifying the signals. The meter is a dc instrument. The British National Physics Laboratory has developed one using a microcomputer with an estimated error of 20 ppm [237].

The Electrostatic Wattmeter

This instrument is in theory independent of frequency and power factor. As the name indicates, the instrument is based on electrostatic forces, in a manner similar to the electrostatic voltmeter. Figure 175 [235].

It can be used for AC and DC with the same calibration. Some disadvantages are low torque and vibration sensitivity. [230] describes its function more in detail.

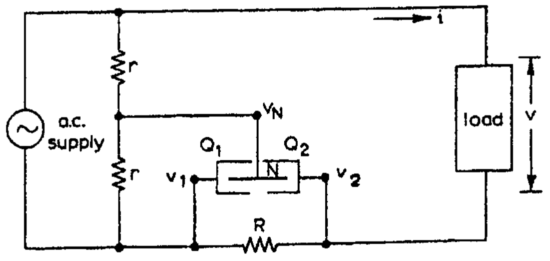

Figure 175 [233]
Quadrant Electrometer used as Wattmeter (incorporating Miles Walker's Compensation for Quadrant-shunt loss)

To use the quadrant electrometer as a wattmeter, a standard resistor called a quadrant shunt is employed in the circuit. The Figure in which R is the quadrant shunt, illustrates a particular case of the well known Miles Walker circuit for power measurement with the quadrant electrometer. In this case, the electrometer is obviously used heterostatically. The expressions for torque is

$T_{inst} = k(viR)$

or $T_{av} = kR$ x (average power in load)

[236] describes the use electronics and feedback to overcome some of its disadvantages.
[237] describes its use in microwave frequencies.

Instead of transforming the current through the voltage and current coil into torque one can let them act as a common core and obtain a "magnetostatic" Watt meter (Fig. 176) [221].

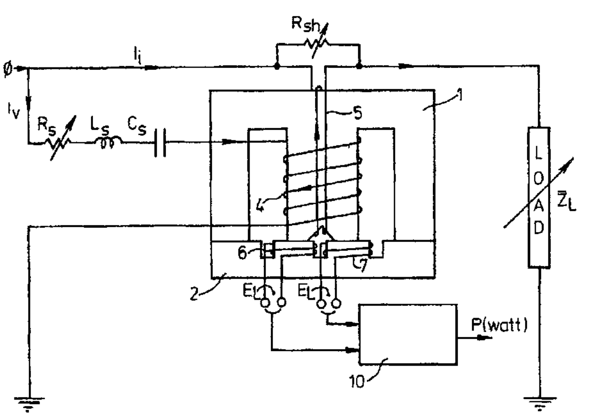

Figure 176 [221]
Magnetostatic Power Meter

HALL ELEMENTS AND FARADAY SENSORS

A Hall element (ch.1.2.7) senses the magnetic field around a conductor, whether it is an alternating or an invariable field. According to Ampere's law (in its special version) the line integral of the field is proportional to the current: $\mu_0 I = \oint \mathbf{B}ds = 2\pi r B\varphi = \mu_0 I$ **(72)**
for a long straight conductor.

I = current in the in circled conductor (A)
B = Magnetic field (T)
ds = line segment (m)
$\oint$ = line integral
μ_0 = permeability in vacuum (Vs/Am)
r = radius (m)
B = circular magnetic field (T)

Cf. section 1.2.1, p. 29-31
Compared with a normal current transformer, that only can measure AC, a Hall element is a small device.

Hall elements are being used as current sensors in power measuring devises. An interesting feature is that they can act as multipliers. As explained in chapter 1.2.7 the output signal from a Hall element is proportional to the magnetic field across it, which in its turn is proportional to the current in the conductor to be measured, and to the current feeding the Hall element.

If we then feed the Hall element with a current proportional to the voltage in the conductor to be measured, we obtain an output proportional to the power supplied by the conductor (U x I)

In Figure 179 (18) is a Hall element being used in this way. (19) detects the output voltage, i.e. the power to be measured.

Typical **problems** to solve are long term stability, sensitivity to interfering fields, low sensitivity and low signal to noise ratio.

In order to increase the sensitivity a magnetic circuit such as a circular iron core can be used for concentrating the flux. The Hall element is then placed in an air-gap in the core (Figs. 177 [224] and 178 B [225]).

An improvement of this construction consist in reducing the section of the magnetic circuit adjacent to the air-gap. This concentrates the flux over the Hall element and thus improves the sensitivity (Fig. 177) [224].
Cf. p. 30-31

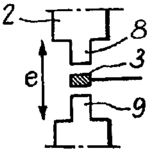

Figure 177 [224]
Flux Concentrator
Current transformer for continuous, alternating or pulsed curents. In the vicinity of the air-gap, the magnetic circuit (2) has at least one portion with reduced section.

A problem in using iron cores is that it has a non-linear magnetization (B-H) curve, as seen in Figure 178 A [225]. The levelling out of the curve for high values of the field strength (H) is caused by saturation of the iron core. The saturation starts at the inner radius of the core and gradually works it way outwards.

By giving the core a shape with a big difference between inner and outer radius, we can achieve an almost linear B-H curve.

The difference in circumference between inner and outer circumference should be at least 3 times, and preferably 5. See Figure 178 B [225].

The air-gap does not have to be in the circumferential direction. See Figure 178 C.

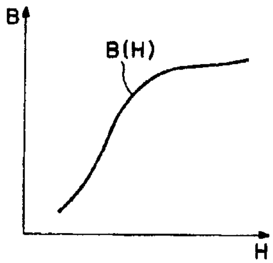

Figure 178 A [225]

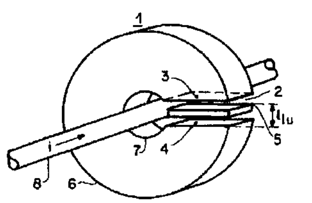

Figure 178 B [225]

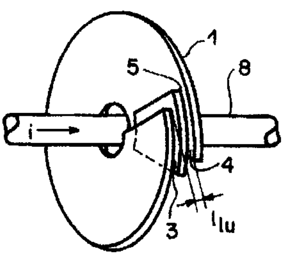

Figure 178 C [225]

Iron Cores with Improved Magnetization Curves

An additional advantage of the device in Figure 178 is that the Hall element is shielded against interfering fields by the iron core.

Offset voltage can be correct by using a second Hall element (Fig. 179) [226].

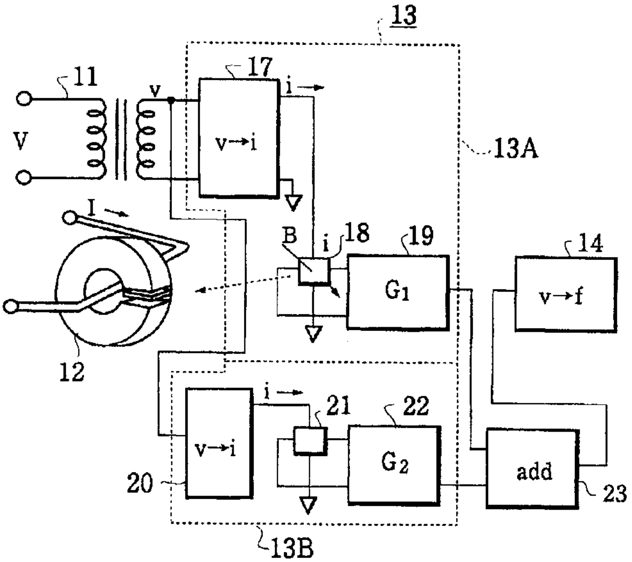

Figure 179 [226]
Electronic Watthour Meter

A first Hall element (18) is supplied with a current proportional to a load voltage and applied with a magnetic field proportional to a load current and produces a voltage proportional to a load power given by the load voltage and the load current. A second Hall element (21) has the same characteristic as that of the first Hall element and supplied with the current proportional to the load voltage and no magnetic field. The output voltages of the first and the second Hall element are combined by combining means (23) to compensate and remove an offset voltage component contained in the output voltage of the first Hall element.

Hall elements are suited for solid state manufacturing technics. Figure 180 [227] shows details of a design.

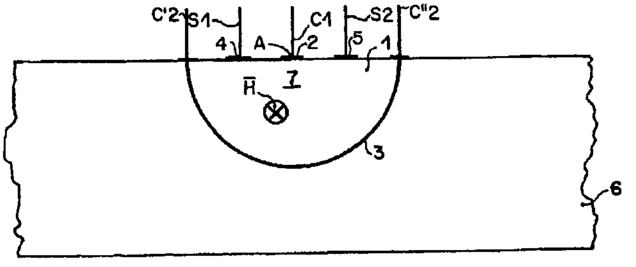

Figure 180 [227]
Integrated Hall Element for Electricity Meter

The Hall element has a semiconductor layer (6) of a single conductivity type carrying two sensor electrodes (4,5) and a current electrode (2). The current electrode lies between the sensor electrodes (4,5) along the centre line between them. An additional current electrode (3) with a semicircular cross-section ensures a vectoral sum current which is perpendicular to the surface of the semiconductor layer (6) adjacent the first current electrode (2).Pref. the second current electrode (3) has its axis symmetrical to a line through the first current electrode (2) normal to the semiconductor surface.

Faraday elements are, as Hall elements, sensitive to the magnetic field. A power measuring set-up can be carried out by arranging a Faraday element as a current sensor (Ch. 2.2) and modulate the light emitting element with the unknown voltage.

One then obtain a power sensor not requiring any current transformer. See Figure 181 [320].

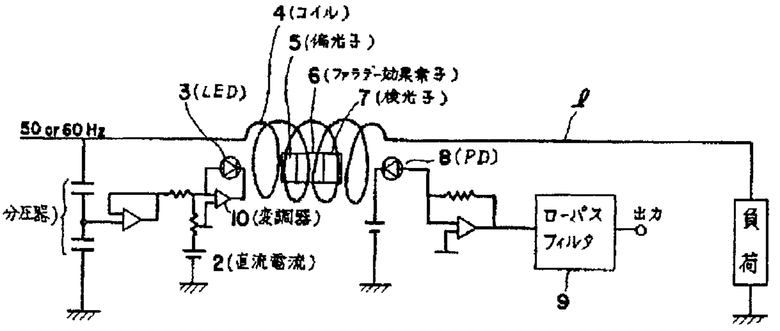

Figure 181 [320]
Power Sensor Comprising a Faraday Cell

PURPOSE: To achieve a smaller size and a lighter weight of the apparatus, by a method wherein a modulation is applied to a light emitting element by a voltage at a measuring point and light thus obtained is passed through a Faraday effect element subjected to a modulation by a current at the measuring point to form a power sensor requiring no current transformer.

- CONSTITUTION:A light emitting element LED 3 is driven with a DC power source 2. As the element is controlled with a modulator 10 with the application of a voltage of a capacitor voltage divider 1 thereto, emission of the LED 3 is turned to a light modulated by a voltage signal. The light modulated generates a Faraday effect in a coil 4 by a magnetic field with a current flowing to the coil 4 through a Faraday effect element 6 placed between a polarizer 5 and an analyser 7 to cause a modulation of light. Light emitted from the analyser 7 is received with a photo diode PD8 to be converted into electricity which is passed through a low pass filter 9. Thus, with the removal of an AC component, a DC component is determined to be measured with a voltmeter.

Thermal converters

These are small, robust, stable in time and have a large frequency range. **Thermocouples** are basically squaring elements, see Chapter 4.2.2.1 above, but connecting two of them together gives a **"sum and difference multiplier"**, an averaging multiplier, Figure 182 [228] shows a circuit design for a thermal Watt meter. The mathematics behind it are:

$$V_{dc} = k / T\int_0^T ((u+i)^2 - (u-i)^2)dt = k / T\int_0^T 4uidt \tag{73}$$

where T stands for time and k is a constant.

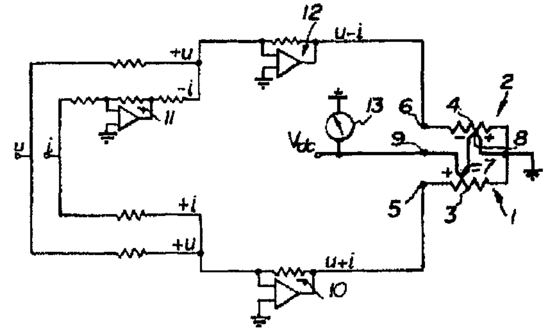

Figure 182 [228]
Differential Thermal Wattmeter

The resistor 4 is heated by a current proportional to u-i, and the resistor 3 by a current proportional to ı+i. This give us the two heat quantities

$$\delta Q(u\text{-}i) = R(u\text{-}i)^2 dt \text{ and } Q(u+i) = R(u+i)^2 dt \text{ (Joule's law)} \qquad \textbf{(74)}$$

n comparison with e.g. electro dynamometers, another type of averaging wattmeter, thermal multi-oliers have a large error (short term instability, low output voltage). They are however small and oortable, insensitive to stock, vibration and attitude [229]. They are used in audio-frequency range, and are good for very distorted wave forms.

The zero instability can be eliminated by automatic reversing [230].This reference describes a Watt meter with a linear scale, a resolution of 10 ppm and a direct reading accuracy of 30 ppm in the 50-1000 ℲZ range.

The problem of the non-quadratic and non-identical response of the thermal converters is solved by ƆC feedback and input interchanges in the already mentioned [228] (Fig. 183).

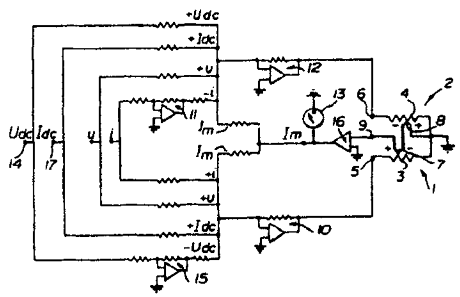

Figure 183 [228]
Wattmeter

A differential qthermal wattmeter of the type disclosed in U.S. Pat.No. 4,045,734 is modified to remove undesirable in-phase a.c. ripple at the fundamental frequency in the feedback path. This result is achieved by a closed loop system in which the in-phase signal in the feedback path is detected and driven to zero by injecting sufficient signal in opposite polarity into the feedback path to cancel the ripple. The advantages are reduction of error and the ability to use standard,low cost components.

With digital sampling technique and a **desktop computer** it is possible to achieve a system with reduced transfer error (accuracy better than 30 ppm at line frequency and all power factors) up to 10 KHz (Fig. 184) [232].

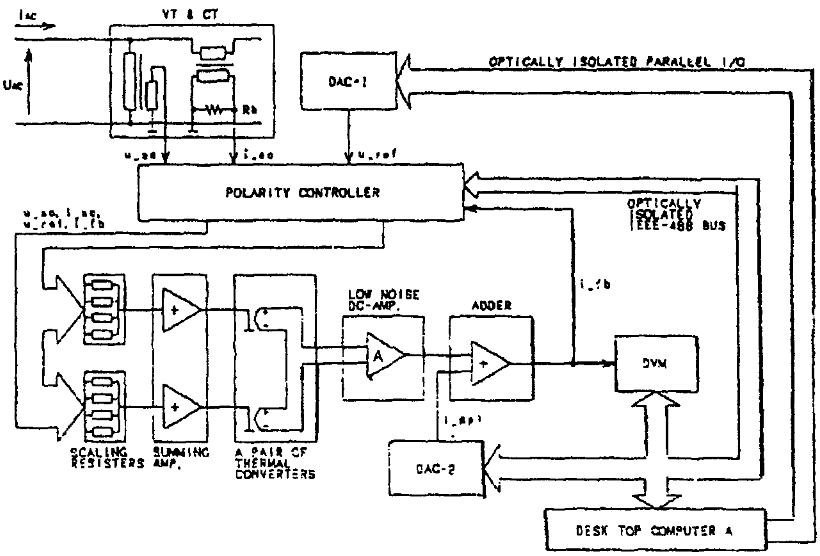

Figure 184 [232] ©1991 IEEE
Block Diagram of the Precision Thermal Wattmeter

[230] describes a thermal instrument for precision measurement of AC voltage, current, power and energy of power frequencies. It has a 0.001% of full scale error for power measurements, and uses digital circuits. The accuracy of this instrument relies on a continous ac/dc transfer.

Electronic Multipliers

Multiplying circuits in general are beyond the scope of this book. For a treatment of analog multipliers, we refer to "Analog Integrated Circuit Design", Chapter 7 [238]. A problem related to multipliers in power measuring is that it is difficult to reach a high precision (1%).

Figure 185 [239] shows an example of using analog four quad multipliers in three phase metering.

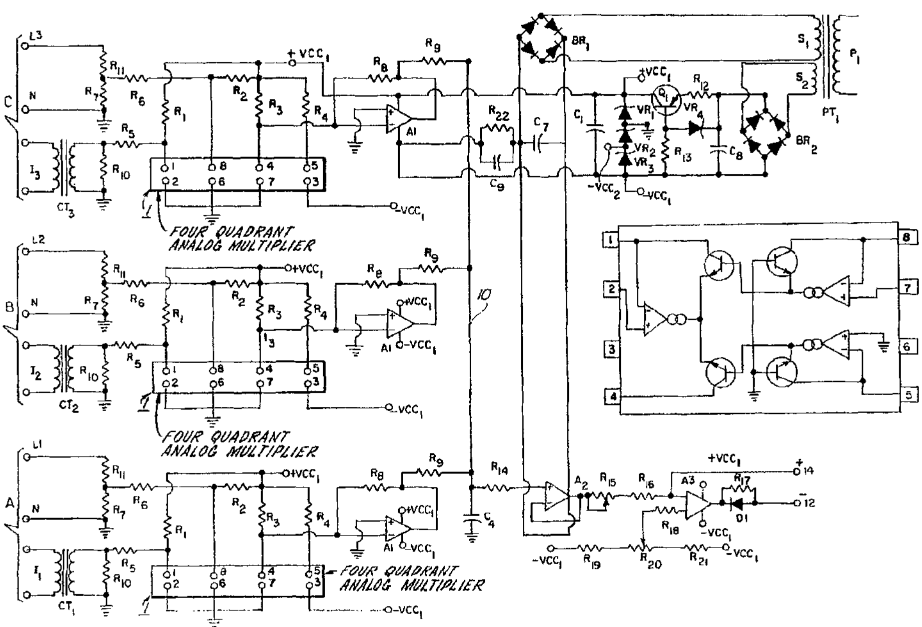

Figure 185 [239]
Alternating Current Watt Transducer

An alternating current watt transducer including an integrated circuit analog multiplier, providing four quadrant multiplication, to the input terminals of which are applied alternating current signals proportional to the voltage and current determinative of the watts to be measured. The integrated circuit analog multiplier provides an alternating current output signal which being proportional to the product of the in-phase components of the input signals, is proportional to the watts being measured. The alternating current signal which is proportional to watts is transformed to a constant-current direct current output.

Figure 186 [240] demonstrates an electronic Wattmeter with a dedicated multiplying circuit

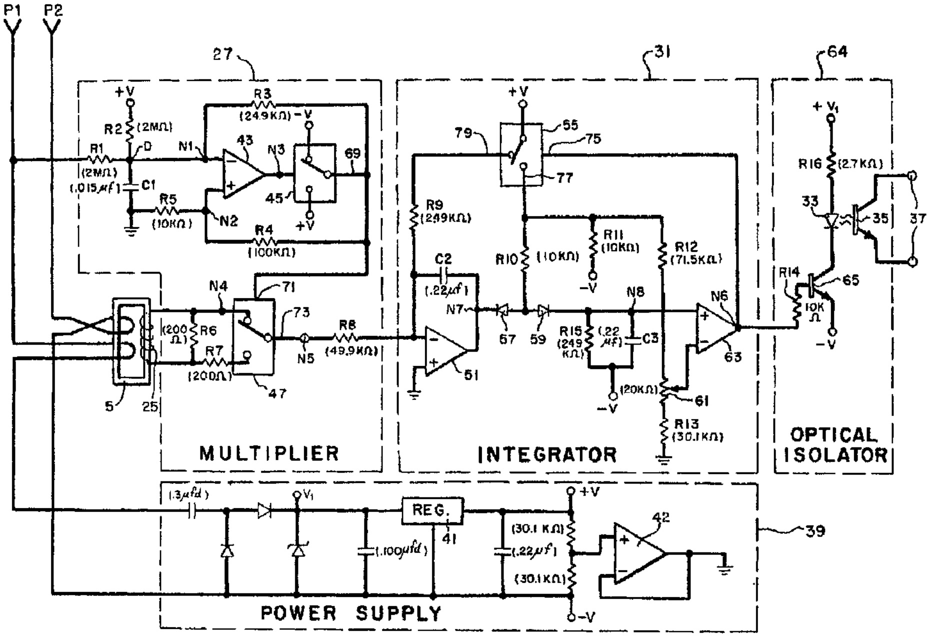

Figure 186 [240]
Electronic Wattmeter

Current and voltage of power lines are monitored and used to generate unitized voltage pulses at a frequency that is proportional to the average power carried by the lines. The current transducer is inductively coupled to the monitored power lines and includes a magnetically permeable frame which has two magnetically permeable, spaced parallel leg members and a magnetically permeable cross-member that is detachably affixed between the leg members. The monitored power lines pass through an aperture defined by the leg members and cross-member of the frame and the frame additively applies the magnetic fields of the conductors to a coil that is inductively coupled to the frame. The coil generates an induced current corresponding to the current of the conductors. A multiplier samples the induced current at a rate defined by the line voltage and generates an output voltage signal that has an average intensity that is representative of the product of the line voltage and the current of the lines. An integrator successively integrates the output voltage signal of the multiplier to a particular magnitude and generates a unitized pulse for each integration up to the particular magnitude. An optial isolator generates an output signal that is modulated by the unitized pulses of the integrator and that is electrically isolated from the line voltage of the power lines.

Log-antilog devices make good multiplication circuits for electric power calculation (Fig. 187) [242].

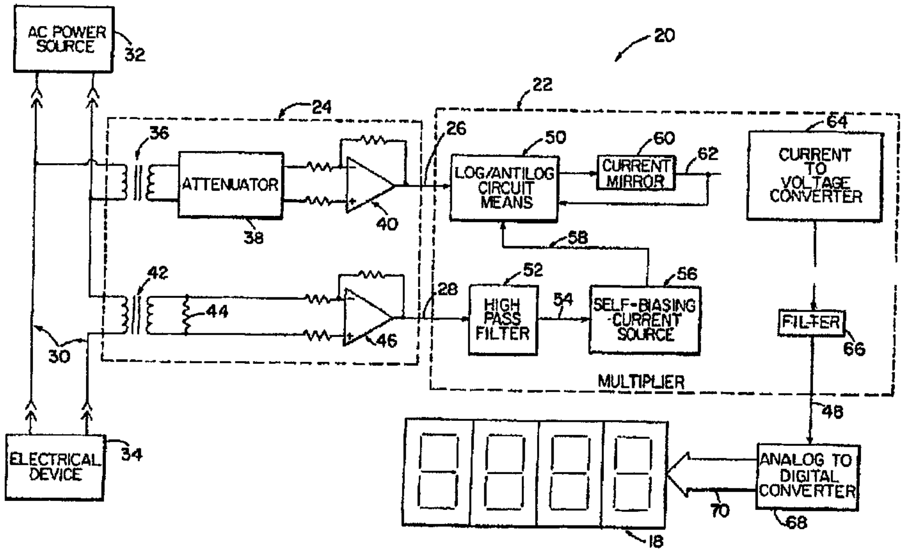

Figure 187 [242]
Power Measuring Appararus

Single components can be used as multipliers. Figure 188 [245] illustrates a minimalistic multiplier based on a single transistor.

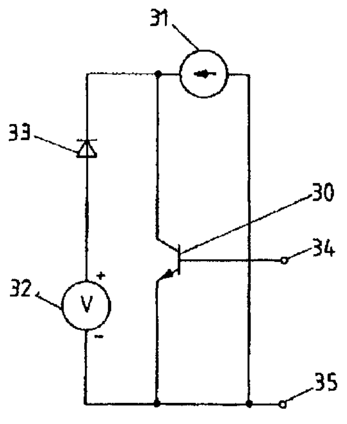

Figure 188 [245]
Multiplier Circuit

The products of the current (31) and the voltage (32) determines the heating of the transistor (30). The heat dependent emitter-base voltage constitutes the output.

An oscilloscope makes a simple multiplier (Fig. 189) [243]. Here the horizontal deflection is driven by a current-proportional signal, and the vertical deflection by a voltage-proportional one. The mapped area is proportional to the power delivered to the load under study.

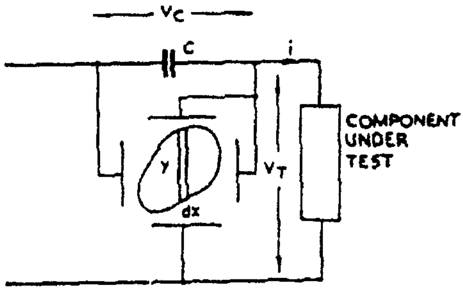

Figure 189 [243]
High Speed Power Analyzer

4.2.5.3 Digital Multiplication

It is not our intention to cover general electronics, but we will give some examples of digital multiplication in watt meters:

Figure 190 [244] gives a schematic overview of the use of a a microprocessor for multiplication and linearization.

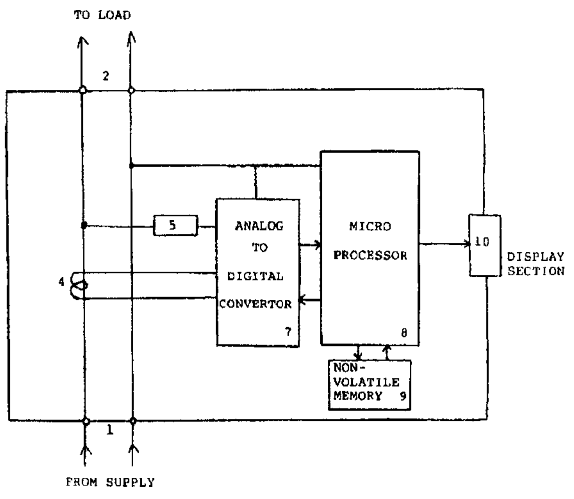

Figure 190 [244]
Improvements in and Relating to Electricty Meters using Current Transformers

Sampling is of particular concern.

The ADC is often of a fast type in order to avoid errors due to un-equal sampling of current and voltage, and in order to capture the true wave forms (Fig. 191) [245]. (Cf. ch. 4.1.1)

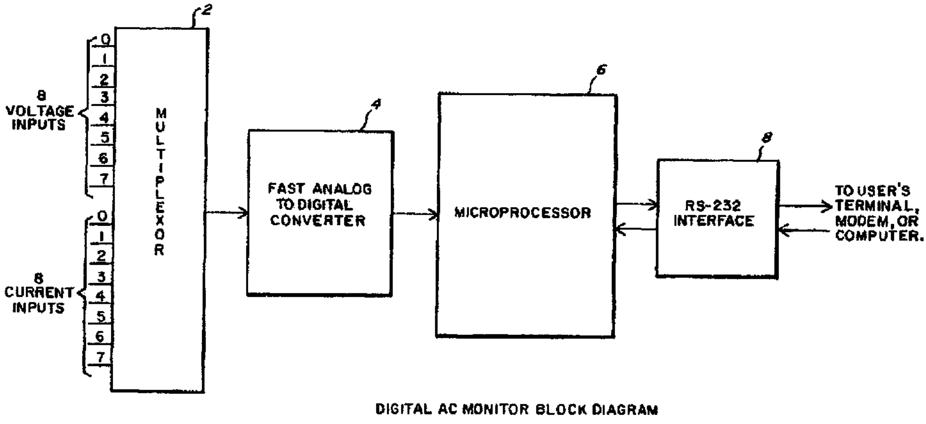

Figure 191 [245]
Digital AC Monitor

An apparatus and method is provided for monitoring a plurality of analog ac circuits by sampling the voltage and current waveform in each circuit at predetermined intervals, converting the analog current and voltage samples to digital format, storing the digitized current and voltage samples and using the stored digitized current and voltage samples to calculate a variety of electrical parameters; some of which are derived from the stored samples. The non-derived quantities are repeatedly calculated and stored over many separate cycles then averaged. The derived quantities are then calculated at the end of an averaging period. This produces a more accurate reading, especially when averaging over a period in which the power varies over a wide dynamic range. Frequency is measured by timing three cycles of the voltage waveform using the upward zero crossover point as a starting point for a digital timer.

Depending on the use of the power measuring apparatus, the requirements on the sampling are different: **Protective circuit breakers** need only a few data points, but require rapid results. **Metering** calculations, on the other hand, do not have to be performed rapidly, but require many sampling points, especially if the signal to be measured is rich in harmonics.

The apparatus of [321] uses **equivalent sampling** to combine the needs of protection and metering in a single device, and with a minimum of computational power. It includes a single standard microprocessor. See Figure 192 [321].

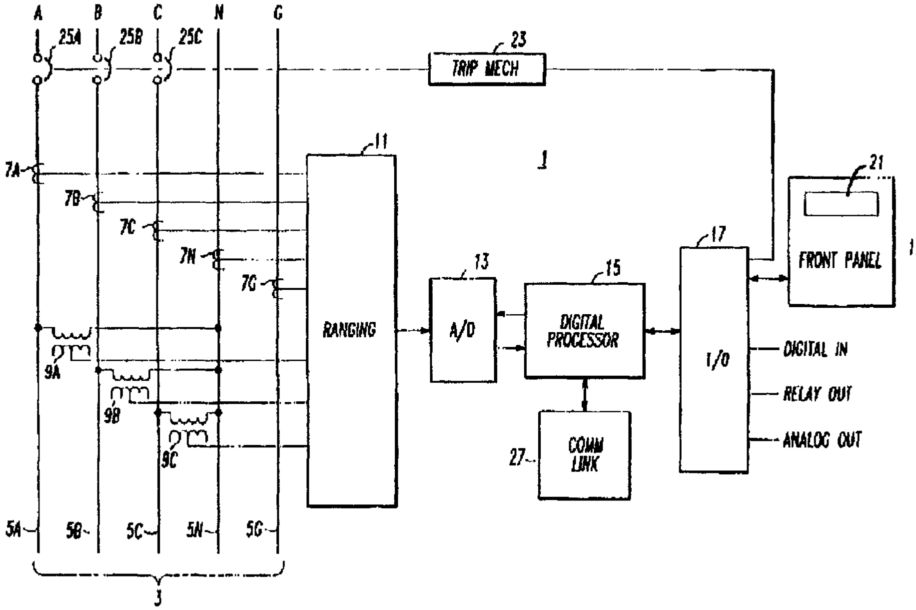

Figure 192 [321]
Equivalent Sampling Power Meter

A circuit interrupter (1) samples waveforms in a protected circuit (3) by taking samples in pairs (P1, P2) spaced 90 electrical degrees apart. The sum of the squares (S2) of samples in each pair, which is representative of the RMS value of the fundamental frequency of the waveform, is used for instantaneous protection (55) by comparing a running sum (S4) of the squares for the two most recent pairs of samples to a threshold representative of the instantaneous trip pick-up value. This sum of the squares (S4) of successive two pairs of samples is also used for short delay protection (61). A delay between successive pairs of samples is varied to produce a selected equivalent sampling rate after a given number of samples. Samples accumulated at this equivalent sampling rate, which is sixty-four samples per cycle in the preferred embodiment, are used for long delay protection (69) and metering.

It is difficult to obtain **simultaneous current and voltage values**.
Elaborate sampling schemes enable the use of a slower, and cheaper, ADC without loosing in precision, given that the signal is reasonably smooth.

A classical method for minimizing the error due to non-identical sampling instants is to periodically reverse the order of the respective voltage and current samples, so that they alternate in leading and lagging every second time, i.e. $p_1=u_1i_2$, $p_2=u_2i_1$, $p_3=u_2i_3$ etcetera. See Figure 193 [322]. The power samples pi are in this device averaged over a great number of samples: $p=1/n(u_0i_1+u_2i_1+....)$.

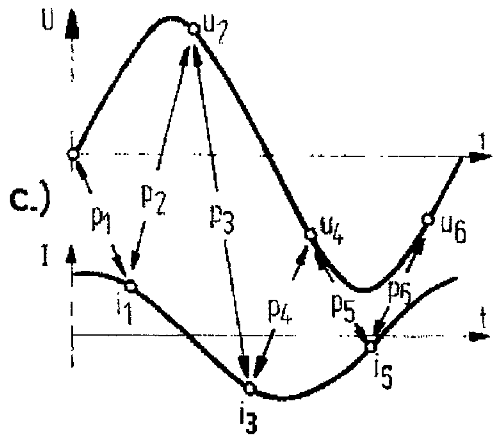

Figure 193 [322]
Sampling Scheme

An alternative is to use interpolation of one of the current/voltage values to the sample instant. See Figure 194 [322].

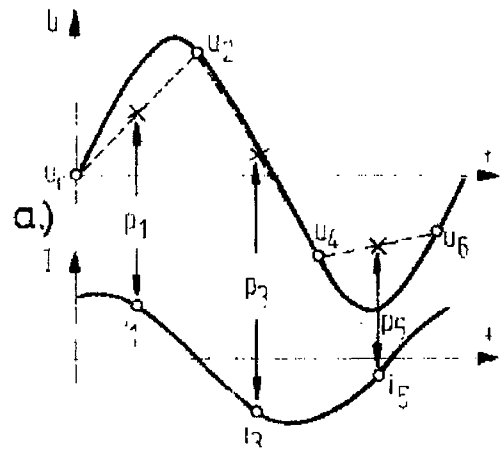

Figure 194 [322]
Sampling Scheme

A simplified sampling scheme reduce the need for computational power, and enables the use of a single processor for measuring, calculating power and performing additional tasks such as controlling a process. [323] illustrates how this can be done. The device applies a correction for the error resulting from the time lag between current and voltage sample: Correction factor=1/cos(T2 f). This factor is deduced by considering that the timelag T between samples has the effect of phase shifting the current and voltage curves. See Figure 195 [323].

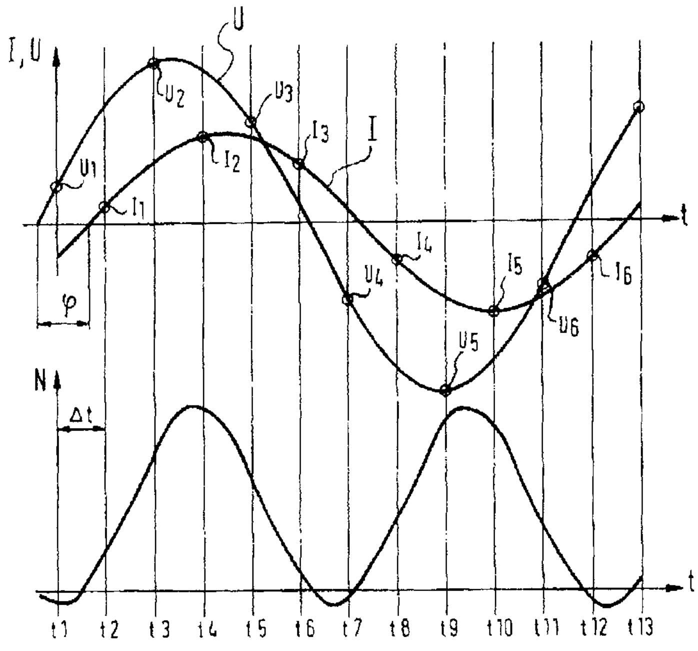

Figure 195 [323]
Sampling Scheme

In a method for measuring the consumption of electrical energy by a consumer the momentary values of the alternating voltage and alternating current are measured alternately in the time periods of a sampling cycle. Each measured momentary value is stored. From the momentary value measured in each sampling period and the stored momentary value the product is formed and the formed products added together. The sum of the products formed is then multiplied by a correction constant depending on the frequency of the alternating current and of the alternating voltage as well as on the sampling period.

ADVANTAGE - Reduces time required for measurement. Since previously microprocessor required complete sampling period to obtain momentary energy consumption and second microprocessor was needed for control procedures, single microprocessor can now perform both measurement and other tasks.

Each of E, I and α can also be separately determined [248], or sampled more or less simultaneously. The series of samples p_1, p_2, p_3 ...(where $p_i = u_i\, i_i \cos\alpha_i$) are then averaged over for example one half period, as in [249]. This is a common method (Fig. 196).

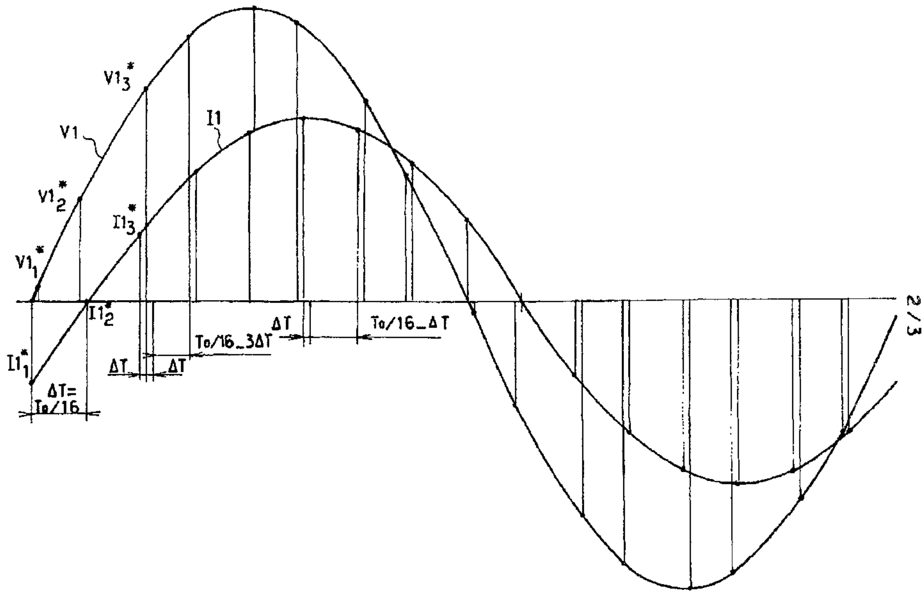

Figure 196 [249]
Process and Device for Measuring Electric Power

A method for measuring the electrical power on an alternative current network, wherein samples taken at different time points and representative of the various network electrical magnitudes related to the power or to each power to be measured are transmitted to a computing device through a single channel, characterized in that, over a determined time period which is equal to or a multiple of the network half-period, sample groups are respectively taken which comprise groups of a first kind each including at least one couple formed by voltage and current samples related to a desired power and taken in a determined order and with a determined time interval, and groups of a second kind in the same number as the groups of the first kind and each including at least one couple of samples of the same voltage and current as said couples in the groups of the first kind, taken with the same time interval but in a revers order to said determined order, each group of both kinds comprising samples which are all taken at different times, the distribution of the samppling times of the first kind groups and the distribution of the sampling times of the second kind groups being symmetrical to one another relative to the middle of the sampling period and, in that the individual powers obtained by multiplying with one another the samples from the couples of the various groups are cumulated.

196], Figure 146 uses exponential averaging of the instantaneous power values to reduce the error 'nduced by sampling voltage and current at different instants.

Pulse width modulation is commonly being used in multiplying currents and voltage values (Fig. 197) [247]. A popular modulation technique is let one input variable, e.g. the voltage, modulate the pulse width, and to let the other variable, i.e. the current, modulate the pulse height.

The resulting digital signal - proportional to power - can easily be exploited to elaborate e.g. average power value by low pass filtering.

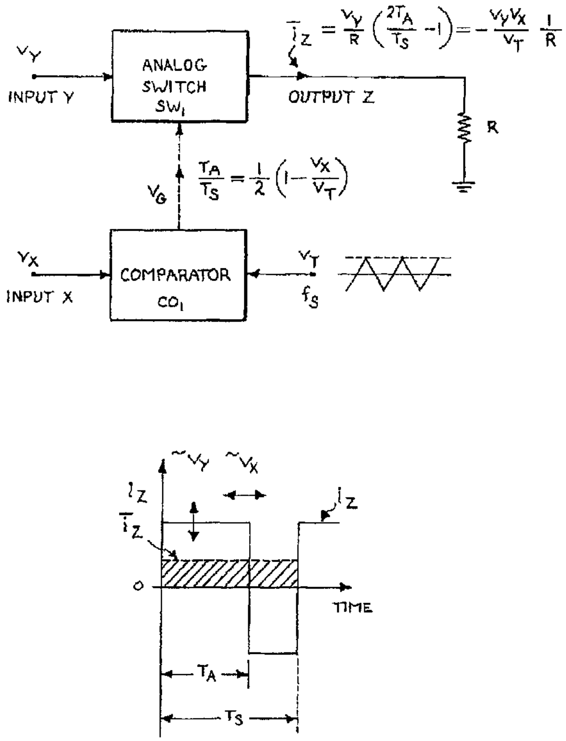

Figure 197 [247]
Electronic Watt Transducer Circuit with Constant DC Current Output Proportional to Watts

An electronic wattmeter in the form of an electronic watt-transducer circuit requiring a minimum number of components that can be fabricated by monolithic semiconductor integrated circuit manufacturing techniques and which provides a direct current output signal that is proportional to watts. The electronic watt transducer circuit comprises a first transformer for developing a first voltage related signal proportional to the input voltage to be measured and a second current transformer for developing a second current related signal proportional to the input current to be measured. A pulse width modulator is connected to receive the first voltage related signal and an input repetitive sampling signal for producing repetitive pulse width modulated output pulses having instantaneous pulse width proportional to the corresponding instantaneous amplitude of the first voltage related signal. Double-pole, double-throw electronic switch multipliers are connected to be automatically switched in response to the repetitive pulse width modulated output signal to develop at the output thereof alternating polarity, pulse width and amplitude modulated signal pulses having instantaneous pulse widths proportional to the first voltage related signal and instantaneous amplitudes proportional to the second current related signal, and a DC component proportional to the product of the two and hence to the power consumption represented by the electric voltage and current being monitored. An averaging type current-to-current converter is connected to the output from the electronic switch multiplier for providing an output analog average direct current electric signal proportional to watts.

A summing arrangement which employs ΣΔ modulation which is suitable for integration on a single chip is illustrated in Figure 198 [324]. This relatively simple arrangement yield sufficient accuracy and dynamic compared to the ones using classic multiplication. "3" denotes a multiplier/adder stage.

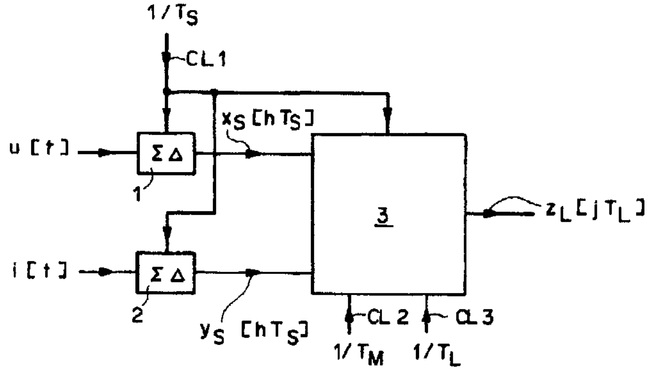

Figure 198 [324]
Integrated Power Measuring Arrangement

Two functions (u, I) of time are input to respective sigma-delta modulators (1, 2) clocked at a first frequency (1/TS). The outputs (xS, yS) pass to a multiplier/adder (3) clocked at the same and two further frequencies (1/TM, 1/TL). Both modulators are pref. of second order and the multiplier/adder comprises two decimation filters, a delay stage (with opt. a decimation-less digital sliding filter), an addn. element and a divide-by-N (over-sampling rate) element.
USE / ADVANTAGE - In e.g. Watt-hour meters for RMS current or voltage values, correlations or averaged powers, the computation requires no multiplication of two R-bit operands, but only simple shifts and algebraic additions.. Maintains precision achievable in conventional multiplication by use of clocked sigma-delta modulators and triply clocked multiplier-adder.

Measuring a plurality of quantities

The versatility of **microcomputers** make them the ideal component for integrating in instruments capable of extracting a multitude of information from the input signals (see Figures 199 [248] and 200 [325].

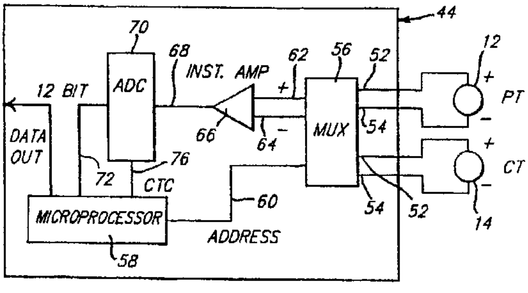

Figure 199 [248]
High Speed Power Analyzer

A method and apparatus for rapidly and continuously sampling AC voltage and current signals in a plurality of power distribution circuits. The sampled signals are then analyzed in a sine board computer to derive the number of fundamental electrical variables. These variables include frequency, RMS volts, RMS amps and a phase angular relationship between the voltage and currents in the system. The computer also performs calibration and compensation functions. From these fundamental variables, other useful parameters can be calculated such as watts, watt-hour, VARS, and power factor.

4.3 COMPONENTS OF POWER

As in all fields of technology, we see an increased use of distributed intelligence in power metering apparatus. Figure 200 [325] illustrates the front panel forming the user interface of a power system monitor. It presents the operator with a large number of parameters.

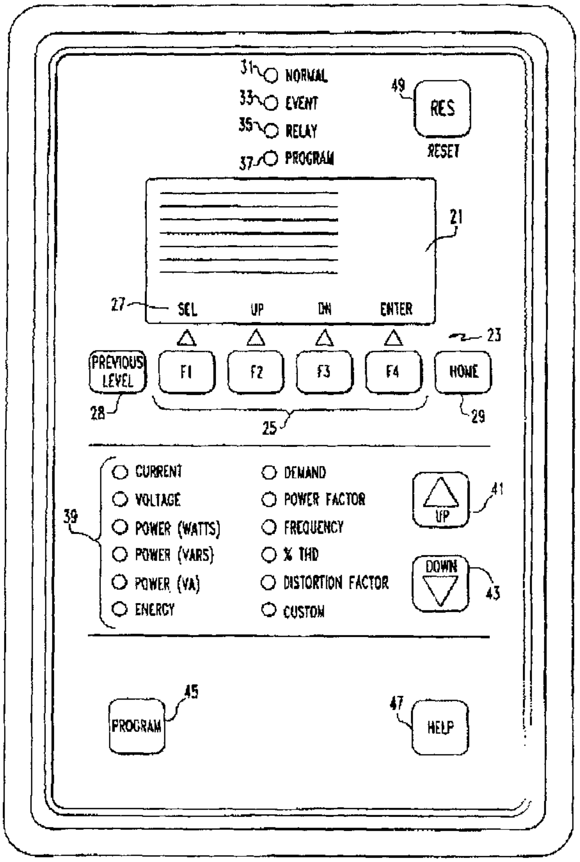

Figure 200 [325]
Front Panel for Power System Monitor

Apparatus for monitoring electrical parameters in an electrical system includes a display on which values of the various monitored electrical parameters are displayed, several at a time. The apparatus can be programmed to generate a custom display presenting selected ones of the many parameters, such as the ones most often referenced by the operator, so that it is not necessary to scroll through the large number of parameters to find those of frequent interest.

A selector is used for selecting the custom set of electrical parameter values for display on the display device the preset number at a time. The custom set includes a number of electrical parameter values which is greater than the preset number of electrical parameter values, and the selector includes a device for sequentially displaying portions of the custom set of electrical parameter values the preset number at a time.

- USE/ADVANTAGE - E.g. for metering systems, and for analysis of parameters such as current, voltage, power, energy, VARs, power factor frequency, harmonic distortion etc. Can also be used to evaluate circuit breakers, or to contactor or motor starter. Allows operator to quickly view values of selected parameters without it being necessary to scroll through large number of parameters to find those of frequent interest.

The complete system is illustrated by Figure 201 [325].

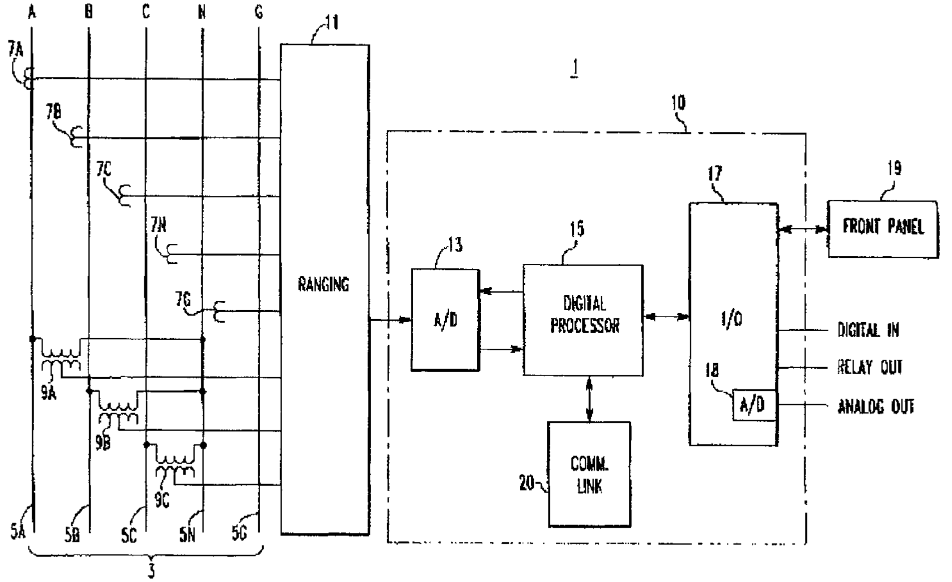

Figure 201 [325]
System Diagram Corresponding to fig. 200
The apparatus for monitoring an electrical system, comprises a device for sensing a number of waveforms in the electrical system. A device generates a predetermined number of electrical parameter values from the sensed waveforms.

4.3.1 Active Power

Active power is proportional to average power as long as I and U remain constant. A way of measuring it is thus to rectify the instantaneous power p(t). The already cited [239] does this, using a 4 quad analog multiplier (IC) and a rectifying circuit.

The Ferraris wheel automatically gives the active power, because the inertia of the wheel acts as an averager.

4.3.2 Instantaneous Power

Sampling the current and the voltage with a small time difference gives raise to an error when multiplying. This error can be reduced by using a particular sampling scheme: Reversing the order of sampling regularly (every full or a multiple period) [249]. Averaging the current samples before and after any specific voltage sample (or vice-versa) improve the accuracy of timing current-voltage couples [245]. See ch. 4.2.5.3 above.

4.3.3 Reactive Power

Remembering that the reactive power, Q, is the quadrature of active power, we see that it can be measured in the same way, employing the factor sinα instead of cosα. Adding a 90° phase shift of α gives the quadrature:

$$P = U\,I\cos\alpha \qquad (63)$$

$$Q = U\,I\sin\alpha = U\,I\cos(\alpha - 90°) \qquad (64)$$

See Figure 202 [250].

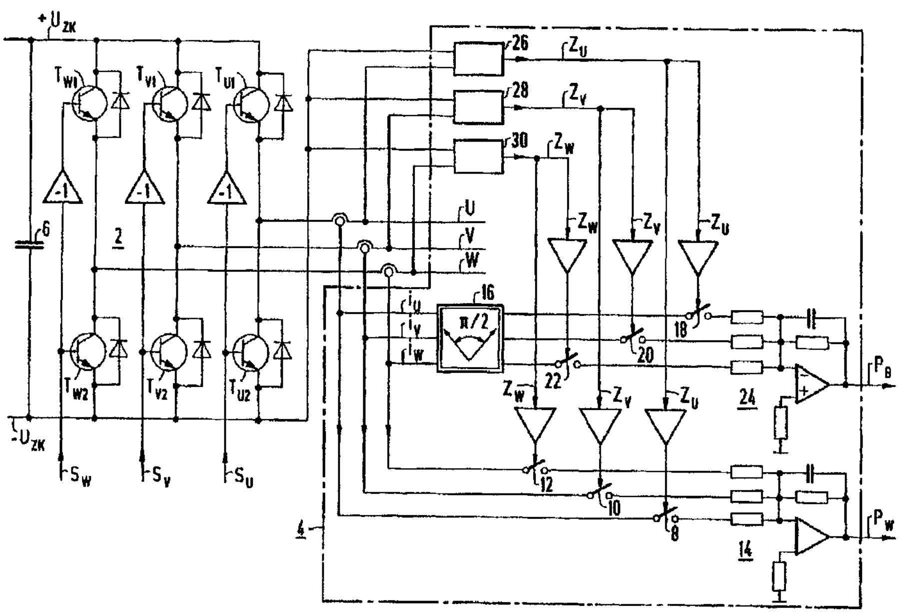

Figure 202 [250]

Circuit for Measuring of the Real and/or Reactive Power at a Converter with Impressed Direct Voltage

The invention relates to a device (4) for measuring real and/or reactive power (PW, PB) at one phase (U, V, W) of an inverter (2), a measurement signal (iU, iV, iW) corresponding to the phase current being connected, directly for detecting the real power (PW) or after phase rotation by pi /2 for detecting the reactive power (PB), to a switch (8, 10, 12 respectively, 18, 20, 22) which can be operated by means of a control signal, the real or reactive power (PW and PB, respectively) corresponding to a smoothed output signal of a ripple section (14 and 24, respectively). According to the invention, the actual switching state (ZU, ZV, ZW) of the converter valve (TU1 to TW2), operating on this phase (U, V, W), of the inverter (2) is provided as control signal, these switching state signals (ZU, ZV, ZW) in each case being determined by means of a detection device (26, 28,30). This provides a device (4) for detecting real and/or reactive power,in which measurement errors due to dead times and/or switching times are avoided.

4.3.4 Power Factor

Power factor = active power/apparent power = P/S=cos α (if u and i are sinusoidal)

In the sine case we can thus measure via the phase: (Fig. 203) [251].

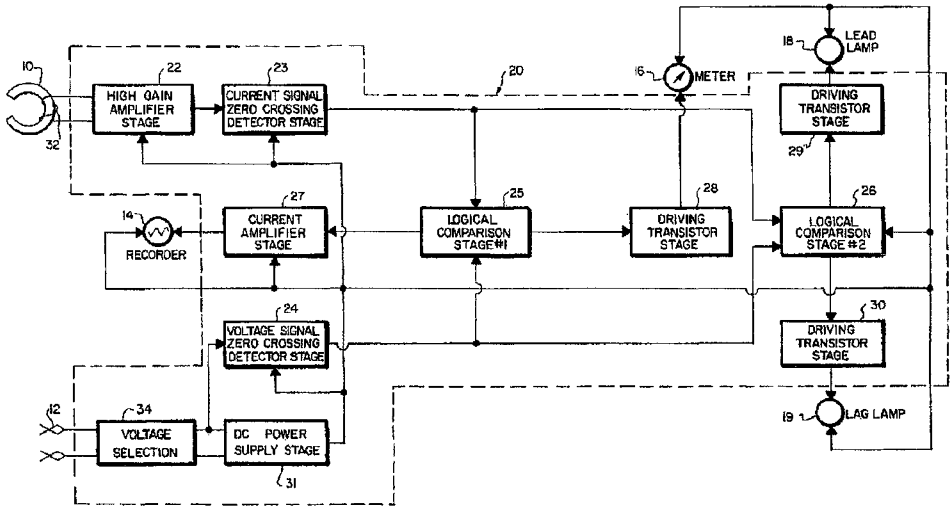

Figure 203 [251]
Power Factor Metering Device

A power factor metering device. The power factor metering device includes a novel electronic circuit for deriving the power factor from a detected voltage and current. The device includes a current clamp that may be clamped onto any conductor of a three-phase or single-phase circuit. Voltage clips are used to detect the circuit's voltage. The current clamp induces a voltage that lags the detected current by 90 electrical degrees. An amplifier stage is coupled to the induced voltage through a low input variable resistance so that the input voltage to the amplifier stage may be adjusted to correct for errors induced in the phase relationship between the detected voltage and current. The output from the amplifier stage is input into a zero crossing detector stage that changes its output state each time the output of the amplifier stage passes through zero. The output of the zero crossing detector stage is applied to one side of a pair of EXCLUSIVE-OR gates, and is also applied to one of the inputs of a bistable multivibrator. The voltage detected by the voltage clips is stepped down by a transformer and is input to a second zero crossing detector stage. The output from the second zero crossing detector stage provides the other input to the EXCLUSIVE-OR gates and the bistable multivibrator. The output of each EXCLUSIVE-OR gate is directly proportional to the phase angle between the detected voltage and current. The outputs from the two EXCLUSIVE-OR gates are amplified and are used to drive a continuous recording device and an instantaneous meter which each display the magnitude of the power factor derived from the detected current and voltage. The output from the bistable multivibrator is used to determine whether the current signal leads or lags the voltage signal.

If we have stored values of P, U and I in a memory, we can use software to calculate the power factor, P/U*I as in [245].

The more complicated case with distorted wave forms is treated below.

4.3.5 Average Power

Low pass filtering is simple way of averaging, see Figure 147 [198] above.

4.4 SPECIAL APPLICATIONS

4.4.1 Power of Distorted Signals

Many power measurements are made supposing simple sinusoidal wave forms. When much harmonics are present, as in systems subject to switching, the simplified phasor formulae cannot be used. Fast digital sampling meters based on multiplying i_i and u_i samples give a correct result for the real power at frequencies under the double Nyquist limit. Note that the power frequency is twice the current frequency (Fig. 144).

Determination of active and reactive components can be done by using the Fourier- developments of the measured current and voltage wave forms; For each frequency the standard formulas are applied. The sum over all frequency then gives the total result i.e.:

$$P_{av} = V_{dc} I_{dc} + \Sigma V_n I_n \cos \alpha_n \tag{75}$$

$$Q_{av} = \Sigma V_n I_n \sin \alpha_n + \ldots \tag{76}$$

V_n, I_n are RMS values. α_n is the phase shift. The measuring principle is thus to sample u, i, and to use fast Fourier Transforms (FFT) to find the magnitude and phase for each frequency. P_{av} is then found by multiplying and adding samples [253] and [254].

Corrections for not sampling i_i and u_i exactly simultaneously must be made as mentioned above.

4.4.2 DC Power and HV Power

As noted above, the Ferraris wheel meter can be used after an AC-DC convertion by e.g. transductors [219]. The use of transductors is shown in Figure 204 [255].

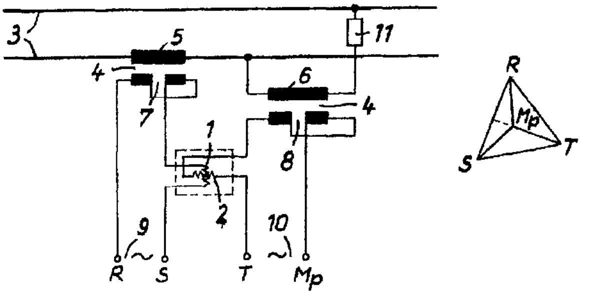

Figure 204 [255]
Transductor Measuring Arrangement

The principles for measuring on HV-lines are the same as for low voltage. What differs is the choice of sensors, see Chapters 1 and 2. Current transformers, Hall devices or Faraday cells are popular current sensors and capacitive transducers or Pockels cells are popular voltage sensors.

Low voltage transducers are being used for high voltage measurements after that the voltage has been divided down to a suitable level. Capacitive voltage dividers are popular, but both resistive and inductive ones can be used.

Usually the quest for safety leads to the use of capacitive or optical sensors. Contactless transmission of measurement values is an alternative for ensuring galvanic separation between the object of measurement and the instrument, in the case there is a risk for contact.

Digital meters measure DC directly. The voltage and current transducers might be different from the AC case. "zero flux" current transducers are suitable for DC, but they are more complicated, and thus more expensive, than the simplest AC transducers.

4.4.3 Polyphase Networks

Measuring the power of each phase and adding them is a straightforward principle (Fig. 205) [256].

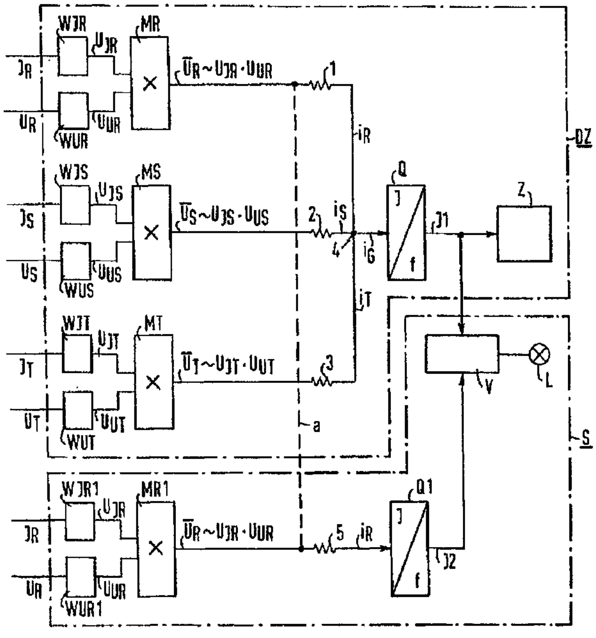

Figure 205 [256]
Electronic Three-Phase Electricity Meter

An electronic three-phase electricity meter, wherein a multiplier unit (MR, MS, MT) is provided for each phase, supplied at its input end with signals proportional to the current and voltage associated with the phase, and emits a power-proportional output signal (~Ur, ~Us, ~Ut) that is added to the output signals of the other multiplier units to form a sum signal which is converted in a quantizer (Q) into a pulse train (I1) having a power-proportional frequency and then integrated with respect to time in a counting device (Z) for the energy to be detected, and the result displayed, characterised in that for one (R) of the three phases (R, S, T) an additional power detection device is provided, consisting at least of one multiplier unit (MR1, MP) and a test quantizer (Q1), which device supplies at its output end a pulse train (I2) having a power-proportional frequency, and that a comparator device (E) is provided for the two pulse trains (I1, I2) supplied by the quantizer (Q) and the power detection device, with comparison device triggers a signal change in a display unit (L) when the ratio of the frequencies of the two pulse trains (I1, I2) exceeds the limits of a specified tolerance band, these limits being selected such that the breakdown of an essential component leads to the exceeding of a limit, existing function elements (WIR, WUR, MR; WIR, WUR, TR, INR) of the three-phase electricity meter (DZ) also being used for the additional power detection device.

Digital addition of each phase's power is shown in Figure 206 [257]. The traditional Two- Watt meter method for 3 phase power measuring is not being treated here.

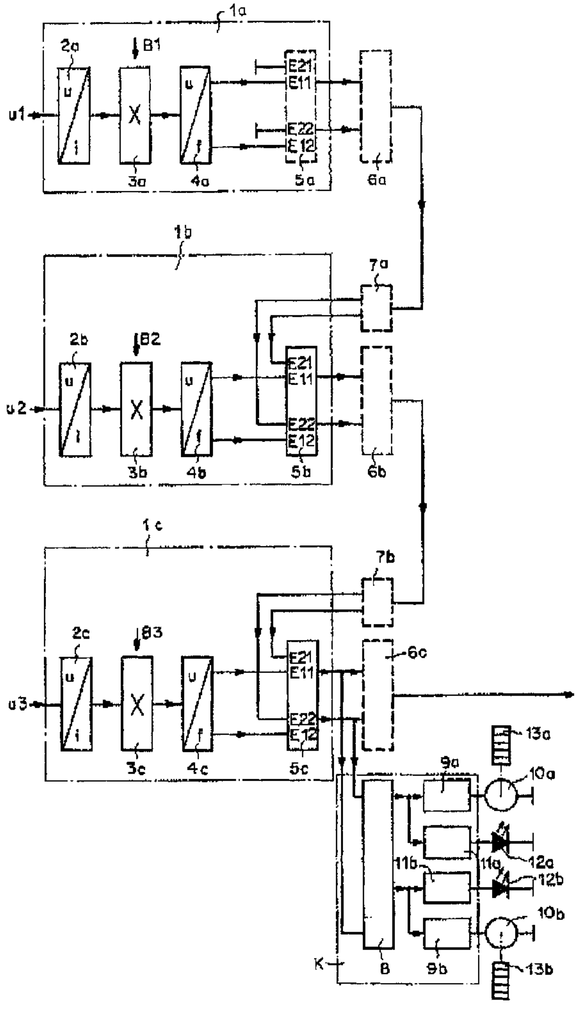

Figure 206 [257]
Three Phase Summing Energy Meter

Each input circuit (1a-1c) comprises a cascade connection of a voltage-to-current converter (2), multiplier (3),voltage-to-frequency converter (4) and adder (5). Output from each ofthe first two adders (5a,5b) is forwarded via a ternary encoder (6a,6b) and decoder (7a,7b) to the adder of the succeeding input circuit. The sum from the final adder (5c) is encoded (6c) for transmission and is also fed to a reversible counter (8) supplying the drivers (9a,9b)of stepper motors (10a,10b) for mechanical indicators (13a,13b). The integrated counter and driver (K) includes also driving circuits (11a,11b) for LEDs (12a,12b) which flash in synchronism with the outputs of the counter (8), one for positive and the otheer for negative sums.

4.4.4 High Frequency Power

We have treated the principles of measurement above in ch. 4.2. The choice of sensor is of particular interest; Bolometric Sensors, thermocouples, hot carrier or Schottky diodes are common. Calorimetry and crystals are also being used. [260].
[331] gives a good overview of detection ranges and reaction time of the various sensors.

[259] states that:
"Average microwave power up to about 10 mW is usually measured by bolometric or thermocouple sensors. The basis for bolmetric power measurement is that when power is dissipated in a resistive element, a corresponding change occurs in the elements resistance. Measuring power with thin-film thermocouples is also widely used in the microwave region. These sensors have the same advantage as diodes in that only a simple dc millivolt meter is needed to display the detected voltage. Moreover, the thin-film thermocouple may be easily matched to transmission line operating as a matched load, and used as broad-band meter. However, high speed can not be achieved in such power sensors, because they depend upon the use of a rise in the lattice temperature. Further, it is necessary to make a power sensor element small compared with the operating wavelength and this causes a decrease in the sensitivity." A sensor exploiting the hot carrier effect of L-H junctions is illustrated in Figure 207 and 208 [259].

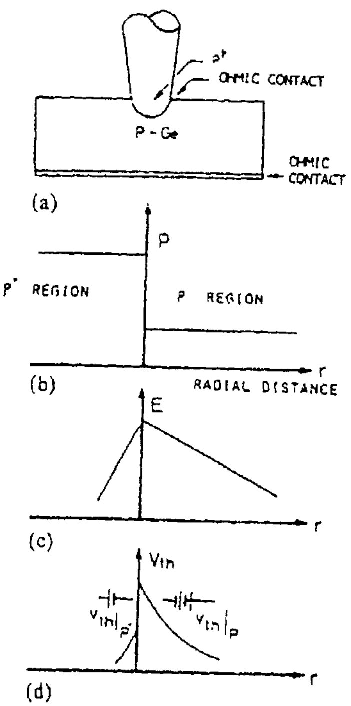

Figure 207 [259] ©1981 IEEE
Charge Carriers Distribution, Electric Field and Thermoelectric Voltage due to Hot Carrier Effect of L-H Junction

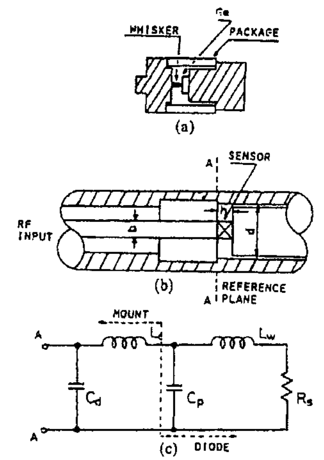

Figure 208 [259] ©1981 IEEE
Hot-carrier Power Sensor, Broad-Band Coaxial Mount and its Equivalent Circuit

Figure 209 [260] shows the use of a diode detector and a pick-up element in a coaxial transmission line.

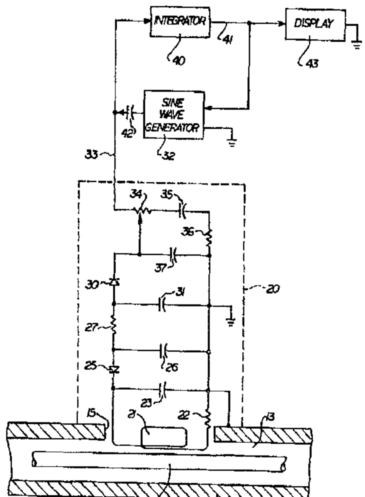

Figure 209 [260]
RF Watt Meter

The induction loop (21) in the pick-up element is connected to a principle detector (25). A secondary detector (30) is connected in opposition to the latter (25) The detectors are close to each other and subject to the same diode thermal environment. A sine wave generator supplies a wave signal to the sec. detector in opposition to the wave signal supplied to the principal detector from the inductive loop. The d.c. portion of the resulting signal representing the difference between the opposed signals is integrated (40) and the integrated output is used as the amplitude in the generated sine wave (32). When the circuit is in balance,the integrated output matches the amplitude of the inductive wave form and can be used as an output indicating (43) measured power in the coaxial transmission cable (11).

A hyper frequent power sensing circuit employing a FET (6) is illustrated in Figure 210 [326].

The FET (6) has a double function: It's gate is grounded and non-polarized, so that it act either as a capacitor or a diode, depending on whether it senses or not a current in the circuit. Additionally, the FET participates with it's equivalent capacitance to the adaption circuit.

The input is at (i).

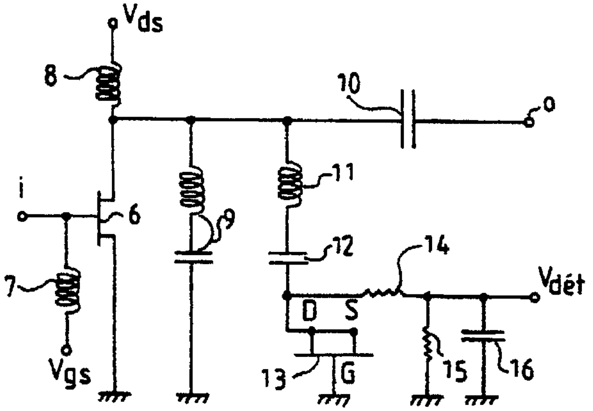

Figure 210 [326]
Hyperfrequent Power Sensing Circuit

Problems with diode detectors

Diode detectors have their particular problems, notably a temperature dependent threshold voltage. Figure 211 [292] shows a circuit that compensates for this via a biasing circuit.

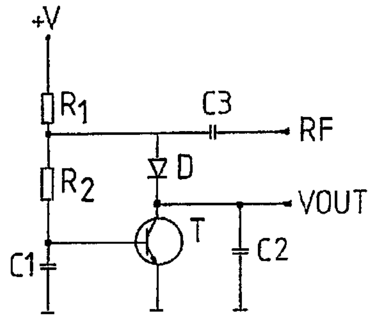

Figure 211 [292]
Biasing Circuitry for a Diode Detector

The invention relates to a biasing circuitry in a power level detector used for power control of a high-frequency power amplifier. According to the invention, to compensate for variation caused in the detector diode (D) threshold voltage by temperature changes, a constant-power source (T, R1, R2) is used by means of which the operating point of the detector diode (D) is set at a constant level and close to the angle point of the threshold voltage of the diode (D).

The problem of limited range(see also Figure 163) has another solution in combining two diodes arranged with different shunt capacitances, so that their sensitivities are different. Figure 212 [327].

D1 and D2 are power sensing Schottky diodes formed on a single IC or individual diodes. Capacitor C+ increases the shunt capacitance , Cd+C1 of D1, so that it is 10 times that of D2. The reduction in sensitivity is 20 dB.

The total range of this arrangement is 40 dB. It is used as a radiation detector.

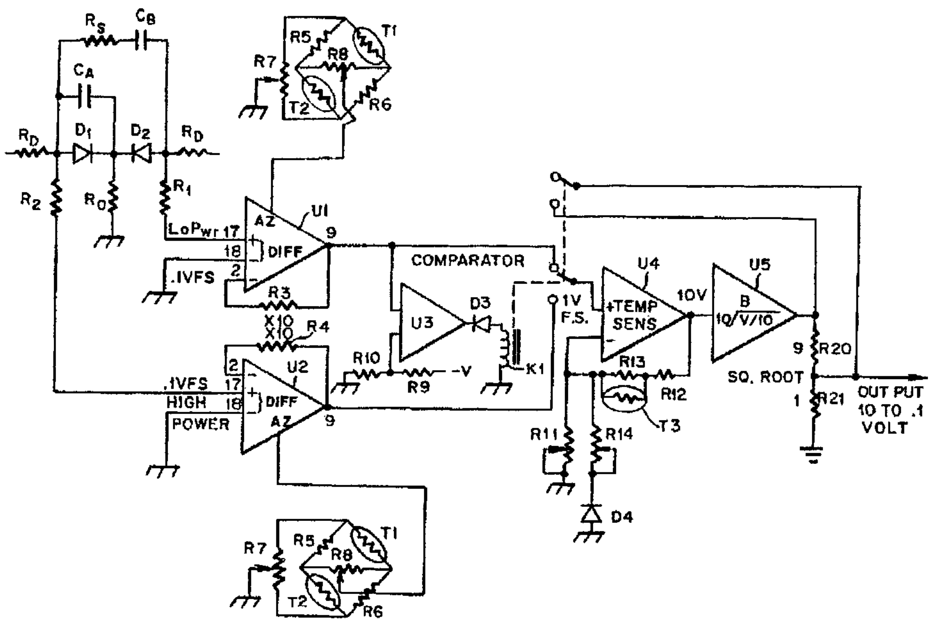

Figure 212 [327]
Wide Power Range Radiation Monitor

A wide power range radiation monitor includes a pair of diodes with their cathodes interconnected and with an additional capacitor coupled in parallel to one of the diodes. The detector of the radiation monitor provides two outputs, a low power output and a high power output, which outputs are connected to the anodes of the detector diodes. The arrangement of dual diodes and capacitance provide the diode detector of the monitor with a greater than 40 dB square law region.

Problems with Ferraris wheel Meters

- The Ferraris wheels response curve is not linear. Extra hardware, such as permanent magnets are being used for compensation (Fig. 170 above).

Figure 173 illustrates the use of a compensating current.

- It is subject to wear.
- The measurement transformers used are unlinear.
- It is inaccurate in measuring higher harmonics. This is of increasing concern because of the proliferation of electronic loads with unlinear characteristics, injecting harmonics into the system. In [289] Elham B. Makram et al [291] and [290] Girgis et al. determine this error.
- The information that it can deliver is very limited.
- It consumes energy: one can regard it as a small motor.

CHAPTER 5

MEASURING ENERGY

5.1 MEASURING PRINCIPLES

The **electric energy** delivered to a load (between time 0 and t1) is defined as:

$$E(t1) = \int_0^{t1} p(t)dt = \int_0^{t1} u(t)i(t)dt \tag{77}$$

The most common technique of measuring electric energy is to **measure the power** with one of the methods described in Chapter 4 (Section 1 - Measuring Principles) and **integrate** over time.

Calorimetric direct measurements are also being done; e.g. with the load completely contained in a liquid. The heat increase of the liquid (plus losses to the environment) is directly proportional to the energy dissipated in the load.

Electrochemical processes such as the ones in Coulombmeters can be used. The advance of an electrochemically driven process is somehow observed.

As a curiosity, we will cite a patent, filed in Thomas Alva Edison's name, for a Ah meters, which were used as energy meter (fixed voltage assumed). In [268], the voltage across a shunt is being used for alternating galvanic deposition and dissolution on two plates (C[1)], (C[2]) held by a balance (A). The oscillating movement is applied to a counter (H) (Fig. 213) [268].

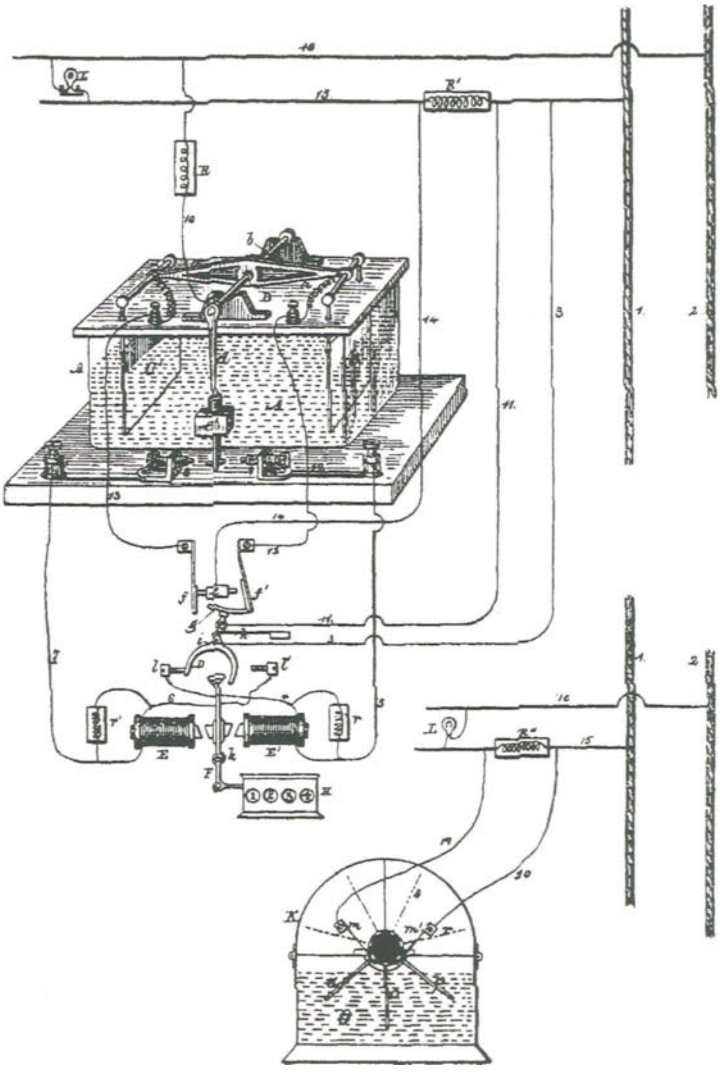

Figure 213 [268]
Ah Meter

In another patent [269] Edison lets the current produce gas, the quantity of which is a measure of current (and energy) consumption. The gas holder is emptied by combustion of the gas, ignited by a platinum coil (x) (Fig. 214).

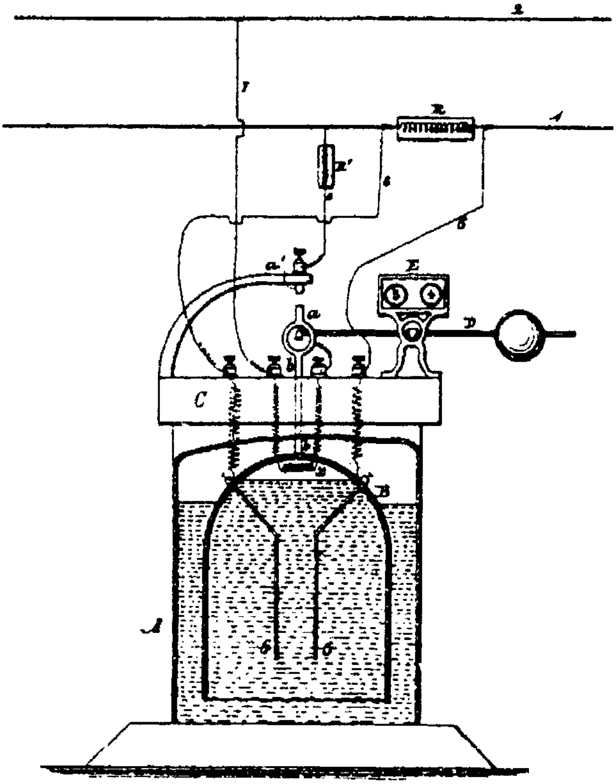

Figure 214 [269]
Ah Meter

5.2 INTEGRATING TECHNIQUES

Electromechanical or solid state integration are of most interest. Electrochemical integration as exemplified by the Edison patents is still in use.
Figures 215 and 216 [298] show a thin film electrochemical cell with, among other things, a use as a charge meter for constant voltage batteries such as lithium batteries. Although it is metering coulombs, it is clear that it also meters energy, as the voltage is constant.

This devise is cost effective, robust and stable over time.

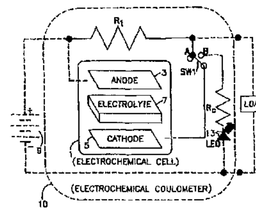

Figure 215 [298]
Electrochemical Integrator

The device consists of a thin film of inexpensive metal such as copper deposited on an inexpensive non-conductor, such as polyethylene to form the anode, and similarly to form the cathode. Electrolyte solution is provided by thin pads of material or structure such as woven fabric which is saturated with the electrolyte. Indications of charge remaining can be provided by LED meters. As current passes through this electrochemical cell, the anode is consumed through oxidation of the metal and the resultant metal ions are then plated at the cathode. Since the anode is consumed, the anode surface area is reduced thereby altering the over all resistivity of the electrochemical cell. The change in resistivity can then be measured in a conventional manner and from this change in resistivity, the number of coulombs passing through the electrochemical cell can be measured.

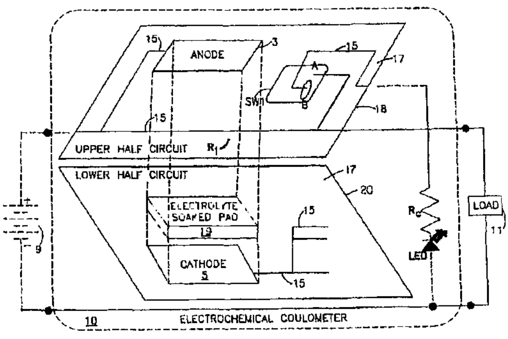

Figure 216 [298]
Electrochemical Integrator

This entire device, with or without the measuring circuit, maybe manufactured as discrete components or as pan of a single unit. One embodiment consists of metal strip-lines **15** such as copper electrolytically deposited on a non-conducting substrate **17** such as polyethylene, for example. $\mathbf{R}_I$ is defined by the sheet resistance of the metal conductors or strips **15**. The anode **3** and cathode **5** are of the same material such as copper, as the strip-lines **15** and of a surface area and thickness to produce the desired measure of charge as described above. An absorbent pad or separator **19** such as non-woven fabric saturated with solution such as copper sulfate in water separates the two electrodes **3** and **5** by a uniform fixed distance and provides the electrolyte **7**, in this example. A press contact switch is used for **SW1** to provide a measuring system such as that shown in the previous figure. The two halves can be placed on the same or separate sheets and the sheet halves glued or sealed together.

5.2.1 Electromechanical and combined Electromechanical-Solid State Integration.

The **Ferraris wheel** described in Chapter 4 (Section 4.2.5.1 "Multiplying Current and Voltage"), translates power consumption into rotational movement of a wheel on an axis. The purely mechanical meter has a decade counter coupled to the axis. See Figure 170 above.

With the privatisation of many of the utility companies providing metered commodities such as electricity, water or gas, and the resultant need to improve efficiency, current trends are towards developing **remote reading** systems which enable a consumer's commodity consumption meter to be read remotely without the need to gain access to the consumer's premises. Remote reading systems require an electronic signal which is related to the rate of consumption, or number of units of the commodity consumed.

Although electronic electricity consumption meters are available with electronic outputs, there are estimated to be in excess of twenty million Ferraris-type mechanical electricity consumption meters currently in operation within the UK, for example, which have an operating life expectancy of up to twenty-five years.

To replace all of these consumption meters with electronic consumption meters would not be cost effective and alternative ways of utilising these existing consumption meters are preferred [329].

The more modern hybrid meter senses the rotation with an Opto-sensor. Each rotation generates an electrical pulse, which is counted digitally. An advantage of the optical sensor/encoder is that it generates output signals suitable for data communication and treatment. Separate optical encoders and signal treatment units exist as "add ons" for conventional (Ferraris) meters (Fig. 217) [272].

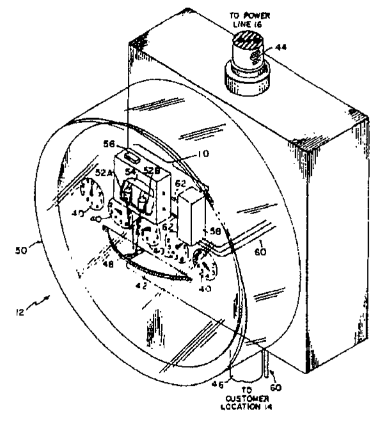

Figure 217 [272]
Automated Power Terminal Meter

An integrated automated meter and load management system comprises terminal units (10) mounted to existing power meters (12). Power usage indicated by the meter (12) is tracked by the terminal unit (10) by tracking rotations of the calibration wheel (42) of the meter (12). Messages representing incremental power usage are transmitted by the terminal unit (10) to a regional control center (18, Fig. 1) over the power lines (16) using a time division multiple access scheme synchronized to the frequency of the power signal. The system includes an initialization unit (64, Fig. 6) for entering through an initialization port 56 the value on the meter (12) when the terminal unit (10) is installed, thereby allowing the control center to track cumulative power usuage. In one embodiment, the terminal unit (10) comprises a load control unit (58) which through load control lines 60 can disconnect loads from the power system in response to commands from the regional control center (18). The regional control center (18) acts as a local communications relay station in relation to a remote central utility control center.

There are several problems with **retrofitted** optical pick-ups for rotation sensing:

- Sensibility to stray light
- Unreliable detection of the mark on the rotating disk due to low sensitivity of the sensor, especially if it is mounted outside of the meter (looking through the transparent cover)
- Reflexions of the light beam may corrupt the counting.

Figures 218 A and 218 B [329] demonstrate a solution to these problems.
The optical pick-up is designed for retrofitting to an existing Ferraris wheel electricity meter. It uses a light beam of a selected frequency, that is modulated by the rotation of the wheel, a synchronous detector (14) for the signal of interest, and performs a correction so as to at least partially cancel the unwanted signal originating in reflected light.

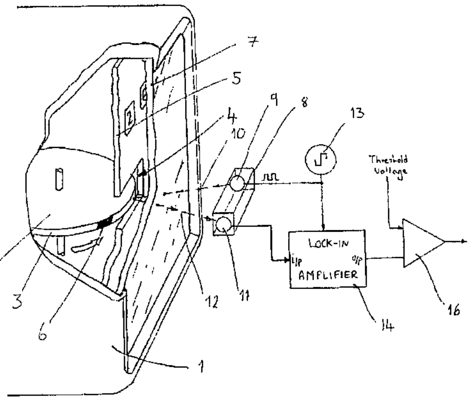

Figure 218 A [329]
Optical Rotation Sensor

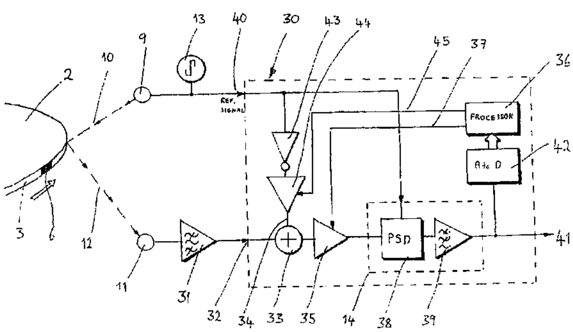

Figure 218 B [329]
Optical Rotation Sensor

An alternative manner of measuring the rotation is to apply **pattern recognition**, e.g. employing artificial intelligence, to the reflected signal [337, 338].

Water and electricity meters are also being retrofitted with analog rotation sensing devices.

Figure 219 [273] shows a dual mode meter, where the mechanical counter's data is electronically encoded and compared to the optical encoder's data, so as to reduce errors.

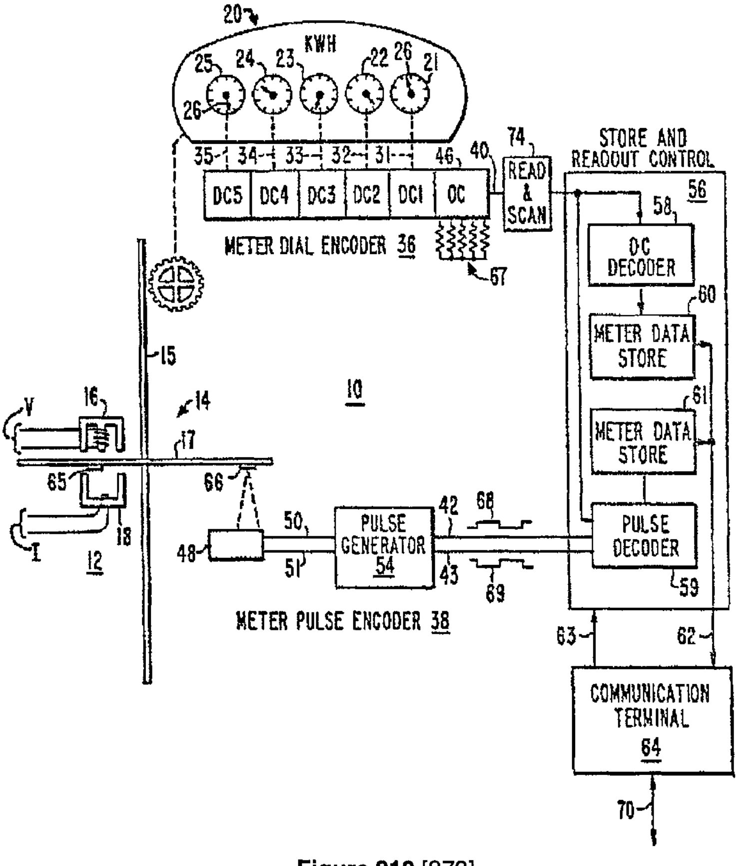

Figure 219 [273]
Dual Mode Meter Reading Apparatus

The apparatus provides a dual mode meter reading apparatus including a first dial register encoder (36) and a second meter pulse encoder (38) both responsive to the measuring element (14) of an integrating meter. Electronic data registers (60, 61) store both non-volatile dial totalized readings and higher resolution pulse augmented readings encoded by the first and second encoders, respectively. Comparison means and a selective logic readout of the two meter readings reduces erroneous meter reading outputs.

The disadvantages of the Electro-mechanical meter is that it consumes energy and that it is subject to wear. The compensation for its non-linearity causes some problems as well. These disadvantages can be eliminated by using a solid state meter, with solid state integrating.

5.2.2 Solid State Integrating

Various types of digital counting are being applied. When analog multiplication is being used for the power calculation, the voltage representing instantaneous power is usually converted into a power-proportional frequency. A succeeding counter then counts cycles, eventually scaled down by a divider, to achieve an energy value (Fig. 220) [274].

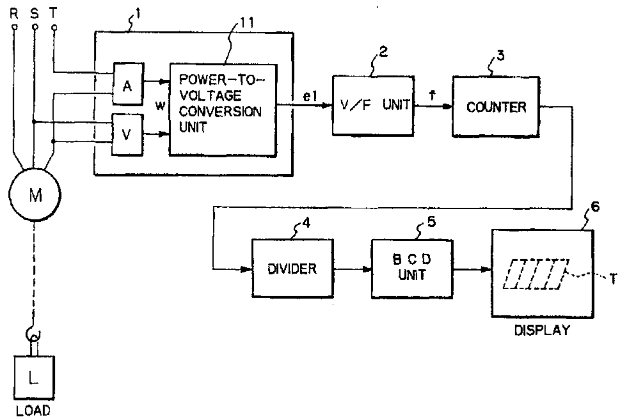

Figure 220 [274]
An Acutual Operating Time Indicator

In the multiphase case, one can cascade the decoders to yield the sum, as illustrated in Figure 206 above.

In the case of digital multiplication, a microprocessor is usually used for integration. The same micro-processor can then be used for the calculation of power and energy (Fig. 221) [276].

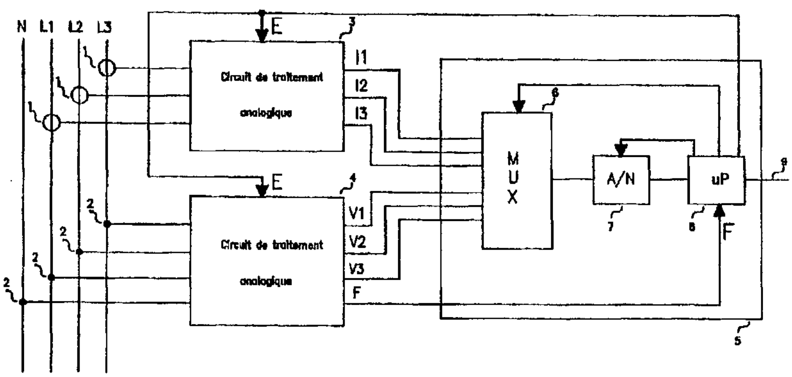

Figure 221 [276]
Power Meter with Microprocessor

The device includes a digital processing circuit (5) calculating a certain number of electrical variables of an electrical network (N, L 1, L2, L3) such as the RMS values of the currents and of the vollages, the values of the active and reactive powers and the values of active and reactive energy consumed. These variables are calculated from digital samples (11, 12,13, V1, V2, V3) which are representative of voltagesand of currents of the network. The number of samples used for the calculation of a variable is a function of the frequency (F) of the network, the samples being accumulated during an integration period corresponding to a whole number of periods of the network.

Digital instruments are suitable for metering non-sinusoidal waveforms. With sufficiently fast and accurate sampling, a straightforward method can be used, and no special precautions need to be taken. See Figures 222 and 223 [277].

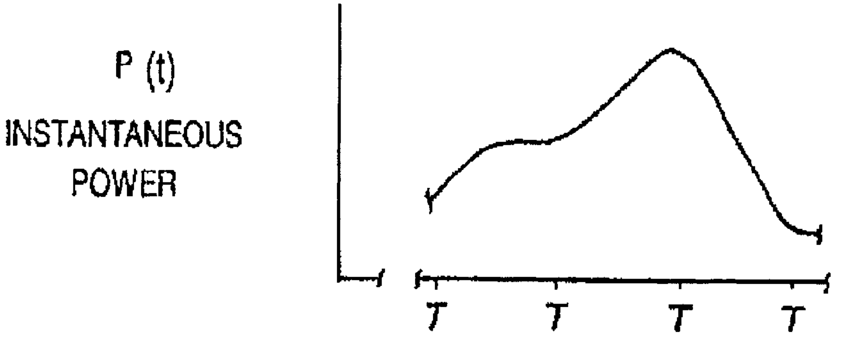

Figure 222 [277]
Waveform Diagram

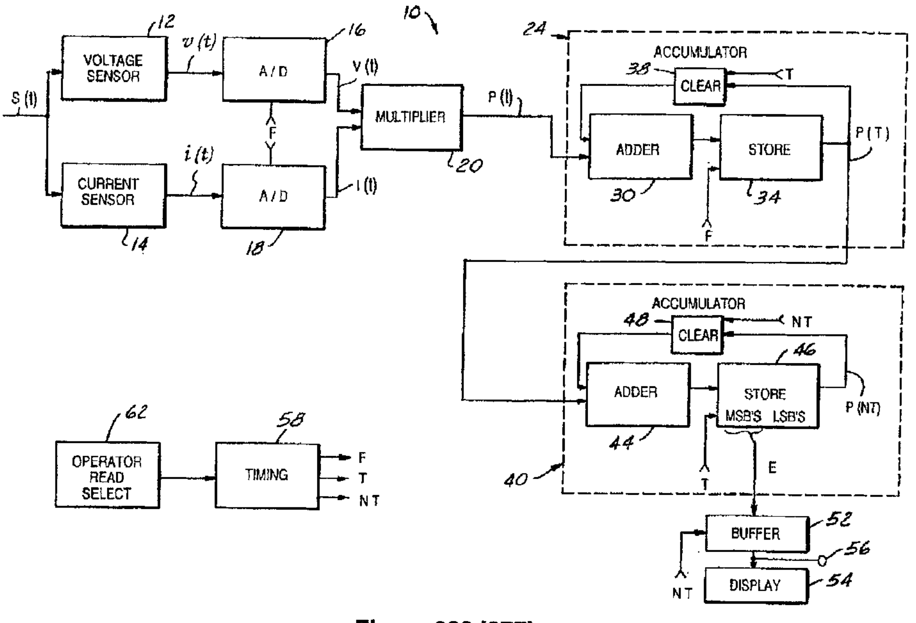

Figure 223 [277]
Digital Energy Meter

A digital energy meter for providing energy measurements of nonsinusoidal waveforms. Voltage and related current components of a digitally sampled waveform are multiplied to form a product representative of instantaneous power. The products are summed or accumulated over a first time period, and the sums then accumulated over a second time period to form a second sum representative of lotalpower over the second time period. An energy measurement is then obtained by an algorithm which requires only a simple division by a power of two.

In chapter 4.4.1 above we have discribed a method involving **Fourier analysis**.

5.3 FEATURES OF ENERGY METERS

5.3.1 Display and Remote-reading

5.3.1.1 Display

General purpose mechanical decade counters and electronic displays need no presentation in this context. One of the features of the Ferraris wheel is that it shows, via the rotational speed, the instantaneous power consumption. Solid state meters lack this feature. To satisfy the need for displaying magnitude and direction of power flow a special display can be added that uses simple arrow representation of power flow direction and magnitude (Fig. 224) [278].

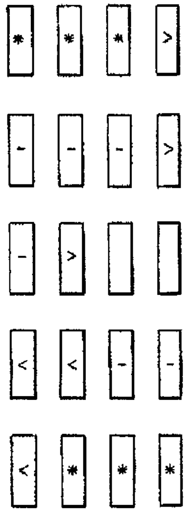

Figure 224 [278]
Solid State Electricity Meter Display

In a solid state electricity meter, a display consisting of a number of juxtaposed display elements provides, in a vector form, an indication of the direction and range of power flow in the line being measured. Circuitry for driving the vector display comprises a first memory storing a plurality of power measurement references and a second memory storing corresponding vector symbols. A microprocessor compares each power measurement with the references stored in the first memory to determine the range of the power measurement and, in response, reads the corresponding vector symbol from the second memory to drive the display.

The **blinking** frequency of a light emitting **diode** can also express the instantaneous power consumption.

Figure 200, Ch. 4.3 above illustrates a visual user interface presenting multiple parameters.

In order to economically manage his use of energy, the consumer needs more information than just the customary value of accumulated kWh or a qualitative display of the instantaneous power consumption.

It would be interesting for him to get an indication of peak power used and to be able to compare the actual consumption with a preset target consumption.

An apparatus featuring such possibilties is illustrated in Figure 225 [328].

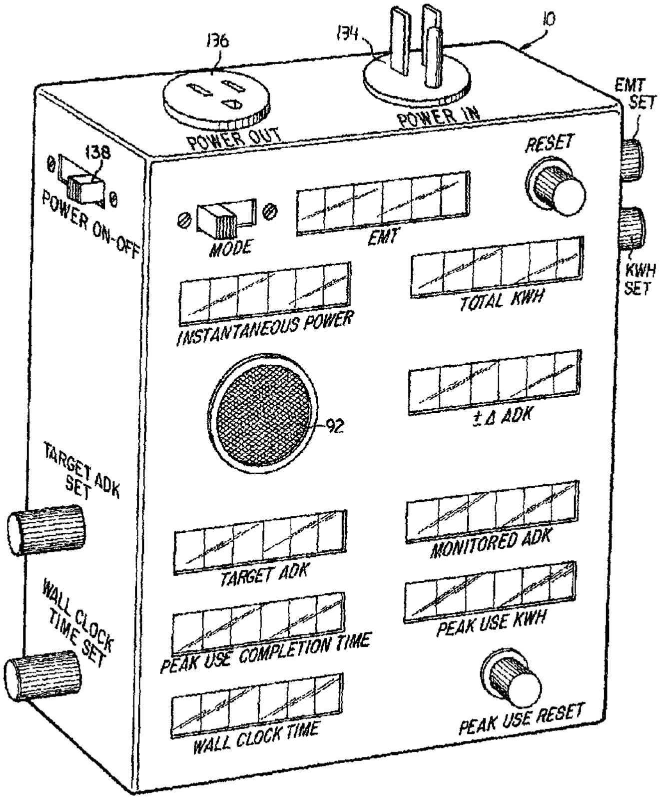

Figure 225 [328]
Integrating electrical power consumption meter - records occurrence of peak consumption and compares daily average with target value.

The meter measures and displays the rate and accumulated amount of total electrical consumption of an installation It computes the average daily consumption, and signals when the average daily consumption exceeds a predetermined target as established by the consumer.
The meter generates an output indicative of peak integrated power consumption over a predetermined time period, and an indication of the precise time of occurrence of this peak, to aid the consumer in his effort to isolate primary sources of power consumption. The meter also computes the difference between the average daily consumption and the target daily consumption, which is displayed in order to provide a measure of the consumer's progress in controlling the amount of useage of 0* system being monitored.

5.3.1.2 Remote Reading

We divide remote reading into two different kinds

(a) short range, up to some tens of meters.

Short range remote reading is done to simplify the reading of electricity meters by service personnel. It involves optical, inductive or radio communications (Fig. 226) [279].

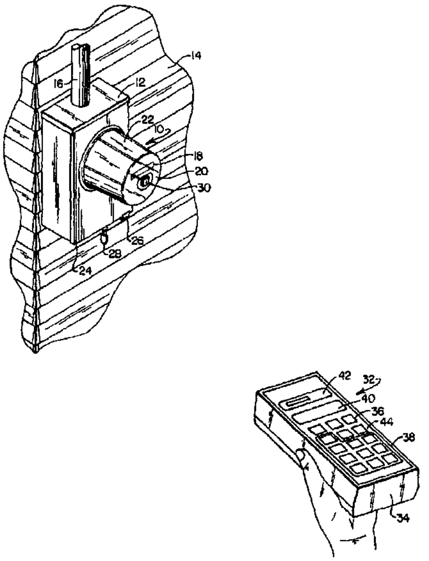

Figure 226 [279]
Electricity Meter with Remote Communications

Apparatus for transmitting electricity meter data in serial form by IR emissions to a remote, hand-held communicator having a front-end delector circuit including a photodiode responding to the meter data and dissipating a d.c. term occasioned by indirect ambient illumination of the photodiode in the IR region. Corresponding control communication from the communicator to the electricity meter is provided by IR emissions directed from an emitter of narrow beam angle to a wider angle receiving photodiode mounted with the meter at a location shielding it from direct sun illumination emanating above a horizontal plane extending from the immediate region of the photoresponsive receiver. Higher date transmission rates of 19.2 Kbaud are available in conjunction with an FSK transmission approach employing two channels.

Long range remote reading involves transmitting power or energy data, usually over telephone-lines or power lines to a central station. LAN's and Radiolinks are also being used.

Remote reading can eliminate certain kinds of fraud and saves manpower, and can be combined with load shedding and surveying.

The previously cited [272] uses the power lines (Fig. 227).

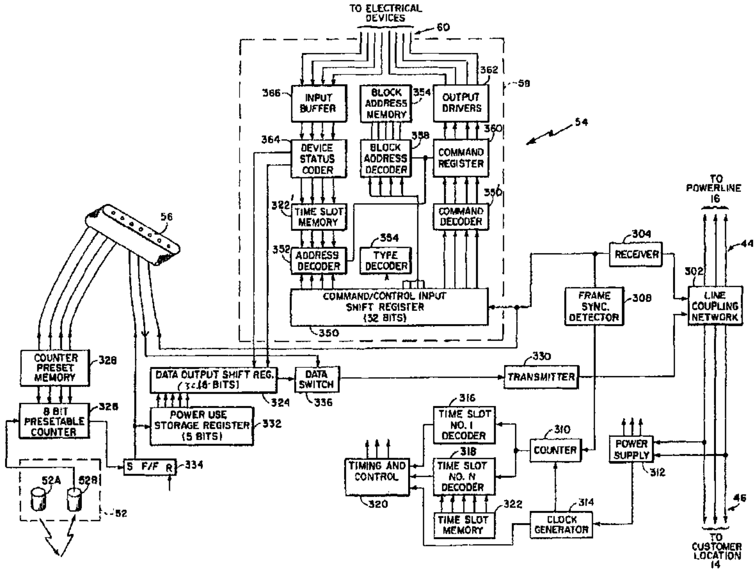

Figure 227 [272-2]
Automated Power System

Figure 228 [280] demonstrates the use of telephone-lines.

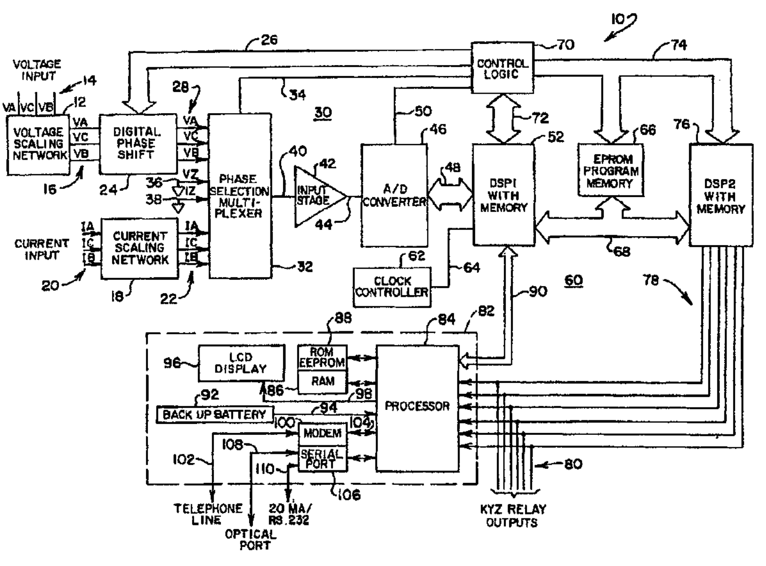

Figure 228 [280]
Power Meter Data Transmission

Collective energy monitoring combines short and long range remote reading/displaying (Fig. 229) [281].

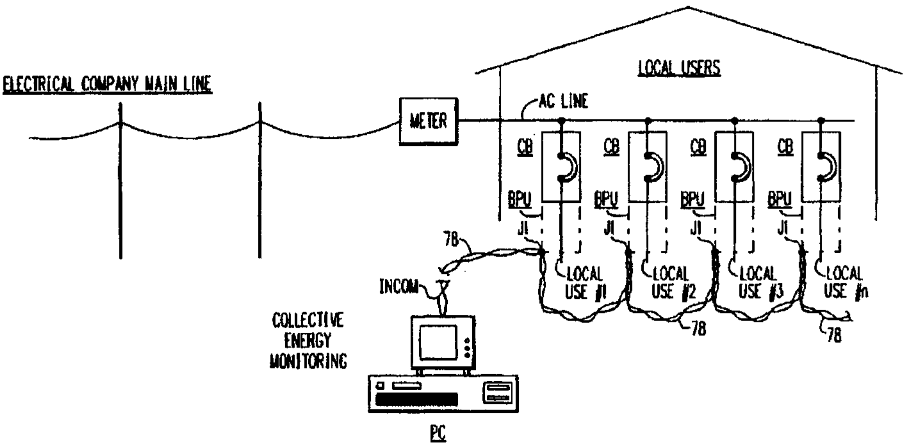

Figure 229 [281]

Energy Monitoring System for a Plurality of Local Stations with Snapshot Polling from a Central Station

PC computer monitors the energy consumed at local stations positioned behind an electrical meter of a utility company for individual biling of the local users using a bidrectional communication line. A command from the PC computer causes at each station the totalized energy to be stored, and then PC computer derives individual biling. A plurality of back-pack units are directly mounted and plugged on panelboard circuit breakers for voltage and current sensing. Each backpack unit incorporates two printed circuits.

5.3.2 Special Purpose Meters

Meters for reactive average etc. energy have been dealt with above in the chapter treating measuring power - see for instance [245] or [331]. A 3-phase meter is illustrated by Figures 205 and 206 above.

Differentiated Tariff Meters

These meters enable consumers to reduce their energy costs by distributing the consumption to different parts of the day, the week, and the year. A meter that can divide the KWH consumption into four categories is shown in Figure 230 [282].

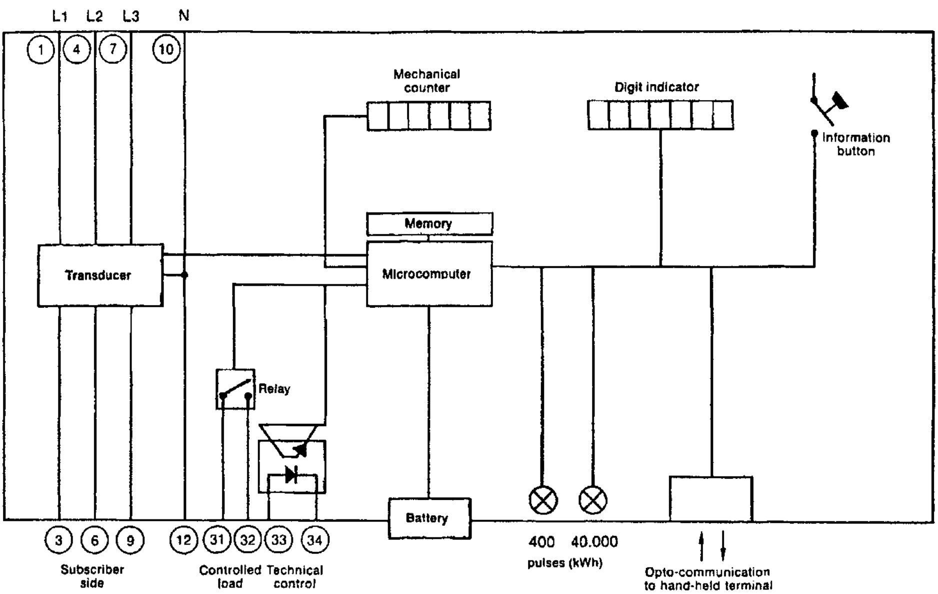

Figure 230 [282]

Simplified Block Diagram of the All-Electric Electricity Meter.

The encircled figures are the numbers of the terminals In the terminal block

Digit indicator

The digit indicator contains seven-segment light emitting diode displays for seven figures, a control digit to the left and six information digits. Normally only the control digit is lit, showing the rate applicable at the moment. When the subscriber depresses the information button the information digits will also light up, and with repeated pressing it is possible to check the state of nine registers. (1-4) show the amount of energy consumed at the rate in question since the meter was last read; (5,6) show the maximum amount of power the consumer has used during a programmable period of time (1-6 hours), (7) shows when the meter was last read, in the form of YEAR, MONTH, DA Y, e.g. 840126; (B) tests the indicator function. All figures should be eights if all segments work property; (9) shows the day and time as DAY, HOUR, MINUTE, e.g. 261114.

Mechanical counter

The mechanical counter in the meter accumulates the number of consumed kWh since the meter was manufactured. It cannot be reset to zero and can, with its six digits, indicate 999 999 kWh. With a normal consumption of 25 000 kWh/year it will take the counter approximately 40 years to step round to zero again.

Relay

A relay in the meter is used to control external load objects, for example water heater and accumulating heating systems. The relay is normally programmed to operate during periods 2 and 4, which is during nights throughout the year and during holidays.

Battery

A battery is necessary to ensure that the clock works even during a power loss. A lithium battery was chosen for the purpose. It is a primary battery with a voltage of approximately 3.4 V.

For the energy consumer who pays for maximum power, a meter with built in **threshold** values and a **load shed relay** is interesting. Such a meter is illustrated in Figure 231 [283].

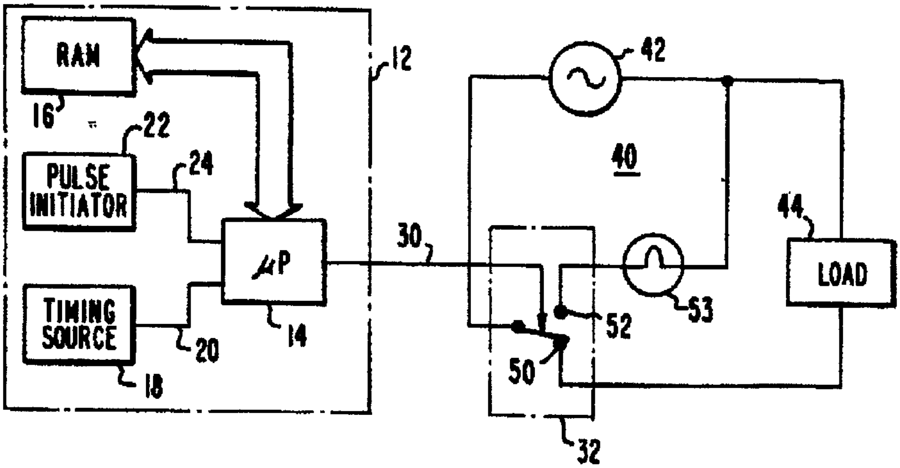

Figure 231 [283]
Watthour Meter with Demand Responsive Load Control Capability

A watthour meter is provided with the ability to maintain a clock and calendar. One or more demand threshold values (16) are defined and associated with periods of electrical demand. The demand meter also defines (14); periods of #me that represent demand intervals and, during each demand interval, electrical energy consumption pulses are accumulated in order to represent the electrical consumption during the demand interval period. The magnitude of electrical consumption that takes place during each demand interval is compared to one of the plurality of demand thresholds in order to determine if the demand threshold for the current period of time has been exceeded. If it is determined that the demand threshold has been exceeded, the demand meter of the present invention outputs a signal to a load shed relay (32); in order to shed a preselected nonessential electrical load (44) so that the electrical energy demand of the consumer is reduced.

Load Identifying Meters

Non-invasive analysis of the use of specific apparatus by a user can be done via the electricity meter. One type of device uses variations of impedance for load identification, and calculates the energy consumption for each type of load [284]. Impedance is determined by amplitude and phase shift. Such a meter has a number of uses:

- Load shedding (chose the least important of the active loads for shedding).
- Monitoring the use of electric devices by elderly or disabled persons for safety purposes.
- Analyzing power use in view of energy savings.
- Consumer studies.

Other types of devices recognize the power drawn by each specific load, and senses when they are switched on or off.

Figure 232 [330] illustrates a transient event detector for the monitoring of electric loads.

Here the unique **pattern** of the start-up transient of each particular load is analyzed and recognised.

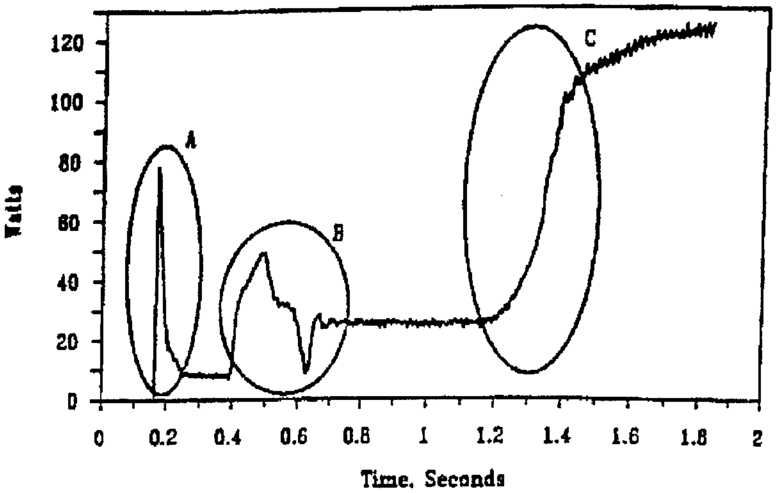

Figure 232 [330]
Transient Event Detector For Monitoring Electrical Loads

A multi-processing transient event detector for use in a nonintrusive electrical load monitoring system has been provided. Templates of transient pattern data associated with each electrical load which may be monitored are stored. Such templates are then used to match and correlate with the actual monitored transient pattern data at the load site. The decomposition in which time scales are changed is accomplished in parallel along with one or more parallel event detection processing modules for each decomposition.

DC-energy Meters

Transforming DC to AC enables using a standard AC energy meter [286] or [219]. See Figure 205 above.

Advanced battery monitors measure the energy going into or out of a battery (Fig. 233) [284].

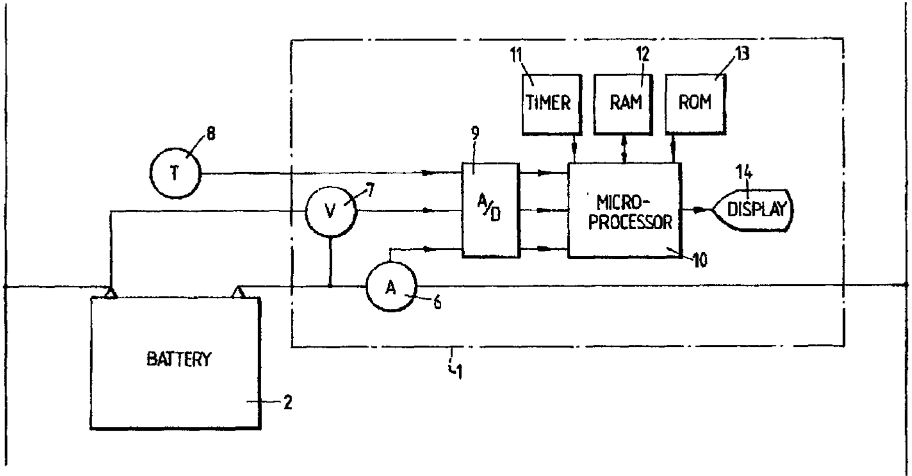

Figure 233 [284]
Battery State of Charge Indicator

A device (1) for indicating changes in the state of charge of a rechargeable battery (2) comprises a current sensor (6) to sense current flow into and out of the battery (2) and to provide an output indicative of both the magnitude and direction of the current flow, timing means (11) to provide a timing signal, and a computer (10) programmed to compute from the output of the current sensor (6) and the timing means (11), a signal representative of the charge dissipated from oraccumulated in the battery (2) over a period of time. Preferably the device (1) includes data storage means (12) to store an indication of the state of charge of the battery (2) and the computer (10) is programmed to use the signal to update the stored data to provide an indication of the current state of charge of the battery (2).

The development of electric vehicles has posed a challange on battery management and energy measurments. [339] measures watt-hours and relates them to remaining battery capacity.

A precise prediction of the capacity requires more data than energy in- and output due to such things as temperature dependence, discharge current intensity, aging and losses during charging and discharging. Advanced battery state of charge meters take these things into consideration.

For the special case of batteries, their energy content can also be determined via their internal resistance or impedance, the density of the electrolyte or the dialectric properties.

5.4 PROBLEMS WITH POWER AND ENERGY METERS

Problems with Solid State Meters Application

Although solid state meters can be made without moving parts they depend on other, more or less costly components:
[288] mentions the following

- power supply
- protection elements against disturbances such as short circuits in loads or transients on lines
- voltage and current sensing elements adopted to interface with the electronic circuits
- electromagnetic shielding.

Hall elements, which are currently used as transducers are temperature sensitive and show long term drift.

A low sampling speed and an imprecise ADC sets limits to the precision and accuracy. Differences in sampling time between current and voltage samples is a source of error. Offset voltage is a source of error. Figure 234 [287] shows a circuit that compensates for the offset error in a power meter multiplier.

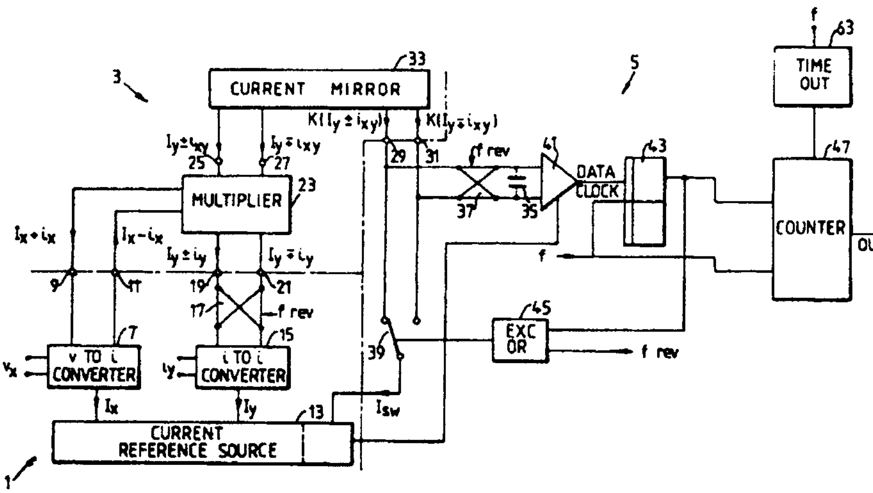

Figure 234 [287]

Electric Power Measuring Device

An electric power measuring device wherein input analogue signals representative of instantaneous values of current and voltage are applied to a multiplier (23) and the product applied to a converter (35, 37 41, 43, 45, 47) to provide a pulse output signal having a frequency representative of the product and hence of the level of power consumption. Compensation for offset errors in the multiplier is effected by periodically reversing the polarity of one of the inputs to the multiplier and effecting corresponding reversals at the input to the converter to avoid irregularities in the output pulse rate when the level of power consumed is low.

Figure 235 [291] illustrates how linearity, frequency and phase corrections come into play in a pulse-width modulation type of Watt meter. Filipski [291] shows that the systematic error of a Time-Division Multiplier (TDM) is below 0-1% if the multivibrator frequency to input frequency ratio is 30 (Fig. 235).

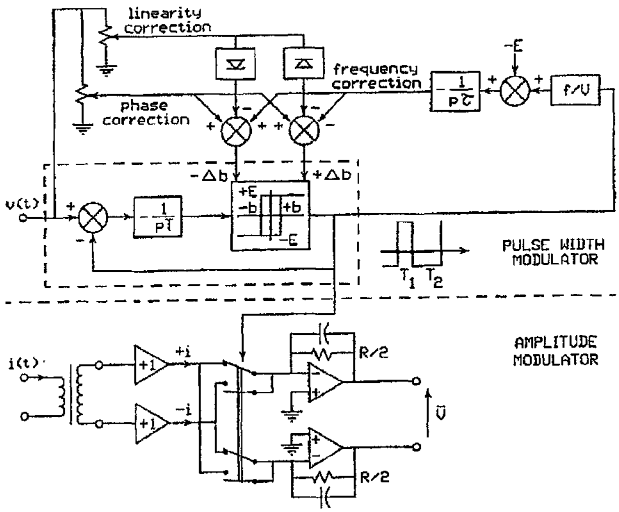

Figure 235 [291]
Watt Meter

The general schematic of the meter is shown in Fig. 1. The input voltage and current modulate the carrier square wave in the pulse-width modulator (PWM) and the amplitude modulator (AM). The integrator -1/pT and comparator with hysteresis ± b form an astable multivibrator. In the absence of the input signal v this multivibrator oscillates symmetrically with instantaneous frequency $f_0 = E/4bT$. When the modulating input signal is applied the output wave is no longer symmetrical, with positive and negative parts of the impulse and instantaneous frequency as follows:

$$T_1=\frac{2bT}{E+\upsilon} \qquad T_2=\frac{2bT}{E-\upsilon} \qquad f_\upsilon=\frac{1}{T_1+T_2}=f_\upsilon(1-\frac{\upsilon^2}{E^2}) \tag{78}$$

The average voltage V at the output of the amplitude modulator is proportional to the product of the inputs.

$$\bar{V}=\frac{T_1 iR}{T^1+T^2}=iR\frac{T^1-T_2}{T_1+T_2}=-\frac{R}{E}\upsilon i \tag{79}$$

When AC voltage and current are applied to the inputs the output becomes proportional to the active power P. Computer analysis of the operation of the wattmeter [3] showed that the AC power conversion error of the wattmeter can be approximated as

$$\Delta P=\frac{1}{11}\left(\frac{\pi}{N}\right)VI\cos\phi \tag{80}$$

where $N = f_0 / f$, f is the input signals frequency, and V, 1, f are rms input voltage, current and relative phase shift. For example, the systematic error given by (3) remains below 0.01% if the multivibrator frequency is at least N = 95 times the input frequency, for 0. 1% systematic error N = 30 is sufficient. The relative conversion error is linear and does not depend on the magnitude of the input. When distorted waveforms are being processed the total conversion error closely follows the resultant error calculated independently for particular harmonics [13]. The meter has no inherent systematic phase error; at power factor of zero the systematic error (3) vanishes. This property makes it particularly attractive for low power factor measurements or for phase sensitive detection.

List of cited documents

CHAPTER ONE

1.	HERING et al.	"Physik für Ingenieure", 4th edition, 1992, VDI Verlag, Düsseldorf
2.	DE 27 27 370	Siemens AG
3.	US 4 866 389	Ventritex
4.	US 4 646 002	Regents of the University of Minnesota
5.	US 3 761 798	Ford Motor Company
6.	US 4 973 910	WILSON
7.	SECKER	Inst. Phys. Conf. Ser. No. 27 (1975), p. 173-181, "The use of field-mill instruments for charge density and voltage measurement"
8.	US 4 878 017	WILLIAMS
9.	US 4 052 665	Snap-on Tools Corporation
10.	EP 0 177 210	GEC Avionics Ltd.
11.	GÖRLICH	Microelectronic Engineering, 16, Nos. 1/4 (1992), p. 349-366, "Electron beam testing versus laser beam"
12.	EP 0 485 202	Texas Instruments Inc.
13.	EP 0 196 475	International Business Machines Corporation
14.	DE KORT	Philips Journal of Research, Vol. 44, nos. 2/3 (1989), p. 295-327, "Integrated Circuit Diagnostic Tools : Underlying Physics and Applications"
15.	WO 92114162	Fraunhofer-Gesellschaft zur Förderung der Angewandten Forschung e.V.
16.	EP 0 440 901	ICT, Gesellschaft für Halbleiterprüftechnik mbH
17.	EP 0 216 077	International Business Machines Corporation
18.	GB 2 239 955	The Electricity Council
19.	GB 2 157 838	Xerox Corporation
20.	WO 96/41201	The Regents of the University of California
21.	WEAVER et al.	Journal of Vacuum Science & Technology B, Vol. 9, No. 3 (1991), p. 1559-1561 "Resolution atomic force microscopy potentiometry"
22.	EP 0 083 196	Sumitomo Electric Industries Limited
23.	EP 0 454 860	Dai Nippon Printing Co. Ltd.
24.	EP 0 453 693	Commissariat à l'Energie Atomique
25.	PHILIP et al.	Measurement Science & Technology, Vol. 2 (1991), p. 565-567, "A high-voltage pulse measuring system based on the Kerr effect"

26. CASSIDY et al. IEEE Transactions on Instrumentation and Measurement, Vol. IM-1 7, No. 4 (1968), p. 313-320, "Calibration of a Kerr Cell System for High-Voltage Pulse Measurements"

27. EP 0 405 802 American Telephone and Telegraph Company

28. EP 0 272 871 Xerox Corporation

29. EP 0 480 206 Siemens AG

30. EP 0 497 616 Eveready Battery Company, Inc.

31. EP 0 433 824 Asea Brown Boveri AG

32. VOH RA et al. Optics Letters, Vol.16, No. 18 (1991), p. 1445-1447, "Fiber-optic dc and low-frequency electric-field sensor"

33. EP 0 701 139 Universidad Pontificia Comillas

34. EP 0 316 619 BBC Brown Boveri AG

35. EP 0 393 382 Asea Brown Boveri AG

36. EP 0 061 033 Matsushita Electric Industrial Co. Ltd.

37. PALMA et al. Journal of Applied Physics, Vol. 58, No. 8 (1958), p. 3265-3267, "Lamb-wave electroacoustic voltage sensor"

38. VOHRA et al. Optics Letters, Vol. 17, No. 5 (1992) p. 372-374, "Fiber-optic ac electric-field sensor based on the electrostrictive effect"

39. EP 0 108 676 Société pour l'Etude et la Fabrication de Circuits Intégrés Spéciaux-E.F.C.I.S.

40. WO 92/13277 ABB Patent GmbH

41. US 4 584 523 RCA Corporation

42. US 4 006 414 The Regents of the University of California

43. WO 86/06173 PARKER

44. US 4 835 476 Three TEC Davis Inc.

45. EP 0 450 938 Eastman Kodak Company

46. WO 90110238 Metricor Inc.

47. US 5087 810 Edjewisse Sensor Products, Inc.,

48. PARK et al. IEEE Transactions on Instrumentation and Measurement, Vol. 39, No. 5 (1990), p. 767-772, "A New Current Measurement Method in Resistance Spot Welding"

49. DE 40 21 358 Siemens AG

50. US 4 348 587 Hughes Aircraft Company

51.	EP 0 107 059	General Electric Company
52.	SCOVILLE et al.	Review of Scientific Instruments, 62, No. 3 (1991), p. 755-760, "A low-cost multiple Hall probe current transducer"
53.	EP 0 438 637	Landis & Gyr Betriebs AG
54.	EP 0 133 695	Borg-Warner Corporation
55.	EP 0 415 439	Kabushiki Kaisha Toshiba
56.	KOLB	Messen Prüfen Automatisieren, No. 12 (1989) p. 600-611, "Neues Messverfahren für Echtzeitstromsensoren und die Anwendung in der Prüftechnik"
57.	LOREIT et al.	Radio Fernsehen Elektronik, Vol. 34, No. 5 (1985), p. 316-319, "Magnetoresistive Sensoren in der Meß- und Speichertechnik"
58.	PARKIN	Annu. Rev. Mat. Sci., Vol. 25 (1995), p. 357-388, "Giant Magnetoresistance in Magnetic Nanostructures"
59.	JIN et al.	Science, Vol. 264 (1994), p. 413-415, "Thousandfold Change in Resistivity in Magneto resistive La-Ca-Mn-O Films"
60.	EP 0 307 729	Siemens AG
61.	EP 0 539 081	Hitachi, Ltd.
62.	DAY et al.	SPIE Vol. 985 Fiber Optic and Laser Sensors V] (1988), p.1 38-150, "Faraday Effect Sensors: The State of the Art"
63.	EP 0 516 562	Merlin Gerin
64.	BARTLETT et al.	Review of Scientific Instruments, Vol. 61, No. 9 (1990), p. 2433-2435, "Current sensing using Faraday rotation and a common path optical fiber heterodyne interferometer"
65.	RASHLEIGH	Optics Letters Vol. 6, No. 1 (1981), p. 19-21, "Magnetic-field sensing with a single-mode fiber"
66.	EP 0 264 612	Siemens AG
67.	JP 58-132670	Mitsubishi Denki K.K.
68.	DE 30 39 679	LGZ Landis & Gyr Zug AG
69.	WEYAND	IEEE Trans. on Instrument & Measurement, Vol. 38, No. 2 (1989), p. 410-414, "An NMR Marginal Oscillator for Measuring Magnetic Fields Below 50 mT"
70.	DURET et al.	Sensors and Actuators -A Physical, Vol. A31, Nos. 1/3 (1992), p. 175-176, "A new current sensor using electron spin resonance"
71.	WO 86/03843	Thomson-CGR
72.	CLARKE	Proceedings of the IEEE, Vol. 77, No. 8 (1989), p 1208-1223, "Principles and Applications of SQUIDS"

73.	GALLOP	Meas. Sci. Technol. Vol. 2 (1991), p. 485-496, "SQUIDS, the Josephson effects and measurement"*
74.	US 4 324 255	BARACH
75.	GIFFARD et al.	Journal of Low Temperature/Physics, Vol.6, No. 5/6 (1972), p. 533-610, "Principles and Methods of Low-Frequency Electric and Magnetic Measurements Using an rf-Biased Point-Contact Superconducing Device"*
76.	CUSHMAN	Electrical Design News, Vol. 14, No. 4 (1969), p. 73-78, "Transistor responds to Magnetic Fields"
77.	US 3 693 085	General Motors Corporation
78.	US 3 801 908	Akzo N.V.
79.	US 4 112 357	The United States of America represented by the Administrator of the National Aeronautics and Space Administration
80.	EP 0 360 574	Kabushiki Kaisha Toshiba
81.	US 4 926 116	Westinghouse Electric Corp.
82.	DE 36 26 328	Klöckner-Moeller Elektrizitäts GmbH
83.	WO 87101812	LGZ Landis & Gyr Zug AG
84.	EP 0 165 835	Merlin Gerin
85.	EP 0 302 747	Mitsui Petrochemical Industries Ltd.
86.	JP 59194544	Yokogawa Hokushin Denki KK
87.	US 4 454 557	McGraw-Edison Company
88.	EP 0 504 674	Vacuumschmelze GmbH
89.	FR 2 638 235	ROBERT
90.	EP 0 284 472	Sangamo Weston, Inc.
91.	EP 0 314 234	Holec Systemen en Componenten B.V.
92.	YAMAGUCHI et al.	IEEE Transactions on Magnetics,Vol. 26, No. 5 (1990), p.1 569-1570, "A planar-type current detector composed of ultra-thin permalloy plates and sputtered electrodes operating over 10MHz"*

CHAPTER TWO

93.	MUHR, Michael	E & I Elektrotechnik und Informationstechnik, 108 (1991) No. 5 "Hochspannungsprüf-und Meßtechnik"*
94.	US 5 153 510	K and M Electronics, Inc.,
95.	LESNE, P.	Electronique Radio Plans, (1990) Juin, No. 511, p. 37-42 "La mesure des tensions élevées"

96.	WO 92/13278	ABB Patent GmbH
97.	CA1063176	Dr.techn. Josef Zelisko Fabrik für Elektrotechnik und Maschinenbau GmbH
98.	KAWAMURA et al.	IEEE Transactions on Instrumentation and Measurement, 37 (1988) Dec., No. 4, p. 564-568 "Development of a High Voltage Sensor Using a Piezoelectric Transducer and a Strain Gage"*
99.	DE 35 44 508	ADOLPH, Ulrich
100.	LIKHACHEV et al.	Measurement Techniques, 32 (1989) January No. 1, p. 92-95 "Modular Transformer Voltage Dividers in Measuring Equipment"*
101.	RAMM et al.	Elektronik, 35 (1986) Aug., No. 16, p. 57-60, "Induktive Spannungsteiler in binärer Schaltungsart"*
102.	US 4 801 937	FERNANDES, Roosevelt A.
103.	FE 2 255 604	Siemens Aktiengesellschaft
104.	US 4 935 693	Square D Company
105.	GB 2 168 495	Licentia Patent-Verwaltungs GmbH (FR Germany)
106.	EP 0 181 054	Niagara Mohawk Power Corporation
107.	US 4 904 996	FERNANDES, Roosevelt A.
108.	US 4 837 503	HASENZAHL, Ernest L.
109.	ZINGALES, G.	Measurement, 8 (1990) Oct./Dec., No. 4, pages 153-157 "New trends in high-voltage measurements"
110.	NIKOLOPOULOS et al.	IEE Proceedings-A, 136 (1989) March, No. 2, Part A, p. 66-72 "Accurate method of representation of high-voltage measuring systems and its application in high-impulse-voltage measurements"*
111.	EP 0 312 050	Hydro-Quebec
112.	GRANDL et al.	GIGRE, International Conference on Large High Voltage Electric Systems, 1988 Session -28th August/3rd September "Studies on very fast Transients (VFT) in a 765kV Substation"*
113.	US 4 594 546	The United States of America as represented by the Secretary of the Army
114.	LUCAS et al.	IEEE Transactions on Instrumentation and Measurement, 40 (1991) April, No. 2, p. 288-290 "Investigations into the Delfection of Relativistic Electrons Inside a Superconducting Cavity Resonator for Measuring High Voltages"*
115.	US 3 944 918	HADERMANN, Albert, WATERS, Paul F., WOO, Jung Woo
116.	EP 0 266 883	Airtech Limited
117.	Anonymous	Research Disclosure, No. 165 (1978.01) p. 6, "Measuring dc voltage in a static converter"*

118. US 4 328 461 McDonnell Douglas Corporation

119. FR 2 605 814 CORDIER, Jacques Henri Emile

120. US 4 095 221 SLOCUM, Chester D.

121. US 4 091 326 The Johns Hopkins University

122. DE 38 33 930 Murata Mfg. Co. Ltd.

123. EP 0 254 601 Commissariat A L'energie Atomique

124. BROADBENT, T.E. Journal of Scientific Instruments (Journal of Physics E)
1968 Series 2 Volume 1, March Nr. 3, p. 341-343
"Absolute measurement of high voltage by a null method using strain gauges"*

125. Not used

126. US 4 025 913 The United States of America as represented by the Secretary of the Navy

127. GB 2 131 961 The Simco Company Inc. (USA-Pennsylvania)

128. US 3 921 087 VOSTEEN, Robert E.

129. US 4 054 835 General Electric Company

130. ANDRÉ, P. Mesures, 52 (1987) 23 mars, No. 4, p. 107,109,110 and 112
"Mesurer un champ électrique en ambiance pertubée"

131. CONCHARENKO, A. N. Measurement Techniques, 29 (1986) August, No. 8, p. 761-763
"Dynamic Meter of Electrostatic Potentials"

132. JOHNSTON et al. Review of Scientific Instruments, 57 (1986) Nov., No. 11, p. 2746
"dc electric field meter with fiber-optic readout"

133. MAENO et al. 1986 Annual Report Conference on Electrical Insulation and Dielectric Phenomena, November 1986 p. 450-455
"Electric Field Measurement in Liquid Dielectrics using a Combination of AC Voltage Modulation and a small Retardation Angle"

134. JOHNSTON et al. N.T.I.S. Technical Notes, (1986) July, No. 7, p 788
"Rotating Capacitor Measures Steady Electric Fields"

135. COMBER et al. IEEE Transactions on Power Apparatus and Systems, Vol. PAS-102 (1983) Nov., No. 11, p. 3549-3557
"Experimental Evaluation of Instruments for Measuring DC Transmission Line Electric Fields and Ion Currents"

136. HORENSTEIN, Mark N. Review of Scientific Instruments, Vol. 54 (1983) May, No. 5, p. 591-593
"Peak sampled vibrating-reed for the measurement of electric fields in the presence of space charge"

137. JONES, B. E. Journal of Scientific Instruments, Vol. 3, Feb. 1970, Nr. 2, p. 101-104
"Clip-on dc voltmeter"

138. AT 389 012 Österreichisches Forschungszentrum Seibersdorft Gmbh

139. TAKAHASHI et al. Journal of Physics E. Scientific Instruments, 19 (1986) Sept., No. 9, p. 705-707
"Polarity-sensing methods for field mills without phase-sensitive detection"

140. DE 33 24 224 LGZ Landis & Gyr Zug AG

141. DE 1 148 654 Siemens-Schuckertwerke Aktiengesellscahft

142. JP 56-151361 Kakaoka Seisakusho K.k.

143. US 4 182 982 Westinghouse Electric Corp.

144. BARNARD, B. R. Journal of Physics E. Scientific Instruments, 17 (1984) Nov., No. 11, p. 1031-1034
"High-resolution SQUID monitor system for large direct currents"

145. RZEWUSKI et al. 5th European Microwave Conference, September 1975, Hamburg, Germany, p. 218-222
"Measurement of Current in EHV and UHV Transmission Lines using YIG-Tuned Devices"*

146. MARRIOT The Marconi Review, p. 79-109 first quarter 1970
"Microwave Devices Using Spheres of Monocrystal-line Garnet Materials"

147. US 3 691 460 Farbenfabriken Bayer Aktiengesellschaft

148. GB 2 081 459 A.R.O. Machinery Co. Ltd.

149. CH 368864 Landis & Gyr AG

150. US 4 529 931 Ford Motor Company

151. US 4 706 016 SCHWITZER, Edmund O.

152. US 4 070 572 General Electric Co.

CHAPTER THREE

154. MEYER, Hg. Technisches Messen T.M., 53 (1986) No. 7/8, p. 266
"Störfestigkeit von Meßsystemen"

155. WEDLOCK Electro/87 and Mini/Micro Northeast, 12 9 (1987) Conference Record, p. 1-10
"Grounding and Shielding Electronic Instrumentation"*

156. KOLNSBERG, A. Messen Prüfen Automatisieren, (1989 September, no. 9, p. 428-430
"Abschätzung Der Wirksamkeit von Störunterdrückungs-Massnahmen bei der Übertragung von Gleichstrom-Mess-signalen"*

157. PELZ, H. Regelungstechnische Praxis, 26 (1984) Sept. No. 9,p, 383-391
"Elektromagnetische Störeinwirkungen auf elektronische Geräte"*

158. MOHR, Richard J. Electro Conference Record, 14 (1989) April 11-13, p. 1-5
"Shielding Design and Application for Electromagnetic Compatibility"

159. KUNKEL, G. M. Measurement + Control, 24 (1991) Nov., No. 9, p. 282-285
"Shielding effectiveness of EMI gasketed joints"

160. US 3 441 852 — Sybron Corporation

161. EP 0 371 672 — International Business Machines Corporation

162. DE 1 466 637 — BAERMANN, Max

163. DE 1 002 459 — Telefunken G.m.b.H.

164. US 5 132 497' — Eaton Corporation

165. US 3 423 670 — Perkin-Elmer Limited

166. EP 469 808 — Nippon Seiki Co. Ltd.

167. EP 0 179 298 — BERTHELSEN, Viggo

168. Not used

169. ter BRAKE et al. — Measurement Science & Technology, 2 (1991) July, No. 7
"Improvement of the performance of a µ-metal magnetically shielded room by means of active compensation"

170. SULLIVAN et al. — Review of Scientific Instruments, 60 (1989) April, No. 4, p. 765-770
"A magnetic shielded room designed for magnetoencephalography"

171. KARTHIKEYAN et al. — Cryogenics, 29 (1989) September, no. 9, p. 915-919
"Plasma sprayed high *T*<*D*>c superconducting magnetic shields"

172. SHIGEMATSU et al. — Japanese Journal of Applied Physics, 28 (1989) May, No. 5.II, p. L813-815
"Magnetic Shield of High-*T*<*D*>c Oxide Superconductors at 77K"

173. KELHÄ, et al. — IEEE Transactions on Magnetics, Vol. MAG-18 (1982) Jan. No. 1,
"Design, Construction, and Performance of a Large-Volume Magnetic Shield"

174. TUCKER, Jonathan — Machine Design, 62 (1990) March 22, No. 6, p. 88-95
"Interfacing Sensors to PCs"

175. EP 0 388 217 — HAMILTON, Sheila

176. POKHILYUK et al. — Instruments & Experimental Techniques, 30 (1987) Jan-Feb., No. 1, Part 2, p. 133-136
"Devices for Wideband-Noise Protection"

177. LEVY, Malcolm — Test & Measurement Word incorp. Electronic Test, 11 (1991) May, Suppl., p. 23-24
" VXIbus Meets the Needs of RF ATE"*

178. SALI, S. — IEE Proceedings-A, 137 (1990) July, No. 4, Part A, p. 165-174
"Triaxial cable designs with optimum braided shields"*

179. — TE/Toute l'Electronique (1989) Février, No. 541,
"Vers un blindge sans faille des connecteurs ronds"

180. MUND, Bernhard — Elektronik, 37 (1988) 2, Sept., No. 18, p. 111, 112 and 114
" Hochgeschirmte HF-Kabel und Anschlußleitungen"

181. AMANO et al. IEEE Trans. on Power Delivery, 4 (1989) April, No. 2, p. 1351-1359
"Study on Reduction in Electric Field, Charged Voltage, ION Current and ION Density under HVDC Transmission Lines by Parallel Shield Wires"*

182. WO 91/19305 LK Lavspænding A/S

183. US 4 795 975 Texas Instruments Incorporated

184. SIMON, Robert M. Product Engineering, Vol. 50 (1979) Dec., No. 12 p. 43
"Shielding from EMI with plastics"

185. MILLER, Walter J. Journal of Vacuum Science & Technology/Section A, 5 (1987) July/August, No. 4, Part IV p. 2706-2708
"Vapor deposited chrome-copper-chrome laminates for electromagnetic interference/radio frequency interference shields"

186. REILLY, John J. Electro, (1984) May, p. 1-10
"Post Mold EMI Shielding Techniques for Plastics"

187. GOLDBLUM, Robert D. Electro. Conf. Record, Vol. 4 (1979-04-24/26), p 6/2
"EMI Testing of Metalized Plastics"

188. MÖBIUS, K.-H. Kunststoffe, 78 (1988) April, No. 4, p. 345
"Elektromagnetische Abschirmung mit elektrisch leitfähigen Kunststoffen"

189. GB 2 144 771 Decospray Limited

190. Electronic Engineering, 62 (1990) may, No. 761, p. 21 + 23
"Shipley offer single-sided shielding for EMC"

191. IBM IBM Technical Disclosure Bulletin, Vol. 32, No. 6B, November 1989, p. 188
"Method to Evaluate the Ability of Conductive Polymer Grommets to remove RF Currents from Cable Shields"

192. US 5 025 211 AT & T Bell Laboratories

193. IBM IBM Technical Disclosure Bulletin, Vol. 32, No. 7 December 1989, p. 386-387
"Grated Ground Plane"*

194. WENAAS et al. IEEE Transactions on Nuclear Science, NS-32 (1985) Dec., No. 6, p. 4346-4348
"EMP Isolation Transformer"

195. PIENKOWSKI et al. IEEE 1989 National Symposium on Electromagnetic Compatibility, May 23-25 1989, p. 380-382
"Measuring the Shielding Effectiveness of Superconductive Composites"*

CHAPTER FOUR

196. EP 0 473 877 Yokogawa Electric Corporation

197. US 3 764 907 Langella et al.

198. GB 2 196 744 Kerry Ultrasonics Limited (Incorporated in United Kingdom)

199. US 5 186 540 Raytheon Company

200. EP 0 330 933 Asea Brown Boveri AG

201. SCHUSTER, Gerhard IEEE Transactions on Instrumentation and Measurement, Vol. IM-29, September 1980, No. 3, p. 153-157
"Thermal Instrument for Measurement of Voltage, Current, Power, and Energy at Power Frequencies"*

202. US 4 628 256 Weinschel Engineering Co., Inc.,

203. US 4 431 951 Westinghouse Electric Corp.,

204. EP 0 320 265 Hewlett-Packard Company

205. EP 0 378 817 Eslab S.r.l.

206. WO 86/06173 PARKER, Robert

207. GB 2 124 392 English Electric Valve

208. GB 2 130 442 The Secretary of State for Defence

209. US 4 008 610 The United States of America as represented by the Secretary of Commerce

210. US 4 977 366 Lucas Weinschel Inc.,

211. EVERETT, Chris EDN, Volume 30, Number 24, October 1985, p. 65, 67,68 and 70-72
"Improved diode detectors increase accuracy of the latest scalar network analyzers"

212. US 4 970 456 Motorola, Inc.,

213. US 4 647 848 Tektronix, Inc.,

214. US 4 080 566 Bird Electronic Corporation

215. US 4 075 554 Bird Electronic Corporation

216. EP 0 218 905 General Electric Company

217. FR 2 594 230 LGZ Landis & Gyr Zug AG.

218. US 2 136 251 General Electric Company

219. US 2 901 701 Aluminum Company of America

220. GB 2 143 955 HUTT, Peter Richard

221. GB 2 034 054 University of Singapore

222. EP 0 456 868 Siemens Aktiengesellschaft

223. US 4 742 296 LGZ Landis & Gyr Zug AG

224. EP 0 354 079 ABB Petercem S.A.

225. EP 0 521 250 Landis & Gyr Betriebs AG

226. EP 0 543 365 Kabushiki Kaisha Toshiba

227. EP 0 148 330 LGZ Landis & Gyr Zug AG

228. US 4 045 734 Canadian Patents and Development Limited

229. KUSTERS et al. IEEE Transactions on Instrumentation and Measurement, Vol. IM-29, No. 4, December 1980 p. 426-431
"The Development of an Automatic-Reversing Differential Thermal Wattmeter"

230. COOPER, D.C. Electronic Instrumentation and Measurement Techniques, Prentice-Hall, Englewood Cliffs, N.J., USA 1970

231. US 4 628 257 Canadian Patents and Development Limited

232. TAKAHASHI, Kunihiko IEEE Transactions on Instrumentation and Measurement, 40 (1991) April, No. 2, p. 388-392
"Precision Thermal Wattmeter Having a Sampling Control System and an Analog Feedback Loop"*

233. FR 674 835 Societe Industrielle pour la Fabrication d'Appareils de Mesure

234. KONDRASKE, George Medical & Biological Engineering & Computing, Vol. 23, No. 4 July 1985

235. CHOUDHURY et al. Proc. IEE, Vol 114, No. 8, August 1987, p. 1171-1173
"Use of an electrostatic wattmeter as ac/dc comparator"*

236. JONES et al. Proc. IEE, Vol. 124, No. 12, December 1977, p. 1259-1261
"Feedback electrostatic wattmeter using a noncontact moving-coil actuator"

237. BARLOW et al. Proc. IEE, Vol. 117, No. 1, January 1970, p. 249-254
"Microwave electrostatic wattmeter"

238. GREBENE, Alan Analog Integrated Circuit Design, Chapter 7, Microelectronics series, Van Nostrand Reinhold Co., New York N.Y., USA, 1972

239. US 4 731 576 Technology Research Corporation

240. GB 2 086 062 Rochester Instrument Systems Inc.

241. EP 0 189 754 REFAC Electronics Corp.

242. EP 0 545 394 Deutsche Zähler-gesellschaft
Nachf. A. Stepper & Co. (Gmbh & Co.)

243. PARKER, E. J. Marconi Instrumentation, Vol. 8, No. 2, June 1961, p. 157-158
"Ac Power Measurement Using An Oscilloscope"

244. EP 0 466 453 Polymeters Response International Limited

245. US 4 672 555 Massachusetts Institute of Technology

246. EP 0 043 958 Litton Systems, Inc.

247. US 4 451 784 General Electric Company

248. US 5 151 866 The Dow Chemical Company

249. EP 0 028 176 Enertec Societe Anonyme

250. EP 0 455 839 Siemens Aktiengesellschaft

251. US 4 321 529 SIMMONDS, Charles W.

252. GB 2 196 744 Kerry Ultrasonics Limited

253. MATOUKA, Michael F. IEEE Transactions on Industrial Electronics, Vol. IE-29, No. 1, February 1982 p.18-31
"A Wide-Range Digital Power/Energy Meter for Systems with Nonsinusoidal Waveforms"

254. SAMRA et al. Proceedings of the 34th Midwest Symposium on Circuits and Systems, Monterey, California, USA, May 14-17 1991, p. 652-655
"Application of Digital Processor Technology to Power Metering of Harmonics"

255. DE 1 541 784 Licentia Patent-Verwaltungs-GmbH

256. EP 0 052 255 Siemens Aktiengesellschaft Berlin und München

257. EP 0 302 170 LGZ LAndis & Gyr Zug AG

258. PFLIER P.M. et al. Elektrische Messgeräte und Messverfahren, 4th edition, Springer Verlag Berlin, Germany 1978

259. KIKUCHI, Kazuo IEEE Transactions on Instrumentation and Measurement, Vol. IM-30, No. 4, December 1981 p. 238-242
"Broad-Band High-Speed Microwave Power Sensor Using Hot Carriers in Semiconductor"*

260. EP 0 104 748 Bird Electronic Corporation

261. GB 2 198 854 Canadian Patents and Development Limited

CHAPTER FIVE

268. DE 16661 EDISON, Thomas Alva

269. DE 17921 EDISON, Thomas Alva

270. Not used

271. US 2 136 251 General Electric Company

272. EP 0 493 964 Raytheon Company

273. EP 0 063 282 Westinghouse Electric Corporation

274. EP 0 560 195 Kabushiki Kaisha Kito

275. EP 0 302 170 LGZ Landis & Gyr Zyg AG

276. EP 0 554 188 Merlin Gerin

277. US 4 795 974 Ford Motor Company

278. EP 0 446 962 Schlumberger Industries Inc.

279. EP 0 342 146 Transdata Inc.

280. EP 0 462 045 Transdata Inc.

281. EP 0 528 634 Westinghouse Electric Corporation

282. BÅNG, Hans Ericsson Review, 62 (1985) Nor. 2, p. 93-95 : "Electronic Electricity Meter for Differentiated Tariffs"

283. EP 0 178 067 Westinghouse Electric Corporation

284. WO 93/04377 Services Industriels De Geneve

285. EP 0 225 106 British Aerospace Public Limited Company

286. DE 1 541 784 Licentia Patent-Verwaltungs GmbH

287. EP 0 267 693 The General Electric Company p.l.c.

288. EP 0 456 868 Siemens Aktiengesellschaft

289. MAKRAM et al. IEEE Transactions on Power Delivery, 7 (1992) July, No. 3, p. 1080-1088 "A Harmonic Analysis Of The Induction Watthour Meter's Registration Error"

290. GIRGIS et al. IEEE Transactions on Industry Applications, 26 (1990) July/August, no. 4, p. 689-695 "Testing the Performance of Three-Phase Induction Watt- hour Meters in the Presence of Harmonic Distortion"

291. FILIPSKI, Piotr S. IEEE Transaction on Instrumentation and Measurement, Vol. IM-39, No.1, February 1990, p. 15-18 "A Tdm Wattmeter With 0.5 Mhz Carrier Frequency"*

292. EP 0 384 615 Nokia Mobile Phones Ltd.

293. FILIPSKI et al. IEEE Transactions on Power Delivery, 7 (1992) October, No. 4, p. 1793-1799 "Evaluation of Reactive Power Meters in the Presence of High Harmonic Distortion"

294. US 3 611 130 The United States of America as represented by the Secretary of Commerce

295. US 3 764 907 LANGELLA Antonio, SAVASTANO Giorgio

296. MENCHETTI et al IMEKO TC-4 (Brussels, May 1993) p. 355-361 "A Wideband Random-sampling Wattmeter"

ADDENDA

297. IEEE Standard Dictionary of Electrical and Electronics Terms. American Standards Institute. Institute of Electrical and Electronics Engineers. 1984. New York. USA

298. US 5 416 406 The United States of America

299. FR 2 564 594 Merlin Gerin

300. US 4 262 265 Mitsubishi

301. EP 556 099 ABB Control

302. Knauer, Evaluation Engineering, November, 1990, pages 150-153 "Fixturing for Low-Current, Low-Voltage Parametric Testing",

303. WO9011529 ABB Strömberg Kojeet Oy, Finland

304. Abd-Elsalam, Abdel-Salam, Wiitanenand Perger Measurement Science & Technology, vol.4, Nr 4, March 1993, Bristol GB "A New Laser-Voltmeter"

305. Karlebo Handbok, Maskinaktiebologet Karlebo, Sweden

306. EP 599 181 Matsushita Electric Ind Co Ltd

307. GB 2 212 265 Hamamatsu Photonics

308. EP 361 832 Westinghouse Electric

309. EP 682 261 ABB Research

310. EP 506 357 Hamamatsu

311. US 4 629 323 Tokyo Shibaura Electric Co

312. EP 586 226 NGK Insulators

313. WO9612195 Siemens

314. US 5 247 244 ABB Power T&D

315. DE 1 9544778 Siemens

316. WO9400768 Sifam

317. EP 740 162 Fuji Electric

318. EP 831 333 Siemens

319. WO9705493 Applied Precision S R O; Grno Ladislav

320. JP 1 162 165 Sumitomo Electric

321. EP 713 279 Eaton Corp

322. DE 2630959 Heliowatt-Werke

323. EP 578 025 Texas Instruments Deutschland

324. EP 681 235 Landis & Gyr

325. EP 793 104 Eaton Corp

326. EP 601 926 Thomson Csf Semiconducteurs

327.	US 5 266 888	Narda Microwave Corp
328.	US 4 253 151	Bouve
329.	EP 738 893	The General Electric Company
330.	WO9725625	Massachussets Institute Of Technology
331.	LANCE	Electronic Test, November 1989, p. 32 and 34, "Microwave Power Measurement"
332.	US 5 017 859	Westinghouse Electric Corp
333.	EP 779 516	Infrarrojo y Microelectronica
334.	DE 566 227	PUNGS, Leo
335.	Göpel et al.	Sensors, Vol. 4, Thermal Sensors, VCH Verlagsgesellschaft, Weinheim, Germany
336.	US 5 291 073	Fluke Mfg Co John
337.	EP 717 286	The General Electric Co
338.	US 5 406 075	GPT Ltd.
339.	US 5 698 983	Yazaki Corp.
340.	EP 826 971	Toshiba
341.	FESER, Kurt	ETZ Elektrotechnische Zeitschrift, 112 (1991) Marz, No. 6/7 p. 292 ,294,296,298,300,302-303 "Trends bei Hochspannungsprüf- und -meßtechnik"*

This Page Intentionally Left Blank

INDEX